Impact de l'adaptation des biofilms bactériens aux biocides désinfectants sur l'antibiorésistance

Raphaël Charron

COLLEGE DOCTORAL BRETAGNE SCIENCES DE LA VIE ET DE LA SANTE

Université de Rennes

Thèse de doctorat de

L'UNIVERSITE DE RENNES I

ECOLE DOCTORALE N° 637
Sciences de la Vie et de la Santé
Spécialité : Microbiologie, Virologie, Parasitologie

Par

Raphaël CHARRON

Impact de l'adaptation des biofilms bactériens aux biocides désinfectants sur l'antibiorésistance

Thèse présentée et soutenue à Rennes le 25 novembre 2024
Unité de recherche : ANSES – Laboratoire de Fougères – Unité Antibiotiques, Biocides, Résidus et Résistance (AB2R)

Composition du Jury :

Président :	Christophe BELOIN	Directeur de recherche – Institut Pasteur
Rapporteurs :	Emmanuelle DÉ	Professeure des universités – Université de Rouen
	Jean-Yves MAILLARD	Professor – Cardiff University, United Kingdom
Examinateurs :	Florie DESRIAC	Maîtresse de conférences – Université de Caen
	Charlotte MICHAUX	Chargée de recherche Inserm – Université de Rennes I
Dir. de thèse :	Arnaud BRIDIER	Chargé de projet, ANSES, Fougères
Co-dir. de thèse :	Romain BRIANDET	Directeur de recherche, INRAE, Jouy-en-Josas

Remerciements

Tout d'abord, je tiens à remercier **Emmanuelle Dé**, **Jean-Yves Maillard**, **Florie Desriac**, **Charlotte Michaux** et **Christophe Beloin** d'avoir accepté de faire partie de ce jury de thèse. J'ai conscience du travail que cela représente et je vous en remercie pour cela.

Arnaud, je ne saurais te remercier assez pour m'avoir aussi bien encadré durant ces 3 ans. J'ai suffisamment d'amis faisant des thèses dans mon entourage pour savoir qu'avoir un directeur qui se rend aussi disponible pour son thésard, c'est aussi rare qu'un soleil en Bretagne ;). Merci d'avoir été autant à l'écoute, tes petits coups de main au labo et ta sympathie. Je garderai bien sûr en mémoire le voyage à Porto et la semaine où tu m'as logé à Fougères, tes pizzas délicieuses, bien au-dessus des restaus d'attrapes-touristes de Porto…
Romain, merci également à toi, pour tous tes précieux conseils, sur la microscopie à fluorescence en particulier, mais aussi sur tous les autres domaines relevant de la thèse. Merci aussi pour m'avoir payé mes fluorophores qui coûtent un bras ;). Toi aussi, merci pour ta sympathie et ton accessibilité.
Dès le premier entretien avec vous deux j'avais un bon pressentiment que ça se passerait bien, et je suis ravi que ça se soit confirmé au fil des 3 ans. En espérant bien sûr que c'était réciproque ;).

Merci à **Astrid Rouillon**, **Pierre-Emmanuel Douarre** et **Christophe Beloin** pour avoir accepté de faire partie de mon Comité de Suivi de Thèse. **Astrid**, merci pour tous tes conseils sur les débouchées professionnelles post-thèse et d'avoir accepté d'être présidente de ce comité de suivi. **Pierre-Emmanuel** merci notamment pour tes conseils sur l'analyse génomique. Enfin, **Christophe**, un remerciement tout particulier pour toi. Tu auras été là à toutes les étapes clés, du M2 Microbio Fonda à Pasteur, le séminaire Pasteur que tu avais donné sur Teams vers juin 2021 auquel j'avais assisté avec Arnaud et Romain et qui constituait mon premier travail de thèse, les deux CSI, et enfin la soutenance de thèse que tu as accepté d'évaluer. Merci pour tous ces précieux conseils depuis 4 ans. Merci également pour m'avoir présenté à toutes ces personnes lors du congrès Eurobiofilms ;).

Bon, pour la suite de l'organisation on va faire dans l'ordre chronologique, donc Fougères d'abord, ne soyez pas jaloux à Jouy ;).
Déjà un petit message général à tous les gens du laboratoire (comme ça je n'oublie personne), vous avez tous été d'une chaleur incroyable, merci pour votre accueil, quand on arrive dans une ville où l'on ne connaît personne, on est bien contents de tomber dans un labo comme ça.
Tahar, tu es la preuve qu'on peut diriger un laboratoire tout entier, mais quand même trouver le temps pour allier discussions professionnelles et extra-professionnelles, mais par dessus tout prendre soin de l'aspect relationnel au sein du laboratoire tout en brisant les barrières hiérarchiques. Merci à toi pour toute ta bienveillance.
Christophe, tu n'es pas en reste. Merci à toi aussi pour ta gentillesse et ton investissement pour que tout se passe bien dans AB2R, pour ton implication dans le projet de thèse et dans Baobab. Et merci pour les petits pains aux réunions d'équipe évidemment :).
Pierre, un immense merci à toi. Je ne sais pas à quoi auraient ressemblé les papiers sans tes analyses génomiques mais ça aurait sans doute eu moins de gueule. En plus de cette aide, merci d'avoir été autant à l'écoute, quand je te demandais de changer une figure pour la 45^{e} fois (t'inquiète je sais ce que c'est aussi de mon côté :')).
Paméla et **Patricia**, merci à toutes les deux pour votre aide dans le projet de thèse. Paméla j'espère que tu ne me maudis pas pour tous ces cryotubes que tu as faits, ou mon écriture en pattes de mouches sur les boîtes de pétri qui ont dû te casser la rétine. Patricia, merci pour les manips que tu as faites quand j'étais à Jouy-en-Josas. Et merci pour toutes les fois où tu m'as trouvé les choses que je cherchais dans le labo ;).

Béatrice et **Charlotte**, bien sûr merci à toutes les deux aussi, honnêtement je pense qu'il y a dû y avoir pas mal de fois où vous m'avez aidé à trouver des trucs dans le L2, sur le LIMS, ou partout ailleurs.
Marine, un remerciement tout particulier à toi. Toute l'aide que tu m'as donné durant ton M2 je ne l'oublierai pas. La biologie c'est cool, mais ça l'est encore plus quand on la fait à 2. Désolé de t'avoir fait faire le sale boulot sur les dénombrements des variants et les photos des boîtes, j'espère que tu ne m'en tiendras pas rigueur et que tu me mettras dans tes remerciements dans un an ;).
Ornella, toi aussi tu t'es investie à fond dans ce projet et bien sûr je t'en remercie aussi. J'espère que ça ne t'a pas traumatisé des RT-q-PCR. Qui dit RT-q-PCR dit **Antoine** bien sûr, je ne t'oublie pas, merci de t'être investi dans le projet, d'avoir supervisé Ornella sur toute la partie sur l'expression de gènes.
Thibaut, merci pour toute ton aide sur le SDS-PAGE, et pour toutes tes explications sur cette manip.
Agnès, merci pour ces discussions sur *Escherichia marmotae* et ta bienveillance. Ravi de partager ce bureau avec toi dans le futur. A propos de partager le bureau…
Maiwenn, on est arrivés en même temps à Fougères, on s'est retrouvés dans le même bureau, et ce fut un plaisir de le partager avec toi. Merci pour ton calme et pour nos discussions, sur Londres, sur Paris.
Alain, **Sylvie**, merci de gérer toute la partie logistique, c'est aussi grâce à vous que cette thèse a pu fonctionner aussi bien. De même pour **Sarah** et **Lucie**, pour l'aide sur les méandres administratifs d'une thèse en co-tutelle.
Estelle, merci pour toutes ces discussions sur nos vies de thésards respectives, à tes conseils de 3e année pour le petit thésard de 1ere année que j'étais. Au moment où j'écris ça, tu dois être en plein dans les derniers préparatifs pour ton mariage, tous mes vœux de bonheur.
Cristina, merci aussi pour tes conseils sur la thèse, à comprendre l'administration de l'école doctorale et Amethis, à ces allers-retours à Nantes pour cette formation de stats, et pour tous les à-côtés de la thèse évidemment.
A tous les grands sportifs de l'ANSES, et Dieu sait que vous êtes nombreux, merci de m'avoir motivé à reprendre le sport. Parmi vous, un remerciement spécial à la team pump du jeudi, **Alexis**, **Thibaut**, **Cristina**, **Marine**, **Annaëlle**, **Mickaël**, **Mickaëlle**, **Sophie** et **Estelle**, à nos jeudi après-midi improductifs et nos vendredi courbaturés. Un remerciement spécial aussi à la team bad du mardi, **Thibaut**, **Pierre**, **Alexis**, **Anne-Louise**, **Darryl**, **Cristina**, **Nelly**, et ceux qui se sont ajoutés dans ma 2e année, **Laura**, **Annaëlle**, **Charlène**, **Gaël**, **Youssef**, désolé si j'en oublie ou si vous n'y étiez pas, j'ai trop passé de temps à côté sur le panier de basket pour me rappeler qui jouait au bad. **Alexis**, **Thibaut**, je vous aurais un jour (ou au moins je vous prendrais un set).
Merci à tous ceux qui ont découvert la nightlife de Fougères avec moi. La team des débuts, avec **Darryl**, **Cristina** (et **Corentin**), **Adrien** et **Marine**. A nos rencontres avec les plus grands phénomènes de Fougères, les soirées lunaires au castle ou au bowling. A nos discussions sur le foot et le sport, aux foulées de l'espoir, à ce weekend à Brest, aux 24 h du Mans, et j'en passe. A **Katherly** pour l'été 2022, nos sorties vélo et le canoë avec l'ACS. A toute la team de la 2e année, **Marine**, **Cristina** et **Corentin** toujours, mais aussi **Laura**, **les deux Pierre**, **Annaëlle**, **Juliette**, **Ornella**, **Saddate**, **Ilhem**, **Maiwenn**, **Youssef**, **Tristan**, **Charlène**, **Gaël**, **Sarah**, **Mariam**, à nos soirées jeux de société au Respawn et nos afterworks au Byggvir.
Merci à tous les gens de l'ACS pour participer à la vie active du labo et pour toutes les sorties organisées au cours des 2 ans.
Merci à toute la team cantine. Bon j'essaye de me refaire mon plan de tête quand j'allais tous vous chercher à midi, mais je sais que je vais forcément en oublier. **Karine** évidemment, je

n'oublierai pas tes critiques sur mon alimentation ;), **Jean-François** et nos discussions voyages et nos discours désespérés sur les passoires thermiques à Fougères :'), **Murielle**, **Sophie**, **Marie-Pierre**, **Béatrice**, **Cristina**, **Darryl**, **Marine**, **Annaëlle**, **Alwena**, **Maiwenn**, **Ilhem**, **Gaël**, **Charlène**, **les deux Pierre**, **Ornella**, **Sarah**, **Saddate**, **Laura**, **Youssef**, et la dernière à nous avoir rejoints juste avant que je parte, **Lucille**.
Enfin, merci à tous les autres (y a encore plein de noms que j'ai en tête), sur qui je n'ai pas forcément une anecdote particulière à raconter, mais tous aussi gentils les uns que les autres.

On passe à Jouy maintenant. Je vous paierai bien ma tournée mais j'ai une réputation de rat à tenir ;).
Florence, merci de m'avoir permis de donner ce cours, une expérience que je ne sais pas encore si j'ai envie de réitérer mais qui m'aura quand même beaucoup apporté.
Vlad, merci pour toutes les discussions sur la microscopie confocale, pour ce petit cours particulier que tu nous auras donné à Virgile et moi, interrompu par l'alarme incendie et qu'on a continué dehors sous la pluie.
Marie-Françoise, merci d'avoir répondu à toutes mes questions sur CRISPR, je ne l'ai pas utilisé durant la thèse, mais pourquoi pas à l'avenir.
Virgile, cher co-premier auteur, merci pour tous tes conseils de thèse. A toutes nos discussions de vie de chercheur qui ont dérivé beaucoup trop de fois, ton gros papier qui je l'espère sortira un jour, et bien sûr à tous les à-côtés de la thèse. Merci aussi pour ce temps passé avec moi au téléphone un vendredi soir pour m'aider à lancer un HCS (que j'aurais quand même réussi à louper…).
Pierre, le GOAT (t'es content, je l'ai écrit). Merci pour toutes nos discussions sur le sport, toutes ces citations d'illustres philosophes tels que Thierry Henry, Kylian Mbappé, ou Thierry Gilardi, que l'on s'est répétés. Merci pour ces ménages P2, avec des musiques discutables. Pas merci, pour toutes ces fois où tu m'as déconcentré quand j'essayais de travailler. Mais t'inquiète pas, tu vas la chercher cette thèse, tu vas la chercher.
Maud, merci d'être partie avec **Pierre** en congrès pendant une semaine pour que je puisse travailler. A nos discussions sur la vie palaisienne également.
Alban, merci à toi aussi pour les discussions sur le sport (enfin avec toi je dois plutôt limiter ça au foot haha), à ces posts insta qui se moquent de CR7 et Mbappé qu'on s'est envoyés. Merci pour toutes les dingueries que tu as pu lâcher avec la voix la plus monotone du monde.
Julien, merci aussi à toi pour toutes ces discussions, sur le tour, sur l'euro, sur les JO, sur les girondins de Bordeaux (RIP). Partenaire de Ferment'heure de la première heure également.
Philippe, pour finir sur la partie sport, j'espère que tu trouveras de nouvelles personnes avec qui échanger quand je serai parti. A ce soporifique France-Belgique, à nos discussions sur les JO et nos messages interposés sous la pluie lors de la cérémonie d'ouverture.
Yasmine, **Aya**, merci pour ces covoiturages et pour la Blablacar money. **Hadi**, merci aussi de nous avoir fait découvrir Blablacar, je vous ramènerai tous des chocolats un jour.
Dimitrios, **Hugo**, thanks for all these walks to the canteen, discussing from all and nothing. **Dimitrios**, to this amazing visit of Versailles we did together. **Hugo**, merci d'être mon sauveur sur R.
Aurore, merci pour l'aide sur toutes les taches administratives, et d'avoir répondu à toutes mes questions, même en distanciel depuis Fougères.
Julia, merci de m'avoir expliqué le confocal pendant une après-midi, tous ces aller retours que t'as dû faire pour les 4000 problèmes que j'avais.
Cécile, merci à toi pour tous ces moments partagés, pas grand-chose de plus à dire mais c'est pour te prouver que je ne t'oublie pas pour une fois ;).
Marina, merci de ramener un peu d'Alsace dans le labo.

Vincent, merci à toi pour les quelques derniers mois à Jouy. On se retrouve à Fougères l'année prochaine de toute façon.
Merci à tous ceux qui auront partagé leurs journées au P2 avec moi, **Merve**, **Alban**, **Pierre**, **Cécile**, **Aurore**, **Matteo**, **Aya**, **Hugo**, **Arthur**, **Hadi**, **Virgile**, merci à ceux « qui étaient là pour mettre la bonne ambiance », pas merci à ceux qui laissaient traîner leur bazar, pas merci à **Pierre** pour les odeurs de saumon pourri. Merci à **Aurore**, **Emilie**, **Inès** et **Pierre** pour avoir été des binômes de ménages tops, pas merci à **Virgile** pour m'avoir abandonné en plein milieu.
Merci à toute la team sport de Jouy, **Arthur**, **Pierre**, **Virgile**, **Alban**, **Cécile**, **Hadi**, bon on n'aura pas tous été les plus réguliers (je ne vise personne), mais ce fut un plaisir de se retrouver là-bas.
Merci à toute la team sorties aussi ici, **Mathilde**, **Arthur**, **Cécile**, **Inès**, **Pierre**, **Virgile**, **Alban, Simon, Dimitrios**, **Daniele**, **Vincent**, **Hugo**, **Hadi**, **Raphaël**, à toutes ces soirées au bureau et au deer'n'beer. A ceux qui viennent de « Pal » (ou plutôt venaient, **Mathilde** lâcheuse), la meilleure ville, **Mathilde** et **Virgile,** pour nos retours à pied ou en Uber ensemble. **Arthur**, je garderai en mémoire, cet afterwork dans Paris qui a mal tourné. **Mathilde** je n'oublierai pas la guigette.
Merci à tous les gens de Doc'J, pour les quelques sorties ensemble, la découverte des alentours de Jouy, **Matteo** « le collègue », **Matthieu**, **Ronan**, **Léa**, **Nathalie**, **Armand**, **Andrea**, **Claire-Jing**, **Victor**, **Alexandre**, **Marie**, **Léa**, **Laura**.
Merci aussi à la dernière team sortie, **Sébastien** et tes idées au top, **Angélique**, **Cécile**, **Aurore**, **Pierre**, **Ronan**, **Léa**, **Claire-Jing**, **Corentin**, **Thibaut**, **Adrien**, à cette soirée karting-laser game-bowling, à nos soirées à désespérer devant le niveau de jeu pitoyable de l'équipe de France à l'euro et les mises en orbite du ballon par Marcus Thuram.

Merci aussi à tous les amis que je côtoie pour certains depuis biiiiiien longtemps, et avec qui j'ai toujours du contact.
Arthur d'abord, merci pour toutes ces soirées au téléphone ou à geeker ensemble, pour m'occuper quand je ne savais pas quoi faire à Fougères. Et évidemment ce petit weekend bien sympa chez toi à, Orléans.
Lucille, merci pour toutes ces fois où tu m'as hébergé quand je revenais faire un petit coucou sur Paname. A ces vacances incroyables en Andalousie, ce weekend au ski chez toi, et ce weekend mémorable à Fougères (oui je parle du bowling). Et évidemment les soirées et les visites de musées gratuits à mon retour sur Paris. A nos discussions sur nos deux thèses respectives, qui se finiront à un jour d'intervalle, trop connectés ;).
Juliette, merci aussi d'être venue à Fougères, à ce festival avec le GOAT Martin Garrix, et aussi ces vacances en Andalousie. A nos discussions sur nos thèses respectives (je répète ce que j'écris à Lucille décidément).
Leon, thank you also to you that you came to visit in Fougères, especially the Mont Saint Michel and Saint Malo, because I don't even know if you remember the name of Fougères haha. Thanks for the geography games we played together and of course thanks for joining to the Oktoberfest.
Célia et **Sacha**, merci pour nos diverses soirées à Rennes, Bédée et Fougères, des jeux de société sans oublier les blindtests évidemment.
Pierre, merci pour les deux nouvel ans chez toi à Paris, ainsi que les quelques soirées qu'on a pu faire depuis mon retour, avec **Antoine** et **Isaure**. Bon courage pour la fin de thèse, bientôt fini !
Tony, merci pour toutes les discussions de sport par message, à la coupe du monde de basket et aux JO, merci pour ce weekend bien stylé à Marseille. Started from the bottom (Poitiers) now we're here (Docteurs de biologie).

Amandine, merci pour le petit weekend chez toi à la fête des Lumières à Lyon, avec **Juliette** et **Lucille**.
To all the Uppsala team that went to Oktoberfest, thanks **Stefan** for hosting, thanks **Nick** for organizing, thanks also to **Pablo**, **Carlos** and **Leon**, amazing weekend, and amazing covid that made me miss one whole week of PhD right after.
Thanks to the other Uppsala bros, **Kevin**, for organizing, and **Kai** for joining, for this amazing ski weekend in Chamonix.
Merci aussi à toute la team de Mulhouse, **Roman**, **Ahmedin**, **Cédric**, **Mathieu**, **Daniel**, **Benjamin**, et ceux qui s'ajoutent par ci par là, pour être toujours au rendez-vous quand je rentre à Noël.
Thanks to all the one-day friends I have made during the congresses and thematic schools I went to, in Rennes, Saint-Malo, Sète, Porto, Hamburg, Copenhagen. I forgot most of your names, but not the moments.

Enfin, merci à ma famille.
Papa et **Maman** d'abord, merci d'avoir toujours été là pour moi, c'est principalement grâce à vous que j'en suis là aujourd'hui, pour toute votre éducation mais aussi pour m'avoir poussé à continuer après le M2, au moment où j'était dégoûté de la recherche. A nos vacances peu exotiques en Bretagne en 2022 et aux JO en 2024, à nos vacances plus exotiques en Tanzanie en 2023.
Alice toi aussi, merci d'être là, d'être une grande sœur aimante, merci d'être là quand j'ai besoin d'une guide après m'être fait opérer des yeux ;), j'essaye de te rendre la pareille quand je ne suis pas tête en l'air. A nos vacances mémorables en Tanzanie également.
Benoît, merci aussi d'être passé à Fougères pour ce petit weekend familial, de m'avoir côtoyé sur la route pour l'Alsace à Noël, avec **Alice**. Au petit verre qu'on a également pris ensemble aux 24h du Mans.
Uli, danke, dass du immer von mich Nachrichten nimmst, auch wenn ich manchmal etwas länger brauche, um zu antworten. Danke dass du mich auch in Fougères besucht hast und dass wir die Gegend zusammen erkundet haben.

J'espère que vous êtes tous prêts à m'appeler Dr. Charron maintenant.

A ceux qui nous aurons quitté pendant cette thèse,

Papi,

Tigris,

et Mireille

Abréviations

AB2R : Antibiotiques, Biocides, Résidus et Résistance

ADN : Acide désoxyribonucléique

ADNe : ADN extracellulaire

ANSES : Agence nationale de sécurité sanitaire de l'alimentation, de l'environnement et du travail

ARN : Acide ribonucléique

BAC : Chlorure de benzalkonium

BTS : Bouillon tryptone soja

CipR : Ciprofloxacin-resistant

CLSM : Microscope confocal à balayage laser

CMI : Concentration Minimale Inhibitrice

ConA : Concanavaline A

Ecoff : Epidemiological cut-off value

ESKAPEE : *Enterococcus faecium, Staphylococcus aureus, Klebsiella pneumoniae, Acinetobacter baumannii, Pseudomonas aeruginosa, Enterobacter, Escherichia coli*

GenR : Gentamicin-resistant

GFP : Green Fluorescent Protein

INRAE : l'Institut national de recherche pour l'agriculture, l'alimentation et l'environnement

HGT : Transfert horizontal de gènes

LNR : Laboratoire National de Référence

LPS : Lipopolysaccharide

MGE : Eléments génétiques mobiles

OMS : Organisation Mondiale de la Santé

PHMB : Polyhexamethylene biguanide

RifR : Rifampicin-resistant

SHY : Sodium Hypochlorite

STEC : *Escherichia coli* productrices de la Shigatoxine

TMN : N-(3-aminopropyl)-N-dodecylpropane-1,3-diamine

WGA : Wheat Germ Agglutinin

WGS : Séquençage du génome complet

Table des matières

Introduction

Introduction

Ce projet de thèse résulte d'un partenariat entre l'Agence nationale de sécurité sanitaire de l'alimentation, de l'environnement et du travail (ANSES) et l'Institut national de recherche pour l'agriculture, l'alimentation et l'environnement (INRAE), qui ont conjointement participé au financement de la bourse doctorale. Ce travail s'inscrit également dans le cadre du projet ANR JCJC BAoBAb (coordonné par Arnaud Bridier), dont il a bénéficié du soutien scientifique et financier. L'objectif principal de cette thèse a été de mieux comprendre le lien entre le mode de vie en biofilm, l'adaptation aux biocides désinfectants et l'émergence de résistances croisées aux antibiotiques chez les bactéries. Ce mode de vie constitue la forme de vie bactérienne la plus courante dans de nombreux environnements, notamment au sein des chaînes de production alimentaire, où les biocides sont fréquemment utilisés.
La première partie de cette thèse a été réalisée au sein du laboratoire de l'ANSES de Fougères, dans l'unité « Antibiotiques, Biocides, Résidus et Résistance » (AB2R) sous la direction d'Arnaud Bridier. Ce laboratoire est reconnu pour son expertise dans le domaine des biocides et de l'étude des résistances aux antimicrobiens. L'unité AB2R héberge également le laboratoire national de référence - Résistance antimicrobienne (LNR-RA), en charge de la réalisation des plans de surveillance annuels de l'antibiorésistance sur la chaîne alimentaire, en lien avec le ministère de l'Agriculture. La seconde partie de la thèse a été réalisée au sein de l'équipe « Biofilms et communautés spatialement organisées » (B3D) de l'unité Micalis, à l'INRAE de Jouy-en-Josas, sous la direction de Romain Briandet. Cette phase s'est concentrée sur l'analyse des dynamiques structurales des biofilms au microscope confocal à fluorescence (CLSM), avec pour objectif de comprendre comment l'organisation spatiale et la différenciation cellulaire influencent la tolérance aux traitements antimicrobiens et l'émergence de variants résistants et observer le comportement de ces derniers au sein de communautés bactériennes complexes.

1. Contexte général

La découverte de la pénicilline par Sir Alexander Fleming en 1928 a marqué un tournant majeur dans l'histoire de la médecine, réduisant considérablement la mortalité humaine dans les décennies suivantes (Ventola, 2015). Les antibiotiques, pour la plupart dérivés de substances produites par des microorganismes, ont été des armes essentielles dans la lutte contre les infections bactériennes. Ces microorganismes, en compétition depuis des millénaires pour l'espace et les ressources, ont cependant développé des stratégies de défenses complexes contre ces substances (Perry et al., 2016). Depuis cette découverte, de nombreuses autres familles d'antibiotiques ont été découvertes et sont utilisées quotidiennement pour traiter aussi bien les humains que les animaux. Cependant, la résistance aux antibiotiques s'est rapidement propagée à travers le monde, exacerbée par l'utilisation abusive et excessive de ces agents antimicrobiens (Ventola, 2015). Bien que ces résistances existent depuis aussi longtemps que ces substances, elles étaient autrefois confinées à certaines niches écologiques. Ce n'est qu'avec l'utilisation extensive des antibiotiques par les humains que la dissémination des résistances à grande échelle a véritablement commencé (Davies and Davies, 2010).

Aujourd'hui, l'émergence de la résistance aux antimicrobiens représente l'une des plus grandes menaces pour la santé publique mondiale, au point d'être un domaine d'action prioritaire pour l'Organisation Mondiale de la Santé (World Health Organization, 2023). Une étude publiée par *The Lancet* en 2019 estimait que la résistance aux antibiotiques était directement responsable annuellement de 1,27 million de décès dans le monde, tout en étant associée à 4,95 millions de décès (Murray et al., 2022). Souvent qualifiée de « *pandémie silencieuse* », cette crise sanitaire touche inégalement les régions du monde, les pays en voie

de développement étant plus gravement affectés. Cette inégalité s'explique par plusieurs facteurs, notamment la difficulté d'accès à certaines molécules et à des diagnostics précis (Chokshi et al., 2019), des conditions d'hygiène insuffisantes (Chokshi et al., 2019), ainsi qu'une pollution environnementale due à des rejets industriels non régulés (Lundborg and Tamhankar, 2017). Un rapport publié en 2014 estimait que, sans intervention, la résistance aux antimicrobiens pourrait devenir, d'ici 2050, la première cause de mortalité dans le monde, avec plus de 10 millions de décès annuels (O'Neill, 2014).

L'utilisation d'antibiotiques, parfois abusive, en médecine humaine est un facteur contributif de sélection connu et a en conséquence fait l'objet de politiques publiques pour limiter la prise non justifiée d'antibiotiques. Cependant, de nombreux autres secteurs peuvent également contribuer à la propagation de bactéries résistantes. Par exemple, les usines de traitement des eaux usées constituent des environnements particulièrement favorables à la propagation de résistances, notamment à travers le rejet d'antibiotiques non métabolisés dans les selles humaines (Sambaza and Naicker, 2023). De plus, dans de nombreux pays, les antibiotiques continuent à être utilisés à des fins non thérapeutiques, ce qui accentue la propagation des résistances. Dans l'agro-industrie, l'utilisation massive d'antibiotiques comme facteurs de croissance chez les animaux (Castanon, 2007) a eu un impact significatif sur l'augmentation de la résistance aux antibiotiques. La chute significative de l'antibiorésistance dans le milieu agro-industriel, depuis la mise en place de certaines mesures, telles que celles impulsées par le plan d'action national Ecoantibio depuis 2012, visant à réduire l'utilisation d'antibiotiques chez les animaux, en témoigne (ANSES, 2023a).

Ainsi, l'identification de l'ensemble des facteurs contribuant activement à la sélection et à la dissémination de résistances aux antimicrobiens au sein des différents secteurs (médecine humaine et vétérinaire, élevage, environnement) est essentielle pour limiter l'émergence de variants résistants. Ces secteurs sont en effet interconnectés et forment un continuum. Ces dernières années, il est apparu qu'une lutte efficace contre la résistance aux antimicrobiens nécessitait une approche intégrée et globale, couvrant l'ensemble des environnements concernés. Ce concept, connu sous le nom de « *One Health* » ou « *une seule santé* », prend en compte cette interconnexion entre santé animale, humaine et environnementale (Velazquez-Meza et al., 2022).

L'utilisation des biocides désinfectants et leur impact constituent un exemple pertinent de cette problématique « *One Health* » (Aslam et al., 2021a). Les biocides, des substances à activité microbicide, sont largement utilisés dans divers domaines. Ils diffèrent des antibiotiques par leur utilisation principalement sur des surfaces inanimées, à l'exception des antiseptiques (McDonnell and Russell, 1999). Un nombre croissant d'études s'intéresse à la pression de sélection exercée par les biocides sur les populations bactériennes et au rôle potentiel que celle-ci pourrait jouer dans la sélection de résistances croisées aux antibiotiques (Maillard, 2018; Charron et al., 2023a). En effet, les mécanismes d'adaptation des bactéries aux biocides peuvent contribuer à la sélection de résistances aux antibiotiques, notamment via des mécanismes partagés comme les pompes d'efflux à large spectre, qui rejettent aussi bien les antibiotiques que les biocides (Langsrud et al., 2004; Karatzas et al., 2007; Pagedar et al., 2011). De plus, une co-sélection indirecte peut également avoir lieu, résultant de la présence de plasmides possédant à la fois des gènes de résistance à des antibiotiques et à des biocides (Russell, 1997; Chen et al., 2013; Roedel et al., 2021). L'omniprésence des biocides dans nos environnements, due à leur utilisation massive et quotidienne dans les milieux anthropisés, et amplifiée par la crise du Covid-19 (Rizvi and Ahammad, 2022), soulève ainsi des questions sur les impacts sanitaires potentiels que pourrait engendrer leur utilisation massive.

Les produits biocides sont massivement utilisés dans les industries agroalimentaires, notamment sur les chaînes de production. En France, 11 000 tonnes sont utilisées chaque année (Oulahal and Degraeve, 2021), pour limiter la transmission de pathogènes via les denrées alimentaires. Pour être efficace sur le terrain, les concentrations de biocides dans les formulations de désinfection sont souvent nettement supérieures à celles nécessaires pour éradiquer les bactéries dans des conditions optimales (Gilbert and McBain, 2003). Cela explique en partie pourquoi le terme « résistance » est souvent débattu lorsqu'il s'agit de biocides, les résistances identifiées en laboratoire n'étant souvent que des baisses de sensibilité, loin des concentrations d'usage sur le terrain (Maillard, 2018). Néanmoins, plusieurs facteurs peuvent limiter les concentrations auxquelles les bactéries sont réellement exposées, réduisant ainsi l'efficacité des procédures de désinfection (Maillard, 2005).

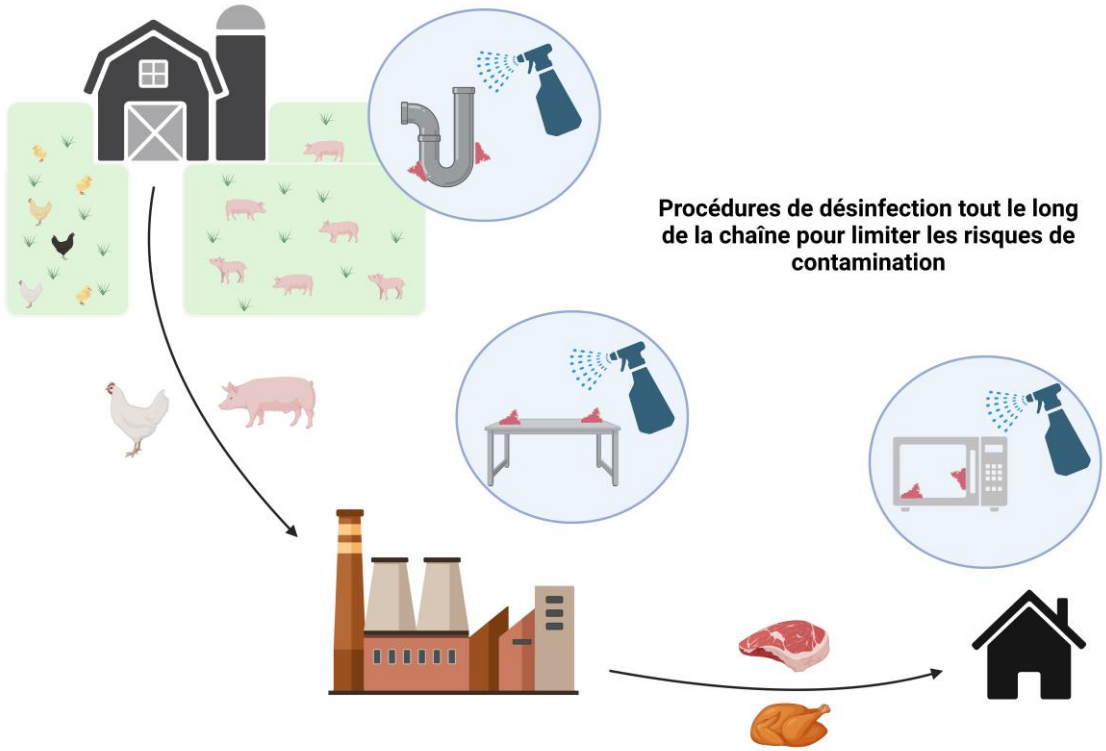

Figure 1 : Schéma représentant les étapes dans lesquelles des procédures de désinfection sont effectuées au sein d'une chaîne de production alimentaire, de « la fourche à la fourchette ». Figure créée avec Biorender.com.

Ces limitations sont souvent liées à des mésusages, notamment des erreurs lors de la préparation et de l'utilisation de la solution de désinfection. De plus, sur les chaînes de production alimentaires, les bactéries vivent principalement au sein de biofilms. Ces derniers sont des communautés structurées de microorganismes, adhérées aux surfaces et englobées dans une matrice extracellulaire composée de polysaccharides, protéines, lipides, ADN extracellulaire (ADNe) et d'autres composés sécrétés par les bactéries ou provenant de l'environnement (Flemming and Wingender, 2010). Les biofilms jouent un rôle crucial dans la survie et l'adaptation des bactéries aux stress antimicrobiens en leur conférant des propriétés fonctionnelles spécifiques (Bridier et al., 2011a; Charron et al., 2023a). La structure tridimensionnelle de cet édifice biologique et les interactions entre certains composés de la matrice et les molécules biocides peuvent limiter la diffusion des biocides, entraînant une

exposition réduite des bactéries situées dans des couches internes (Bridier et al., 2011b). Par exemple, de nombreux biocides sont des substances cationiques positivement chargées (Fox et al., 2022), qui peuvent interagir avec l'ADNe présent dans la matrice, lui-même chargé négativement (Mulcahy et al., 2008). De plus, la membrane des bactéries est également négativement chargée (Chen and Cooper, 2002), ce qui permet aux bactéries situées dans les couches internes d'être protégées par celles en périphérie du biofilm.

Les biofilms limitent également la diffusion d'autres substances, telles que les nutriments ou l'oxygène (Høiby et al., 2010), créant ainsi une hétérogénéité des ressources qui engendre une hétérogénéité des métabolismes au sein du biofilm. Les bactéries situées à la surface ont généralement un accès privilégié à ces composés, tandis que celles situées dans les couches internes y ont un accès réduit (Høiby et al., 2010). Ainsi, certaines bactéries dans les couches internes peuvent présenter une croissance ralentie, et dans certains cas, entrer dans une phase de dormance, comme c'est le cas pour les cellules persistantes et les cellules viables mais non cultivables (Uruén et al., 2020). Leur activité métabolique étant réduite, les cibles de certains antimicrobiens ne seront plus disponibles, limitant ainsi leur efficacité (Wood et al., 2013). Les bactéries en biofilms peuvent ainsi généralement survivre à des concentrations qui sont plusieurs milliers de fois supérieures à celles nécessaires à éliminer les mêmes niveaux de populations planctoniques (Trubenová et al., 2022). De ce fait, les biofilms posent des problèmes sanitaires importants, car ils peuvent être à l'origine de la persistance de souches pathogènes sur les chaînes de production, malgré les opérations de nettoyage et désinfection (Bridier et al., 2015).

Cette hétérogénéité phénotypique au sein des biofilms, causée par des gradients chimiques de nutriments et de biocides, ainsi que par la réponse des bactéries à leur microenvironnement immédiat, pourrait également influencer le devenir évolutif des bactéries (Sadiq et al., 2017). D'une part, cette hétérogénéité est décrite comme un avantage adaptatif, offrant aux populations bactériennes une forme d'assurance face aux perturbations environnementales (Bódi et al., 2017). D'autre part, les biofilms pourraient favoriser l'apparition et la sélection de mutations génétiques (Conibear et al., 2009; Ryder et al., 2012). L'augmentation de la fréquence des mutations dans certaines conditions présentes dans les biofilms pourrait donc accroître la probabilité d'émergence de résistances et de résistances croisées.

Cependant, il est important de souligner que la majorité des données disponibles sur le développement de résistances croisées entre biocides et antibiotiques proviennent d'études sur des suspensions planctoniques. Or, comme cela a été exposé, la vie en biofilm influence profondément la manière dont les bactéries s'adaptent aux stress biocides, ce qui pourrait avoir un impact direct sur le développement de résistances croisées aux antibiotiques.

Dans ce contexte, l'objectif de cette thèse a été de répondre à plusieurs questions clés :

- Comment le mode de vie « biofilm » influe-t-il sur l'adaptation des bactéries aux biocides, et quel rôle joue-t-il dans l'émergence de résistances croisées ?
- Quels sont les déterminants génétiques et les mécanismes moléculaires impliqués dans ces résistances croisées ?
- Quelles variations phénotypiques sont observées chez les variants, et comment impactent-elles leur capacité de dissémination au sein de la chaîne alimentaire ?

Ces travaux contribueront à l'identification de marqueurs moléculaires et phénotypiques liés à l'adaptation aux biocides et au développement de résistances croisées. A terme, ceux-ci pourraient être utilisés pour développer des outils de surveillance dans la chaîne alimentaire.

2. Etude bibliographique

2.1. Escherichia coli, un modèle d'étude pertinent

Escherichia coli est à ce jour l'une des espèces bactériennes les mieux étudiées et caractérisées. Bacille à gram négatif appartenant à la famille des Enterobacteriaceae, cette espèce a été identifiée pour la première fois en 1885 par Theodore Escherich (Friedmann, 2014). Sa découverte ancienne, combinée à sa facilité de culture, ont fait de cette bactérie un modèle d'étude privilégié. Dans des conditions de cultures optimales, certaines souches d'*E. coli* peuvent se répliquer en moins de vingt minutes, ce qui facilite les études expérimentales et renforce son statut d'organisme modèle. Souvent pionnière dans la recherche, elle a notamment été l'une des premières espèces bactériennes à être intégralement séquencée, avec le génome de la souche de référence K-12 publié en 1997, deux ans après le séquençage du premier génome bactérien (Koonin, 1997). La richesse de la littérature existante sur cette espèce, notamment dans des expériences d'évolutions (McDonald, 2019; Lenski, 2023), offre ainsi de nombreux points de comparaison, et sa facilité de manipulation en laboratoire est renforcée par l'existence de nombreux outils, en, particulier en biologie moléculaire.
E. coli représente également un excellent modèle d'étude dans le cadre de cette thèse et du projet ANR BAoBAb. Son ubiquité en fait un modèle représentatif des bactéries présentes aussi bien dans les chaînes de production alimentaires que dans les isolats cliniques, en parfaite adéquation avec le concept « *One Health* ». De plus, la capacité de certaines souches à former des biofilms structurés justifie son utilisation pour étudier l'effet de substances actives représentatives des solutions désinfectantes employées dans les chaînes de production. Enfin, les problèmes de résistance aux antimicrobiens posés par *E. coli*, membre du groupe des ESKAPEE (Partridge et al., 2018), renforcent la pertinence de ce modèle pour étudier l'évolution de la résistance aux antibiotiques.

2.1.1. Diversité intra-espèce chez E. coli

L'une des particularités d'*E. coli* réside dans la grande diversité au sein de l'espèce (Jang et al., 2017). Ubiquitaire, cette espèce peut être retrouvée dans une grande variétés d'environnements (Jang et al., 2017). La grande plasticité de son génome entraîne des disparités significatives au sein de l'espèce, certaines souches partageant peu de similarités génotypiques (Denamur et al., 2021), tout comme des différences phénotypiques marquées, avec des profils très distincts. *E. coli* est notamment souvent un organisme commensal présent dans le tractus gastro-intestinal humain, mais certaines souches possèdent un potentiel pathogène, provoquant diverses infections selon les souches (Denamur et al., 2021). Ces infections peuvent avoir lieu aussi bien au niveau de la paroi intestinale (Nguyen and Sperandio, 2012) qu'au niveau du tractus urinaire (Figure 2) (Terlizzi et al., 2017). Par exemple, le sérotype O157:H7, connu pour sa virulence, est responsable de 64% des hospitalisations liées à *E. coli* en Europe entre 2002 et 2006 (Brugère et al., 2012). Ce sérotype appartient aux *E. coli* entérohémorragiques (EHEC), un sous-groupe des *E. coli* productrices de la shigatoxine (STEC).

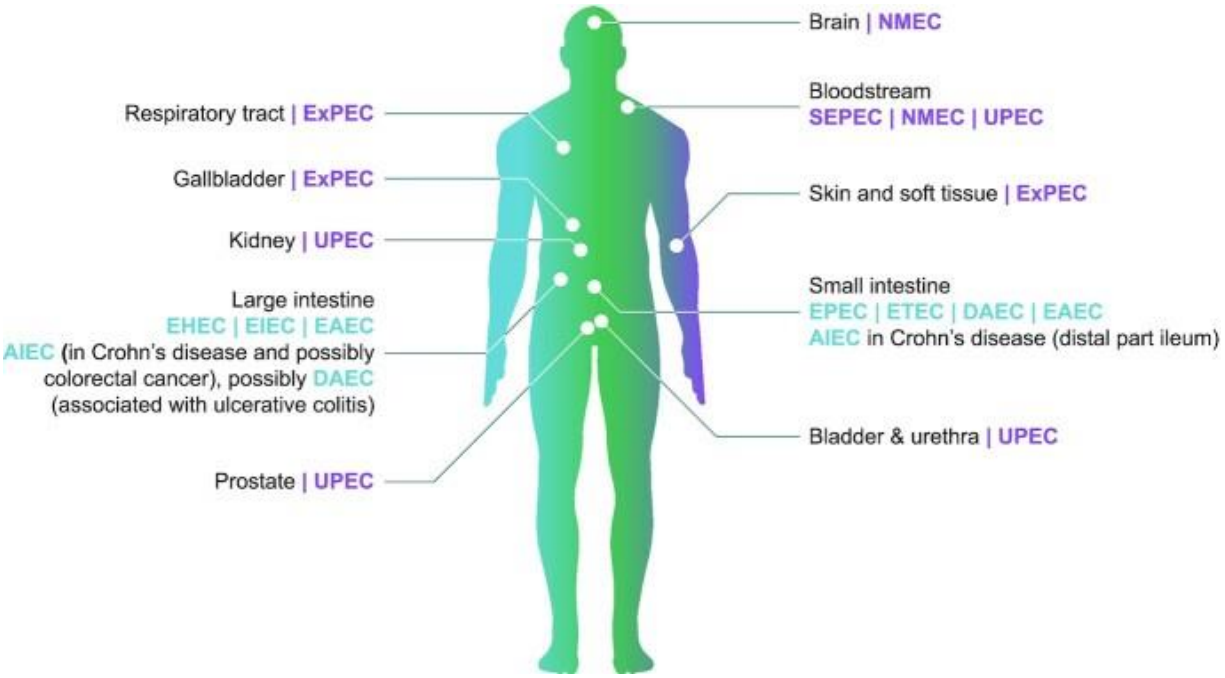

Figure 2 : Représentation des différents pathotypes de E. coli et des différentes cibles cellulaires sujettes à des infections. Ceux-ci se divisent en deux groupes, InPec (Intestinal pathogenic E. coli) et ExPec (Extraintestinal pathogenic E. coli). Dans le premier groupe on retrouve les EPEC (Enteropathogenic E. coli), les ETEC (Enterotoxigenic E. coli), les EIEC (Enteroinvasive E. coli), les EAEC (Enteroaggragative E. coli), les DAEC (Diffuse adhering E. coli), les AIEC (Adherent-invasive E. coli) et donc les EHEC (Enterohemorrhagic E. coli) dans lesquelles on retrouve les STEC et les VTEC (Verocytotoxin-producing E. coli). Chacun de ces pathotypes possède ses propres gènes de virulence spécifiques, qui définissent leurs modes d'infection au sein du tractus gastro-intestinal. Les pathotypes du second groupe sont principalement classées par l'organe qu'ils infectent. On y retrouve toutes les infections non-intestinales, avec les UPEC (Uropathogenic E. coli), les NMEC (Neonatal meningitis E. coli) et MAEC (meningitis-associated E. coli), les APEC (Avian pathogenic E. coli), les SEPEC (Sepsis-associated E. coli) et d'autres Expec n'appartenant à aucune des catégories précédemment citées. (Issu de (Geurtsen et al., 2022))

2.1.2. E. coli dans les chaînes de production alimentaire

Etant donnée sa prévalence chez les humains et les animaux, *E. coli* est fréquemment rencontrée sur les chaînes de production alimentaires. La surveillance des souches pathogènes, notamment dans les filières bovines (Dong et al., 2020), porcines (Colello et al., 2016), avicoles (Alonso et al., 2012) et laitières (Farrokh et al., 2013), est cruciale pour prévenir leur propagation. En France, les toxi-infections alimentaires provoquent chaque année entre 232 et 358 décès ainsi que jusqu'a 21200 hospitalisations, engendrant un coût économique considérable (Van Cauteren et al., 2018). Bien que *E. coli* ne soit pas l'agent pathogène le plus fréquent (Figure 3), il reste essentiel de limiter les risques associés. Entre 2008 et 2013, les estimations font état, en France, de 8200 à 38600 infections symptomatiques, 317 à 2238 hospitalisations et 2 à 12 décès annuels, liés à des infections alimentaires par des souches STEC (Figure 3) (Van Cauteren et al., 2018). Ces cas sont parfois très médiatisés, comme l'a montré le scandale sanitaire qui a eu lieu en France, en 2022, où la contamination de pizzas surgelées de la marque Buitoni par *E. coli* a provoqué des

dizaines d'hospitalisations, principalement des enfants, dont deux sont décédés (Santé Publique France, 2022).
Si les bactéries proviennent souvent directement des pièces de viande, la manipulation de ces dernières peut entraîner la propagation des bactéries sur les surfaces présentes en industrie, augmentant ainsi les risques de contamination des lots suivants. *E. coli*, notamment les souches STEC, a déjà été isolée sur des surfaces industrielles agro-alimentaires (Aslam et al., 2004; Rivera-Betancourt et al., 2004; Vogeleer et al., 2014). Ces souches sont capables d'adhérer aux surfaces et de former des biofilms, renforçant ainsi leur persistance dans l'environnement (Dourou et al., 2011; Nesse et al., 2014).

A

Estimations (5%, 50% et 95% de l'estimation finale) du nombre annuel moyen de cas symptomatiques, par agent pathogène, France métropolitaine, 2008-2013

Agent pathogène	Toute transmission*			Proportion de transmission alimentaire	Transmission alimentaire*			Proportion du nombre total de cas**
	5%	50%	95%		5%	50%	95%	
Bacillus cereus	32 841	69 468	164 316	100%	32 841	69 468	164 316	4,6
Campylobacter spp.	272 669	492 705	1 078 543	73-86%	215 216	392 177	862 747	26,1
Clostridium botulinum	11	21	41	100%	11	21	41	0,0
Clostridium perfringens	47 922	119 632	332 244	100%	47 922	119 632	332 244	8,0
STEC	11 523	24 710	52 295	59-87%	8 206	17 927	38 668	1,2
Listeria monocytogenes	328	402	497	100%	328	402	497	0,0
Salmonella spp.	108 805	198 047	410 817	91-95%	102 041	183 002	387 599	12,2
Shigella spp.	6 206	11 082	23 143	23-40%	1 837	3 449	7 555	0,2
Staphylococcus aureus	21 058	73 021	271 056	100%	21 058	73 021	271 056	4,9
Yersinia spp.	12 175	23 674	54 388	80-100%	10 799	21 330	49 477	1,4

B

Estimations (5%, 50% et 95% de l'estimation finale) du nombre annuel moyen de cas d'hospitalisations, par agent pathogène, France métropolitaine, 2008-2013

Agent pathogène	Toute transmission*			Proportion de transmission alimentaire	Transmission alimentaire*			Pourcentage du nombre total de cas hospitalisés**
	5%	50%	95%		5%	50%	95%	
Bacillus cereus	216	457	1 080	100%	216	457	1 080	2,6
Campylobacter spp.	5 138	6 943	9 510	73-86%	4 039	5 524	7 595	31,4
Clostridium botulinum	10	19	37	100%	10	19	37	0,1
Clostridium perfringens	317	811	2 238	100%	317	811	2 238	4,6
STEC	199	514	1 259	59-87%	143	372	928	2,1
Listeria monocytogenes	258	310	375	100%	258	310	375	1,8
Salmonella spp.	3 927	4 415	4 983	91-95%	3 644	4 106	4 632	23,3
Shigella spp.	204	248	305	23-40%	56	78	104	0,4
Staphylococcus aureus	141	486	1 827	100%	141	486	1 827	2,8
Yersinia spp.	180	222	278	80-100%	158	200	255	1,1

C

Estimations (5%, 50% et 95% de l'estimation finale) du nombre annuel moyen de cas décédés, par agent pathogène, France métropolitaine, 2008-2013

Agent pathogène	Toute transmission*			Proportion de transmission alimentaire	Transmission alimentaire*			Pourcentage du nombre total de cas décédés**
	5%	50%	95%		5%	50%	95%	
Bacillus cereus	1	1	3	100%	1	1	3	0,4
Campylobacter spp.	33	52	82	73-86%	26	41	65	16,0
Clostridium botulinum	0	0	4	100%	0	0	4	0,1
Clostridium perfringens	1	2	6	100%	1	2	6	0,8
STEC	2	6	16	59-87%	2	4	12	1,6
Listeria monocytogenes	47	65	90	100%	47	65	90	25,4
Salmonella spp.	62	72	84	91-95%	57	67	78	26,2
Shigella spp.	0	1	4	23-40%	0	0	1	0,1
Staphylococcus aureus	0	1	4	100%	0	1	4	0,5
Yersinia spp.	1	10	108	80-100%	1	9	96	3,5

Figure 3 : Estimation du nombre annuel moyen d'infections symptomatiques (A), d'hospitalisations (B) et de décès (C) liés à des infections par des pathogènes bactériens alimentaires entre 2008 et 2013. (Adapté de (Van Cauteren et al., 2018))

2.1.3. Les biofilms chez E. coli

Les biofilms d'*E. coli* ont été largement caractérisés, ce qui a permis de mieux comprendre les différentes étapes de leur formation et la composition de leur matrice extracellulaire (Figure 4). L'adhésion initiale aux surfaces est médiée par divers gènes, notamment ceux de l'opéron *fimAICDFGH*, impliqués dans la formation de fimbriae de type 1, ainsi que par les opérons *csgBA* et *csgDEFG*, responsables de la production de fibres amyloïdes appelées curli. D'autres facteurs, tels que les pili conjugatifs, codés par des gènes que l'on peut retrouver sur les plasmides, participent également à ce processus (Beloin et al., 2008). Ces décorations de surface permettent l'adhésion à des substrats biotiques et abiotiques, tout en contribuant à la structuration des biofilms. Cette organisation spatiale est renforcée par des facteurs agrégatifs comme l'auto-transporteur Ag43, participant à l'adhésion entre les bactéries (Beloin et al., 2008).
Comme de nombreuses autres espèces bactériennes, *E. coli* produit plusieurs exopolysaccharides, essentiels à la matrice du biofilm, notamment le β-1,6-*N*-acetylglucosamine (PNAG), codé par l'opéron *pgaABCD*, et la cellulose, codée par les opérons *bcsABZC* et *bcsEFG*, qui assurent la formation d'un biofilm dense et rigide (Sharma et al., 2016). Le PNAG joue un rôle crucial lors des phases initiales du biofilm en facilitant également la fixation aux surfaces et entre les cellules (Sharma et al., 2016). L'acide colanique, codé par l'opéron *rcsABCDF* est un autre polysaccharide, qui enrobe généralement les cellules bactériennes et les protège de divers stress environnementaux (Sharma et al., 2016). De plus, d'autres éléments polysaccharidiques présents à la surface des bactéries, tels que le lipopolysaccharide ou la capsule, sont également essentiels à l'adhésion, l'agrégation et la structuration du biofilm (Beloin et al., 2008).
Parmi les autres composés présents dans la matrice du biofilm de *E. coli*, l'ADNe, libéré notamment par la lyse bactérienne, joue un rôle clé dans le maintien et l'intégrité de la structure du biofilm (Hufnagel et al., 2015) (Okshevsky et al., 2015). La charge négative de l'ADNe permet également la capture de certaines molécules antimicrobiennes chargées positivement (Laverty et al., 2011; Charron et al., 2023a).
La formation de biofilms et la synthèse des différents composés de la matrice sont des processus finement régulés, impliquant divers mécanismes. En réponse aux stimuli environnementaux, des régulateurs globaux comme *rpoS* et H-NS, ainsi que des systèmes à deux composants, comme CpxA/CpxR et EnvZ/OmpR, contrôlent la formation de biofilms (Beloin et al., 2008). Ces régulateurs réagissent notamment aux variations de pH, d'oxygène, de nutriments ou encore de température (Ballén et al., 2022).
La communication entre bactéries, médiée par des systèmes de quorum sensing, joue également un rôle clé dans la formation de biofilms. Chez *E. coli*, la molécule AI-2, synthétisée par LuxS, module la production de biofilms en fonction de sa concentration dans le milieu (Sharma et al., 2016).
Au sein de la cellule, la concentration en seconds messagers tels que le c-di-GMP ou le (p)ppGpp est modulée en réponse aux différents stimuli, qui vont réguler l'activité de certains activateurs et répresseurs de la transcription des gènes impliqués dans la formation des biofilms. Certains composants sont également régulés par des mécanismes de variation de phase, comme les fimbriae de type I et l'Ag43. Les gènes *fimA* (pour les fimbriae) et *flu* (pour l'Ag43) sont généralement en phase OFF. En réponse à certain stimuli respectivement, une inversion dans l'ADN et une méthylation permettent à ces deux gènes de passer en phase ON et d'être transcrits (Beloin et al., 2008). Les fimbriae étant principalement impliqués dans l'adhésion initiale et l'Ag43 principalement dans l'agrégation entre les bactéries suivant la phase initiale, ces derniers ne sont pas activés simultanément. Il a été démontré que ces deux

processus sont liés, la surexpression des fimbriae de type I pouvant entraîner la répression de l'Ag43 (Beloin et al., 2008).
Ainsi, la formation de biofilms par *E. coli* est complexe et pose de nombreux défis, tant dans les contextes cliniques, où ces biofilms peuvent adhérer sur les cellules humaines (Beloin et al., 2008), que dans les environnements industriels où leur élimination par des biocides peut s'avérer difficile (Charron et al., 2023a). Une partie détaillée sur les différents facteurs propres aux biofilms qui permettent la survie des bactéries face aux biocides a fait l'objet d'une valorisation sous forme de revue, qui est présentée dans la partie 2.3.

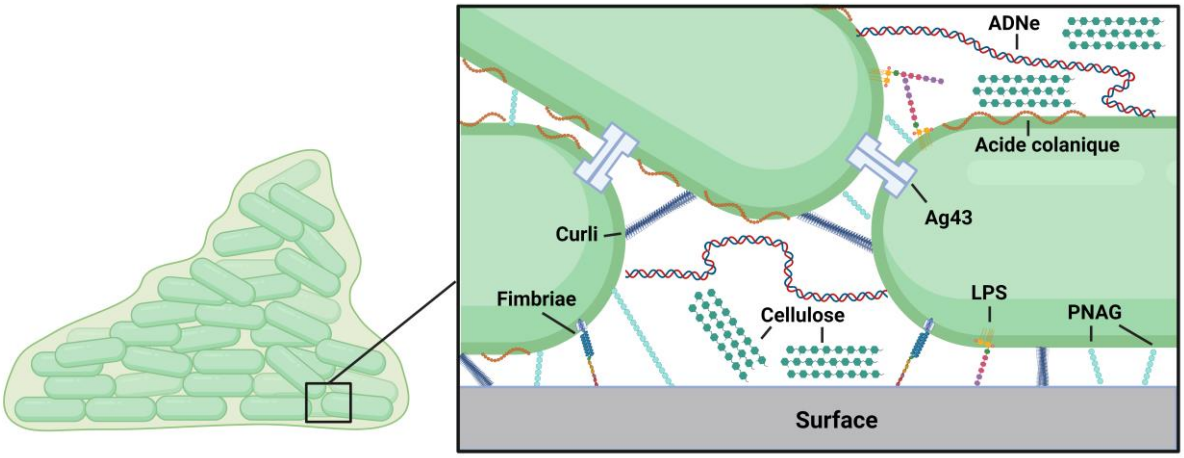

Figure 4 : Schéma illustrant les différents composés de la matrice de E. coli et les interactions auxquelles ces derniers participent. Figure créée avec Biorender.com.

2.1.4. La résistance aux antibiotiques chez E. coli

L'utilisation parfois abusive d'antibiotiques a favorisé la propagation de souches résistantes, les souches en contact direct avec ces antibiotiques étant les plus impactées. *E. coli*, présente aussi bien chez les humains que chez les animaux d'élevage, est donc particulièrement concernée par ce risque d'antibiorésistance (Tadesse et al., 2012). *E. coli* fait notamment partie du groupe ESKAPEE, qui regroupe plusieurs agents pathogènes présentant un risque élevé d'antibiorésistance : *Enterococcus faecium*, *Staphylococcus aureus*, *Klebsiella pneumoniae*, *Acinetobacter baumannii*, *Pseudomonas aeruginosa*, *Enterobacter* et *E. coli* (Partridge et al., 2018). L'OMS classe également *E. coli* parmi les pathogènes prioritaires pour la surveillance des résistances antimicrobiennes (World Health Organization, 2024). Pour cette raison, *E. coli* est une bactérie sentinelle, dont les isolats sont régulièrement prélevés pour mesurer leur résistance à plusieurs familles d'antibiotiques, permettant ainsi de suivre l'évolution des résistances au fil des années (Tadesse et al., 2012). Le LNR-RA du laboratoire de Fougères participe à ce plan de surveillance, en analysant les résistances d'échantillons de *E. coli* isolés sur des pièces de viande provenant d'animaux sains dans les chaînes de production alimentaire. Des résultats de ce plan de surveillance sont détaillés dans la figure 5. On y observe une certaine diversité entre les filières, les souches isolées dans des élevages avicoles possédant plus souvent des résistances que celles provenant d'élevages bovins et ovins. Des disparités existent également entre les familles d'antibiotiques, certaines résistances étant très prévalentes (plus de 50% dans les élevages avicoles), tandis que d'autres sont inexistantes. Ceci s'explique par la date de mise sur le marché de ces substances antibiotiques, ainsi que par le choix des antibiotiques utilisés dans ces filières (Poirel et al.,

2018). Dans de nombreuses familles, la baisse de la prévalence des résistances au fil des années témoigne également de la hausse des contrôles sur l'utilisation d'antibiotiques en médecine vétérinaire, visant à réguler et réduire leur usage (ANSES, 2023a). Le plan Ecoantibio a notamment permis de réduire l'exposition des animaux d'élevage aux antibiotiques en France de 52% entre 2011 et 2022 (ANSES, 2023b), et de plus de 90% pour les antibiotiques critiques pour la santé humaine, comme les céphalosporines de 3e et 4e génération (ANSES, 2023a).

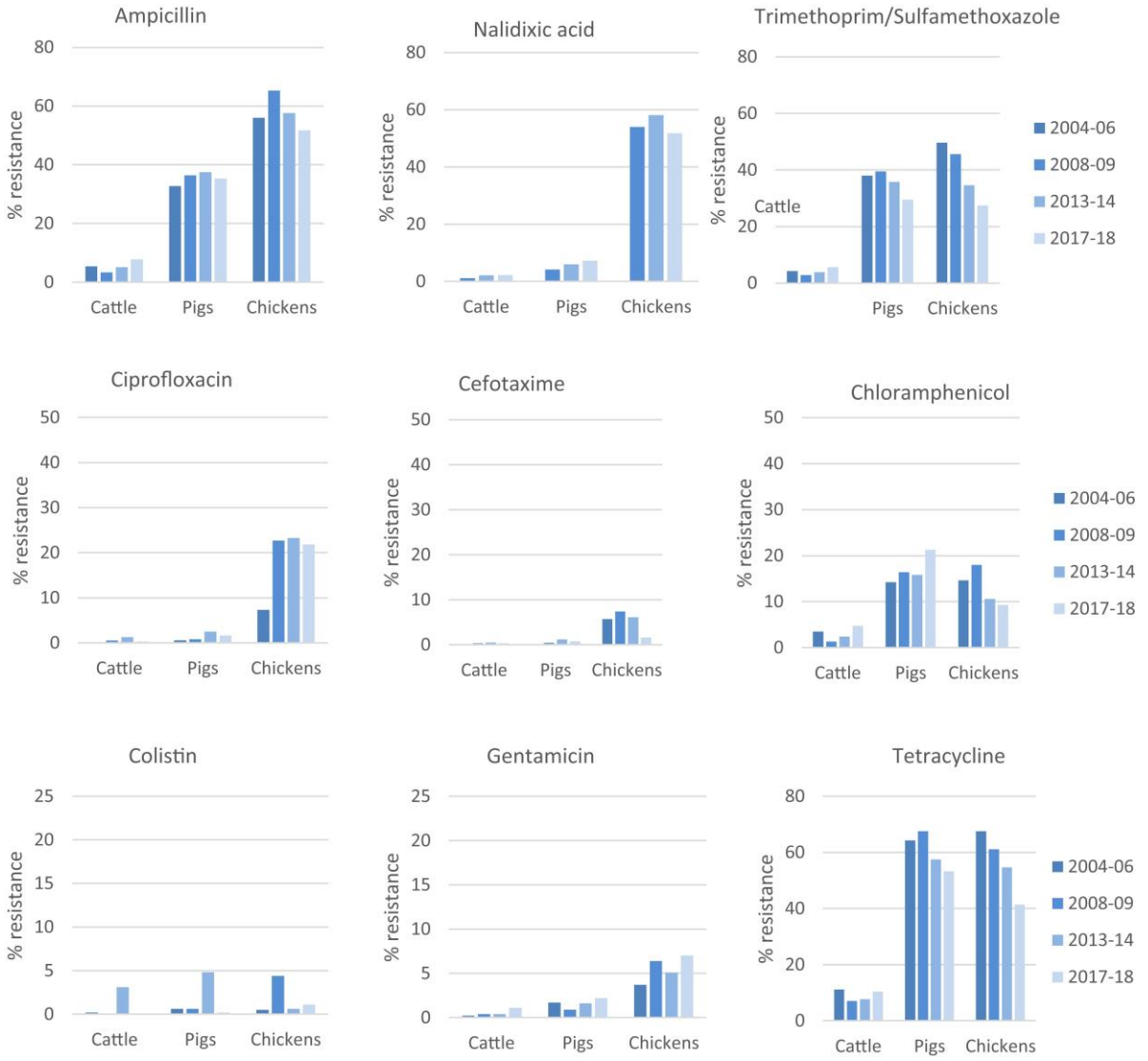

Figure 5 : Prévalence de souches de E. coli résistantes à différents antibiotiques, provenant d'animaux sains, en Europe, de 2004 à 2018. NB : Les résistances à la céfépime, les méropénèmes et la tigécycline ont également été analysées, mais aucune résistance n'ayant été découverte, elles ne sont pas présentes sur cette figure. (Issu de (De Jong et al., 2022))

2.2. Les biocides

2.2.1. Introduction

Les produits biocides sont des substances actives utilisées pour éliminer ou contrôler les organismes nuisibles, allant des microorganismes aux insectes et rongeurs (European Chemicals Agency, 2012). Ils sont classés en plusieurs catégories (European Chemicals Agency, 2012) :

- **Désinfectants :** substances ou mélanges destinés à détruire les microorganismes
- **Produits de protection :** produits de prévention appliqués sur des surfaces pour empêcher la fixation d'organismes, comme les produits de protection du bois ou les produits anti-biofilm
- **Produits de lutte contre les nuisibles :** produits utilisés contre des espèces non-microscopiques, comme les rongeurs (rodenticides), les oiseaux (avicides), les poissons (piscicides) ou les insectes (insecticides)
- **Autres produits biocides :** produits ne rentrant dans aucune autre catégorie tels que les peintures anti-salissure utilisées en milieu aquatique, pour protéger la coque des navires, ou les produits utilisés pour préserver des cadavres humains ou animaux dans le cadre d'embaumement et de taxidermie.

Cette thèse se concentre exclusivement sur les désinfectants. Le terme « biocide » utilisé se réfèrera donc uniquement à cette catégorie. Parmi les désinfectants, on distingue plusieurs sous-catégories en fonction du domaine d'application (European Chemicals Agency, 2012) :

- **Hygiène humaine :** produits utilisés pour désinfecter la peau ou le cuir chevelu
- **Désinfectants et produits algicides non destinés à l'application directe sur des êtres humains ou des animaux :** produits utilisés pour désinfecter tout type d'équipement qui n'est pas en contact avec des denrées alimentaires, tels que les produits de traitement des piscines, aquariums, air, eau, textile, etc
- **Hygiène vétérinaire :** produits utilisés pour désinfecter les surfaces associées à des environnements dans lesquels se trouvent des animaux, ainsi que des produits d'hygiène buccale ou des savons
- **Surfaces en contact avec les denrées alimentaires et les aliments pour animaux :** produits utilisés pour désinfecter tout type de matériel qui pourrait rentrer en contact avec des denrées alimentaires
- **Eau potable :** produits utilisés pour traiter l'eau potable consommée par les humains et les animaux

Les biocides peuvent également être classés en fonction de leur mode d'action et de leur structure moléculaire. Le tableau 1 regroupe les principales familles de biocides, leurs substances actives, leurs cibles au sein de la bactérie, ainsi que les secteurs industriels où ils sont utilisés :

Famille	Substances actives	Cibles et mode d'action	Filière
Ammoniums quaternaires	- Chlorure de benzalkonium - Chlorure de didecydimethylamonium	- Interaction avec les lipides et protéines membranaires - Déstructuration de la membrane cellulaire et modification de la perméabilité	- Viande/Charcuterie - Produits de la mer
Peroxydes	- Peroxyde d'hydrogène - Acide peracétique - Ozone	- Production de radicaux libres - Oxydation des lipides, protéines (groupements-SH) et acides nucléiques - Désorganisation des membranes	- Viande/Charcuterie - Laitière - Végétaux - Produits de la mer - Viticole
Halogénés	- Chlore - Hypochlorite de sodium - Dioxyde de chlore	- Halogénation des protéines, carbohydrates, lipides et acides nucléiques - Désorganisation de la membrane	- Viande/Charcuterie - Laitière - Végétaux - Produits de la mer - Viticole
Alcools	- Ethanol - Alcool isopropylique	- Perturbation de la membrane cellulaire par liaison aux phospholipides - Dénaturation des protéines - Inhibition de la synthèse des acides nucléiques et des protéines	- Viande/Charcuterie - Laitière
Aldéhydes	- Glutaraldéhyde - Formaldéhyde	- Réticulation des protéines - Inhibition de la synthèse des acides nucléiques et des protéines - Altération de la paroi cellulaire	- Viande/Charcuterie
Biguanides	- Chlorhexidine - Polyhexaméthylène biguanide	- Fuite des constituants cytoplasmiques par désorganisation de la bicouche lipidique - Précipitation des protéines et acides nucléiques	- Viande/Charcuterie - Produits de la mer
Triamines	- N-(3-aminopropyl)-N-dodecylpropane-1,3-diamine	- Déstructuration de la membrane cellulaire et modification de la perméabilité	- Viande/Charcuterie - Laitière - Produits de la mer

Tableau 1 : Familles de biocides leur cibles cellulaires et leurs modes d'actions (Adapté de (Bridier et al., 2021))

2.2.2. Procédures de nettoyage et désinfection

Les procédures de nettoyage et désinfection suivent un cheminement précis, étape par étape, ayant pour objectif d'augmenter au maximum l'efficacité du traitement (CRITT IAA, 2015) :

- **Pré-Nettoyage :** élimination des salissures visibles en utilisant de l'eau chaude et rangement de la zone à nettoyer.
- **Nettoyage :** utilisation de détergents pour éliminer les souillures visibles restantes, qui pourraient interférer avec le désinfectant. La matière organique peut notamment influer sur le pH, un facteur limitant pour de nombreux biocides. Il est donc important à cette étape de respecter les temps d'application du détergent pour améliorer son efficacité.
- **Rinçage intermédiaire :** élimination des souillures détachées durant l'étape de nettoyage ainsi que les traces de détergent, suivi d'un séchage pour éviter la dilution du désinfectant à l'étape suivante

- **Désinfection :** application du biocide pour éliminer les microorganismes. Il est important de respecter le temps d'application recommandé du fournisseur du biocide.
- **Rinçage final :** élimination des résidus de biocides, qui pourraient diriger l'évolution de futures bactéries. Certains de ces produits étant toxiques, ce rinçage permet également d'éviter qu'ils ne se retrouvent dans l'alimentation.
- **Séchage :** cette dernière étape sert à éviter de futures multiplications de bactéries et à préserver les surfaces de la corrosion.

Chacune de ces étapes est adaptée au sein de l'entreprise, dans un plan de nettoyage précis, afin de correspondre au mieux aux machineries qui y sont présentes, ainsi qu'aux aliments qui y sont manipulés (CRITT IAA, 2015). De nombreux tests simples existent en guise de contrôle pour évaluer l'efficacité de chaque étape. On retrouve par exemple des tests de détection des protéines et des sucres pour l'étape de nettoyage, des boîtes de contact ou petrifilms pour les contrôles de la désinfection et des tests de pH ou des tests spécifiques aux biocides pour l'étape de rinçage (CRITT IAA, 2015).

2.2.3. Facteurs limitants l'efficacité des biocides

Les réglementations en place concernant le nettoyage et la désinfection des chaînes de production sont strictes et doivent être scrupuleusement respectées. Cependant, la réduction en bactéries sur les surfaces n'est souvent que partielle (Luyckx et al., 2016), malgré l'utilisation de concentrations théoriquement léthales pour ces microorganismes. Plusieurs facteurs expliquent cette survie. Tout d'abord, les machineries présentes dans les industries sont souvent complexes, et certaines parties difficiles d'accès peuvent favoriser l'implantation de microorganismes. La matière organique non éliminée, due à des erreurs ou à un manque de temps alloué à ces procédures, peut avoir un impact significatif sur l'efficacité du biocide en réduisant l'exposition des bactéries ou en modifiant le pH local (Russell, 2003; Cerf et al., 2010). Les périodes de nettoyage et désinfection ont des durées importantes et sont considérées par les entreprises comme des pertes de productivité. Une désinfection incomplète permet l'établissement et le maintien de biofilms, augmentant la survie des bactéries lors des expositions futures aux biocides et favorisant la sélection de souches adaptées (Charron et al., 2023a). Ce phénomène augmente non seulement les risques de contamination pour les consommateurs, mais aussi celui de l'émergence de bactéries résistantes aux biocides, et possiblement de manière croisée à certains antibiotiques, (Aslam et al., 2021a).

2.2.4. Résistances aux biocides

Contrairement aux antibiotiques, les biocides peuvent être utilisés à de très fortes concentrations, car leur utilisation n'est pas limitée par la toxicité sur les humains (Charron et al., 2023a). Cette particularité leur confère une grande efficacité, notamment grâce à un effet multi-ciblé sur les cellules bactériennes (Gilbert and McBain, 2003; Maillard, 2018). Alors que les antibiotiques ont généralement une cible spécifique au sein de la cellule, réduisant ainsi les risques d'effets secondaires délétères sur les cellules humaines, ce n'est pas le cas des biocides. Ces derniers ont, pour la plupart, des effets concomitants sur la paroi, la membrane, les protéines ou encore les acides nucléiques (Donaghy et al., 2019). Cet effet multi-cibles dirige généralement l'évolution vers des adaptations bactériennes globales, et non spécifiques comme peuvent l'être les adaptations aux antibiotiques, pour lesquels on retrouve

souvent des mutations entraînant la modification de la cible de l'antibiotique (Poole, 2002). Parmi celles-ci on retrouve la mutation du gène *rpoB*, codant pour l'acide ribonucléique (ARN) polymérase, permettant la résistance à la rifampicine (Lambert, 2005), ou bien la mutation du gène *gyrA*, codant pour la gyrase de l'ADN, conférant une résistance aux fluoroquinolones (Lambert, 2005). Parmi les adaptations les plus connues aux biocides on retrouve notamment l'utilisation accrue de systèmes d'extrusions actifs tels que les pompes d'efflux, ou la réduction de l'abondance de transporteurs membranaires passifs, comme les porines, diminuant la perméabilité de la membrane externe des bactéries (Maillard, 2018). Ces modifications ayant cependant un effet général, il n'est pas rare qu'elles aient des effets croisés sur d'autres substances bactéricides. Ainsi, plusieurs résistances aux antibiotiques ont été observées sur des bactéries après adaptation à des stress biocides (Poole, 2002; Kampf, 2018; Charron et al., 2023a). Un tableau détaillé présentant les cibles génétiques qui ont déjà été associées à des résistances croisées entre biocides et antibiotiques, a fait l'objet d'une valorisation dans l'article présenté dans la partie 2.3. Bien que leur utilisation soit cruciale pour limiter la propagation des bactéries pathogènes dans les industries agroalimentaires, elle doit être rigoureusement encadrée pour prévenir l'apparition de résistances.

2.3. Article 1 : Les biofilms et leurs impacts sur les résistances aux biocides

Cette revue a été écrite dans le cadre d'une étude bibliographique visant à évaluer les différentes formes de tolérance intrinsèques au mode de vie biofilm conférant aux bactéries une survie accrue aux biocides. Elle se divise en deux parties. La première partie discute les aspects purement liés au biofilm, séparés en trois axes : la façon dont la matrice du biofilm protège les bactéries, la façon dont les modifications physiologiques au sein du biofilm impactent la survie aux biocides et enfin comment le mode de vie biofilm peut également favoriser l'apparition de résistances acquises dans le génome. La seconde partie se concentre sur les effets secondaires potentiels qui suivent l'émergence de résistances aux biocides. Cette partie est également divisée en trois axes, abordant les risques pour l'humain d'une adaptation aux biocides avec, tout d'abord, une partie sur les capacités de colonisation et dissémination des variants, puis une partie sur l'émergence de résistances croisées aux antibiotiques et enfin les potentiels effets sur la virulence des souches. Cette revue a été valorisée dans le journal « *Microbiology* » en juin 2023.

« Biofilms as protective cocoons against biocides: from bacterial adaptation to One Health issues », *Microbiology*, 2023

Raphaël Charron, Marine Boulanger, Romain Briandet, Arnaud Bridier

MICROBIOLOGY

REVIEW
Charron *et al.*, *Microbiology* 2023;169:001340
DOI 10.1099/mic.0.001340

MICROBIOLOGY SOCIETY
OPEN ACCESS

Biofilms as protective cocoons against biocides: from bacterial adaptation to One Health issues

Raphaël Charron[1,2,*], Marine Boulanger[1], Romain Briandet[2] and Arnaud Bridier[1,*]

Abstract

Bacteria in the food chain mostly live in communities associated with surfaces known as biofilms, which confer specific survival and adaptive abilities. In such communities, the bacteria mostly exhibit higher tolerance to external stress, and their recurrent exposure along the food chain to biocides used during cleaning and disinfection procedures raises concern about the adaptation routes they develop, both at single-cell and communal levels. In recent years, an increasing number of research subjects have focused on understanding the specific features of biofilms that enable bacterial populations to adapt to biocide exposure within a 'protective cocoon'. The first part of this review concentrates on the diversity of adaptive strategies, including structural modulation of these biofilms, physiological response or the acquisition of genetic resistance. The second part discusses the possible side effects of biofilm adaptation to biocides on antimicrobial cross-resistance, virulence and colonization features from a One Health perspective.

INTRODUCTION

The increase in antimicrobial resistance over the past 60 years has become a major public health concern and has raised questions about the drivers of this emergence of resistant bacteria. Many review papers have focused on antibiotics used to treat bacterial infections and the link between antibiotic use, resistance selection and underlying mechanisms in many areas [1–3]. However, other substances — such as biocides — are used daily to control bacterial contamination of surfaces in diverse environments and to prevent the transmission of pathogens to humans or animals. Unlike antibiotics, which often have a specific mode of action based on one or only few bacterial targets, chemical biocides mostly act on multiple targets [4]. Through a variety of complex mechanisms, resistance to most of the biocides in use has already been documented [5]. Because of the large-scale and repeated use of biocides, resistant bacteria can quickly propagate and colonize new environments, thereby accelerating the spread of resistant clones. In 2014, Zou *et al.* documented the prevalence of several quaternary ammonium compound (QAC) resistance genes in *Escherichia coli* isolated from retail meat and identified the major prevalence of five genes, reaching 100% for *ydgE/F* genes [6]. However, it is important to clarify that the term biocide resistance is still confusing as it encompasses various definitions, illustrating a high diversity of practical situations in terms of levels of susceptibility loss [5]. If the term antibiotic resistance is usually based on the clinical concentration used, biocides are in general used at high concentrations where the vast majority of bacteria are eliminated. Some resistances are in fact just describing a decrease of susceptibility for the bacteria, which would not survive efficient treatment, at an in-use concentration. A consensus in the scientific community to define which threshold could be used to differentiate between a susceptible and a resistant strain is still required. However, susceptibility reductions could still confer an advantage to the cells with inaccurate application of the treatment, which would ultimately increase the risks of human infections and should thus be considered as seriously as the evolution of antibiotic resistances. In this context, resistance to biocides also needs to be taken seriously because of the mechanisms that potentially confer cross-resistance among the two families of molecules, i.e. biocides and antibiotics. Indeed, although both this phenomenon and its importance in the development of antimicrobial resistance need to be fully understood, several studies have demonstrated a relationship between

Received 08 February 2023; Accepted 09 May 2023; Published 02 June 2023
Author affiliations: [1]Antibiotics, Biocides, Residues and Resistance Unit, Fougères Laboratory, French Agency for Food, Environmental and Occupational Health & Safety (ANSES), 35300 Fougères, France; [2]Université Paris-Saclay, INRAE, AgroParisTech, Micalis Institute, 78350, Jouy-en-Josas, France.
***Correspondence:** Raphaël Charron, raphael.charron@inrae.fr; Arnaud Bridier, arnaud.bridier@anses.fr
Keywords: antimicrobial resistance; bacterial adaptation; biocides; biofilm; food chain; One Health.
Abbreviations: BAC, benzalkonium chloride; CSP, competence-stimulating peptide; DDAC, didecyldimethylammonium chloride; ECM, extracellular matrix; eDNA, extracellular DNA; EPS, extracellular polymeric substance; HGT, horizontal gene transfer; MFS, major superfacilitator superfamily; PAA, peracetic acid; PDH, pyruvate dehydrogenase; PHMB, polyhexamethylene biguanide; QAC, quaternary ammonium compound; QS, quorum sensing; RND, resistance–nodulation–cell division; ROS, reactive oxygen species; SMR, small multidrug resistance; VBNC, viable but non-culturable.

biocide exposure and antibiotic resistance selection [7–9]. For example, multidrug efflux systems [10–14], cell wall permeability modifications [12, 13] or alterations in metabolic cascades [15] have all been associated with bacterial resistance to both antibiotics and biocides. It is thus of prime importance to understand the evolution and adaptation of bacteria to biocide actions so as to unravel possible side effects on global resistance to antimicrobials (including antibiotics). Studies on other possible impacts of biocides on dissemination of antibacterial resistance, colonization of new environments and bacterial virulence also need to be taken into account when identifying the One Health effects of the use of biocides.

In their natural environments, most microorganisms live in spatially organized communities called biofilms, which are associated with surfaces [16]. In these biostructures, microbial cells are embedded in self-produced extracellular polymeric substances (EPSs). This matrix is typically composed of water and a mixture of polysaccharides, DNA, proteins and lipids [17]. This organic slime confers broad protection to the bacteria against environmental stresses such as dehydration or exposure to antimicrobial compounds [18–20]. Molecular diffusion/reaction limitations participate in biofilm resistance because gradients of nutrients and oxygen are induced in the 3D structure. As a consequence, biofilm phenotypes tend to be highly heterogeneous compared with planktonic populations, since different bacterial subpopulations adapt to their local microenvironments [21]. While bacteria living in the external layers grow at a normal speed, those in the inner layers are often subject to the activation of stress responses triggered by local nutrient depletion, leading to the appearance of particular subpopulations such as persisters or viable but non-culturable (VBNC) cells [22]. This heterogeneity can also influence bacterial survival, as some of these populations become highly tolerant or even resistant to curative treatments [23].

The recurrent exposure of biofilms to biocides in multiple environments has led us to explore in this review the adaptation routes of bacteria at cellular and populational scales to understand how biofilms can drive resistance. The second part of this paper explores, from a One Health viewpoint, the possible side effects that adaptation to biocides could have in newly resistant subpopulations in terms of antimicrobial cross-resistance, virulence and colonization features.

STRUCTURAL MODULATIONS OF BIOFILMS IN RESPONSE TO BIOCIDES

Biofilms are dynamic structures whose shapes and sizes are driven by the bacterial responses to environmental conditions and stresses. Bacteria can adapt to changing conditions through regulation of matrix component production, biofilm spatial organization, cannibalism or vascularization [24]. In this part, we will focus on the biofilm's structural plasticity as a response to biocide exposure, especially through the modulation of extracellular matrix composition and the bacteria's collective behaviour (Fig. 1) .

Intrinsic features of the extracellular matrix

The structural integrity of a biofilm is maintained through an extracellular matrix (ECM) produced by bacteria during biofilm maturation. Its composition can differ regarding the species embedded in the biofilm, local stresses or nutrient availability. It can be composed of water, polysaccharides, proteins, lipids, surfactants, glycolipids, extracellular DNA (eDNA), membrane vesicles and ions, all in various quantities. However, polysaccharides, proteins and eDNA are the three main components found for many bacteria [17, 25]. If bacteria are considered bricks, then ECM is the cement that provides mechanical biofilm resistance and can mitigate biocide effects within the 3D structure [17, 26].

Spatiotemporal patterns of inactivation in the biofilm architecture are highly biocide- and strain-specific, as demonstrated by time-lapse confocal laser scanning microscopy approaches [27–29]. Penetration of the 3D biofilm structure by biocides depends on interactions between the biocide molecules and ECM components, and can be slowed through the sorption of positive/negative charges or hydrophobic interactions. For instance, it takes about 25 min for glutaraldehyde to diffuse inside a *Staphylococcus epidermidis* biofilm, whereas its antimicrobial action in the absence of sorption reactions is estimated to be 24 s [27]. Sometimes, antimicrobial substances cannot even penetrate the biofilm to reach their biotargets, bacteria. For example, a synergistic combination of the biochemical nature of the ECM and biofilm roughness and topography has been shown to confer non-wetting properties to *Bacillus subtilis* biofilm surfaces [30]. It can be viewed as an impermeable coat that prevents antimicrobial actions, as biocides are not able to fully penetrate the biofilm [30]. Kobayashi's team indicated that the amphiphilic protein BslA could be partially responsible for the surface repellency of *B. subtilis* biofilms by forming a protective monolayer at the biofilm's interface with air [26].

Upon exposure to a biocide, the structural organization of a biofilm can be modified directly as a consequence of biocide action or through the defensive adaptive responses of bacteria. The main mechanisms involved in such modulations are described below.

Modulations of extracellular matrix composition

As mentioned above, the ECM is composed of different macro- and micro-molecules according to various conditions, including which strains are embedded in the biofilm and environmental fluctuations. In response to biocide exposure, it is also common to observe an increase in biofilm production, characterized by an increase in the ECM that acts as a protective shield for bacteria, which are thus exposed to sublethal biocide concentrations, allowing their survival. Modulation of the biofilm density has already

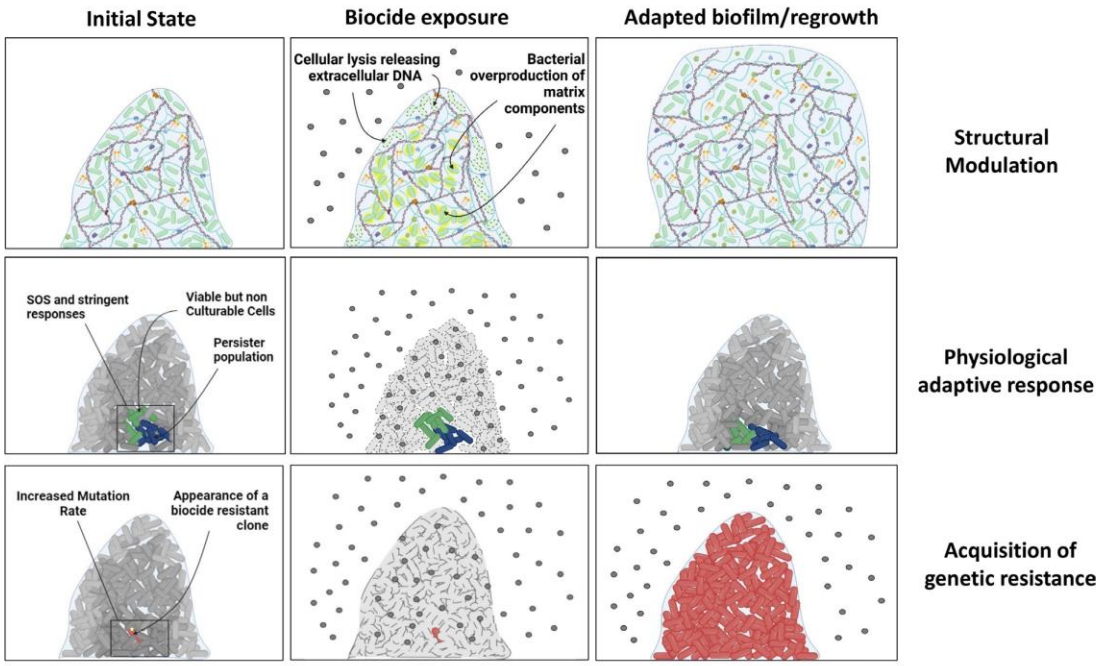

Fig. 1. Structural modulation: exposure to biocides induces stress responses, which lead to upregulation of matrix component production. Cells lysed by the biocide release their eDNA into the biofilm, thus reinforcing it. Physiological adaptive response: nutrients and oxygen gradients lead to specific physiological states, such as persister cells or VBNC cells. These cells can tolerate temporary exposure to biocides, while the rest of the biofilm will be eliminated. If the exposure to biocides stops, the surviving cells will again become active and regrow a new biofilm, with new persister populations in the inner layers. Acquisition of genetic resistance: stressful conditions in the inner layers can increase the mutation rate, which can randomly lead to the appearance of a biocide-resistant clone. If this clone is then exposed to a biocide, all the other cells will be eliminated while this cell will survive and develop a new biofilm, independently of the presence or absence of the biocide.

been associated with increased survival against different biocide families [31]. After being stressed by sublethal doses of ClO_2, the quantity of matrix has been shown to increase in biofilm formed by *B. subtilis* [32]. As another example, the crystal violet assay, commonly used to graduate biofilm formation, has shown that uropathogenic *E. coli* displayed a significant increase in biofilm production, especially after exposure to triclosan and benzalkonium chloride (BAC) [33]. It has also been shown that a previous adaptation by *E. coli* to biocides sodium nitrite and sodium hypochlorite could enhance biofilm formation with or without further exposure to a biocide [34]. The production of EPSs such as polysaccharides is one of the most frequent responses to biocide exposure. A large number of biocides have been shown to induce EPS production in different bacterial species through the activation of different pathways and regulators [32, 35, 36]. Polysaccharides are not the only component activitated during biocide exposure, as the overproduction of amyloid fibres has also been associated with the exposure of biofilms to different classes of biocides, e.g. the production of Curli proteins in *E. coli* biofilm exposed to various biocide substances, including glutaraldehyde, isopropanol, chlorophene and chlorhexidine [35].

Role of extracellular DNA in interfering with biocide action

eDNA is another major component of the ECM released through cell lysis, membrane vesicles or dedicated secretion systems [37]. It can remain in the environment for some time until degradation or effective removal by mechanical and chemical action. It is of real importance for bacteria, as it can be a source of resistance genes through horizontal gene transfer as described further below. Its involvement in biofilm adhesion to surfaces and its ability to interact with the bacterial cell wall has already been demonstrated by its anionic properties that allow binding to positively charged molecules, proteins or polysaccharides [38]. Jennings *et al*. showed that in the *Pseudomonas aeruginosa* matrix, the presence of partially acetylated GalNAc and GlcNAc on a cationic exopolysaccharide Pel allows cross-links with eDNA, which is therefore partially responsible for the integrity of the biofilm's structure [39]. This negative charge could also be involved in the capture of cationic biocides, which could limit penetration through to the deepest biofilm layers and decrease antimicrobial efficiency. Such a process has already been observed with cationic antibiotics [40, 41] and antimicrobial peptides [25], and is likely to occur with positively charged biocides such as QACs. Moreover, the amount of eDNA produced, which is directly linked to its

release in the biofilm ECM, can be promoted with the use of biocides. In *P. aeruginosa* and *Staphylococcus aureus*, Moshynets *et al.* [42] showed an increase in eDNA release after exposure to alcohols, hydrogen peroxide (H_2O_2) and QACs resulting from exposed cell lysis.

Production of protective exoenzymes

Inactivation by enzymes has not yet been fully described in the literature but exoenzymes synthesized and released into the ECM may be another strategy used by biofilms to combat oxidative biocide exposure (e.g. hypochlorite solutions). Oxidoreductase enzymes such as catalase and superoxide dismutase can be expressed and released into the exopolymeric matrix by certain bacterial species entrapped in the biofilm. They can be exploited by enzyme non-producing bacteria, thereby behaving as public goods [43]. Their presence in the ECM can be stimulated after exposure to oxidative biocides. Exposure to 5 mM sodium hypochlorite (NaOCl) or 50 µM H_2O_2 led to a higher catalase activity in *S. epidermidis* biofilm compared with their planktonic homologues [44]. It has also been demonstrated that penetration of *P. aeruginosa* catalase-deficient (*katA* gene knock-out) biofilms by the active form of H_2O_2 was facilitated when compared with the wild-type isogenic strain, suggesting that catalase activity plays a protective role [45]. Disruption of the *katA* gene has also been shown to affect *Proteus mirabilis* biofilm sensitivity to H_2O_2 through the modification of matrix composition, such as a reduction in carbohydrate content [46]. Similarly, superoxide dismutases have been shown to protect bacteria from the action of H_2O_2. In *E. coli*, the *sodC* chromosomal gene encoding superoxide dismutase confers higher survival rates against H_2O_2, while also being associated with increased biofilm formation [47].

Quorum sensing as a cooperative communication system

Bacterial cooperation plays a key role in biofilm adaptation to biocide exposure. This cooperation can be triggered by inducing quorum-sensing (QS) mechanisms present in many bacterial species [48]. This system is based on the secretion of signalling molecules by bacteria which will in turn interact with a receptor protein in neighbouring bacterial cells, regulating gene expression in the population above a critical threshold [49]. QS systems have been widely associated with every step of biofilm formation, from initial attachment to dispersal [50]. A deficient QS system has already been associated with a large defect in biofilm formation, as demonstrated by Sakuragi *et al.* [51] in *P. aeruginosa* biofilms, where mutants of *lasI* and *rhlI*, which are QS effectors, were severely hampered in their ability to produce exopolysaccharide components. QS systems are essential for coordinating a cooperative mutualistic action. Synergistic biofilm formation between two different species also require an efficient QS system, as described by Rickard *et al.* [52], where the AI-2 molecule was required by *Actinomyces naeslundii* and *Streptococcus oralis* to build a common biofilm structure. Additionally, in Gram-positive cells, the release of eDNA inside the bacterial structure can also be mediated by a QS molecule called the CSP (competence-stimulating peptide), which regulates the expression of an autolysin, LytA, and two putative bacteriocins, triggering cell lysis and consequently DNA release. The CSP is essential for stabilizing the biofilm structure in several species of the genus *Streptococcus* [53]. By regulating the biofilm structure and components, QS can therefore enhance the chances of bacteria surviving exposure to a biocide, fostering bacterial cohesion in order to form a structured, protective matrix. The use of furanone, an inhibitor of the QS molecule AI-2, has already been associated with increased efficiency of hypochlorite and BAC against *Salmonella enterica* [54]. QS molecules LasR and RhlR have also been associated with a decreased susceptibility of *P. aeruginosa* against oxidative stressors such as H_2O_2, with the regulation of catalase and superoxide dismutase genes [55]. Finally, direct responses to biocide stress through QS regulators have also been reported. In fact, Gholamrezazadeh *et al.* reported that the use of BAC, nanosilver and acid-based formulations induced the expression of the QS regulator RhlR in *P. aeruginosa* isolates [56].

Role of ecological interactions

In their natural environments, mono-species biofilms can be found in specific biotopes, but the vast majority of biofilms are multi-species [57]. Microbial species are not spatially distributed randomly in a diversified biofilm. Beneficial or negative interactions between species can lead to a specific arrangement of the biofilm surface area, and can depend on morphological or bacterial structural properties [58]. The spatial organization has an impact on the biofilm's structural ability to resist a stress such as exposure to a biocide [59]. Microorganisms can also use specific species-related interactions as an adaptive strategy to counter biocide exposure. Some species can be protected by others from exposure to and the action of biocides within the biofilm's 3D structure [29, 60, 61]. As mentioned above, it is quite common to observe an increase in ECM production in single-strain biofilms exposed to biocides. The same is true when biofilms comprise multiple strains. In a dual-species biofilm, the production of EPSs can be increased, thus acting as a more efficient protective shield. Pang *et al.* demonstrated that more EPSs were produced in a biofilm composed of *P. aeruginosa* with non-cellulose-producing *Salmonella enterica* serovar Enteritidis [62], while Burmølle *et al.* demonstrated a synergistic interaction between four different species in response to hydrogen peroxide [63]. Some pathogenic strains of *E. coli* have already been shown to be able to increase the production of EPS components by other non-pathogenic strains via the secretion of matrix-stimulating metabolites [64]. Based on the hypothesis that the biochemical composition of the ECM is even more heterogeneous in a multi-species biofilm, this may increase biocide deactivation by diffusion and/or sorption reactions [61].

The complexity of a multispecies biofilm's reactions to biocide exposure also resides in its production of biomolecules. The natural diversity of microorganisms in biofilms reflects a full range of biomolecules found in the ECM, including cooperative public goods [65]. This phenomenon may allow susceptible bacteria that do not produce biomolecules to become tolerant to antimicrobials simply by the presence in its environment of bioproducts synthesized by its neighbouring bacteria. For example, *P. aeruginosa* is able to produce SdsA1, an SDS-hydrolase enzyme [66] which, produced individually by a single strain, can protect the whole community in a mixed-species biofilm [59]. Similarly, the matrix component produced by *B. subtilis* NDmed protects *S. aureus* from the actions of disinfectants [60]. In the event of environmental stresses such as starvation or antimicrobial addition, some subpopulations inside biofilms can even enter a specific lifestyle, including cannibalism. In *B. subtilis*, some subpopulations inside biofilms have been shown to secrete toxins able to lyse neighbouring non-immunized cells, which would then release nutrients inside the biofilm. Interestingly, the cells that could enter this cannibal state are the same ones that previously produced the ECM [67]. It has also been shown that selected bacilli swimmers can infiltrate and vascularize *S. aureus* biofilm by creating transient pores, offering direct routes for antimicrobials to reach the deepest populations of biofilm communities [68, 69]. In conclusion, intra- and inter-species interactions play an important, but still largely unexplored, role in modulating the spatial organization of the biofilm's structure and functions.

BACTERIAL PHYSIOLOGICAL MODULATIONS AND ACTIVE RESPONSES

One of the main differences between biofilms and planktonic cultures is their divergence in phenotypes. While planktonic cultures are usually exposed to homogeneous conditions and therefore have similar phenotypes, biofilms are composed of a multitude of microenvironments, exposing some of the cells in the inner layers of the biofilm to very low concentrations of nutrients and oxygen, consequently increasing the heterogeneity of physiological states [70]. These conditions promote stress responses in biofilms that completely remodel the physiology of these cells, triggering differential gene expression and thus new phenotypes, including reduced growth and potentially increased tolerance. Among these phenotypes, the development of persisters and VBNC cell populations is frequent in biofilms [22]. These populations are marked by their inability to grow, and are often challenging to eradicate due to the inactivation of certain antimicrobial targets. These recalcitrance phenomena often occur during antibiotic treatments because of the target-specific nature of antibiotics. For biocides, the multiplicity of targets usually prevents these limitations on planktonic cells. However, their diffusion-reaction limitation in biofilms can reduce the number of impacted targets for some treatments [71]. A recent study by Fernandes *et al.*, described the ability of *Pseudomonas fluorescens* and *Bacillus cereus* biofilm populations to regrow after different biocide treatments [72]. They observed that persister populations were able to survive BAC, glyoxal and glycolic acid treatments. *B. cereus* endospores were quite resilient to biocide treatments, while a considerable number of VBNCs were found among the surviving *P. fluorescens* populations. Peracetic acid (PAA) had a stronger effect, being able to eliminate all the *B. cereus* population, but not *P. fluorescens* VBNCs. The surviving populations were able to regrow in planktonic and biofilm conditions but the new population usually had the same susceptibility as the initial one, demonstrating that their survival was only due to their transitory persisting metabolism. Some studies have demonstrated that exposure to biocides can trigger the emergence of a VBNC population [73, 74]. In this section, we will focus on the different stress responses and physiological modulations in the biofilm that can lead to biocide-resilient populations (Fig. 1).

The stringent response

The stringent response is a key regulatory mechanism within bacteria. This stress response is activated in the event of nutrient depletion [75] to remodulate the cellular functions and limit gene expression to those that are essential. Thus, the inner layers of biofilms can be subject to a stringent response triggered by the lack of nutrients in certain strata or niches. Briefly, the stringent response can be induced through two homologous proteins: RelA and SpoT. These two proteins are activated through different external stresses, such as carbon and lipid starvation or internal consequences, such as amino acid deprivation [18]. They are both able to synthesize an alarmone called (p)ppGpp. This molecule targets many cellular functions, being involved in nucleotides, lipids, phosphates and amino acid metabolism, and acting on DNA replication, DNA transcription and RNA translation [76]. Through this process, bacteria can reduce their activities and focus on essential functions such as amino acid biosynthesis and nutrient uptake [75], while inhibiting growth processes such as replication, transcription and translation [77]. Thus, the stringent response often occurs in the inner layers of biofilms where nutrient availability can be reduced. Many studies have shown that the stringent response has, in addition, a direct regulatory role in biofilm formation and dispersion, being involved in the regulation of motility and EPS production [78, 79]. Within biofilms, the stringent response has been associated with an increased bacterial tolerance to antibiotics [80]. Similar effects are observed with biocides, and results from the inhibition of their targets are in keeping with the inhibition of cell functions. Both reduced growth rates and nutrient limitation have been associated with reduced sensitivity to biocides, demonstrating a possible effect of the stringent response on biocide tolerance [81–83]. The stringent response has also been shown to control the activity of catalases and hence to mediate the survival of bacteria against oxidative stressors, as demonstrated with hydrogen peroxide [84, 85]. A link between chlorhexidine and the stringent response has also been observed in *Enterococcus faecium* [86]. Recently, another study led by Nordholt *et al.* [87] used BAC to periodically disinfect *E. coli*, the goal being to simulate industrial conditions where bacteria are routinely exposed to biocides. They indicated that this periodic process induced a bacterial tolerance strongly linked to the triggering of the stringent response.

SOS response

The SOS response is a bacterial defence system involved in the restoration of damaged DNA. It is controlled by more than 50 genes regulated by inducer RecA and repressor LexA. Activated when ssDNA is starting to accumulate in the cell due to a polymerase being unable to fulfil its function while a helicase continues to unbind DNA upstream, RecA will induce an autocleavation of LexA and derepress the genes involved in the SOS response [88]. These genes code for polymerases that will repair the damaged DNA and therefore provide a level of tolerance to the deleterious effects of some biocides. The general environmental stress to which bacteria evolving in biofilms are exposed promotes the SOS response. In fact, six genes of the SOS response have already been positively associated with the accumulation of (p)ppGpp in *E. coli*, including RecA [89], demonstrating a link between stringent and SOS responses. The constant activation of the SOS response could hence be another argument for affirming that biofilms are a favourable condition for the emergence of tolerant clones. Several biocide families target DNA, and their effects may thus be directly impacted by the SOS repair system. In fact, the use of polyhexamethylene biguanide (PHMB) has already been associated with the triggering of DNA repair systems [90]. Peroxide-based biocides, such as PAA and H_2O_2, induce the appearance of reactive oxygen species (ROS), which damage DNA. These two biocides have already been associated with the triggering of an SOS response [91, 92]. In a similar manner, chlorine-releasing compounds such as NaOCl and chlorhexidine can also increase ROS production and have also been associated with instigation of the SOS response [13, 92, 93].

Toxin–antitoxin modules

Toxin–antitoxin modules are also systems able to promote the emergence of bacterial tolerance. These modules work through the action of a toxin, which inhibits several essential cellular processes such as DNA synthesis, DNA translation and cell wall synthesis [94]. The effects of these toxins are regulated by the antitoxins binding them, which are degraded in the event of external stress [18]. Thus, the toxin can be released and interfere with cellular functions, which will in turn slow bacterial growth and reduce biocide targets. Toxin–antitoxin systems are usually closely linked to stringent and SOS responses. In fact, the TisB/IstR-1 system is regulated by RecA and thereby strongly associated with the SOS response. This system has been associated with persister formation by the regulation of the proton motive force leading to a reduction of ATP in the cell, which will shut down multiple targets [95]. The HipA/HipB toxin–antitoxin system has itself been associated with (p)ppgpp and the stringent response. Two hypotheses have been forwarded regarding the way this system functions. One has suggested that HipA phosphorylates elongation factor EF-Tu, which ultimately leads to growth inhibition [96], while the other has rejected this hypothesis and has instead suggested that HipA phosphorylates the glutamyl-tRNA-synthetase GltX [97]. This phosphorylation interferes with the aminoacylation of tRNA-Glu, which directly leads to the accumulation of uncharged structures in the ribosomal A site, triggering RelA and the subsequent synthesis of (p)ppgpp. Logically, biofilms are thus a privileged zone for the development of toxin–antitoxin responses and the formation of persister cells [98]. Furthermore, research tends to show that toxin–antitoxin systems can even promote biofilm formation [99–101]. While no articles have directly linked the tolerance of bacteria in biofilms to biocides through toxin–antitoxin systems, some nonetheless have shown a link between the presence of some of these systems and the emergence of biocide tolerance. The PemI/PemK system has been identified on a chlorhexidine-tolerant *Klebsiella pneumoniae* plasmid [102]. Another study, performed on *Acinetobacter baumannii*, showed an association between the AbkA/AbkB system and chlorhexidine tolerance [103].

Active and passive trans-membrane transport

Efflux is an active pumping mechanism by which bacteria reject molecules that enter their inner structure from their environment, thus enabling the bacteria to survive. Efflux pumps are therefore strongly associated with tolerance, and have already been shown to be upregulated in dormant bacteria [104]. In addition, efflux pumps and biofilms are closely linked [105, 106]. This could be explained by the use of some broad-spectrum efflux pumps in functions other than the rejection of antimicrobials that could drive biofilm formation, for example the secretion of ECM components produced by bacteria [105]. Some efflux pumps are also involved in the secretion of QS compounds, which play a major role in the communication of bacteria inside biofilms [105]. Among the different efflux pumps, some have already been associated with both biofilm formation and biocide tolerance, demonstrating that biofilm cells could be less susceptible to biocides. The resistance–nodulation–cell division (RND) type of efflux pump is predominant. This superfamily is composed of many multidrug efflux pumps usually with a broad efflux spectrum. The AcrAB system may be the most well characterized. It has been shown to be involved in tolerance to several classes of biocides in different species, including *E. coli* [107] and *K. pneumoniae* [108]. AcrAB also appears to be essential for biofilm maintenance at a high level [109]. Amongst the other RND efflux pumps, the AdeABC efflux system of *A. baumannii* or the MexCD-oprJ system of *P. aeruginosa* have also been associated with both biofilm formation [110, 111] and antimicrobial tolerance [112–114]. Other efflux pump families are also involved in both biofilm formation and biocide tolerance, such as the major superfacilitator superfamily (MFS) and the small multidrug resistance (SMR) families. The MFS efflux pump NorA, present in *Staphylococcus aureus*, has been involved in tolerance to chlorhexidine, cetrimide and BAC [115, 116], while also contributing to biofilm formation [117]. In the SMR family, the *Listeria monocytogenes* EmrE efflux pump confers tolerance to QACs [118] while being essential in biofilm formation [119]. Additionally, the SMR SugE efflux pump has been shown to confer greater tolerance to QACs in *E. coli* biofilms than in planktonic cultures [120].

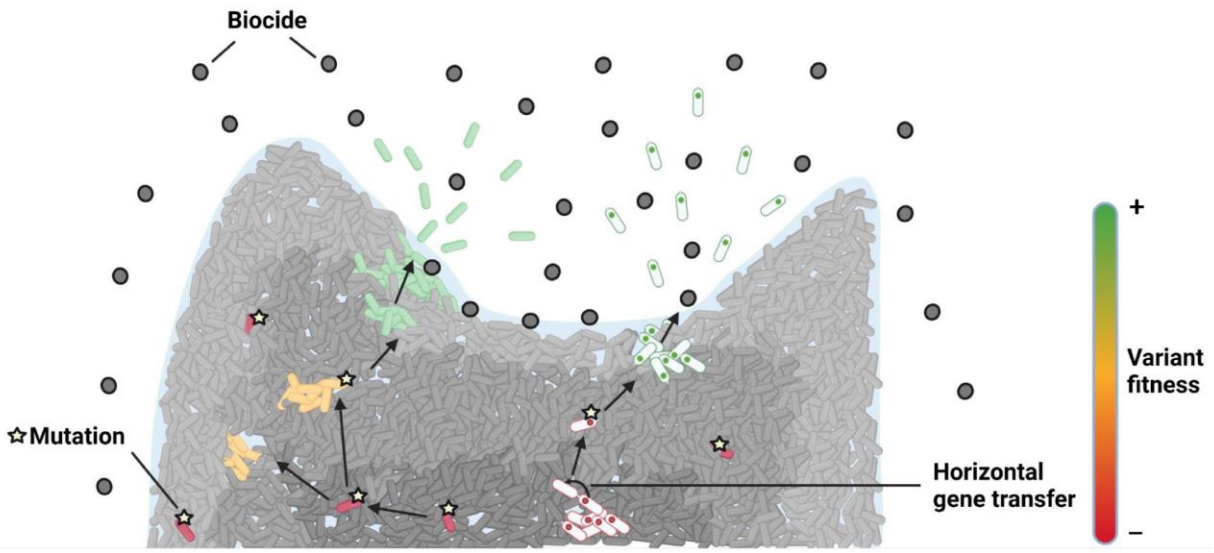

Fig. 2. Resistance can occur through mutational events or plasmid carriage. However, it is often associated with a fitness cost. The biofilm protects unfit variants, which can become fit to multiply and finally disseminate in a biocide-full environment through compensatory mutational events.

Joint regulation mechanisms between passive and active transport also occur in bacterial cells. While efflux pumps are upregulated, porins —transmembrane channels used for internalizing molecules and nutrients — are downregulated to limit the entry of new antimicrobials and facilitate the externalization of those already inside [121]. For example, in *E. coli*, three global regulators – MarA, SoxS and Rob – regulate both porins and efflux systems at the same time, upregulating AcrAB, TolC and MicF, the last being a known repressor of OmpF [122]. Porins are usually essential for biofilm formation [123, 124], which is in opposition to resistance mechanisms, as upregulation facilitates the entry of antimicrobials into the cell. Indeed, porins can contribute to cell adhesion and autoaggregation [125, 126] but also to the export of matrix components, such as the Pel polysaccharide in *P. aeruginosa* [127]. This therefore contrasts with biofilm tolerance and biocide tolerance, as bacteria usually decrease porin expression during biocide exposure [128, 129].

ACQUISITION OF GENETICALLY MEDIATED RESISTANCE

Although modulation of the biofilm's structure and the inner physiological state of certain populations inside the matrix can confer tolerance against biocides, they cannot be considered as resistance mechanisms, as the bacteria's survival is only mediated by genetic regulation cascades which will disappear immediately once the stress is removed. In contrast, genetically mediated resistances are anchored in the genome and will last even if the bacteria disseminate in another less stressful environment. Genetically mediated resistances will also be transmitted to the bacterial daughter cells, spreading the resistance rapidly in the biotope. In this section, we will focus on how biofilms and biocide exposure can influence and select the emergence of biocide-resistant genetic variants, and how such resistant variants can fix and evolve in the protective environment conferred by the biofilm (Fig. 2) .

From physiological adaptation to genetic resistance

In recent years, several studies have revealed a relationship between tolerance and the emergence of resistance. Indeed, some studies have shown that tolerance often precedes resistance in a bacterial cell population, especially when cells are exposed to high concentrations of antimicrobials [87, 130, 131]. The explanation for this phenomenon could be that the tolerant metabolism facilitates emergence of the resistant phenotype. In a bacterial population, a resistant phenotype often requires the previous appearance of several partial resistances that provide weaker protections but also entail fewer fitness costs. These are sometimes not strong enough to survive the antimicrobial attack, and this is where tolerance could play a role: the longer time required to eliminate such cells with an antimicrobial treatment could give the cells enough time to go through these different steps and gain full resistance. Biofilm tends to promote physiological heterogeneity and cell tolerance due to its 3D structure, which can work in favour of the proportion of tolerant cells in the population, thereby substantially contributing to the emergence of resistance against biocides.

Simultaneously, high mutation rates have been associated with biofilms [132], specifically in persister populations [133], hence increasing the chances of acquiring genetic resistances. This could be due to the use of error-prone polymerases during the SOS response, which ultimately leads to higher probability of mutational events and fixation of some resistance mechanisms [134, 135]. Deletion of the SOS response activator RecA has already been associated with a delay in the acquisition of antibiotic resistance in *E. coli* [136], and could therefore play a major role in the acquisition of biocide resistance.

Physiological responses to biocide exposure can also stimulate mutation rates. The addition of chlorhexidine, didecyldimethylammonium chloride (DDAC), copper, permethrin and propiconazole have been demonstrated to activate global stress responses, such as the RpoS-mediated response and the SOS response in *E. coli*, subsequently increasing the mutation rate [137]. Oxidizing agents such as H_2O_2 and PAA can also induce the formation of ROS [138, 139] that are toxic for the cells and damage DNA. Nevertheless, the protection conferred by the biofilm could limit exposure effects so they remain sublethal. These concentrations could increase DNA instability, which would ultimately lead to mutations, but the concentrations would not be high enough to be lethal for the bacterial cell. Exposure to H_2O_2 has, for example, been shown to markedly increase the mutation rates in yeasts [140].

Finally, an increase in mutation rate has also been associated with efflux pumps. A recent study associated the upregulation of *acrB* with a higher mutation rate [141]. This efflux pump is one of the most strongly associated with antimicrobial survival and, as previously noted, has already been linked to biocide tolerance [108]. Hence, its overexpression would allow the bacteria to both survive biocide exposure and simultaneously induce mutations in the population.

Triggering of genetic exchanges

Biofilms are hotspots for horizontal gene transfers (HGTs) between bacteria [142]. The density of bacteria is higher than in planktonic cultures and bacteria stay physically close together, thus increasing the probability of DNA exchange. This can happen in mono-species biofilms but also between two different species in multi-species biofilms, which are frequent in natural environments [143].

Different transfer mechanisms support HGTs, and bacterial conjugation is one of the best described. Proximity between bacteria facilitates intercommunication. It has already been shown that plasmids are better conserved in biofilms [144] and that exchanges are also fostered by other mechanisms intrinsic to biofilms, such as the SOS response, which is interlinked with bacterial conjugation [145, 146]. In addition, the 3D structure of biofilms may facilitate plasmid stability and persistence even under non-selective conditions [147, 148].

Reciprocally, plasmids can also contribute to biofilm formation and development. Conjugative pili are, for example, known to facilitate biofilm formation thanks to their aggregative properties, which improve cell–cell fixation properties [147]. Ghigo [149] demonstrated that conjugative pili could also increase cell-surface adherence and increase the chances of initial attachment. This could be due to the upregulation of curli and colanic acid production associated with the conjugative plasmid [150]. While conjugative pili are naturally present on every plasmid as a backbone gene essential for the plasmid's horizontal transmission, other genes able to facilitate biofilm formation have been found on some plasmids. Of these, fimbriae and type IV pili — important genes in the adhesion step — are frequently found on plasmids [147].

Resistance plasmids are of concern because of their fast and efficient exchange of resistance genes. Additionally, the use of a single antimicrobial substance can select for multidrug-resistant bacteria as plasmids often carry a large number of genes, conferring broad resistances. Some biocide resistance genes have already been observed on plasmids [6, 151–155] and could spread easily between different bacterial populations. Moreover, the addition of certain biocides, such as chlorine, chloramine and hydrogen peroxide, could directly enhance conjugation events, probably by inducing bacterial stress responses [156].

While the acquisition of bacterial plasmids could thus be facilitated in biofilms, other HGT methods can also be induced. Bacteria may also acquire resistance genes through the transformation of genetic material. The large quantities of eDNA in the biofilm matrix can be acquired by neighbouring bacteria and hence spread acquired bacterial resistance mechanisms. Indeed, bacterial transformation is generally induced inside biofilms due to the eDNA in their matrix [157].

Furthermore, by lysing their targets, biocides could actually induce this type of genetic exchange. Indeed, many biocides lyse cells by inducing a loss of membrane integrity, thereby releasing intracellular content into the biofilm matrix [158, 159]. Some tolerant bacteria that survived exposure would be able to transform some of the genetic material released, and could thereby acquire resistance genes [160–162].

Protective incubation of newborn variants

The superposition of metabolic and biocide gradients resulting from the 3D structure increase the chances of tolerant subpopulations developing resistance without being eliminated by the treatment. However, resistant phenotypes are often associated with a fitness cost that can be caused by a mutation of the bacterial target, inhibiting the effect of the biocide, but also altering its function. It can also be a consequence of elevated energy costs, brought about by efflux pump upregulations [163] or the addition of a plasmid to the bacterial genome [164]. New research, however, tends to characterize biofilms as 'diversity incubators' [165],

boosting the appearance of variants and greatly helping them to survive and settle in the population. In addition to their ability to promote the appearance of variants, biofilms could play a major role in the fixation of these variants in the environment. Indeed, protective microenvironments will permit variants to survive in biofilms, while in a well-mixed suspension they would probably be directly outcompeted by strains with higher fitness once selective pressure is removed after the end of biocide exposure. The cooperative behaviour in biofilms and the protective effects of the structure will actually provide mutants with the opportunity to survive and develop, potentially allowing the acquisition of additional mutations in daughter cells. Consequently, some of these bacteria will earn compensatory mutations, which will restore or even increase their fitness, hence allowing mutants to fix in the population, and be able to disseminate and colonize new environments. France *et al.* have studied the fixation of gentamicin- and rifampicin-resistant mutants in biofilm and planktonic populations after initial antibiotic exposure [166]. They showed that the gentamicin-resistant clones, which suffered severe fitness costs, could remain in the same quantities in biofilms even 45 days after the antibiotic exposure, while the number of resistant variants in planktonic conditions declined greatly over time. On the other hand, the rifampicin-resistant clones, whose mutations do not usually involve fitness costs, could persist in the same quantities in both planktonic and biofilm conditions.

IMPACT OF BACTERIAL ADAPTATION TO BIOCIDES IN THE LIGHT OF THE ONE HEALTH CONCEPT

Recent health crises have increased the general public's concern about food processing procedures. The impacts of such procedures, in particular hygiene and disinfection, need to be investigated from farm to fork in the light of the One Health concept, which recognizes that human, animal and environmental health are intricately linked. Hence, studies on the side effects of bacterial adaptation to biocides have to be enforced to identify potential impacts on and risks to public health issues. More especially, the biofilm model needs to be integrated because it is a main way that bacteria can adapt along the food chain [167]. This section will thus summarize the main possible effects of biocide use on pathogens that can have a food safety impact from a One Health perspective.

Colonization and dissemination

Biocide use may affect the ability of the exposed bacterial populations to disseminate and colonize new environments, especially after several industrial disinfection cycles. Any misuse of biocides could increase the dissemination of viable cells by the superficial disruption of the biofilm without being strong enough to eradicate bacterial cells inside the biofilm. The effects of BAC and NaOCl on *L. monocytogenes* were studied by Rodriguez-Melcon *et al.* [168], who found that the use of both biocides at 0.5, 1.0 and 1.5 MICs could reduce the biofilm's biovolumes of the different strains. However, only NaOCl was able to kill the vast majority of the cells, while MICs of BAC were not able to reduce the number of viable cells. The same effects have been observed with PAA and BAC on *Yersinia enterocolitica* and *Cronobacter sakazakii* [169]. A sub-optimal biocide treatment could thereby lead to a detachment of viable cells that could easily recolonize new surfaces.

An increase in adhesion properties has also been observed in sulphate-reducing bacteria after exposure to glutaraldehyde [170]. Likewise, NaOCl and acetic acid could enhance the surface adhesion force of *Campylobacter jejunii* [171]. This can be explained by the overexpression of adhesion-related genes [172, 173] and the downregulation of motility-related genes [174]. New surface colonization could thereby be facilitated for the biofilm-detached exposed cells.

Finally, several studies have already associated biocide exposure with changes in biofilm formation, thus potentially increasing the faculty of bacteria to form stronger biofilms on the newly colonized surfaces. A study on uropathogenic *E. coli* has shown a positive association between biofilm formation and both triclosan and BAC [33]. A positive association with biofilm formation has also been reported for sodium nitrite and NaOCl in *E. coli* [34], while *Salmonella enteritidis* biofilm capabilities have been enhanced upon exposure to NaOCl and H_2O_2 at sublethal concentrations [175].

Food processing industries usually employ high concentrations of biocides during cleaning procedures, which should prevent these events from happening. However, the presence of biofilms, combined with other limitations related to surface topology, the presence of interfering matter, or even misuse, for instance, could lead to a decrease in the final biocide concentrations applied to bacteria. Adaptation to such low biocide concentrations may thus provide bacteria with an opportunity to propagate in the food chain through a higher adhesion or biofilm production capabilities, thus increasing the chance of reaching the consumer at the end of the process.

Antimicrobial cross-resistance

The possible dissemination of biocide-exposed pathogens along the food chain towards consumers raises concerns about the impact of biocide exposure on antibiotic resistance. This potential side effect of biocides has been gaining interest due to the growing threat of antimicrobial resistance worldwide. Numerous classes of biocides and antibiotics have indeed been associated with cross-resistances [9], notably because of the similar mechanisms bacteria use to fight against both kinds of molecules (see Table 1). Multidrug efflux pump overexpression is one of the main co-selection mechanisms reported between

Table 1. List of genetic targets directly or indirectly associated with a decreased antibiotic susceptibility due to biocide cross-selection

Modulation of cellular functions underlying cross-resistance	Genetic target	Biocidal active substances	Reduced antibiotic susceptibility	Bacterial species	Reference
Efflux activity	AbeM	TCS	Cip, Dox, Min	*Acinetobacter baumannii*	[129]
	AcrAB/TolC	FOR+GLU+QAC	Acr, Amp, Cm, Tet	*Salmonella enterica*	[197]
		TCS	Acr, Amp, Cm, Tet	*Salmonella enterica*	[197]
		FOR+GLU+QAC	Amp, Cip, Cm, Tet	*Salmonella enterica*	[200]
		FOR+GLU+QAC	Amp, Cip, Cm, Tet	*Salmonella enterica*	[200]
		OCB	Amp, Cip, Cm, Tet	*Salmonella enterica*	[200]
		OCB	Amp, Cip, Cm, Tet	*Salmonella enterica*	[200]
	AcrEF/TolC	ALD+QAC	Cm, Cip, Nal, Tet	*Salmonella enterica*	[201]
		OCB	Cm, Cip, Nal, Tet	*Salmonella enterica*	[201]
	AcrR	BAC	Amp, Cm	*Escherichia coli*	[7]
		TCS	Amp, Cm, Lev	*Escherichia coli*	[202]
		TCS	Amp, Azi, Cfc, Cfp, Cfz, Cxm, Cip, Ery, Gen, Lin, Lom, Oxa, Tet	*Escherichia coli*	[12]
		BAC	Amp, Cm, Tet	*Escherichia coli*	[203]
		DDAC	Amp, Cm, Tet	*Escherichia coli*	[203]
	AdeB	CHX	Ami, Cip, Dox, Gen, Imi, Mer, Min, Net, Sul, Tob	*Acinetobacter baumannii*	[129]
		BAC	Ami, Cip, Dox, Gen, Imi, Mer, Min, Net, Sul, Tob	*Acinetobacter baumannii*	[129]
	AdeJ	TCS	Cip, Dox, Min	*Acinetobacter baumannii*	[129]
	AdeS	CHX	Ami, Cip, Dox, Gen, Imi, Mer, Min, Net, Sul, Tob	*Acinetobacter baumannii*	[129]
		BAC	Ami, Cip, Dox, Gen, Imi, Mer, Min, Net, Sul, Tob	*Acinetobacter baumannii*	[129]
	CepA	CHX	Col	*Klebsiella pneumoniae*	[204]
	CmeB	TCS	Amp, Cip, Cm, Ery, Tet,	*Campylobacter jejuni*	[205]
	DinF	DDAC	Amp, Tet	*Escherichia coli*	[203]
	FepR	BAC	Cip	*Listeria monocytogenes*	[10]
	MdfA	CHP	Amp, Cm	*Escherichia coli*	[7]
		TCS	Amp, Azi, Cfc, Cfp, Cfz, Cxm, Cip, Ery, Gen, Lin, Lom, Oxa, Tet	*Escherichia coli*	[12]
	MepA	BAC	Acr, Cip, Nor	*Staphylococcus aureus*	[206]
		CHX	Acr, Cip, Nor	*Staphylococcus aureus*	[206]
		CHX	Cip, Mup	*Staphylococcus aureus*	[116]
	MexAB/OprN	TCS	Cip, Ery, Gen, Tet, Tmp	*Pseudomonas aeruginosa*	[207]
	MexCD/OprJ	BAC	Nor	*Pseudomonas aeruginosa*	[208]
		CHX	Nor	*Pseudomonas aeruginosa*	[208]
		TCS	Cip, Ery, Tet, Tmp	*Pseudomonas aeruginosa*	[207]

Continued

Table 1. Continued

Modulation of cellular functions underlying cross-resistance	Genetic target	Biocidal active substances	Reduced antibiotic susceptibility	Bacterial species	Reference
	MexX	CHX	Ami, Cef, Cip, Mer	*Pseudomonas aeruginosa*	[209]
	MexXY/OprM	TCS	Cip, Ery, Gen, Tet, Tmp	*Pseudomonas aeruginosa*	[207]
	MsbA	DDAC	Amp, Cm, Tet	*Escherichia coli*	[203]
	NorA	CHX	Cip, Mup	*Staphylococcus aureus*	[116]
	NorE	TCS	Amp, Azi, Cfc, Cfp, Cfz, Cxm, Cip, Ery, Gen, Lin, Lom, Oxa, Tet	*Escherichia coli*	[12]
	OqxAB	BAC	Cip, Cm, Flu, Nal, Nor, Tmp	*Escherichia coli*	[210]
		TCS	Cip, Cm, Flu, Nal, Nor, Tmp	*Escherichia coli*	[210]
	PmpM	BAC	Acr, Cip, Nor	*Pseudomonas aeruginosa*	[211]
	SmeDEF	TCS	Cip, Cm, Tet	*Stenotrophomonas maltophilia*	[212]
	YihV	TCS	Amp, Azi, Cfc, Cfp, Cfz, Cxm, Cip, Ery, Gen, Lin, Lom, Oxa, Tet	*Escherichia coli*	[12]
	CarO	BAC	Ami, Cip, Dox, Gen, Imi, Mer, Min, Net, Sul, Tob	*Acinetobacter baumannii*	[129]
		TCS	Ami, Cip, Dox, Gen, Min, Net	*Acinetobacter baumannii*	[129]
	EnvZ	CHP	Amp, Cm, Nor	*Escherichia coli*	[7]
	FabH	TCS	Cip	*Staphylococcus aureus*	[213]
	MipA	BAC	Amp, Cm, Tet	*Escherichia coli*	[203]
	OmpA	OCB	Amp, Cip, Cm, Tet	*Salmonella enterica*	[200]
		FOR+GLU+QAC	Amp, Cip, Cm, Tet	*Salmonella enterica*	[200]
		BAC	Ami, Cip, Dox, Gen, Imi, Mer, Min, Net, Sul, Tob	*Acinetobacter baumannii*	[129]
Membrane permeability		CHX	Ami, Cip, Dox, Gen, Imi, Mer, Min, Net, Sul, Tob	*Acinetobacter baumannii*	[129]
		TCS	Ami, Cip, Dox, Gen, Min, Net	*Acinetobacter baumannii*	[129]
	OmpC	OCB	Amp, Cip, Cm, Tet	*Salmonella enterica*	[200]
		FOR+GLU+QAC	Amp, Cip, Cm, Tet	*Salmonella enterica*	[200]
	OmpF	OCB	Amp, Cip, Cm, Tet	*Salmonella enterica*	[200]
		FOR+GLU+QAC	Amp, Cip, Cm, Tet	*Salmonella enterica*	[200]
	OmpR	CHP	Amp, Cm, Nor	*Escherichia coli*	[7]
		POV	Amp, Cm, Nor	*Escherichia coli*	[7]
	PmrB	BAC	Pol	*Pseudomonas aeruginosa*	[14]
	SbmA	BAC	Amp, Cm, Tet	*Escherichia coli*	[203]
Central metabolism	AceE	PHMB	Gen	*Escherichia coli*	[15]

Continued

Table 1. Continued

Modulation of cellular functions underlying cross-resistance	Genetic target	Biocidal active substances	Reduced antibiotic susceptibility	Bacterial species	Reference
Biofilm formation	Aes	GLU	Cm	*Escherichia coli*	[7]
	Flu	CHX	Amp	*Escherichia coli*	[7]
	PyrE	GLU	Amp, Cm, Nor	*Escherichia coli*	[7]
	YeaW	GLU	Amp, Cm, Nor	*Escherichia coli*	[7]
Modification of specific target	FabI	TCS	Cip	*Staphylococcus aureus*	[213]
		HAL	Cip, Nal	*Salmonella enterica*	[8]
		OCB	Cip, Nal	*Salmonella enterica*	[8]
	GrlA	TCS	Cip	*Staphylococcus aureus*	[213]
	GrlB	TCS	Cip	*Staphylococcus aureus*	[213]
	GyrA	TCS	Cip	*Staphylococcus aureus*	[213]
		HAL	Cip, Nal	*Salmonella enterica*	[8]
		OCB	Cip, Nal	*Salmonella enterica*	[8]
	InhA	TCS	Iso	*Mycobacterium tuberculosis*	[214]
	RpoA	AQAS	Cm, Nal, Tet	*Salmonella enterica*	[8]
		GLU	Cm	*Escherichia coli*	[7]
	RpoB	PER	Amp, Cm	*Escherichia coli*	[7]
		BAC	Amp	*Escherichia coli*	[7]
		BAC	Rif	*Escherichia coli*	[203]
		DDAC	Rif	*Escherichia coli*	[203]
	RpoC	PER	Amp, Cm	*Escherichia coli*	[7]
		BAC	Rif	*Escherichia coli*	[203]
		DDAC	Rif	*Escherichia coli*	[203]
Global regulator activity	Crp	BAC	Amp, Cm, Tet	*Escherichia coli*	[203]
		DDAC	Amp, Cm, Tet	*Escherichia coli*	[203]
	GdpP	SHY	Oxa	*Staphylococcus aureus*	[215]
	Lon	BAC	Amp, Cm, Tet	*Escherichia coli*	[203]
	FrdD	TCS	Amp, Amx, Cep	*Escherichia coli*	[202]
	MarA	BAC	Cip, Cm, Ctf, Cxm, Flo, Nal	*Escherichia coli*	[128]
	MarR	TCS	Cm, Lev, Nor, Tet	*Escherichia coli*	[202]
		BAC	Amp, Cm, Tet	*Escherichia coli*	[203]
		DDAC	Amp, Cm, Tet	*Escherichia coli*	[203]
	PhoPQ	CHX	Col	*Klebsiella pneumoniae*	[198]
	RamR	QAC	Cm, Nal, Tet	*Salmonella enterica*	[8]
		ALD+QAC	Cm, Nal, Tet	*Salmonella enterica*	[8]

Continued

Table 1. Continued

Modulation of cellular functions underlying cross-resistance	Genetic target	Biocidal active substances	Reduced antibiotic susceptibility	Bacterial species	Reference
	SoxR	TCS	Amp, Cm, Lev	*Escherichia coli*	[202]
		BAC	Amp, Cm, Tet	*Escherichia coli*	[203]
		DDAC	Amp, Cm, Tet	*Escherichia coli*	[203]
	SoxS	BAC	Cip, Cm, Ctf, Cxm, Flo, Nal	*Escherichia coli*	[128]

Acr, acriflavine; ALD, aldehydes; Ami, amikacin; Amp, ampicillin; Amx, amoxicillin; Azi, azithromycin; BAC, benzalkonium chloride; Cep, cephalexin; Cfc, cefaclor; Cfp, cefepime; Cfz, Cefazolin; CHP, chlorophene; CHX, chlorhexidine; Cip, ciprofloxacin; Cm, chloramphenicol; Col, colistin; Ctd, ceftiofur; Cxm, cefotaxime; DDAC, didecyldimethylammonium chloride; Dox, doxycycline; Ery, erythromicin; Flu, flumequine; FOR, formaldehyde; Gen, gentamicin; GLU, glutaraldehyde; HAL, chlorophene tertiary amine compound; Imi, imipenem; Iso, isoniazid; Lev, levofloxacin; Lin, linezolid; Lom, lomefloxacin; Mer, meropenem; Min, minocycline; Mup, mupirocin; Nal, nalidixic acid; Net, netilmicin; Nor, norfloxacin; OCB, oxidising compound blend; Oxa, oxacillin; PER, hydrogen peroxide; PHMB, polyhexamethylene biguanide; PIO, piovidone iodine; Pol, polymixin B; QAC, quaternary ammonium compound; Rif, rifampicin; Sul, sulbactam; TCS, triclosan; Tet, tetracycline; Tmp, trimethoprim; Tob, tobramycin.

biocides and antibiotics. As previously stated, efflux pumps play an important role in biofilm formation and defence against biocides, but their non-specificity also leads them to play an important role in antibiotic resistance. Several studies have directly associated some efflux pumps with cross-resistance against different classes of biocides and antibiotics, in various foodborne pathogens [176, 177]. Cross-resistance through modifications to cell permeability via porin mutations has also been documented [176, 178, 179]. Changes in metabolism can also affect both tolerance to biocides and antibiotics, which is particularly relevant in biofilms, as shown in 2021 by Cuzin *et al.*, who exposed *E. coli* biofilms to PHMB and isolated a gentamicin-resistant variant with lower susceptibility to PHMB from the exposed biofilm population [15]. Decreases in antimicrobial susceptibility are related to a single nonsense mutation in the gene *aceE* encoding the pyruvate dehydrogenase E1 component of the pyruvate dehydrogenase (PDH) complex that catalyses the conversion of pyruvate to acetyl-CoA and CO_2 upstream of the tricarboxylic acid cycle [15].

Additionally, plasmids containing genes conferring resistance to both biocides and antibiotics have already been identified, notably QAC efflux pumps that are often found on multidrug resistance plasmids [151, 155, 180–182]. However, numerous studies have also failed to identify a direct link between biocide exposure and an increase in antibiotic resistance [5, 183, 184]. Another study by Li *et al.* showed that, under their conditions, resistance to triclosan could induce some physiological modifications which conferred tolerance to antibiotics by inducing the formation of biofilm and reducing membrane permeability, without, however, inducing irreversible modifications which would lead to permanent resilience [185]. The link between both antimicrobial classes is not always clear and the emergence of resistance to antibiotics has already been observed after biocide exposure without having any effect on the biocide MICs [186, 187]. Finally, biocide exposure can even increase the susceptibility of bacteria to some antibiotic classes [183, 188], with some resistance mutations having occasional global effects on the bacterial cell that disrupt the effect of other mechanisms [189]. Hence, additional studies are needed to improve our understanding of the role of biocides in the emergence of antibiotic resistance from a One Health perspective.

Virulence and pathogenicity

Another interesting line of research in keeping with a One Health approach is the study of the potential impact of biocides on the virulence and pathogenicity of strains. The global risk of consumer contamination would be instantly increased if adaptation to biocides likewise increases the strain's ability to infect its host. One of the impacts that biocides have on efflux pumps could, for example, be increased virulence. Several efflux systems have been associated with the ability of some pathogens to infect and colonize human cells [190]. The AcrAB-TolC complex has been directly linked to the faculty of *S. enterica* serovar Typhimurium to infect macrophage cells [191], probably by controlling the expression of pathogenicity islands SPI-1 and SPI-2 [192]. It has also been associated with survival against bile salts found in the gastrointestinal tract [193]. The invasiveness of *P. aeruginosa* has been shown to be greatly reduced following mutation of the MexAB-OprM system [194]. ROS-degrading enzymes are also important proteins in both biocide resistance and virulence. The RcsA peroxidase of *P. aeruginosa* has been found to be associated with both *in vivo* bacterial survival in *Caenorhabditis elegans* and *Drosophila melanogaster* and an increase in the survival rate against sodium hypochlorite and hypochlorous acid [195]. However, despite the different possible links between virulence and biocide resistance, the studies that have investigated virulence after exposure to biocides did not find any positive impact of biocide exposure on the pathogens' natural virulence. Exposure of *S. enterica* serovar Typhimurium to several classes of biocides (a tar oil phenol, an oxidizing agent, an aldehyde agent and a QAC agent) has been found not to affect virulence in chicks [196]. Another study performed on *S. enterica*

serovar Typhimurium has even shown a significantly reduced invasiveness of triclosan-exposed and QAC-exposed bacterial cells [197]. Henly *et al.* [33] showed more mixed results on uropathogenic *E. coli*. Triclosan exposure was indeed found to reduce virulence in 5/8 strains and BAC in 6/8 strains although virulence of the least pathogenic strain was nevertheless induced after BAC exposure. Contrasting results were also observed with PHMB (1/8 showed increased virulence and 3/8 reduced virulence). The last biocide tested, silver nitrate, was actually the only one that never reduced pathogenicity, and in fact increased it in 2/8 strains tested. Wand *et al.* [198] also showed contrasting results with 4/6 strains that had a significant loss of virulence after CHX exposure while the last two did not seem to have an impact on the survival of *Galleria mellonella* larvae. Another study has shown that hypervirulent strains of *L. monocytogenes* were positively associated with a plasmid carrying the *emrC* gene coding BAC efflux pumps, which could show a positive selection of virulent clones through the use of this biocide, but no direct link has been made to confirm the efflux pump's direct role on the virulence of these strains [199]. To conclude, no general link between biocide exposure and virulence has yet been proven, but the fitness costs induced by triclosan and QAC exposure seem to have, in general, a deleterious effect on cells. More studies will be required on different biocide classes to identify potential links between pathogenicity and biocide adaptation.

CONCLUSION

Considerable progress has been made in the last few decades on our understanding of how biofilms adapt to their environment. The heterogeneity of phenotypes caused by the 3D structure facilitates tolerance against external stresses. New studies are exploring the link between bacterial tolerance and the appearance of acquired resistances, paving the way for future research on a possible link between biofilms and the propagation of harmful bacterial variants. The constant exposure of biofilms to biocides in food chain industries raises the question of potential effects of biocide exposure on the development and propagation of antimicrobial resistance variants via the food chain, resulting in a possible public health risk. Field studies linking all these characteristics in natural environments are required to evaluate the risk associated with these phenomena.

Funding information
R.C. was a recipient of an Anses-INRAE doctoral fellowship. ANR JCJC BAoBAb (ANR-21-CE35-0001) also supported this work (including M.B.'s internship).

Author contributions
Writing – original draft preparation, R.C., M.B., A.B.; writing – review and editing, R.C., A.B., R.B.; supervision and funding acquisition, A.B., R.B. All authors have read and agreed to the published version of the manuscript. Images were created using BioRender.com software. All the authors have read and agreed to the published version of the manuscript.

Conflicts of interest
The authors declare no conflict of interest.

References

1. **Larsson DGJ**, **Flach C-F**. Antibiotic resistance in the environment. *Nat Rev Microbiol* 2022;20:257–269.
2. **Founou LL**, **Founou RC**, **Essack SY**. Antibiotic resistance in the food chain: a developing country-perspective. *Front Microbiol* 2016;7:1881.
3. **Avershina E**, **Shapovalova V**, **Shipulin G**. Fighting antibiotic resistance in hospital-acquired infections: current state and emerging technologies in disease prevention, diagnostics and therapy. *Front Microbiol* 2021;12:707330.
4. **Butucel E**, **Balta I**, **Ahmadi M**, **Dumitrescu G**, **Morariu F**, ***et al.*** Biocides as biomedicines against foodborne pathogenic bacteria. *Biomedicines* 2022;10:379.
5. **Maillard J-Y**. Resistance of Bacteria to Biocides. *Microbiol Spectr* 2018;6.
6. **Zou L**, **Meng J**, **McDermott PF**, **Wang F**, **Yang Q**, ***et al.*** Presence of disinfectant resistance genes in *Escherichia coli* isolated from retail meats in the USA. *J Antimicrob Chemother* 2014;69:2644–2649.
7. **Merchel Piovesan Pereira B**, **Wang X**, **Tagkopoulos I**. Biocide-induced emergence of antibiotic resistance in *Escherichia coli*. *Front Microbiol* 2021;12:640923.
8. **Webber MA**, **Whitehead RN**, **Mount M**, **Loman NJ**, **Pallen MJ**, ***et al.*** Parallel evolutionary pathways to antibiotic resistance selected by biocide exposure. *J Antimicrob Chemother* 2015;70:2241–2248.
9. **Kampf G**. Biocidal agents used for disinfection can enhance antibiotic resistance in gram-negative species. *Antibiotics* 2018;7:110.
10. **Douarre P-E**, **Sévellec Y**, **Le Grandois P**, **Soumet C**, **Bridier A**, ***et al.*** FepR as a central genetic target in the adaptation to quaternary ammonium compounds and cross-resistance to ciprofloxacin in *Listeria monocytogenes*. *Front Microbiol* 2022;13:864576.
11. **Amsalu A**, **Sapula SA**, **De Barros Lopes M**, **Hart BJ**, **Nguyen AH**, ***et al.*** Efflux pump-driven antibiotic and biocide cross-resistance in *Pseudomonas aeruginosa* isolated from different ecological niches: a case study in the development of multidrug resistance in environmental hotspots. *Microorganisms* 2020;8:1647.
12. **Sonbol FI**, **El-Banna TE**, **Abd El-Aziz AA**, **El-Ekhnawy E**. Impact of triclosan adaptation on membrane properties, efflux and antimicrobial resistance of *Escherichia coli* clinical isolates. *J Appl Microbiol* 2019;126:730–739.
13. **Tong C**, **Hu H**, **Chen G**, **Li Z**, **Li A**, ***et al.*** Chlorine disinfectants promote microbial resistance in *Pseudomonas* sp. *Environ Res* 2021;199:111296.
14. **Kim M**, **Weigand MR**, **Oh S**, **Hatt JK**, **Krishnan R**, ***et al.*** Widely used benzalkonium chloride disinfectants can promote antibiotic resistance. *Appl Environ Microbiol* 2018;84:e01201-18.
15. **Cuzin C**, **Houée P**, **Lucas P**, **Blanchard Y**, **Soumet C**, ***et al.*** Selection of a gentamicin-resistant variant following polyhexamethylene biguanide (PHMB) exposure in *Escherichia coli* biofilms. *Antibiotics (Basel)* 2021;10:553.

16. **Flemming H-C, van Hullebusch ED, Neu TR, Nielsen PH, Seviour T, *et al.*** The biofilm matrix: multitasking in a shared space. *Nat Rev Microbiol* 2023;21:70–86.
17. **Karygianni L, Ren Z, Koo H, Thurnheer T.** Biofilm matrixome: extracellular components in structured microbial communities. *Trends Microbiol* 2020;28:668–681.
18. **Uruén C, Chopo-Escuin G, Tommassen J, Mainar-Jaime RC, Arenas J.** Biofilms as promoters of bacterial antibiotic resistance and tolerance. *Antibiotics (Basel)* 2020;10:3.
19. **Bridier A, Briandet R, Thomas V, Dubois-Brissonnet F.** Resistance of bacterial biofilms to disinfectants: a review. *Biofouling* 2011;27:1017–1032.
20. **Koechler S, Farasin J, Cleiss-Arnold J, Arsène-Ploetze F.** Toxic metal resistance in biofilms: diversity of microbial responses and their evolution. *Res Microbiol* 2015;166:764–773.
21. **Jo J, Price-Whelan A, Dietrich LEP.** Gradients and consequences of heterogeneity in biofilms. *Nat Rev Microbiol* 2022;20:593–607.
22. **Ayrapetyan M, Williams TC, Oliver JD.** Bridging the gap between viable but non-culturable and antibiotic persistent bacteria. *Trends Microbiol* 2015;23:7–13.
23. **Ciofu O, Moser C, Jensen PØ, Høiby N.** Tolerance and resistance of microbial biofilms. *Nat Rev Microbiol* 2022;20:621–635.
24. **Bridier A, Piard J-C, Pandin C, Labarthe S, Dubois-Brissonnet F, *et al.*** Spatial organization plasticity as an adaptive driver of surface microbial communities. *Front Microbiol* 2017;8:1364.
25. **Campoccia D, Montanaro L, Arciola CR.** Extracellular DNA (eDNA). A major ubiquitous element of the bacterial biofilm architecture. *Int J Mol Sci* 2021;22:9100.
26. **Kobayashi K, Iwano M.** BslA(YuaB) forms a hydrophobic layer on the surface of *Bacillus subtilis* biofilms. *Mol Microbiol* 2012;85:51–66.
27. **Davison WM, Pitts B, Stewart PS.** Spatial and temporal patterns of biocide action against *Staphylococcus epidermidis* biofilms. *Antimicrob Agents Chemother* 2010;54:2920–2927.
28. **Bridier A, Dubois-Brissonnet F, Greub G, Thomas V, Briandet R.** Dynamics of the action of biocides in *Pseudomonas aeruginosa* biofilms. *Antimicrob Agents Chemother* 2011;55:2648–2654.
29. **Bridier A, Sanchez-Vizuete MDP, Le Coq D, Aymerich S, Meylheuc T, *et al.*** Biofilms of a bacillus subtilis hospital isolate protect *Staphylococcus* aureus from biocide action. *PLoS One* 2012;7:e44506.
30. **Epstein AK, Pokroy B, Seminara A, Aizenberg J.** Bacterial biofilm shows persistent resistance to liquid wetting and gas penetration. *Proc Natl Acad Sci* 2011;108:995–1000.
31. **Bas S, Kramer M, Stopar D.** Biofilm surface density determines biocide effectiveness. *Front Microbiol* 2017;8:2443.
32. **Shemesh M, Kolter R, Losick R.** The biocide chlorine dioxide stimulates biofilm formation in *Bacillus subtilis* by activation of the histidine kinase KinC. *J Bacteriol* 2010;192:6352–6356.
33. **Henly EL, Dowling JAR, Maingay JB, Lacey MM, Smith TJ, *et al.*** Biocide exposure induces changes in Susceptibility, Pathogenicity, and Biofilm Formation in Uropathogenic *Escherichia coli*. *Antimicrob Agents Chemother* 2019;63:e01892-18.
34. **Capita R, Riesco-Peláez F, Alonso-Hernando A, Alonso-Calleja C.** Exposure of *Escherichia coli* ATCC 12806 to sublethal concentrations of food-grade biocides influences its ability to form biofilm, resistance to antimicrobials, and ultrastructure. *Appl Environ Microbiol* 2014;80:1268–1280.
35. **Merchel Piovesan Pereira B, Wang X, Tagkopoulos I.** Short- and long-term transcriptomic responses of *Escherichia coli* to biocides: a systems analysis. *Appl Environ Microbiol* 2020;86:e00708-20.
36. **Singkham-In U, Phuengmaung P, Makjaroen J, Saisorn W, Bhunyakarnjanarat T, *et al.*** Chlorhexidine promotes Psl expression in *Pseudomonas aeruginosa* that enhances cell aggregation with preserved pathogenicity demonstrates an adaptation against antiseptic. *Int J Mol Sci* 2022;23:8308.
37. **Campoccia D, Montanaro L, Arciola CR.** Tracing the origins of extracellular DNA in bacterial biofilms: story of death and predation to community benefit. *Biofouling* 2021;37:1022–1039.
38. **Panlilio H, Rice CV.** The role of extracellular DNA in the formation, architecture, stability, and treatment of bacterial biofilms. *Biotechnol Bioeng* 2021;118:2129–2141.
39. **Jennings LK, Storek KM, Ledvina HE, Coulon C, Marmont LS, *et al.*** Pel is a cationic exopolysaccharide that cross-links extracellular DNA in the *Pseudomonas aeruginosa* biofilm matrix. *Proc Natl Acad Sci*2015;112:11353–11358.
40. **Tseng BS, Zhang W, Harrison JJ, Quach TP, Song JL, *et al.*** The extracellular matrix protects *Pseudomonas aeruginosa* biofilms by limiting the penetration of tobramycin. *Environ Microbiol* 2013;15:2865–2878.
41. **Chiang W-C, Nilsson M, Jensen PØ, Høiby N, Nielsen TE, *et al.*** Extracellular DNA shields against aminoglycosides in *Pseudomonas aeruginosa* biofilms. *Antimicrob Agents Chemother* 2013;57:2352–2361.
42. **Moshynets OV, Baranovskyi TP, Iungin OS, Kysil NP, Metelytsia LO, *et al.*** eDNA inactivation and biofilm inhibition by the PolymericBiocide polyhexamethylene guanidine hydrochloride (PHMG-Cl). *Int J Mol Sci* 2022;23:731.
43. **Heilmann S, Krishna S, Kerr B.** Why do bacteria regulate public goods by quorum sensing?-How the shapes of cost and benefit functions determine the form of optimal regulation. *Front Microbiol* 2015;6:767.
44. **Olwal CO, Ang'ienda PO, Ochiel DO.** Alternative sigma factor B (σ^B) and catalase enzyme contribute to *Staphylococcus epidermidis* biofilm's tolerance against physico-chemical disinfection. *Sci Rep* 2019;9:5355.
45. **Stewart PS, Roe F, Rayner J, Elkins JG, Lewandowski Z, *et al.*** Effect of catalase on hydrogen peroxide penetration into *Pseudomonas aeruginosa* biofilms. *Appl Environ Microbiol* 2000;66:836–838.
46. **White AN, Learman BS, Brauer AL, Armbruster CE.** Catalase activity is critical for *Proteus mirabilis* biofilm development, extracellular polymeric substance composition, and dissemination during catheter-associated urinary tract infection. *Infect Immun* 2021;89:e0017721.
47. **Scotti R, Nicolini L, Stringaro A, Gabbianelli R.** A study on prophagic and chromosomal sodC genes involvement in Escherichia coli O157:H7 biofilm formation and biofilm resistance to H_2O_2. *Ann Ist Super Sanita* 2015;51:62–66.
48. **Mukherjee S, Bassler BL.** Bacterial quorum sensing in complex and dynamically changing environments. *Nat Rev Microbiol* 2019;17:371–382.
49. **Abisado RG, Benomar S, Klaus JR, Dandekar AA, Chandler JR, *et al.*** Bacterial quorum sensing and microbial community interactions. *mBio* 2018;9:e02331-17.
50. **Nadell CD, Xavier JB, Foster KR.** The sociobiology of biofilms. *FEMS Microbiol Rev* 2009;33:206–224.
51. **Sakuragi Y, Kolter R.** Quorum-sensing regulation of the biofilm matrix genes (pel) of *Pseudomonas aeruginosa*. *J Bacteriol* 2007;189:5383–5386.
52. **Rickard AH, Palmer RJ, Blehert DS, Campagna SR, Semmelhack MF, *et al.*** Autoinducer 2: a concentration-dependent signal for mutualistic bacterial biofilm growth. *Mol Microbiol* 2006;60:1446–1456.
53. **Spoering AL, Gilmore MS.** Quorum sensing and DNA release in bacterial biofilms. *Curr Opin Microbiol* 2006;9:133–137.
54. **Vestby LK, Lönn-Stensrud J, Møretrø T, Langsrud S, Aamdal-Scheie A, *et al.*** A synthetic furanone potentiates the effect of disinfectants on Salmonella in biofilm. *J Appl Microbiol* 2010;108:771–778.
55. **Hassett DJ, Ma JF, Elkins JG, McDermott TR, Ochsner UA, *et al.*** Quorum sensing in *Pseudomonas aeruginosa* controls expression of catalase and superoxide dismutase genes and mediates biofilm susceptibility to hydrogen peroxide. *Mol Microbiol* 1999;34:1082–1093.
56. **Gholamrezazadeh M, Shakibaie MR, Monirzadeh F, Masoumi S, Hashemizadeh Z.** Effect of nano-silver, nano-copper, deconex and benzalkonium chloride on biofilm formation and expression of transcription regulatory quorum sensing gene (rh1R) in

drug-resistance *Pseudomonas aeruginosa* burn isolates. *Burns* 2018;44:700–708.

57. **Winans JB**, **Wucher BR**, **Nadell CD**. Multispecies biofilm architecture determines bacterial exposure to phages. *PLoS Biol* 2022;20:e3001913.
58. **Booth SC**, **Rice SA**. Influence of interspecies interactions on the spatial organization of dual species bacterial communities. *Biofilm* 2020;2:100035.
59. **Lee KWK**, **Periasamy S**, **Mukherjee M**, **Xie C**, **Kjelleberg S**, ***et al***. Biofilm development and enhanced stress resistance of a model, mixed-species community biofilm. *ISME J* 2014;8:894–907.
60. **Sanchez-Vizuete P**, **Le Coq D**, **Bridier A**, **Herry J-M**, **Aymerich S**, ***et al***. Identification of ypqP as a new *Bacillus subtilis* biofilm determinant that mediates the protection of *Staphylococcus aureus* against antimicrobial agents in mixed-species communities. *Appl Environ Microbiol* 2015;81:109–118.
61. **Sanchez-Vizuete P**, **Orgaz B**, **Aymerich S**, **Le Coq D**, **Briandet R**. Pathogens protection against the action of disinfectants in multispecies biofilms. *Front Microbiol* 2015;6:705.
62. **Pang XY**, **Yang YS**, **Yuk HG**. Biofilm formation and disinfectant resistance of *Salmonella* sp. in mono- and dual-species with *Pseudomonas aeruginosa*. *J Appl Microbiol* 2017;123:651–660.
63. **Burmølle M**, **Webb JS**, **Rao D**, **Hansen LH**, **Sørensen SJ**, ***et al***. Enhanced biofilm formation and increased resistance to antimicrobial agents and bacterial invasion are caused by synergistic interactions in multispecies biofilms. *Appl Environ Microbiol* 2006;72:3916–3923.
64. **Vacheva A**, **Ivanova R**, **Paunova-Krasteva T**, **Stoitsova S**. Released products of pathogenic bacteria stimulate biofilm formation by *Escherichia coli* K-12 strains. *Antonie Van Leeuwenhoek* 2012;102:105–119.
65. **Özkaya Ö**, **Xavier KB**, **Dionisio F**, **Balbontín R**, **O'Toole G**. Maintenance of microbial cooperation mediated by public goods in single- and multiple-trait scenarios. *J Bacteriol* 2017;199:e00297-17.
66. **Hagelueken G**, **Adams TM**, **Wiehlmann L**, **Widow U**, **Kolmar H**, ***et al***. The crystal structure of SdsA1, an alkylsulfatase from *Pseudomonas aeruginosa*, defines a third class of sulfatases. *Proc Natl Acad Sci*2006;103:7631–7636.
67. **López D**, **Vlamakis H**, **Losick R**, **Kolter R**. Cannibalism enhances biofilm development in Bacillus subtilis. *Mol Microbiol* 2009;74:609–618.
68. **Houry A**, **Gohar M**, **Deschamps J**, **Tischenko E**, **Aymerich S**, ***et al***. Bacterial swimmers that infiltrate and take over the biofilm matrix. *Proc Natl Acad Sci*2012;109:13088–13093.
69. **Ravel G**, **Bergmann M**, **Trubuil A**, **Deschamps J**, **Briandet R**, ***et al***. Inferring characteristics of bacterial swimming in biofilm matrix from time-lapse confocal laser scanning microscopy. *Elife* 2022;11:e76513.
70. **Boles BR**, **Thoendel M**, **Singh PK**. Self-generated diversity produces "insurance effects" in biofilm communities. *Proc Natl Acad Sci*2004;101:16630–16635.
71. **Maillard J-Y**. Bacterial target sites for biocide action. *J Appl Microbiol* 2002;92:16S–27S.
72. **Fernandes S**, **Gomes IB**, **Sousa SF**, **Simões M**. Antimicrobial susceptibility of persister biofilm cells of *Bacillus cereus* and *Pseudomonas fluorescens*. *Microorganisms* 2022;10:160.
73. **Noll M**, **Trunzer K**, **Vondran A**, **Vincze S**, **Dieckmann R**, ***et al***. Benzalkonium chloride induces a VBNC state in *Listeria monocytogenes*. *Microorganisms* 2020;8:184.
74. **Robben C**, **Fister S**, **Witte AK**, **Schoder D**, **Rossmanith P**, ***et al***. Induction of the viable but non-culturable state in bacterial pathogens by household cleaners and inorganic salts. *Sci Rep* 2018;8:15132.
75. **Wilmaerts D**, **Windels EM**, **Verstraeten N**, **Michiels J**. General mechanisms leading to persister formation and awakening. *Trends Genet* 2019;35:401–411.
76. **Kushwaha GS**, **Oyeyemi BF**, **Bhavesh NS**. Stringent response protein as a potential target to intervene persistent bacterial infection. *Biochimie* 2019;165:67–75.
77. **Pacios O**, **Blasco L**, **Bleriot I**, **Fernandez-Garcia L**, **Ambroa A**, ***et al***. (p)ppGpp and its role in bacterial persistence: new challenges. *Antimicrob Agents Chemother* 2020;64:e01283-20.
78. **Yin W-L**, **Xie Z-Y**, **Zeng Y-H**, **Zhang J**, **Long H**, ***et al***. Two (p)ppGpp synthetase genes, *relA* and *spoT*, are involved in regulating cell motility, exopolysaccharides production, and biofilm formation of *Vibrio alginolyticus*. *Front Microbiol* 2022;13:858559.
79. **Kim H-M**, **Davey ME**. Synthesis of ppGpp impacts type IX secretion and biofilm matrix formation in *Porphyromonas gingivalis*. *NPJ Biofilms Microbiomes* 2020;6:5.
80. **Nguyen D**, **Joshi-Datar A**, **Lepine F**, **Bauerle E**, **Olakanmi O**, ***et al***. Active starvation responses mediate antibiotic tolerance in biofilms and nutrient-limited bacteria. *Science* 2011;334:982–986.
81. **Ortega Morente E**, **Fernández-Fuentes MA**, **Grande Burgos MJ**, **Abriouel H**, **Pérez Pulido R**, ***et al***. Biocide tolerance in bacteria. *Int J Food Microbiol* 2013;162:13–25.
82. **Du Z**, **Nandakumar R**, **Nickerson KW**, **Li X**. Proteomic adaptations to starvation prepare *Escherichia coli* for disinfection tolerance. *Water Res* 2015;69:110–119.
83. **Zhang S-P**, **Feng H-Z**, **Wang Q**, **Quan S-W**, **Yu X-Q**, ***et al***. Proteomic analysis reveals the mechanism of different environmental stress-induced tolerance of *Pseudomonas aeruginosa* to monochloramine disinfection. *J Hazard Mater* 2021;417:126082.
84. **Fortuna A**, **Collalto D**, **Schiaffi V**, **Pastore V**, **Visca P**, ***et al***. The Pseudomonas aeruginosa DksA1 protein is involved in H_2O_2 tolerance and within-macrophages survival and can be replaced by DksA2. *Sci Rep* 2022;12:10404.
85. **Khakimova M**, **Ahlgren HG**, **Harrison JJ**, **English AM**, **Nguyen D**. The stringent response controls catalases in *Pseudomonas aeruginosa* and is required for hydrogen peroxide and antibiotic tolerance. *J Bacteriol* 2013;195:2011–2020.
86. **Bhardwaj P**, **Hans A**, **Ruikar K**, **Guan Z**, **Palmer KL**. Reduced chlorhexidine and daptomycin susceptibility in vancomycin-resistant *Enterococcus faecium* after serial chlorhexidine exposure. *Antimicrob Agents Chemother* 2018;62:e01235-17.
87. **Nordholt N**, **Kanaris O**, **Schmidt SBI**, **Schreiber F**. Persistence against benzalkonium chloride promotes rapid evolution of tolerance during periodic disinfection. *Nat Commun* 2021;12:6792.
88. **Podlesek Z**, **Žgur Bertok D**. The DNA damage inducible SOS response is a key player in the generation of bacterial persister cells and population wide tolerance. *Front Microbiol* 2020;11:1785.
89. **Durfee T**, **Hansen A-M**, **Zhi H**, **Blattner FR**, **Jin DJ**. Transcription profiling of the stringent response in *Escherichia coli*. *J Bacteriol* 2008;190:1084–1096.
90. **Allen MJ**, **White GF**, **Morby AP**. The response of *Escherichia coli* to exposure to the biocide polyhexamethylene biguanide. *Microbiology (Reading)* 2006;152:989–1000.
91. **Ceragioli M**, **Mols M**, **Moezelaar R**, **Ghelardi E**, **Senesi S**, ***et al***. Comparative transcriptomic and phenotypic analysis of the responses of *Bacillus cereus* to various disinfectant treatments. *Appl Environ Microbiol* 2010;76:3352–3360.
92. **Peeters E**, **Sass A**, **Mahenthiralingam E**, **Nelis H**, **Coenye T**. Transcriptional response of *Burkholderia cenocepacia* J2315 sessile cells to treatments with high doses of hydrogen peroxide and sodium hypochlorite. *BMC Genomics* 2010;11:90.
93. **Wang S**, **Xiao X**, **Qiu M**, **Wang W**, **Xiao Y**, ***et al***. Transcriptomic responses of *Salmonella enterica* serovars enteritidis in sodium hypochlorite. *Front Cell Infect Microbiol* 2022;12:853064.
94. **Gerdes K**, **Maisonneuve E**. Bacterial persistence and toxin-antitoxin loci. *Annu Rev Microbiol* 2012;66:103–123.
95. **Dörr T**, **Vulić M**, **Lewis K**. Ciprofloxacin causes persister formation by inducing the TisB toxin in *Escherichia coli*. *PLoS Biol* 2010;8:e1000317.

96. Schumacher MA, Piro KM, Xu W, Hansen S, Lewis K, *et al*. Molecular mechanisms of HipA-mediated multidrug tolerance and its neutralization by HipB. *Science* 2009;323:396–401.
97. Germain E, Castro-Roa D, Zenkin N, Gerdes K. Molecular mechanism of bacterial persistence by HipA. *Mol Cell* 2013;52:248–254.
98. Karimaei S, Kazem Aghamir SM, Foroushani AR, Pourmand MR. Antibiotic tolerance in biofilm persister cells of *Staphylococcus aureus* and expression of toxin-antitoxin system genes. *Microb Pathog* 2021;159:105126.
99. Chan W, Domenech M, Moreno-Córdoba I, Navarro-Martínez V, Nieto C, *et al*. (n.d.) The *Streptococcus pneumoniae* yefM-yoeB and relBE toxin-antitoxin operons participate in oxidative stress and biofilm formation. *Toxins*;10:378.
100. Sun C, Guo Y, Tang K, Wen Z, Li B, *et al*. MqsR/MqsA toxin/antitoxin system regulates persistence and biofilm formation in *Pseudomonas putida* KT2440. *Front Microbiol* 2017;8:840.
101. Wang X, Wood TK. Toxin-antitoxin systems influence biofilm and persister cell formation and the general stress response. *Appl Environ Microbiol* 2011;77:5577–5583.
102. Bleriot I, Blasco L, Delgado-Valverde M, Gual de Torella A, Ambroa A, *et al*. Mechanisms of tolerance and resistance to chlorhexidine in clinical strains of *Klebsiella pneumoniae* producers of carbapenemase: role of new type II toxin-antitoxin system, PemIK. *Toxins* 2020;12:566.
103. Fernández-García L, Fernandez-Cuenca F, Blasco L, López-Rojas R, Ambroa A, *et al*. Relationship between tolerance and persistence mechanisms in acinetobacter baumannii strains with AbkAB toxin-antitoxin system. *Antimicrob Agents Chemother* 2018;62:e00250-18.
104. Pu Y, Zhao Z, Li Y, Zou J, Ma Q, *et al*. Enhanced efflux activity facilitates drug tolerance in dormant bacterial cells. *Mol Cell* 2016;62:284–294.
105. Alav I, Sutton JM, Rahman KM. Role of bacterial efflux pumps in biofilm formation. *J Antimicrob Chemother* 2018;73:2003–2020.
106. Kvist M, Hancock V, Klemm P. Inactivation of efflux pumps abolishes bacterial biofilm formation. *Appl Environ Microbiol* 2008;74:7376–7382.
107. Bay DC, Stremick CA, Slipski CJ, Turner RJ. Secondary multidrug efflux pump mutants alter *Escherichia coli* biofilm growth in the presence of cationic antimicrobial compounds. *Res Microbiol* 2017;168:208–221.
108. Wand ME, Darby EM, Blair JMA, Sutton JM. Contribution of the efflux pump AcrAB-TolC to the tolerance of chlorhexidine and other biocides in *Klebsiella* spp. *J Med Microbiol* 2022;71:001496.
109. Yamasaki S, Wang L-Y, Hirata T, Hayashi-Nishino M, Nishino K. Multidrug efflux pumps contribute to *Escherichia coli* biofilm maintenance. *Int J Antimicrob Agents* 2015;45:439–441.
110. Richmond GE, Evans LP, Anderson MJ, Wand ME, Bonney LC, *et al*. The *Acinetobacter baumannii* two-component system AdeRS regulates genes required for multidrug efflux, biofilm formation and virulence in a strain-specific manner. *mBio* 2016;7:e00852-16.
111. Gillis RJ, White KG, Choi K-H, Wagner VE, Schweizer HP, *et al*. Molecular basis of azithromycin-resistant *Pseudomonas aeruginosa* biofilms. *Antimicrob Agents Chemother* 2005;49:3858–3867.
112. Fraud S, Campigotto AJ, Chen Z, Poole K. MexCD-OprJ multidrug efflux system of *Pseudomonas* aeruginosa: involvement in chlorhexidine resistance and induction by membrane-damaging agents dependent upon the AlgU stress response sigma factor. *Antimicrob Agents Chemother* 2008;52:4478–4482.
113. Migliaccio A, Esposito EP, Bagattini M, Berisio R, Triassi M, *et al*. Inhibition of AdeB, AceI, and AmvA efflux pumps restores chlorhexidine and benzalkonium susceptibility in *Acinetobacter baumannii* ATCC 19606. *Front Microbiol* 2021;12:790263.
114. Short FL, Liu Q, Shah B, Clift HE, Naidu V, *et al*. The *Acinetobacter baumannii* disinfectant resistance protein, AmvA, is a spermidine and spermine efflux pump. *Commun Biol* 2021;4:1114.
115. LaBreck PT, Bochi-Layec AC, Stanbro J, Dabbah-Krancher G, Simons MP, *et al*. Systematic analysis of efflux pump-mediated antiseptic resistance in *Staphylococcus aureus* suggests a need for greater antiseptic stewardship. *mSphere* 2020;5:e00959-19.
116. Truong-Bolduc QC, Wang Y, Reedy JL, Vyas JM, Hooper DC. *Staphylococcus aureus* efflux pumps and tolerance to ciprofloxacin and chlorhexidine following induction by mupirocin. *Antimicrob Agents Chemother* 2022;66:e0184521.
117. Zimmermann S, Klinger-Strobel M, Bohnert JA, Wendler S, Rödel J, *et al*. Clinically approved drugs inhibit the *Staphylococcus aureus* multidrug NorA efflux pump and reduce biofilm formation. *Front Microbiol* 2019;10:2762.
118. Kovacevic J, Ziegler J, Wałecka-Zacharska E, Reimer A, Kitts DD, *et al*. Tolerance of *Listeria monocytogenes* to quaternary ammonium sanitizers is mediated by a novel efflux pump encoded by emrE. *Appl Environ Microbiol* 2016;82:939–953.
119. Matsumura K, Furukawa S, Ogihara H, Morinaga Y. Roles of multidrug efflux pumps on the biofilm formation of *Escherichia coli* K-12. *Biocontrol Sci* 2011;16:69–72.
120. Slipski CJ, Jamieson TR, Zhanel GG, Bay DC. Riboswitch-associated guanidinium-selective efflux pumps frequently transmitted on proteobacterial plasmids increase *Escherichia coli* biofilm tolerance to disinfectants. *J Bacteriol* 2020;202:e00104-20.
121. Vergalli J, Bodrenko IV, Masi M, Moynié L, Acosta-Gutiérrez S, *et al*. Porins and small-molecule translocation across the outer membrane of gram-negative bacteria. *Nat Rev Microbiol* 2020;18:164–176.
122. Li X-Z, Plésiat P, Nikaido H. The challenge of efflux-mediated antibiotic resistance in gram-negative bacteria. *Clin Microbiol Rev* 2015;28:337–418.
123. Orme R, Douglas CWI, Rimmer S, Webb M. Proteomic analysis of *Escherichia coli* biofilms reveals the overexpression of the outer membrane protein OmpA. *Proteomics* 2006;6:4269–4277.
124. Gao J, Han Z, Li P, Zhang H, Du X, *et al*. Outer membrane protein F is involved in biofilm formation, virulence and antibiotic resistance in *Cronobacter sakazakii*. *Microorganisms* 2021;9:2338.
125. Sauer K. The genomics and proteomics of biofilm formation. *Genome Biol* 2003;4:219.
126. El-Khatib M, Nasrallah C, Lopes J, Tran Q-T, Tetreau G, *et al*. Porin self-association enables cell-to-cell contact in *Providencia stuartii* floating communities. *Proc Natl Acad Sci* 2018;115:E2220–E2228.
127. Whitfield GB, Marmont LS, Ostaszewski A, Rich JD, Whitney JC, *et al*. Pel polysaccharide biosynthesis requires an inner membrane complex comprised of PelD, PelE, PelF, and PelG. *J Bacteriol* 2020;202:e00684-19.
128. Bore E, Hébraud M, Chafsey I, Chambon C, Skjæret C, *et al*. Adapted tolerance to benzalkonium chloride in *Escherichia coli* K-12 studied by transcriptome and proteome analyses. *Microbiology (Reading)* 2007;153:935–946.
129. Fernández-Cuenca F, Tomás M, Caballero-Moyano F-J, Bou G, Martínez-Martínez L, *et al*. Reduced susceptibility to biocides in *Acinetobacter baumannii*: association with resistance to antimicrobials, epidemiological behaviour, biological cost and effect on the expression of genes encoding porins and efflux pumps. *J Antimicrob Chemother* 2015;70:3222–3229.
130. Levin-Reisman I, Ronin I, Gefen O, Braniss I, Shoresh N, *et al*. Antibiotic tolerance facilitates the evolution of resistance. *Science* 2017;355:826–830.
131. Levin-Reisman I, Brauner A, Ronin I, Balaban NQ. Epistasis between antibiotic tolerance, persistence, and resistance mutations. *Proc Natl Acad Sci* 2019;116:14734–14739.
132. Wang D, Ning Q, Deng Z, Zhang M, You J. Role of environmental stresses in elevating resistance mutations in bacteria: phenomena and mechanisms. *Environ Pollut* 2022;307:119603.
133. Windels EM, Michiels JE, Fauvart M, Wenseleers T, Van den Bergh B, *et al*. Bacterial persistence promotes the evolution of antibiotic resistance by increasing survival and mutation rates. *ISME J* 2019;13:1239–1251.

134. **Crane JK**, **Alvarado CL**, **Sutton MD**. Role of the SOS response in the generation of antibiotic resistance *in vivo*. *Antimicrob Agents Chemother* 2021;65:e0001321.

135. **Meunier A**, **Nerich V**, **Fagnoni-Legat C**, **Richard M**, **Mazel D**, ***et al***. Enhanced emergence of antibiotic-resistant pathogenic bacteria after *in vitro* induction with cancer chemotherapy drugs. *J Antimicrob Chemother* 2019;74:1572–1577.

136. **Händel N**, **Hoeksema M**, **Freijo Mata M**, **Brul S**, **ter Kuile BH**. Effects of stress, reactive oxygen species, and the SOS response on De Novo acquisition of antibiotic resistance in *Escherichia coli*. *Antimicrob Agents Chemother* 2015;60:1319–1327.

137. **Schmidt SBI**, **Rodríguez-Rojas A**, **Rolff J**, **Schreiber F**. Biocides used as material preservatives modify rates of de novo mutation and horizontal gene transfer in bacteria. *J Hazard Mater* 2022;437:129280.

138. **Russell AD**. Similarities and differences in the responses of microorganisms to biocides. *J Antimicrob Chemother* 2003;52:750–763.

139. **Ryder VJ**, **Chopra I**, **O'Neill AJ**. Increased mutability of *Staphylococci* in biofilms as a consequence of oxidative stress. *PLoS One* 2012;7:e47695.

140. **Qi L**, **Wu X-C**, **Zheng D-Q**. Hydrogen peroxide, a potent inducer of global genomic instability. *Curr Genet* 2019;65:913–917.

141. **El Meouche I**, **Dunlop MJ**. Heterogeneity in efflux pump expression predisposes antibiotic-resistant cells to mutation. *Science* 2018;362:686–690.

142. **Lee IPA**, **Eldakar OT**, **Gogarten JP**, **Andam CP**. Bacterial cooperation through horizontal gene transfer. *Trends Ecol Evol* 2022;37:223–232.

143. **Abe K**, **Nomura N**, **Suzuki S**. Biofilms: hot spots of horizontal gene transfer (HGT) in aquatic environments, with a focus on a new HGT mechanism. *FEMS Microbiol Ecol* 2020;96:fiaa031.

144. **Stalder T**, **Cornwell B**, **Lacroix J**, **Kohler B**, **Dixon S**, ***et al***. Evolving populations in biofilms contain more persistent plasmids. *Mol Biol Evol* 2020;37:1563–1576.

145. **Beaber JW**, **Hochhut B**, **Waldor MK**. SOS response promotes horizontal dissemination of antibiotic resistance genes. *Nature* 2004;427:72–74.

146. **Baharoglu Z**, **Bikard D**, **Mazel D**. Conjugative DNA transfer induces the bacterial SOS response and promotes antibiotic resistance development through integron activation. *PLoS Genet* 2010;6:e1001165.

147. **Madsen JS**, **Burmølle M**, **Hansen LH**, **Sørensen SJ**. The interconnection between biofilm formation and horizontal gene transfer. *FEMS Immunol Med Microbiol* 2012;65:183–195.

148. **Røder HL**, **Trivedi U**, **Russel J**, **Kragh KN**, **Herschend J**, ***et al***. Biofilms can act as plasmid reserves in the absence of plasmid specific selection. *NPJ Biofilms Microbiomes* 2021;7:78.

149. **Ghigo JM**. Natural conjugative plasmids induce bacterial biofilm development. *Nature* 2001;412:442–445.

150. **May T**, **Okabe S**. *Escherichia coli* harboring a natural IncF conjugative F plasmid develops complex mature biofilms by stimulating synthesis of colanic acid and Curli. *J Bacteriol* 2008;190:7479–7490.

151. **Russell AD**. Plasmids and bacterial resistance to biocides. *J Appl Microbiol* 1997;83:155–165.

152. **LaBreck PT**, **Rice GK**, **Paskey AC**, **Elassal EM**, **Cer RZ**, ***et al***. Conjugative transfer of a novel *Staphylococcal* plasmid encoding the biocide resistance gene, *qacA*. *Front Microbiol* 2018;9:2664.

153. **Kropac AC**, **Eshwar AK**, **Stephan R**, **Tasara T**. New insights on the role of the pLMST6 plasmid in *Listeria monocytogenes* biocide tolerance and virulence. *Front Microbiol* 2019;10:1538.

154. **Vijayakumar R**, **Sandle T**. A review on biocide reduced susceptibility due to plasmid-borne antiseptic-resistant genes-special notes on pharmaceutical environmental isolates. *J Appl Microbiol* 2019;126:1011–1022.

155. **Roedel A**, **Vincze S**, **Projahn M**, **Roesler U**, **Robé C**, ***et al***. Genetic but no phenotypic associations between biocide tolerance and antibiotic resistance in *Escherichia coli* from German broiler fattening farms. *Microorganisms* 2021;9:651.

156. **Zhang Y**, **Gu AZ**, **He M**, **Li D**, **Chen J**. Subinhibitory concentrations of disinfectants promote the horizontal transfer of multidrug resistance genes within and across genera. *Environ Sci Technol* 2017;51:570–580.

157. **Li Y-H**, **Lau PCY**, **Lee JH**, **Ellen RP**, **Cvitkovitch DG**. Natural genetic transformation of *Streptococcus mutans* growing in biofilms. *J Bacteriol* 2001;183:897–908.

158. **Jakubovics NS**, **Burgess JG**. Extracellular DNA in oral microbial biofilms. *Microbes Infect* 2015;17:531–537.

159. **Jones IA**, **Joshi LT**. Biocide use in the antimicrobial era: a review. *Molecules* 2021;26:2276.

160. **Itzek A**, **Zheng L**, **Chen Z**, **Merritt J**, **Kreth J**. Hydrogen peroxide-dependent DNA release and transfer of antibiotic resistance genes in *Streptococcus gordonii*. *J Bacteriol* 2011;193:6912–6922.

161. **Hannan S**, **Ready D**, **Jasni AS**, **Rogers M**, **Pratten J**, ***et al***. Transfer of antibiotic resistance by transformation with eDNA within oral biofilms. *FEMS Immunol Med Microbiol* 2010;59:345–349.

162. **Liu S-S**, **Qu H-M**, **Yang D**, **Hu H**, **Liu W-L**, ***et al***. Chlorine disinfection increases both intracellular and extracellular antibiotic resistance genes in a full-scale wastewater treatment plant. *Water Res* 2018;136:131–136.

163. **Olivares Pacheco J**, **Alvarez-Ortega C**, **Alcalde Rico M**, **Martínez JL**, **Davies JE**. Metabolic compensation of fitness costs is a general outcome for antibiotic-resistant *Pseudomonas aeruginosa* mutants overexpressing efflux pumps. *mBio* 2017;8:e00500-17.

164. **San Millan A**, **MacLean RC**, **Baquero F**, **Bouza E**, **Gutiérrez-Fuentes JA**. Fitness costs of plasmids: a limit to plasmid transmission. *Microbiol Spectr* 2017;5.

165. **Penesyan A**, **Paulsen IT**, **Kjelleberg S**, **Gillings MR**. Three faces of biofilms: a microbial lifestyle, a nascent multicellular organism, and an incubator for diversity. *NPJ Biofilms Microbiomes* 2021;7:80.

166. **France MT**, **Cornea A**, **Kehlet-Delgado H**, **Forney LJ**. Spatial structure facilitates the accumulation and persistence of antibiotic-resistant mutants in biofilms. *Evol Appl* 2019;12:498–507.

167. **Jacques M**, **Malouin F**. One health-one biofilm. *Vet Res* 2022;53:51.

168. **Rodríguez-Melcón C**, **Riesco-Peláez F**, **García-Fernández C**, **Alonso-Calleja C**, **Capita R**. Susceptibility of *Listeria monocytogenes* planktonic cultures and biofilms to sodium hypochlorite and benzalkonium chloride. *Food Microbiol* 2019;82:533–540.

169. **Capita R**, **Vicente-Velasco M**, **Rodríguez-Melcón C**, **García-Fernández C**, **Carballo J**, ***et al***. Effect of low doses of biocides on the antimicrobial resistance and the biofilms of *Cronobacter sakazakii* and *Yersinia enterocolitica*. *Sci Rep* 2019;9:15905.

170. **Zhang Y**, **Ge H**, **Lin W**, **Song Y**, **Ge F**, ***et al***. Effect of different disinfection treatments on the adhesion and separation of biofilm on stainless steel surface. *Water Sci Technol* 2021;83:877–885.

171. **Techaruvichit P**, **Takahashi H**, **Kuda T**, **Miya S**, **Keeratipibul S**, ***et al***. Adaptation of *Campylobacter jejuni* to biocides used in the food industry affects biofilm structure, adhesion strength, and cross-resistance to clinical antimicrobial compounds. *Biofouling* 2016;32:827–839.

172. **Daer S**, **Goodwill JE**, **Ikuma K**. Effect of ferrate and monochloramine disinfection on the physiological and transcriptomic response of *Escherichia coli* at late stationary phase. *Water Res* 2021;189:116580.

173. **Slany M**, **Oppelt J**, **Cincarova L**. Formation of *Staphylococcus aureus* biofilm in the presence of sublethal concentrations of disinfectants studied via a transcriptomic analysis using transcriptome sequencing (RNA-seq). *Appl Environ Microbiol* 2017;83:e01643-17.

174. **Forbes S**, **Morgan N**, **Humphreys GJ**, **Amézquita A**, **Mistry H**, ***et al***. Loss of function in *Escherichia coli* exposed to environmentally relevant concentrations of benzalkonium chloride. *Appl Environ Microbiol* 2019;85:e02417-18.

175. **Romeu MJ**, **Rodrigues D**, **Azeredo J**. Effect of sub-lethal chemical disinfection on the biofilm forming ability, resistance to

antibiotics and expression of virulence genes of *Salmonella* Enteritidis biofilm-surviving cells. *Biofouling* 2020;36:101–112.

176. **Langsrud S**, **Sundheim G**, **Holck AL**. Cross-resistance to antibiotics of *Escherichia coli* adapted to benzalkonium chloride or exposed to stress-inducers. *J Appl Microbiol* 2004;96:201–208.
177. **Pagedar A**, **Singh J**, **Batish VK**. Efflux mediated adaptive and cross resistance to ciprofloxacin and benzalkonium chloride in *Pseudomonas aeruginosa* of dairy origin. *J Basic Microbiol* 2011;51:289–295.
178. **Tattawasart U**, **Maillard J-Y**, **Furr JR**, **Russell AD**. Outer membrane changes in *Pseudomonas stutzeri* resistant to chlorhexidine diacetate and cetylpyridinium chloride. *Int J Antimicrob Agents* 2000;16:233–238.
179. **Gadea R**, **Fernández Fuentes MÁ**, **Pérez Pulido R**, **Gálvez A**, **Ortega E**. Adaptive tolerance to phenolic biocides in bacteria from organic foods: effects on antimicrobial susceptibility and tolerance to physical stresses. *Food Res Int* 2016;85:131–143.
180. **Russell AD**, **Tattawasart U**, **Maillard JY**, **Furr JR**. Possible link between bacterial resistance and use of antibiotics and biocides. *Antimicrob Agents Chemother* 1998;42:2151.
181. **Chen L**, **Chavda KD**, **Fraimow HS**, **Mediavilla JR**, **Melano RG**, ***et al***. Complete nucleotide sequences of blaKPC-4- and blaKPC-5-harboring IncN and IncX plasmids from *Klebsiella pneumoniae* strains isolated in New Jersey. *Antimicrob Agents Chemother* 2013;57:269–276.
182. **Kücken D**, **Feucht H**, **Kaulfers P**. Association of qacE and qacE-Delta1 with multiple resistance to antibiotics and antiseptics in clinical isolates of gram-negative bacteria. *FEMS Microbiol Lett* 2000;183:95–98.
183. **Cottell A**, **Denyer SP**, **Hanlon GW**, **Ochs D**, **Maillard J-Y**. Triclosan-tolerant bacteria: changes in susceptibility to antibiotics. *J Hosp Infect* 2009;72:71–76.
184. **Futoma-Kołoch B**, **Dudek B**, **Kapczyńska K**, **Krzyżewska E**, **Wańczyk M**, ***et al***. Relationship of triamine-biocide tolerance of *Salmonella enterica* serovar Senftenberg to antimicrobial susceptibility, serum resistance and outer membrane proteins. *Int J Mol Sci* 2017;18:1459.
185. **Li M**, **He Y**, **Sun J**, **Li J**, **Bai J**, ***et al***. Chronic exposure to an environmentally relevant triclosan concentration induces persistent triclosan resistance but reversible antibiotic tolerance in *Escherichia coli*. *Environ Sci Technol* 2019;53:3277–3286.
186. **Adkin P**, **Hitchcock A**, **Smith LJ**, **Walsh SE**. Priming with biocides: a pathway to antibiotic resistance? *J Appl Microbiol* 2022;133:830–841.
187. **Knapp L**, **Rushton L**, **Stapleton H**, **Sass A**, **Stewart S**, ***et al***. The effect of cationic microbicide exposure against *Burkholderia cepacia* complex (Bcc); the use of *Burkholderia lata* strain 383 as a model bacterium. *J Appl Microbiol* 2013;115:1117–1126.
188. **Curiao T**, **Marchi E**, **Grandgirard D**, **León-Sampedro R**, **Viti C**, ***et al***. Multiple adaptive routes of *Salmonella enterica* typhimurium to biocide and antibiotic exposure. *BMC Genomics* 2016;17:491.
189. **Pál C**, **Papp B**, **Lázár V**. Collateral sensitivity of antibiotic-resistant microbes. *Trends Microbiol* 2015;23:401–407.
190. **Li X-Z**, **Nikaido H**. Efflux-mediated drug resistance in bacteria: an update. *Drugs* 2009;69:1555–1623.
191. **Buckley AM**, **Webber MA**, **Cooles S**, **Randall LP**, **La Ragione RM**, ***et al***. The AcrAB-TolC efflux system of *Salmonella enterica* serovar Typhimurium plays a role in pathogenesis. *Cell Microbiol* 2006;8:847–856.
192. **Webber MA**, **Bailey AM**, **Blair JMA**, **Morgan E**, **Stevens MP**, ***et al***. The global consequence of disruption of the AcrAB-TolC efflux pump in Salmonella enterica includes reduced expression of SPI-1 and other attributes required to infect the host. *J Bacteriol* 2009;191:4276–4285.
193. **Alcalde-Rico M**, **Hernando-Amado S**, **Blanco P**, **Martínez JL**. Multidrug efflux pumps at the crossroad between antibiotic resistance and bacterial virulence. *Front Microbiol* 2016;7:1483.
194. **Hirakata Y**, **Srikumar R**, **Poole K**, **Gotoh N**, **Suematsu T**, ***et al***. Multidrug efflux systems play an important role in the invasiveness of *Pseudomonas aeruginosa*. *J Exp Med* 2002;196:109–118.
195. **Nontaleerak B**, **Duang-Nkern J**, **Wongsaroj L**, **Trinachartvanit W**, **Romsang A**, ***et al***. Roles of RcsA, an AhpD family protein, in reactive chlorine stress resistance and virulence in *Pseudomonas aeruginosa*. *Appl Environ Microbiol* 2020;86:e01480-20.
196. **Randall LP**, **Cooles SW**, **Coldham NG**, **Penuela EG**, **Mott AC**, ***et al***. Commonly used farm disinfectants can select for mutant *Salmonella enterica* serovar Typhimurium with decreased susceptibility to biocides and antibiotics without compromising virulence. *J Antimicrob Chemother* 2007;60:1273–1280.
197. **Karatzas KAG**, **Webber MA**, **Jorgensen F**, **Woodward MJ**, **Piddock LJV**, ***et al***. Prolonged treatment of *Salmonella enterica* serovar typhimurium with commercial disinfectants selects for multiple antibiotic resistance, increased efflux and reduced invasiveness. *J Antimicrob Chemother* 2007;60:947–955.
198. **Wand ME**, **Bock LJ**, **Bonney LC**, **Sutton JM**. Mechanisms of increased resistance to chlorhexidine and cross-resistance to colistin following exposure of *Klebsiella pneumoniae* clinical isolates to chlorhexidine. *Antimicrob Agents Chemother* 2017;61:e01162-16.
199. **Kremer PHC**, **Lees JA**, **Koopmans MM**, **Ferwerda B**, **Arends AWM**, ***et al***. Benzalkonium tolerance genes and outcome in *Listeria monocytogenes* meningitis. *Clin Microbiol Infect* 2017;23:265.
200. **Karatzas KAG**, **Randall LP**, **Webber M**, **Piddock LJV**, **Humphrey TJ**, ***et al***. Phenotypic and proteomic characterization of multiply antibiotic-resistant variants of *Salmonella enterica* serovar typhimurium selected following exposure to disinfectants. *Appl Environ Microbiol* 2008;74:1508–1516.
201. **Whitehead RN**, **Overton TW**, **Kemp CL**, **Webber MA**. Exposure of *Salmonella enterica* serovar typhimurium to high level biocide challenge can select multidrug resistant mutants in a single step. *PLoS One* 2011;6:e22833.
202. **Lu J**, **Jin M**, **Nguyen SH**, **Mao L**, **Li J**, ***et al***. Non-antibiotic antimicrobial triclosan induces multiple antibiotic resistance through genetic mutation. *Environ Int* 2018;118:257–265.
203. **Jia Y**, **Lu H**, **Zhu L**. Molecular mechanism of antibiotic resistance induced by mono- and twin-chained quaternary ammonium compounds. *Sci Total Environ* 2022;832:155090.
204. **Zhang Y**, **Zhao Y**, **Xu C**, **Zhang X**, **Li J**, ***et al***. Chlorhexidine exposure of clinical *Klebsiella pneumoniae* strains leads to acquired resistance to this disinfectant and to colistin. *Int J Antimicrob Agents* 2019;53:864–867.
205. **Pumbwe L**, **Randall LP**, **Woodward MJ**, **Piddock LJV**. Evidence for multiple-antibiotic resistance in *Campylobacter jejuni* not mediated by CmeB or CmeF. *Antimicrob Agents Chemother* 2005;49:1289–1293.
206. **Kaatz GW**, **McAleese F**, **Seo SM**. Multidrug resistance in *Staphylococcus* aureus due to overexpression of a novel multidrug and toxin extrusion (MATE) transport protein. *Antimicrob Agents Chemother* 2005;49:1857–1864.
207. **Chuanchuen R**, **Beinlich K**, **Hoang TT**, **Becher A**, **Karkhoff-Schweizer RR**, ***et al***. Cross-resistance between triclosan and antibiotics in *Pseudomonas aeruginosa* is mediated by multidrug efflux pumps: exposure of a susceptible mutant strain to triclosan selects nfxB mutants overexpressing MexCD-OprJ. *Antimicrob Agents Chemother* 2001;45:428–432.
208. **Morita Y**, **Murata T**, **Mima T**, **Shiota S**, **Kuroda T**, ***et al***. Induction of mexCD-oprJ operon for a multidrug efflux pump by disinfectants in wild-type *Pseudomonas aeruginosa* PAO1. *J Antimicrob Chemother* 2003;51:991–994.
209. **Tag ElDein MA**, **Yassin AS**, **El-Tayeb O**, **Kashef MT**. Chlorhexidine leads to the evolution of antibiotic-resistant *Pseudomonas aeruginosa*. *Eur J Clin Microbiol Infect Dis* 2021;40:2349–2361.
210. **Hansen LH**, **Jensen LB**, **Sørensen HI**, **Sørensen SJ**. Substrate specificity of the OqxAB multidrug resistance pump in *Escherichia coli* and selected enteric bacteria. *J Antimicrob Chemother* 2007;60:145–147.

211. **He G-X**, **Kuroda T**, **Mima T**, **Morita Y**, **Mizushima T**, ***et al***. An H(+)-coupled multidrug efflux pump, PmpM, a member of the MATE family of transporters, from *Pseudomonas aeruginosa*. *J Bacteriol* 2004;186:262–265.

212. **Sanchez P**, **Moreno E**, **Martinez JL**. The biocide triclosan selects *Stenotrophomonas maltophilia* mutants that overproduce the SmeDEF multidrug efflux pump. *Antimicrob Agents Chemother* 2005;49:781–782.

213. **Tkachenko O**, **Shepard J**, **Aris VM**, **Joy A**, **Bello A**, ***et al***. A triclosan-ciprofloxacin cross-resistant mutant strain of *Staphylococcus aureus* displays an alteration in the expression of several cell membrane structural and functional genes. *Res Microbiol* 2007;158:651–658.

214. **Parikh SL**, **Xiao G**, **Tonge PJ**. Inhibition of InhA, the enoyl reductase from *Mycobacterium tuberculosis*, by triclosan and isoniazid. *Biochemistry* 2000;39:7645–7650.

215. **Speck S**, **Wenke C**, **Feßler AT**, **Kacza J**, **Geber F**, ***et al***. Borderline resistance to oxacillin in *Staphylococcus aureus* after treatment with sub-lethal sodium hypochlorite concentrations. *Heliyon* 2020;6:e04070.

Stratégie expérimentale et méthodologie

La thèse s'est articulée autour de trois parties distinctes (Figure 6). La première partie a consisté en un criblage, où les biofilms sélectionnés ont été exposés à différents biocides. L'objectif était d'observer comment cette exposition influençait l'évolution de la résistance aux antibiotiques (2.1). Après la collecte des variants et la réalisation des premiers tests de validation, une analyse complète de leur génome a été effectuée par séquençage (WGS), permettant d'identifier des cibles génétiques récurrentes associées à des résistances croisées (2.2). Enfin, la dernière partie a porté sur une caractérisation détaillée des variants présentant les particularités génomiques les plus intéressantes. Cette section a inclus l'étude des mécanismes moléculaires sous-jacents, ainsi que l'évaluation du profil de résistance, des capacités de survie et du potentiel de dissémination des variants. Pour établir le lien avec l'adaptation en biofilms, la structure spatiale des biofilms produits par ces variants a été caractérisée à l'aide du CLSM (2.3). Ces grandes étapes dessinent la démarche adoptée au cours de la thèse et résument la stratégie expérimentale globale. Certaines approches méthodologiques centrales dans cette démarche expérimentale ont été valorisées à travers des chapitres d'ouvrage, et sont présentés dans cette section. Cependant, ceux-ci ne couvrent pas de manière exhaustive l'ensemble des aspects méthodologiques de la thèse, qui sont présentés de manière détaillée dans le matériel et méthodes des articles présents dans la partie Résultats.

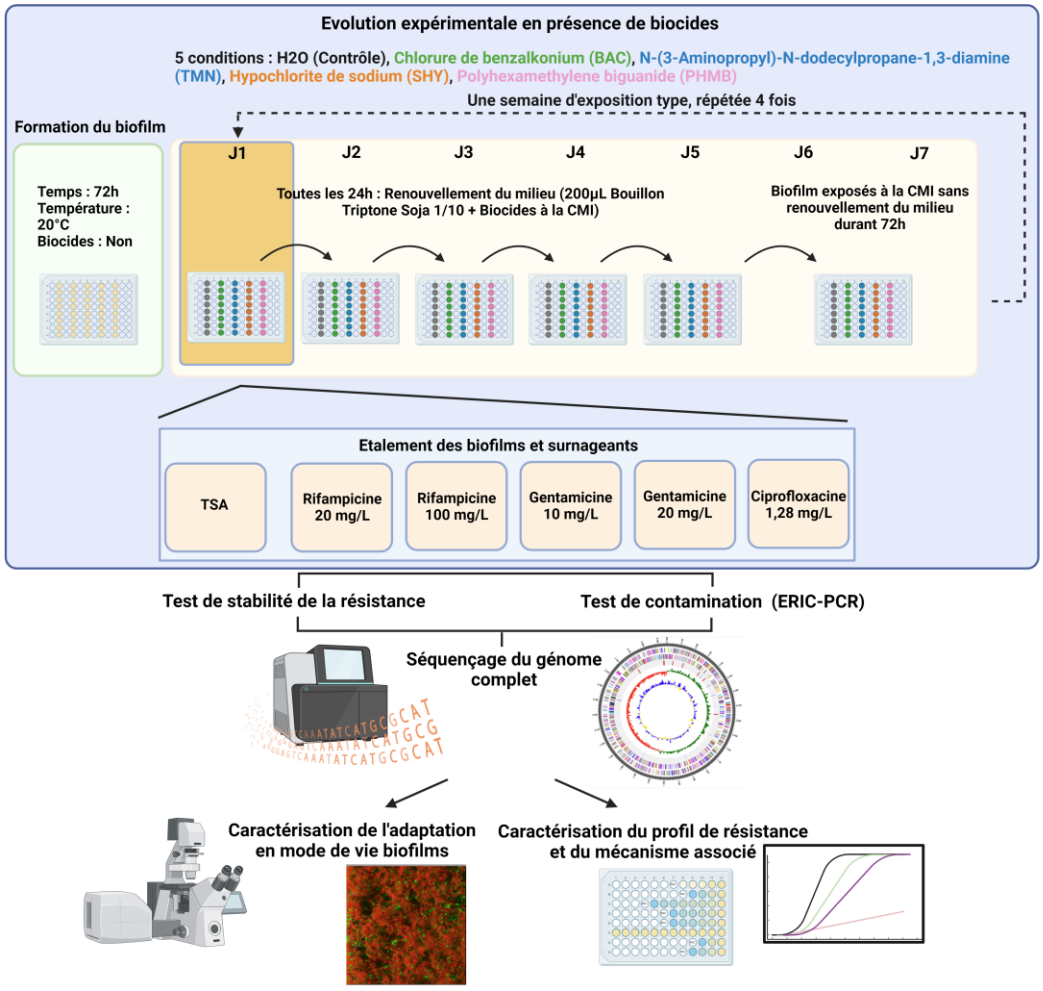

Figure 6 : Schéma récapitulatif de la stratégie expérimentale globale. Figure créée avec Biorender.com.

1. Matériel

1.1. Souches utilisées

Les souches bactériennes utilisées dans l'étude ont été principalement sélectionnées au sein de la collection du LNR-RA hébergé dans l'unité AB2R du laboratoire de Fougères. Cette collection rassemble plus de 12000 souches de *E. coli* isolées dans l'industrie agroalimentaire au cours de 20 dernières années dans le cadre des plans nationaux de surveillance de l'antibiorésistance, pilotés par la direction générale de l'alimentation (DGAL) du ministère de l'agriculture.
Un panel de 60 souches a été sélectionné, représentant des prélèvements réalisés entre 2014 et 2019, à raison de 10 souches par année. La sélection a été faite sur la base de leur profil de résistance à 14 antibiotiques afin d'avoir une image pertinente de la diversité présente sur la chaîne alimentaire. Parmi les 10 souches choisies pour chaque année, 5 étaient sensibles à tous les antibiotiques testés tandis que les autres présentaient des résistances spécifiques variées : 1 souche résistante à l'ampicilline, 1 résistante à la tétracycline, 1 résistante à la ciprofloxacine, 1 résistante à la céfotaxime et 1 souche résistante à la gentamicine. Cette sélection visait à constituer un échantillon représentatif permettant d'évaluer si les souches déjà résistantes présentaient une capacité accrue à développer des résistances supplémentaires. A ces 60 souches ont été ajoutées 4 autres souches : la souche de référence Ec1655, ainsi que 3 autres souches utilisées dans les deux laboratoires pour leur capacité à former des biofilms : la souche SS2 isolée d'un site agroalimentaire en 2014 et les souches CIRMBP-0248 et CIRMBP-0223 (collection INRAE), qui ont été isolées sur de la volaille respectivement en 1975 et 1977.

1.2. Biocides utilisés

Pour conduire les expérimentations d'adaptation aux biocides, quatre substances actives représentatives des agents désinfectants couramment utilisés dans les chaînes de production alimentaire ont été retenues. Le choix s'est porté sur des substances actives plutôt que sur des solutions commerciales afin d'attribuer les effets observés directement à ces substances et non à d'autres composants présents dans les solutions commerciales (conservateur, texturant, agent moussant, etc.).
Les quatre substances choisies appartiennent à des familles différentes, afin d'avoir une diversité de mécanismes d'action et leurs effets potentiels sur les bactéries. Il s'agit du chlorure de benzalkonium (BAC), du polyhexaméthylène biguanide (PHMB), du N-(3-aminopropyl)-N-dodecylpropane-1,3-diamine (TMN) et de l'hypochlorite de sodium (SHY). Le BAC fait partie de la famille des ammoniums quaternaires. Ces biocides sont utilisés depuis de nombreuses années et ont été intensivement étudiés, notamment en ce qui concerne leurs effets sur la résistance aux antibiotiques. Le BAC a ainsi été choisi pour permettre des comparaisons avec la littérature existante. Le PHMB fait partie de la famille des biguanides. Bien que ce biocide soit moins caractérisé, des composés similaires, comme la chlorhexidine, ont fait l'objet de recherches plus approfondies. La TMN, quant à elle, fait partie de la famille des triamines. Malgré son utilisation croissante dans diverses filières (Tableau 1), les informations disponibles sur ce biocide sont encore limitées, en particulier sur ses effets sur l'antibiorésistance. Enfin, le SHY issu de la famille des halogènes, est un biocide très largement employé en élevage et en production alimentaire.

2. Méthodologie

2.1. Evolution expérimentale en présence de biocides

L'exposition des souches aux différents biocides a été réalisée sur une période d'un mois. Le milieu de culture supplémenté en biocides était renouvelé quotidiennement en semaine, tandis qu'une exposition continue, sans renouvellement, était maintenue pendant 72h, du vendredi au lundi. Pour chaque biocide, la concentration d'exposition utilisée correspondait à la Concentration Minimale Inhibitrice (CMI) déterminée pour les souches en phase planctonique. Afin d'exploiter la diversité entre les souches, toutes ont été exposées à une concentration unique, correspondant à la CMI la plus basse parmi les 10 souches.
Le choix de se porter sur la CMI sous forme planctonique a été retenu pour garantir un impact suffisant sur les souches, même au sein des biofilms, afin de permettre une évolution dirigée par le biocide. Du Bouillon Tryptone Soja (BTS), dilué au 1/10^{e} a été choisi comme milieu de culture. La matière organique pouvant jouer un rôle dans l'interférence et l'inactivation des substances actives biocides, il a été décidé de diluer le milieu de culture afin de limiter ces interactions, tout en conservant un milieu de culture suffisamment riche pour ne pas entraver la croissance bactérienne, simulant ainsi les environnements des agro-industries, où les bactéries évoluent souvent dans des environnements riches en nutriments. Le choix de la température s'est lui porté sur une température ambiante, couramment retrouvée dans les industries agro-alimentaires.
Les biofilms et surnageants ont été étalés sur des géloses supplémentées ou non en antibiotiques. Les surnageants ont été étalés afin d'avoir un point de comparaison avec les souches présentes au sein du biofilm, la concentration d'exposition étant trop élevée pour avoir un contrôle représenté par des bactéries issues de culture planctoniques. Les antibiotiques choisis pour le crible étaient la ciprofloxacine, la rifampicine et la gentamicine. Ces antibiotiques appartiennent à différentes familles d'antibiotiques, respectivement les fluoroquinolones, les rifamycines et les aminoglycosides. Leurs cibles au sein de la bactérie sont également différentes, ciblant chacune une étape différente de la synthèse protéique : les fluoroquinolones ciblent la réplication de l'ADN, les rifamycines ciblent la transcription de l'ADN en ARN et les aminoglycosides ciblent la traduction de l'ARN en protéine (Figure 7).

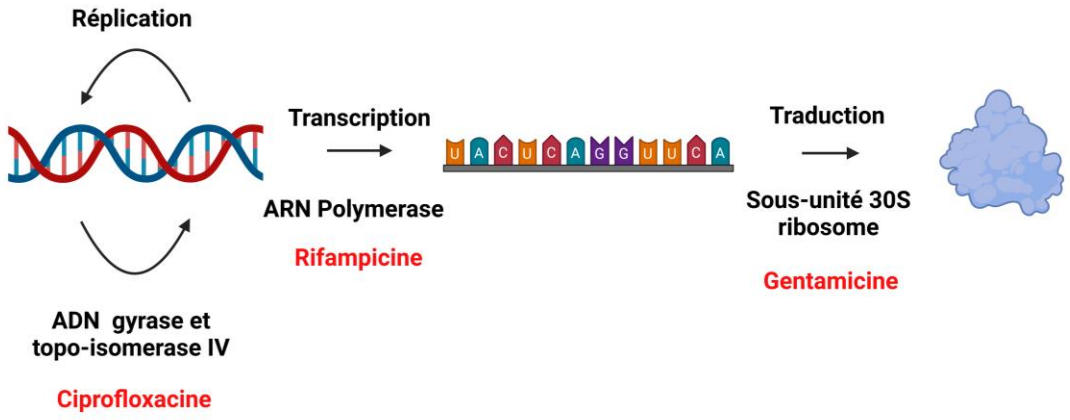

Figure 7 : Cibles cellulaires de la ciprofloxacine, de la rifampicine et de la gentamicine. Figure créée avec Biorender.com.

Les concentrations choisies se basent sur plusieurs critères. La rifampicine a été utilisée à une concentration de 20 mg/L, la plus faible permettant de différencier une souche sensible d'une souche résistante. Une concentration plus élevée, à 100 mg/L a également été utilisée, permettant de sélectionner les variants présentant les résistances les plus fortes. Pour la gentamicine et la ciprofloxacine, les concentrations ont été basées sur les valeurs Ecoff (Epidemiological cut-off values) définies par l'EUCAST (European Committee on Antimicrobial Susceptibility Testing), qui détermine le seuil à partir duquel la majorité des souches d'une espèce ne peuvent plus croître. Des tests ont été effectués sur les géloses afin d'identifier la concentration minimale pour empêcher toute croissance des 10 souches. La concentration choisie pour la ciprofloxacine correspondait à 20 fois l'Ecoff, tandis que pour la gentamicine, des concentrations de 5 fois et 10 fois l'Ecoff ont été choisies. Comme pour la rifampicine, deux concentrations ont été retenues pour la gentamicine, afin de distinguer les souches faiblement résistantes de celles possédant des résistances plus élevées. Cette approche n'a pas été appliquée à la ciprofloxacine car des tests antérieurs avaient montré que la concentration sélectionnée limitait déjà suffisamment le nombre de variants.
Enfin, une gélose sans antibiotiques a été utilisée pour collecter l'ensemble de la population, permettant de vérifier si des phénotypes particuliers étaient associés au variant. Les variants obtenus ont ensuite été soumis à plusieurs étapes de validation. La première étape consistait à vérifier la stabilité de la résistance. Il est en effet possible que des modifications physiologiques, plutôt que génétiques, soient à l'origine de la survie de la bactérie, celles-ci sont cependant moins « pertinentes » dans le cadre d'une analyse « *One Health* » car elles peuvent disparaitre une fois le stress éliminé, rendant les bactéries sensibles lors d'une future exposition aux antibiotiques chez l'humain. De plus, les variants étant destinés à être séquencés, il était important de s'assurer qu'il y avait bien une modification génétique. Les tests de stabilité ont été effectués en repiquant les variants sur des géloses non supplémentées en antibiotique, 5 jours d'affilée, et le 6^{e} jour à nouveau avec antibiotique. Ainsi, les variants étant toujours capables de se développer sur gélose supplémentée était ceux, qui même sans pression de sélection, avaient conservé leur phénotype de résistance.
Tous les variants ayant passé ce premier test ont été testé par ERIC-PCR (Enterobacterial Repetitive Intergenic Consensus Polymerase Chain Reaction**).** Cette technique permet l'amplification de plusieurs séquences spécifiques aux entérobactéries et d'avoir ainsi un profil de bandes amplifiées différent en fonction de la souche choisie. Ce test a permis de vérifier que les variants sélectionnés avaient bien le même profil que leur souche parentale, excluant ainsi la possibilité d'une contamination.
Enfin, une fois ces deux tests passés, les variants ont été conservés dans des cryotubes à -80°C.

2.2. Article 2 : Analyse génomique comparative des variants et de leurs souches parentales

Parmi les variants ayant passé les tests préalables, 235 ont été sélectionnés pour un séquençage génomique complet (WGS). La sélection de ces variants s'est faite selon plusieurs critères. Tous les variants collectés résistants à la gentamicine (GenR) ont été envoyés pour séquençage. Les variants résistants à la rifampicine (RifR) étant trop nombreux, un choix arbitraire a été fait : des variants RifR ont été choisis dans les conditions pertinentes, en choisissant des variants provenant de toutes les souches et toutes les semaines, afin d'avoir une représentation générale des variants ayant émergé au fil de l'expérimentation. Aucun variant résistant à la ciprofloxacine (CipR) n'ayant été isolé au cours de l'exposition, aucun n'a donc été envoyé à séquencer. Le génome de ces variants a ensuite été comparé à celui de la souche parentale dont ils étaient issus, afin d'identifier des mutations à l'origine du profil de résistance.

La méthodologie de l'analyse des mutations, survenant chez les variants résistants aux antibiotiques, développée dans le cadre de cette thèse et du projet ANR JCJC BAoBAb a été valorisée dans un chapitre de la seconde édition du livre « Foodborne Bacterial Pathogens » (série *Methods in Molecular Biology*, Springer) qui sera publié fin 2024. Ce protocole reprend de façon détaillée les étapes de traitement des séquences, assemblage et annotation du génome, analyse de la qualité du séquençage, et comparaison des génomes, en présentant les packages utilisés pour chaque étape. Un exemple d'application est présenté à la fin, utilisant des analyses du séquençage qui n'ont pas été publiées dans les autres articles de la thèse. Des analyses des variants provenant d'une espèce de *Escherichia marmotae* y sont présentées. Bien que cette souche ait initialement été caractérisée comme appartenant à l'espèce *E. coli*, l'analyse de séquençage a révélé qu'elle appartenait à une autre espèce, ce qui nous a conduit à l'exclure des autres études.

« Genomic pipeline for analysis of mutational events in bacteria », Foodborne Bacterial pathogens-2nd edition, *Methods in Molecular Biology*, 2024

Pierre Lemée, Raphaël Charron, Arnaud Bridier

Chapter 15

Genomic Pipeline for Analysis of Mutational Events in Bacteria

Pierre Lemée, Raphaël Charron, and Arnaud Bridier

Abstract

Unveiling the strategies of bacterial adaptation to stress constitute a challenging area of research. The understanding of mechanisms governing emergence of resistance to antimicrobials is of particular importance regarding the increasing threat of antibiotic resistance on public health worldwide. In the last decades, the fast democratization of sequencing technologies along with the development of dedicated bioinformatical tools to process data offered new opportunities to characterize genomic variations underlying bacterial adaptation. Thereby, research teams have now the possibility to dive deeper in the deciphering of bacterial adaptive mechanisms through the identification of specific genetic targets mediating survival to stress. In this chapter, we proposed a step-by-step bioinformatical pipeline enabling the identification of mutational events underlying biocidal stress adaptation associated with antimicrobial resistance development using *Escherichia marmotae* as an illustrative model.

Key words Bacterial adaptation, Antimicrobial resistance, Variant, Whole genome sequencing, Variant calling, Mutation

1 Introduction

Microbial adaptive evolution has shaped and continues to drive the microbial communities and their impacts in pristine and anthropized environments worldwide. Bacterial ecosystems are mostly very competitive, and bacteria undergoing a mutational event conferring them an advantage in specific conditions have the potential to outcompete their unmutated counterparts. Mutations improving nutrient absorption or metabolization [1] or bettering survival upon stress exposure, for example, to an antibiotic and/or a biocide, have already been reported, for instance [2–4]. Bacteria can evolve quickly, since some species are able to double their population size in less than 10 min [5]. Consequently, it is possible to study the genetic adaptation and evolutionary drift of the population upon various exposure conditions using laboratory-scaled experiences known as adaptive laboratory experiments (ALE)

Arnaud Bridier (ed.), *Foodborne Bacterial Pathogens: Methods and Protocols*, Methods in Molecular Biology, vol. 2852,
https://doi.org/10.1007/978-1-0716-4100-2_15,

[6]. Some works thereby demonstrated that bacterial populations evolve continuously, even under stable environmental conditions, and that new mutational events recurrently occur leading to the propagation of mutants with increased fitness [7, 8]. Lenski demonstrated that even after 25 years of cultivation and 60,000 generations, new variants with new genome modifications are still appearing and can exhibit an increased fitness and spread in the bacterial population [9].

ALE have been harnessed in various fields to decipher bacterial adaptive strategies. For instance, developments of dedicated experimental setups have been conducted to investigate the effects of various drug concentrations on antimicrobial resistance emergence [10]. Such approaches enabled the identification of mechanisms involved in adaptation and resistance emergence, highly supported by the democratization of bacterial genome sequencing and analysis [2]. Since the discovery of the Sanger method in the 1970s [11], numerous innovative technologies have indeed been developed. Initially restrained to the analysis of specific genes in the genome, next-generation sequencing (NGS) enables today the reliable and accurate analysis of complete genomes of bacterial strains through an affordable and fast process [12]. Such technological advances highly contributed these last years to the identification of genetic targets governing bacterial adaptation in various environments and under different stresses (including antimicrobials). Whole genome sequencing (WGS) and comparative genomic approaches indeed provide the possibility to identify specific mutations between a wild-type (*parental strain*) and an adapted derivative strain (called hereafter *variant strain*), thus revealing the metabolic pathways involved in adaptation processes.

As an illustration, we presented in this chapter the bioinformatical pipeline of analysis developed in the frame of BAoBAb project (https://anr.fr/Project-ANR-21-CE35-0001). Using ALE combined with WGS, the objective of the project was to investigate the mechanism of bacterial adaptation to biocides by comparing genomes of parental strains and biocide-adapted variants to identify mutational events involved in biocidal stress adaptation.

2 Materials

Whole genome sequencing analysis requires several resources. First, to be able to run all the software, sufficient computing resources are needed. All these resources can be found in a public remote computing cluster. It is important to note that all the methodology presented is carried out in a UNIX environment using Bash consoles. Knowledge of this environment and of the Bash language is therefore necessary to carry out this analysis. Analyses must be

Table 1
Software used to analyze WGS data

Name	Description	Reference
Bakta	Annotate bacterial genomes from genome files in fasta format. It uses a database implemented in the software to annotate.	[13]
fastp	Trim bad-quality reads and eliminate the completely bad ones. It uses raw fastq files as input.	[14]
Quast	Assess the quality of a de novo assembly.	[15]
snippy	Variant calling of bacterial strains using a bacterial reference genome	[16]
Unicycler	Assemble a de novo genome from reads.	[17]

performed on DNA from pure strain cultures with no contaminants. Sequencing is then achieved using Illumina whole genome sequencing instrument. For each strain, a pair of fastq files containing small reads (150 nt) will be generated and used (*see* **Note 1**).

Various software packages are used in the analysis and must be installed before starting the analysis (Table 1). All these software should preferably be installed in different mamba (*see* **Note 2**) environments to avoid package versioning and conflicts.

3 Methods

The bioinformatical method described here enables to highlight mutations through the comparison of bacterial genomes. The genome of a parental strain not exposed to the stress (biocides, antibiotics, chemicals) is compared to the genome of the same strain having undergone a phase of exposure to stress which potentially led to adaptive mutations (*variant strain*). Effects of mutations found in genes or in a family of genes linked to a specific metabolic pathway can then be deeply investigated to understand biological mechanisms at the origin of the adaptation to stress in variant.

Bioinformatical analysis begins with the raw reads processing (trimming and filtering) for both parental and variant strains. Then a de novo assembly is carried out from the parental strain reads, as well as a gene annotation of the newly constituted genome to constitute a reference genome. Finally, processed raw reads of variants are aligned on the annotated reference genome of the parental strain to identify discrepancies between parental and variant genome strains (mutational events) (Fig. 1) (*see* **Note 3**).

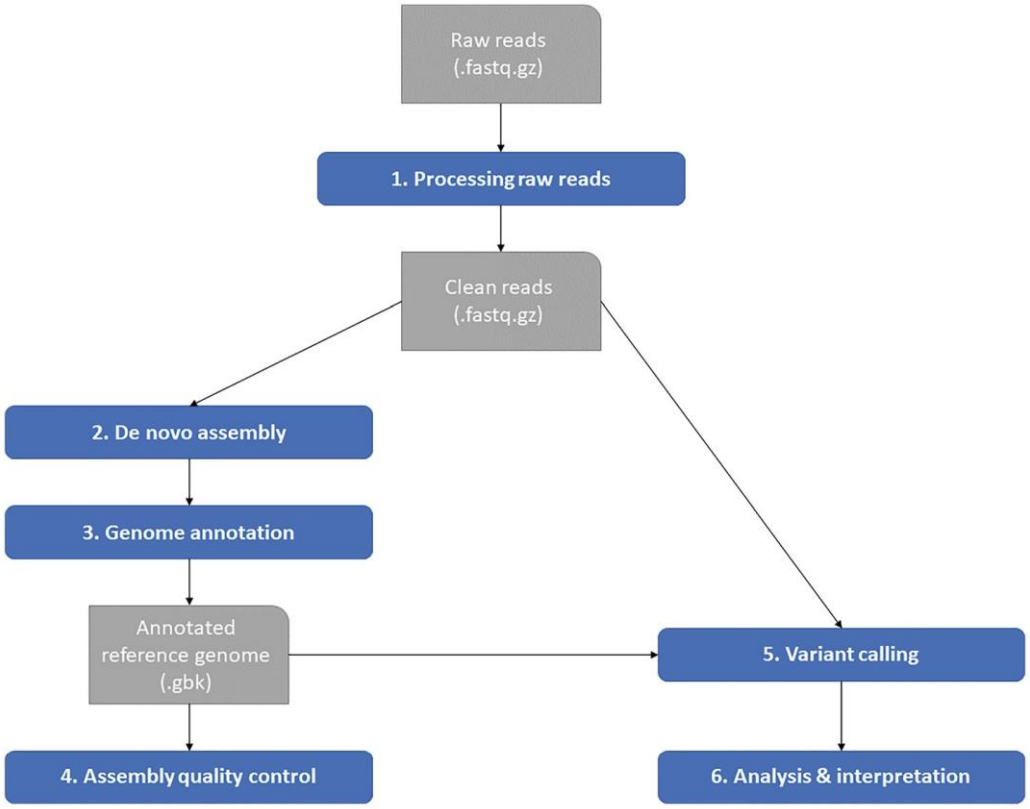

Fig. 1 Analysis pipeline of whole genome sequencing data (https://github.com/AB2R/WGS_pipeline)

3.1 Raw Reads Processing

Raw reads processing filters out reads of poor quality and eliminates any adapters (*see* **Note 4**) used during sequencing. The fastq file obtained after sequencing contains all the reads. These reads are associated with a quality score generated by the sequencer which will be used by the fastp software to eliminate bad-quality reads. This step is done in the same way with the reads of the parental strain and the reads of the mutated strains.

```
fastp -i $FASTQ_R1 -I $FASTQ_R2 -o $FASTQ_CLEAN_R1 -O $FASTQ_CLEAN_R2 --unpaired1 $FASTQ_UNPAIRED --unpaired2 $FASTQ_UNPAIRED -h $FASTQ_REPORT_HTML --detect_adapter_for_pe -M 25 -5 -r --correction
```

Where:

- `-i` is an option to input the first fastq reads file of a strain `$FASTQ_R1`.
- `-I` is an option to input the second fastq reads file of a strain `$FASTQ_R2`.
- `-o` is an option to output the first fastq reads file processed by fastp `$FASTQ_CLEAN_R1`.

- `-O` is an option to output the second fastq reads file processed by fastp `$FASTQ_CLEAN_R2`.
- `--unpaired1,2` are two options to output reads that are no longer paired with their second reads. For example, read1 passed quality control but not read2; read1 will not be paired anymore. All unpaired reads are stocked in the same file `$FASTQ_UNPAIRED`.
- `-h` is an option to output quality control report of the reads in HTML file `$FASTQ_REPORT_HTML`.
- `--detect_adapter_for_pe` is an option to detect and remove automatically sequencing adapters. It is only used for paired data.
- `-M` is an option to specify the quality threshold for `-5` and `-r` options. Here the threshold is set up on 25.
- `-5` is an option to drop the bases with bad quality at the start of the read. It uses a sliding window and cuts if the mean quality of the bases in the window is below the thresholds specified by option `-M`.
- `-r` is almost the same option as `-5`. The sliding window cuts the right part of the read if the mean quality of the bases in the window is below the thresholds specified by option `-M`.
- `--correction` is an option to enable base correction in overlapped regions.

The reads files are now properly filtered and cleaned. They can now be used either to assemble the reference genome with the reads of the parental strain or to call variants with the mutated strains.

3.2 Parental Strain Genome

A de novo assembly can be made from the parental strains reads. This assembly will then be followed by a genome annotation from online databases. Finally, a quality control of this assembly will be established.

3.2.1 De novo Assembly

De novo assembly is done using the Unicycler software.

```
unicycler -1 $PARENTAL_FASTQ_CLEAN_R1 -2
$PARENTAL_FASTQ_CLEAN_R2 -s $FASTQ_UNPAIRED -o $ASSEMBLY_-
FOLDER --min_fasta_length 200
```

Where:

- `-1` is an option to input the first fastq reads file of the parental strain `$PARENTAL_FASTQ_CLEAN_R1`.
- `-2` is an option to input the second fastq reads file of the parental strain `$PARENTAL_FASTQ_CLEAN_R2`.

- `-s` is an option to input the unpaired reads file of the parental strain `$FASTQ_UNPAIRED`.
- `-o` is an option to output all the results in a directory `$ASSEMBLY_FOLDER`. The `$PARENTAL_GENOME_FASTA` assembly in fasta format is stored in this directory under the name "assembly.fasta."
- `--min_fasta_length` is an option to specify the minimum length of a contig that makes up the assembly. Here, below 200 nt, contigs are removed from the assembly.

The output folder of Unicycler contains the newly formed assembly composed of contigs of different sizes. Now the genome has to be annotated to get information about the genes composing it.

3.2.2 Genome Annotation

Genome annotation is done with the Bakta software. It uses a database carrying information on the genes of different bacterial species. We will therefore first have to download the database before launching Bakta (*see* **Note 5**).

```
bakta_db download --output $BAKTA_DATABASE --type full
```

Where:

- `download` is an option to download the Bakta database.
- `--output` is an option to specify the output directory of the Bakta database `$BAKTA_DATABASE`.
- `--type` is an option to specify the database to download (full, light).

Now that the Bakta database has been downloaded, annotation can be carried out on the genome of the parental strain. It is possible to specify the bacterial species of the samples as an argument to facilitate annotation (*see* **Note 6**). Here, the species *Escherichia marmotae* will be indicated.

```
bakta --db $BAKTA_DATABASE --output $ANNOTATION_FOLDER --prefix PARENTAL --genus Escherichia --species marmotae $PARENTAL_GENOME_FASTA
```

Where:

- `--db` is an option to specify the directory of the Bakta database `$BAKTA_DATABASE`.
- `--output` is an option to specify the output directory of the Bakta annotation. `$ANNOTATION_FOLDER`. This folder will contain all the annotation files.

- `--prefix` is an option to specify the start of the name of each file in annotation directory.
- `--genus` and `--species` are options to specify the bacterial species of the parental strain. This option optimizes the annotation according to the species provided.
- `$PARENTAL_GENOME_FASTA` is the input fasta file for the genome assembly contained in the `$ASSEMBLY_FOLDER` folder under the name "assembly.fasta."

The genome of the parental strain is annotated, and all that remains is to assess the quality of the assembly. The annotations obtained are also used in this evaluation to obtain as much information as possible.

3.2.3 Assembly Quality

Quality of the assembly is assessed using Quast software. It will not directly indicate whether the assembly is of good or poor quality but rather provides information about its content. For example, it can give information about the number of contigs and the size of the longest contig. The longer the contigs, the fewer they will be, and the better will be the quality of the assembly.

```
quast –o $ASSEMBLY_QUALITY_FOLDER –g $PARENTAL_ANNOTATION_GFF –
1 $PARENTAL_FASTQ_CLEAN_R1 -2 $PARENTAL_FASTQ_CLEAN_R2 --sin-
gle $FASTQ_UNPAIRED $PARENTAL_GENOME_FASTA
```

Where:

- `-o` is an option to specify the output directory for Quast analyses.
- `-g` is an option to specify the annotation file `$PARENTAL_ANNOTATION_GFF` contained in the `$ANNOTATION_FOLDER` folder in .gff format.
- `-1` and, `-2` are options to specify the two fastq reads files of the parental strain `$PARENTAL_FASTQ_CLEAN_R1` and `$PARENTAL_FASTQ_CLEAN_R2`.
- `--single` is an option to specify the fastq file of unpaired reads `$FASTQ_UNPAIRED`.
- `$PARENTAL_GENOME_FASTA` is the genome assembly contained in the parental strain.

A report is provided in the Quast results file. This contains all the statistics needed to establish the quality of the assembly made from the reads of the parent strain. The reference genome used to compare the mutated strains is now ready for the next step: variant calling from the genome of the parental strain.

3.3 Variant Calling

Variant calling will be used to detect spontaneous mutations in stress-exposed strains. This is done by aligning the reads of mutated strains with the reference genome of the parental strain. The most identified variants are single-nucleotide polymorphism (SNP). Insertions and deletions of a few nucleotides can also be detected. Snippy software is used for variant calling. The reads of the mutated strains that have been filtered in the fastp step can now be used. This process must be carried out for each stress-exposed strain to be analyzed.

```
snippy --outdir $VARIANT_CALLING_FOLDER --prefix MUTATED_-
STRAIN --ref $PARENTAL_ANNOTATION_GBFF --R1 $MUTATED_FASTQ_-
CLEAN_R1 --R2 $MUTATED_FASTQ_CLEAN_R2
```

Where:

- `--outdir` is an option to specify the output directory `$VARIANT_CALLING_FOLDER` containing all the variants.
- `--prefix` is an option to specify the start of the name of each file in the output directory. It is important to indicate the exact strain in this parameter to identify the files to be analyzed for each strain.
- `--ref` is an option to specify the annotated genome file `$PARENTAL_ANNOTATION_GBFF` used as a reference in the analysis. This .gbff file is in the folder `$ANNOTATION_FOLDER`.
- `--R1` and `--R2` are options to specify the two fastq reads files of the mutated strain `$MUTATED_FASTQ_CLEAN_R1` and `$MUTATED_FASTQ_CLEAN_R2`.

The mutations found by snippy are stored in files in the output folder. It is now possible to analyze the variants for each mutated strain.

3.4 Analysis of the Results: The Example of BAoBAb Project

Based on all the previous analyses, we can now study the results of the variants obtained for each mutated strain. Variants can be found either in genes directly or in intergenic areas. However, they can also be found in hypothetical proteins that were located during the initial stages of genome annotation but were subsequently not identified in the databases.

As an example, we will study a strain that was used in the BAoBAb project. Biofilms of an *Escherichia marmotae* strain (named Ec219) were exposed to various biocides for 4 weeks. Resistant variants to antibiotics emerging in biofilms were selected by plating on rifampicin-supplemented plates at various times upon exposure. Finally, the whole genome of the resistant variants was sequenced through short-reads technology and compared to the genome of the parental strain of *E. marmotae*. Mutations in these

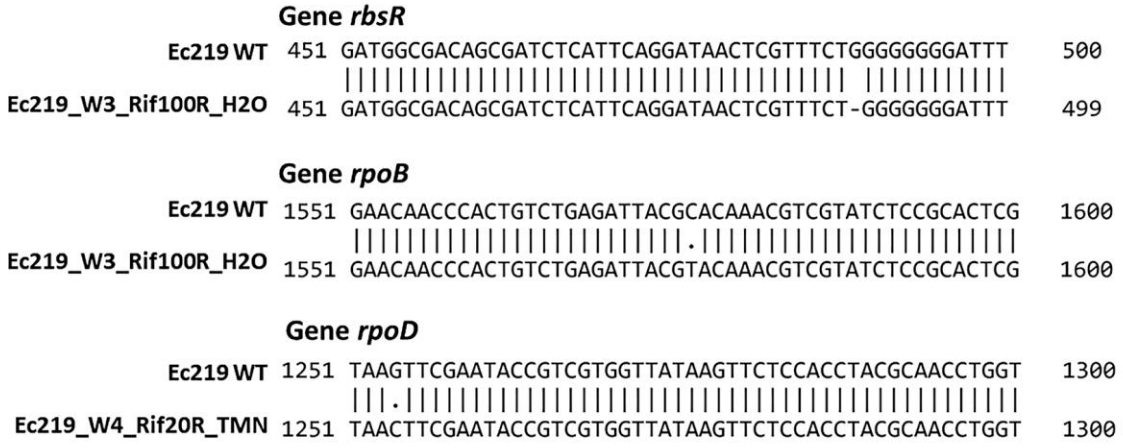

Fig. 2 Comparison of *rbsR*, *rpoB*, and *rpoD* DNA sequences between the Ec219 parental strain and the two variants Ec219_W3_Rif100R_H2O and Ec219_W4_Rif20R_TMN

different variants can thereby be analyzed, in the objective of characterizing mechanisms of cross-resistance between antibiotics and biocides.

Two variants from the study were selected here as illustrative examples (Fig. 2):

- Ec219_W3_Rif100R_H2O: a resistant variant emerged after 3 weeks of exposure in Ec219 biofilms exposed to H_2O and selected on 100 mg/L rifampicin-supplemented plates
- Ec219_W4_Rif20R_TMN: a resistant variant emerged after 4 weeks of exposure in Ec219 biofilms exposed to N-(3-aminopropyl)-N-dodecylpropane-1,3-diamine and selected on 20 mg/L rifampicin-supplemented plates

The genome of the parental strain Ec219 was assembled and annotated using, respectively, Unicycler (Subheading 3.2.1) and Bakta (Subheading 3.2.2). After the analysis of the assembly quality using Quast (Subheading 3.2.3), we ended up with a genome that had a final size of 4,531,508 bp. The genome was made up of 48 contigs with the largest contig being 632,041 bp in size and an N50 of 322,084 bp. The N50 is a measure of the size of the contig halfway through the genome. All contigs larger than or equal to the N50 constitute 50% of the genome. The average sequencing depth was 189. Depth is an important measure because it indicates the average number of reads stacked on top of each other for a given nucleotide. The greater the depth, the more precise is the information contained in the genome. If a mutation is found in a low depth zone (<10), then it is difficult to conclude on the truthfulness of the mutation as it may be due to a sequencing error.

Table 2
Mutations in resistant variants of *Escherichia marmotae* Ec219

Variant	Contig	Position	Type	Reference	Alternate	Effect	Gene
Ec219_W3_Rif100R_H2O	7	284,902	del	TG	T	Frameshift variant	*rbsR*
Ec219_W3_Rif100R_H2O	22	5608	snp	C	T	Missense variant	*rpoB*
Ec219_W4_Rif20R_TMN	2	42,8187	snp	G	C	Missense variant	*rpoD*
Ec219_W4_Rif20R_TMN	13	5453	snp	C	T	–	–

del deletion, *snp* single-nucleotide polymorphism

Both variants exhibited each two mutations (Table 2).

Ec219_W3_Rif100R_H2O is mutated in the *rbsR* gene, encoding a transcriptional repressor for the ribose rbsDACBK operon, with a deletion of a guanine (G) at position 284,902 of the seventh contig of the genome. This mutation causes a shift in the reading frame of the protein. This type of mutation mainly causes the appearance of an early stop codon in the protein, resulting in partial or total loss of the protein's activity. The second mutation in the Ec219_W3_Rif100R_H2O variant is in the *rpoB* gene encoding the beta subunit of DNA-directed RNA polymerase and already described to be involved in rifampicin resistance. It is a single-nucleotide polymorphism (snp), meaning that there has been a change from a cytosine to a thymine nucleotide at position 5608 at the 22nd contig. This mutation causes a change in the code of the three-nucleotide codon, resulting in a change of an amino acid in the final protein. Depending on the polarity of this amino acid compared with the base amino acid, the protein's conformation and affinity in the active site may be affected.

Ec219_W4_Rif20R_TMN shows a snp in the *rpoD* gene encoding the RNA polymerase sigma factor. There is a guanine to cytosine nucleotide change at position 428,187 of the second contig, also causing an amino acid change. The second mutation is located in an intergenic region between two genes. Nevertheless, it can still have an effect as it could be located on a promoter or suppressor site of a gene. In conclusion, different types of mutation can emerge, and it is important to analyze all of them carefully to draw out all the possible interpretations.

4 Notes

1. During the presentation of the method, the files and folders used during the analysis are all named in the form of the variable `$FILE_NAME`. Each call to this variable corresponds to the same file or folder.
2. Mamba is a conda extension that works in the same way as conda. However, it is an optimized version of conda and runs faster for each command. All the software used can be installed via conda and therefore via mamba.
3. It is important to differentiate sequential reads from parental and mutated strains. Despite the similarity of the analyses at the beginning of the pipeline, the reads will not be used by the same tools.
4. Adapters are short-nucleotide sequences that are added to reads. They enable the sequences to bind with the flow cell (the support used for sequencing). They also enable sequences to be enriched via PCR. In some cases, they can be used to index different samples, enabling sequencing with mixed DNA.
5. Bakta has two databases that can be installed via a command: full or light. The full database is downloaded in the presented method to have the best annotation results. However, this database is very heavy in terms of storage. So, if you are having trouble installing the database, it is better to download the light database.
6. In the Bakta options, it is possible to enter information about a bacterial species to facilitate annotation of the genome. It is also possible to add the `—strain` option to provide information at strain level.

5 Data Availability

All the data used as examples in this work are available on NCBI in the BioProject PRJNA947807.

Acknowledgments

This research was funded by the l'Agence Nationale de la Recherche (ANR), project JCJC BAoBAb (ANR-21-CE35-0001). RC is a recipient of an Anses-INRAE doctoral fellowship. French general directorate for food (DGAL) and the National Reference Laboratory "Résistance Antimicrobienne" hosted in the Anses laboratory of Fougères were thanked for the availability of *E. marmotae* strain.

References

1. D'Souza G, Kost C (2016) Experimental evolution of metabolic dependency in bacteria. PLoS Genet 12:e1006364. https://doi.org/10.1371/journal.pgen.1006364
2. Marciano DC, Wang C, Hsu T-K, Bourquard T, Atri B, Nehring RB, Abel NS, Bowling EA, Chen TJ, Lurie PD, Katsonis P, Rosenberg SM, Herman C, Lichtarge O (2022) Evolutionary action of mutations reveals antimicrobial resistance genes in Escherichia coli. Nat Commun 13:3189. https://doi.org/10.1038/s41467-022-30889-1
3. Douarre P-E, Sévellec Y, Le Grandois P, Soumet C, Bridier A, Roussel S (2022) FepR as a central genetic target in the adaptation to quaternary ammonium compounds and cross-resistance to ciprofloxacin in Listeria monocytogenes. Front Microbiol 13:864576. https://doi.org/10.3389/fmicb.2022.864576
4. Charron R, Lemée P, Huguet A, Minlong O, Boulanger M, Houée P, Soumet C, Briandet R, Bridier A (2023) Polyhexamethylene biguanide promotes adaptive cross-resistance to gentamicin in Escherichia coli biofilms. Front Cell Infect Microbiol 13:1324991. https://doi.org/10.3389/fcimb.2023.1324991
5. Weissman JL, Hou S, Fuhrman JA (2021) Estimating maximal microbial growth rates from cultures, metagenomes, and single cells via codon usage patterns. Proc Natl Acad Sci USA 118:e2016810118. https://doi.org/10.1073/pnas.2016810118
6. Bennett AF, Hughes BS (2009) Microbial experimental evolution. Am J Phys Regul Integr Comp Phys 297:R17–R25. https://doi.org/10.1152/ajpregu.90562.2008
7. Wiser MJ, Ribeck N, Lenski RE (2013) Long-term dynamics of adaptation in asexual populations. Science 342:1364–1367. https://doi.org/10.1126/science.1243357
8. Lenski RE, Wiser MJ, Ribeck N, Blount ZD, Nahum JR, Morris JJ, Zaman L, Turner CB, Wade BD, Maddamsetti R, Burmeister AR, Baird EJ, Bundy J, Grant NA, Card KJ, Rowles M, Weatherspoon K, Papoulis SE, Sullivan R, Clark C, Mulka JS, Hajela N (2015) Sustained fitness gains and variability in fitness trajectories in the long-term evolution experiment with Escherichia coli. Proc Biol Sci 282:20152292. https://doi.org/10.1098/rspb.2015.2292
9. Lenski RE (2017) Experimental evolution and the dynamics of adaptation and genome evolution in microbial populations. ISME J 11:2181–2194. https://doi.org/10.1038/ismej.2017.69
10. Vinchhi R, Jena C, Matange N (2023) Adaptive laboratory evolution of antimicrobial resistance in bacteria for genetic and phenotypic analyses. STAR Protoc 4:102005. https://doi.org/10.1016/j.xpro.2022.102005
11. Sanger F, Nicklen S, Coulson AR (1977) DNA sequencing with chain-terminating inhibitors. Proc Natl Acad Sci USA 74:5463–5467. https://doi.org/10.1073/pnas.74.12.5463
12. Shendure J, Ji H (2008) Next-generation DNA sequencing. Nat Biotechnol 26:1135–1145. https://doi.org/10.1038/nbt1486
13. Schwengers O, Jelonek L, Dieckmann MA, Beyvers S, Blom J, Goesmann A (2021) Bakta: rapid and standardized annotation of bacterial genomes via alignment-free sequence identification. Microbial Genomics 7:000685. https://doi.org/10.1099/mgen.0.000685
14. Chen S, Zhou Y, Chen Y, Gu J (2018) fastp: an ultra-fast all-in-one FASTQ preprocessor. Bioinformatics 34:i884–i890. https://doi.org/10.1093/bioinformatics/bty560
15. Gurevich A, Saveliev V, Vyahhi N, Tesler G (2013) QUAST: quality assessment tool for genome assemblies. Bioinformatics 29:1072–1075. https://doi.org/10.1093/bioinformatics/btt086
16. Seeman T (2018) Snippy: fast bacterial variant calling from NGS reads. https://github.com/tseemann/snippy
17. Wick RR, Judd LM, 1Gorrie CL, Holt KE (2017) Unicycler: resolving bacterial genome assemblies from short and long sequencing reads. PLoS Comput Biol 13:e1005595. https://doi.org/10.1371/journal.pcbi.1005595

2.3. Article 3 : Analyse structurale des biofilms par CLSM

A la suite de l'analyse génomique, des analyses phénotypiques ont été effectuées sur les variants présentant les cibles génétiques les plus intéressantes, en particulier à l'aide de la microscopie confocale à balayage laser (CLSM). Des caractérisations du profil des biofilms des souches parentales ont été effectuées au CLSM, avec plusieurs marqueurs de la matrice de *E. coli*, afin d'expliquer les différences d'émergences de variants entre les souches dans la partie Résultats 2.1. Des analyses de biovolumes et spatiales ont été effectuées avec un double marquage comprenant du Syto9, marquant les bactéries, et de la concanavaline A (ConA), marquant les composés polysaccharidiques comprenant du α-D-glucose ou du α-D-mannose, ou du WGA (Wheat Germ Agglutinin), marquant les polysaccharides possédant des résidus N-acétylglucosamine. Les biofilms des souches ont également été observés en présence de PHMB au CLSM, sur des expériences de courte durée dans la partie Résultats 2.2.1. La structure et le biovolume de ceux-ci ont été analysés, avec du Syto 9 et du Congo Red, marquant la cellulose et les curli dans le biofilm. Enfin, des analyses avec de la ConA ont également été effectuées pendant un mois, en présence de PHMB, spécifiquement sur Ec1655 et Ec223, dans la partie Résultats 2.2.2. Pour évaluer la compétitivité des variants émergeant dans la partie Résultats 3, dans un environnement biofilm, des co-cultures ont été réalisées avec leurs souches parentales. Afin de pouvoir différencier les deux souches, elles ont été transformées, l'une avec un plasmide contenant le gène codant pour la GFP (Green Fluorescent Protein), et l'autre avec le même plasmide mais cette fois-ci contenant le gène codant pour la mCherry. Ainsi, des co-cultures ont pu être réalisées, avec la souche parentale fluoresçant dans une certaine longueur d'onde et le variant dans une autre. De telle manière, la distribution spatiale et le biovolume de chaque souche de la co-culture, avec ou sans biocide, ont pu être analysés.

Cet article a été publié en mai 2023 dans le volume 53 du livre « Methods in Microbiology » et présente les méthodes d'analyse de biofilms multi-espèces. Il est divisé en deux parties. Une première partie sert d'analyse bibliographique et présente les différentes méthodes utilisables à chaque étape essentielle du processus d'analyse de biofilms au CLSM. La première étape se concentre sur les méthodes pour établir un biofilm. La seconde se concentre sur les différentes méthodes permettant le marquage des bactéries au sein du biofilm. La suivante présente les méthodes d'imagerie qui peuvent permettre l'observation de biofilms multi-espèces. Enfin, la dernière étape se concentre sur les nouvelles méthodes d'analyse d'images et de traitement des données. La deuxième partie du chapitre présente un protocole détaillé permettant l'observation en microplaques de biofilms de *Bacillus spp*. et *E. coli* en reprenant les étapes présentées dans la partie bibliographique, sur un exemple appliqué.

« Spatial analysis of multispecies bacterial biofilms », *Methods in Microbiology*, 2023

Virgile Guéneau*, Raphaël Charron*, Vlad Costache, Arnaud Bridier, Romain Briandet

***Ces auteurs ont contribué de manière égale**

Spatial analysis of multispecies bacterial biofilms

Virgile Guéneau[a,b,†], Raphaël Charron[a,c,†], Vlad Costache[a,d], Arnaud Bridier[c,*], and Romain Briandet[a,*]

[a]*Université Paris-Saclay, INRAE, AgroParisTech, Micalis Institute, Jouy-en-Josas, France*

[b]*Lallemand SAS, Blagnac, France*

[c]*Antibiotics, Biocides, Residues and Resistance Unit, Fougères Laboratory, French Agency for Food, Environmental and Occupational Health & Safety (ANSES), Fougères, France*

[d]*MIMA2 Imaging Facility, Microscopie et Imagerie des Microorganismes, Animaux et Aliments, INRAE, Jouy-en-Josas, France*

**Corresponding authors: e-mail address: arnaud.bridier@anses.fr; romain.briandet@inrae.fr*

1 Introduction

Life in sessile communities known as biofilms constitutes the main microbial state over the earth. Biofilms profoundly affect our everyday life through their involvement in natural and ecological processes as well as through their deleterious impact on health or industrial productivity. In such biological structures, bacteria are close to each other and embedded in a complex 3D polymeric matrix, which shapes the specific features of the biofilm and is composed of diverse polysaccharides, proteins, nucleic acids and lipids (Karygianni, Ren, Koo, & Thurnheer, 2020). This communal lifestyle greatly influences the emergence of functional properties, which directly result from the biofilm spatial organization, phenotypic heterogeneity and social interactions of individuals in the community (Arnaouteli, Bamford, Stanley-Wall, & Kovács, 2021; Jo, Price-Whelan, & Dietrich, 2022; Sadiq et al., 2021). Recently, Díaz-Pascual et al. (2021) demonstrated that alanine metabolism is spatially and temporally heterogeneous and determines local growth dynamics in *E. coli* colonies. They highlighted an interplay between the anoxic base of the colony close to nutritive agar where alanine was secreted and the oxic nutrient-deprived region at the top of the colony where alanine was then used as a carbon source. This resulted in the metabolic specialization of subpopulations according to their spatial location and governed the shaping of the colony architecture and functions. Likewise, focusing on dental caries Kim et al. (2020) revealed a corona-like 3D

[†]These authors contributed equally.

Methods in Microbiology, ISSN 0580-9517, https://doi.org/10.1016/bs.mim.2023.03.002

architecture of polymicrobial biofilm with the pathogen *Streptococcus mutans* in the inner core. They observed that such specific micron-scale spatial organization modulated pathogen virulence potential and interactions with the host. Such findings illustrate the close relationships between spatial organization and functions in multicellular bacterial communities. Reciprocally, the plasticity of biofilm architecture constitutes a collective way to adapt to the dynamics of such internal subpopulation interactions and to face the environmental fluctuations that finally affect the survival of biofilm-dwelling cells (Bridier et al., 2017). Several studies reported, for instance, the effective protection against antibiotic or biocidal stresses of bacteria living in a biofilm in comparison to their planktonic counterparts (Bowler, Murphy, & Wolcott, 2020; Bridier, Briandet, Thomas, & Dubois-Brissonnet, 2011; Høiby, Bjarnsholt, Givskov, Molin, & Ciofu, 2010).

In industrial and natural environments, biofilms are mostly complex associations of different bacterial strains or species rather than pure cultures. Such ecological heterogeneity reinforces the complexity of social relationships within the biofilm 3D structure depending on the cooperative or competitive nature of social phenotypes and their dynamics, and greatly affects bacterial phenotype and fitness (Elias & Banin, 2012). Along the food chain, in certain conditions, some bacteria are poor biofilm formers alone, but benefit from the association with other species in mixed communities. It has been reported that biofilms of various foodborne pathogens including *Listeria monocytogenes*, *E. coli,* or *Salmonella enterica* may thus be promoted by the presence of other bacteria in mixed communities (Giaouris et al., 2015; Xu, Hu, Han, & Chen, 2022). Moreover, interactions in multispecies biofilms can also lead to a better tolerance of bacterial subpopulations to disinfectants (Li et al., 2021). Phenomena of pathogen protection by resident flora against the effect of biocides, especially due to spatial organization and matrix components sharing was indeed described as reviewed earlier (Sanchez-Vizuete, Orgaz, Aymerich, Le Coq, & Briandet, 2015). Recent work performed on meat processing plant microcosms showed, for instance, that resident microflora may affect the colonization and the subsequent sanitizer tolerance of the pathogen *E. coli* O157:H7 (Chitlapilly Dass et al., 2020). Observations indicated a link between the degree of species diversity of resident biofilm and the level of protection provided. Conversely, the presence of resident microbiota can limit the colonization of surfaces by pathogenic bacteria due to nutrient and spatial competition. Relations between the composition and diversity of the resident microflora and the presence of specific bacterial species have also been associated with a lower prevalence of *L. monocytogenes* in mixed communities (Fagerlund, Langsrud, & Møretrø, 2021). A better deciphering of these ecological interactions and their impact on biofilm emergent properties is therefore of prime importance from a health perspective and constitutes a scientific challenge.

In this perspective, the analysis of species spatial organization gives crucial information on the nature of interactions in 3D multicellular communities since specific architectural patterns reflect the way individual bacterial strains interplay through deleterious, neutral or beneficial processes (Liu et al., 2016). Different studies using synthetic communities and/or computational approaches indeed demonstrated

that the analysis of spatiotemporal community structures enabled a comprehensive understanding of the roles of pairwise social interactions in the structuration of dual-species agar colonies (Blanchard & Lu, 2015; Bonicoli, Angelini, Riela, & Taiani, 1987). In previous work, we proposed an approach relying on the comparison of 4D confocal image series of biofilm development in flow-cells with a simple mathematical null model of biofilm growth to detect non-trivial interspecific interactions between pairs of *Pseudomonas* species expressing distinct fluorescent proteins (Bridier, Briandet, Bouchez, & Jabot, 2014). Such a structure-based approach has proven to be successful to identify how bacterial interactions vary depending on bacterial strains.

These last years, dramatic improvements in biofilm imaging methods were achieved, through the development of microscopy techniques, fluorescence-associated tools, genetic engineering, computing and artificial intelligence for image processing, and their integration, which provide an unprecedented opportunity to dive deep into our understanding of bacterial interactions in biofilms (Bridier & Briandet, 2022). The possibility of differentially tagged distinct species in biofilm structure using specific fluorescent genetic constructs makes it possible to monitor independently each subpopulation at the single-cell resolution during biofilm development.

2 General workflow for biofilms spatial analysis

The experimental process for biofilm spatial analysis is composed of four major steps: the biofilm model choice, the fluorescent probe choice and labelling, the image vizualisation and the data treatment. All these steps are summarized in Fig. 1.

2.1 Generating and capturing biofilms for spatial analysis

2.1.1 In vitro *biofilms*

Many setups with different geometries and hydrodynamics have been developed to study biofilms *in vitro* (Azeredo et al., 2017). The choice of the assay will deeply impact the observed effects on biofilm formation as illustrated in Yarwood, Bartels, Volper, and Greenberg (2004). Historically, the first setups allowed axenic biofilms to grow reproducibly in the lab compatibly with Confocal Laser Scanning Microscopy (CLSM) were based on millifluidic flowcells mounted on microscopic grade glass slides (Habimana, Guillier, Kulakauskas, & Briandet, 2011; Pamp, Sternberg, & Tolker-Nielsen, 2009; Tolker-Nielsen & Sternberg, 2011, 2014). The main drawback of these millifluidic systems was the low throughput of experiments (typically only a few flowcells every week). To overcome this limitation, protocols of biofilm formation based on microscopic grade microtiter plates were combined with High-Content-Screening CLSM, both in static (Bridier, Dubois-Brissonnet, Boubetra, Thomas, & Briandet, 2010) or dynamic microfluidic systems (Pouget et al., 2021). These high-throughput approaches allowed the exploration of

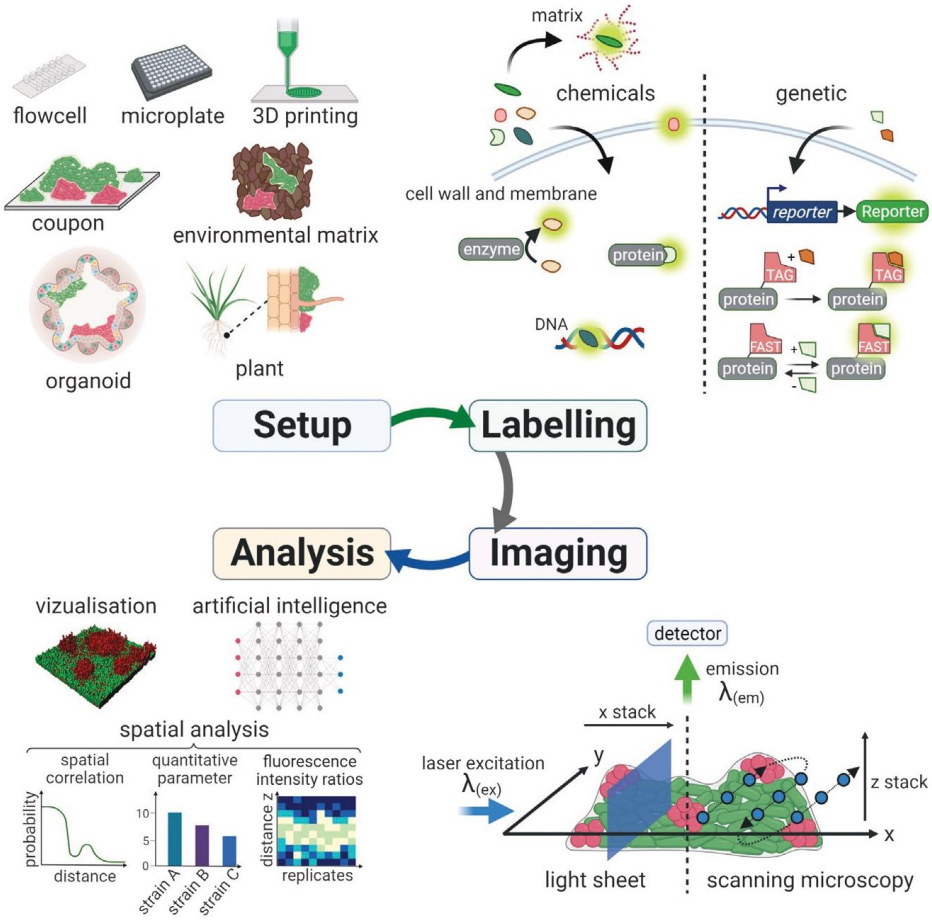

FIG. 1

Workflow to study mixed biofilms using fluorescence microscopy. First, the biofilm type of growth must be chosen from a large list of *in vitro*, *ex situ* and *in vivo* methods available. Then, genetic and chemical fluorescent markers are used to stain bacterial cells inside the biofilm. Consequently, excitation of these markers allows for the observation of the biofilms under fluorescence microscopy. Finally, images can be processed using various softwares to perform 3D reconstruction, spatial quantitative analysis or more in-depth analysis using artificial intelligence. Figure created with https://biorender.com/.

interspecies diversity of biofilms formation and to pinpoint genetic determinants and their regulations, but also to access dynamic processes at different time scales (Béchon et al., 2022; Canette, Deschamps, & Briandet, 2019; Guilbaud, Piveteau, Desvaux, Brisse, & Briandet, 2015; Sanchez-Vizuete et al., 2022).

Polymeric 3D printing was recently used to generate a large variety of device geometries to grow biofilms *in vitro* under various hydrodynamic regimes (Hall, Palmer, Ji, Ehrlich, & Król, 2021; Kristensen, Leonhardt, Neland, & Schlafer, 2020; Zaborskytė, Wistrand-Yuen, Hjort, Andersson, & Sandegren, 2021).

To study the impact of the local microenvironment on biofilm formation, bacteria can be loaded on hydrogels with specific compositions (Heumann et al., 2020; Saint Martin et al., 2022). Depending on the texture of the gel and its physicochemical properties, different morphologies of biofilms can emerge and affect microbial behaviour (van Tatenhove-Pel et al., 2021). 3D bioprinting of simplified structured matrixes with patterned microbial ecosystems allows the exploration of cellular diversification and modelling of interaction between species within structured communities (Connell, Ritschdorff, Whiteley, & Shear, 2013; Huang, Xia, Yang, & Jin, 2018; Krishna Kumar et al., 2021; Ning et al., 2019). An illustrative example of these 3D polymicrobial structures is the formation of autoreplicative kefir granules used in fermented beverages with reported beneficial effects on health. These granule starters that can measure up to a couple of centimetres in diameter are symbiotic communities (often described as functional superorganisms) including lactic acid bacteria and yeasts embedded in a dense extracellular polymeric matrix (Lu et al., 2014). Nowadays, no report has described sucessful initiation of kefir grain from assembled planktonic communities and 3D bioprinting is envisioned to nucleate such communities in synthetic ecology approaches.

2.1.2 Environmental samples

Numerous techniques using swabs, wipes or sponges are used to collect environmental biofilms for studying their composition using DNA sequencing or enumeration on agar. However, these techniques can at best recover <90% of the biofilm community (Grand et al., 2011). In addition, these approaches are based on biofilm disruption for their collection and hence are not compatible with microscopic exploration (Guéneau et al., 2021). As it has been demonstrated that biofilm spatial organization is an important trait of biofilm properties, microscopy has been applied on environmental samples that could be transferred to a lab, or on coupons of relevant materials previously deposited on the surface and sampled *in situ* after biofilms developed in the local ecosystem (Douterelo, Jackson, Solomon, & Boxall, 2016; Guéneau et al., 2021; O'Donnell, Young, Rushton, Shirley, & Crawford, 2007; Romani, Carrion, Fernandez, Lebaron, & Lami, 2021; Shank et al., 2011; Silva et al., 2018).

2.1.3 Biofilms associated with host cells

Tissues and associated biofilms removed from the host (biopsies) can be analysed under the microscope to visualize patterns of the microbial–host interaction. As an example, dental plaque can be sampled and marked with a genus-specific fluorescent label to show the highly complex stratification of surface communities attached to teeth (Mark Welch, Rossetti, Rieken, Dewhirst, & Borisy, 2016; Zijnge et al., 2010). Microscopic observations of histological sections of mouse gastrointestinal tract tissues pinpointed *in vivo* biofilm formation by bacterial pathobionts (Barnes et al., 2017). Organoid 3D models of cell cultures are increasingly being developed. The advantage of these models is that they mimic the organization of organs using human cells, sometimes taken directly from patients (Clevers, 2016). Interaction studies between organoids and microorganisms can be done using

fluorescence microscopy (Dekkers et al., 2019; Han et al., 2021). A human epidermis organoid model was developed to study the development of methicillin-resistant *Staphylococcus aureus* and *P. aeruginosa* biofilms (Wu et al., 2021). Organoids can also mimic the natural environment of the pathogen (*Helicobacter pylori*) responsible for gastric cancer, increasing the knowledge about this bacterium (Amieva & Peek, 2016). Gut-on-chips that mimic the organization of digestive tract tissues are also used to study biofilm formation on epithelial tissue cells (Yuan et al., 2020).

Plant–microbe interactions are also intensively explored by imaging technologies: plants are, for example, used as laboratory models to study bacterial colonization on roots. *P. fluorescens* and *B. subtilis* biofilm formation on *Populus tremuloides* roots were studied using microfluidic chips coupled with confocal microscopy (Noirot-Gros et al., 2020). Exclusion of the fungal pathogen *Trichoderma aggressivum* by *B. velezensis* that developed on hyphae of *Agaricus bisporus* was also deciphered with fluorescent tools (Pandin et al., 2019). Interactions between microalgae and bacteria can be studied in polymicrobial biofilms taking advantage of the autofluorescence of photosynthetic organisms to discriminate the different species in the community (Doiron et al., 2012).

2.2 Biofilm labelling for fluorescence microscopy

2.2.1 Chemical fluorophores

2.2.1.1 Geolocation of cells and matrix components

Fluorophores that specifically target cell compounds can be used to label biofilms. Probes able to penetrate cells and intercalate into the nucleic acids such as 4′,6-diamidino-2-phenylindole (DAPI) or SYTO fluorescently label the entire microbial population (Johnson & Criss, 2013). These treatments do not destructure the biofilm organization but are toxic to the bacteria and they can not be used for live dynamic experiments. In contrast, cell membrane-intercalating markers such as FM4-64 or matrix contrasting EbbaBiolight can be used to perform real-time kinetics of biofilm formation when used at an appropriate concentration (Bassères et al., 2021; Choong et al., 2021; Sanchez-Vizuete et al., 2022). Immunofluorescence can be used to pinpoint a specific organism within the community by using antibodies targeting specific surface antigens. Primary antibodies targeting several pathogenic microorganisms such as *Staphylococcus aureus* and *Listeria monocytogenes* are commercially available (Kühbacher, Cossart, & Pizarro-Cerdá, 2021). Antibodies can be directly coupled with a fluorophore, or a second fluorescent antibody directed towards antibodies produced by a specific animal species can be used in a second reaction (Deshmukh, Joshi, Bhand, & Roy, 2016).

Fluorescent *In Situ* Hybridization (FISH) is based on fluorescent oligonucleotides able to fix a strain-specific sequence of the genome allowing the visualization of specific members in the microbial community (Frickmann et al., 2017). Biofilms must be chemically fixed and cells permeabilized to allow the probes to penetrate the cells, thus altering the native biofilm architecture. The coupling of several

species-specific oligonucleotides tagged with different fluorophores allowed the visualization of the very specific and stratified spatial organization of environmental multispecies biofilms (Mark Welch et al., 2016).

A biofilm matrix is a complex mixture of extracellular biomolecules. It is often described as the biofilm *dark matter* as it is complex to visualize (Flemming, Neu, & Wingender, 2017). No universal matrix dyes exist and it is often necessary to use a combination of probes to obtain only partial contrast of this biofilm component. Exopolysaccharides can be contrasted by fluorescent lectins such as concanavalin A or wheat germ agglutinin (WGA) (Farasin et al., 2017; Neu & Lawrence, 1999). However, a biofilm matrix is often a mixture of several polysaccharides and often there is no other choice than to screen different lectins to find the ones reacting with the sample being studied. Around 80 fluorescent lectins are commercially available and some suppliers provide kits with small aliquots of dozen of lectins to screen them. Another important component of the biofilm matrix is extracellular DNA (eDNA). It can be targeted by several nucleic acid binding fluorophores, but the preferred molecules would be cell impermeant so they do not label intracellular DNA. This is the case for SYTOX green or TOTO1 (Béchon et al., 2022). Dyes labelling proteins (Sypro Ruby, DyLight) or amyloid plaque core proteins (Thioflavin T) were also used to contrast specific regions of the matrices (Bridier, Meylheuc, & Briandet, 2013; Hernández-Galán et al., 2017).

2.2.1.2 Microbial physiology

Several fluorophores have specific functions, providing information on the physiological state of the biofilm organisms, thereby the coupling of these fluorophores can provide a large panel of information on global lifestyle. Several fluorophore combinations can be used to discern living from dead bacteria (Tawakoli, Al-Ahmad, Hoth-Hannig, Hannig, & Hannig, 2013). For example, the use of the cell-permeant SYTO 9 which targets nucleic acids, marking the whole population in green, coupled with the cell impermeant propidium iodide that only marks the DNA of bacteria whose membrane is damaged, allows the spatial visualization and quantification of the dead microbial fraction (Dubois et al., 2019). Some non-fluorescent molecules can enter cells and be metabolized to release a fluorophore. Calcein-AM, cFDA or triembarine are used to visualize metabolically active bacteria by fluorescently reporting esterase activity *in situ* (Guéneau et al., 2021; Guilini et al., 2015). A bias of this labelling is the existence of strains able to expel these fluorophores by efflux pumps, especially within Gram-negative bacterial species (Reuter et al., 2020). Reactive nitrogen and oxygen intermediates involved in many metabolism pathways inside biofilms can also be quantified using fluorescent molecules (Barraud et al., 2006).

Studying the different expression profiles of several genes at the same time and at the single-cell level within a biofilm without the loss of structural information is a challenge. Using *P. aeruginosa* as a biofilm-forming bacterium model, Daniel Dar et al. recently developed the parallel sequential fluorescence *in situ* hybridization (par-seqFISH) technique for this purpose (Dar, Dar, Cai, & Newman, 2021).

Some general drawbacks of the use of chemical fluorophores within a biofilm are their non-specific reactions that can contrast untargeted biofilm compartments and possible diffusion-reaction limitations that can prevent their availability at the target sites (Flemming et al., 2016).

2.2.2 Genetically encoded fluorescent proteins

Genetically encoded reporters represent the second important family of microbial fluorescent markers. As for chemical reporters, they can be used for several types of analyses.

Soluble fluorescent proteins can be expressed under constitutive promoters for live geo-localization purposes (Bridier, Piard, Briandet, & Bouchez, 2020). They can also be expressed under the natural promoter of a specific gene of interest, which leads to fluorescence proportional to gene expression (transcriptional fusion) (Hautefort, Proença, & Hinton, 2003). DNA sequences can be engineered to fuse the fluorescent protein-coding sequence to a specific protein-coding sequence, which allows protein location analysis in the cell or in the environment (translational fusion) (Billaudeau, Yao, Cornilleau, Carballido-López, & Chastanet, 2019).

2.2.2.1 Fluorescent proteins

The Green Fluorescent Protein (GFP) has been, over the last decades, extensively used as a fluorescent marker in biological organisms. Originating from the medusa *Aequoria victoria,* this protein was purified in 1962 (Shimomura, Johnson, & Saiga, 1962). Since then, this protein has been much studied and the mechanism implicated in its fluorescence unravelled. The protein is composed of 11 beta-sheets enrolled in a cylinder structure that surrounds the fluorochrome, composed of three amino acids, Ser65-Tyr66-Gly67. This fluorochrome matures in three steps: cyclisation, dehydration and oxidation of these amino acids (Day & Davidson, 2009). This maturation is induced by a 488 nm wavelength and generates an emission of 509 nm wavelength, causing the green fluorescence of the protein. Through molecular engineering, this protein has been adapted in numerous clones, to enable emission in other wavelengths, covering a large part of the visible spectrum (Day & Davidson, 2009). The large list of fluorochromes available (GFP, YFP, CFP, etc.) allows *in vivo* multi staining and multispecies biofilm studies (Lee et al., 2014; Oliveira et al., 2015).

Another fluorescent protein is DsRed, originating from *Discosoma* corals, and has been one of the main precursors for Red Fluorescent Proteins (RFP). Several proteins derived from DsRed have been engineered and called mFruits (Shaner et al., 2004). These proteins emit in different wavelengths, between 550 and 650 nm, and are more efficient than the initial natural DsRed, in terms of photostability, maturation speed and brightness (Shaner et al., 2004). They also work in a similar manner to GFP, notably with the absolute need for oxygen to fluoresce. The best known of these proteins is mCherry, a protein emitting fluorescence at 610 nm. This efficient fluorescent protein has been used in many studies and notably

in several studies analysing multispecies biofilms, thanks to its different emission spectrum from GFP (Bridier et al., 2020; Lagendijk, Validov, Lamers, de Weert, & Bloemberg, 2010; Lee et al., 2014).

However, the main problem with these markers is the requirement of oxygen in the maturation steps of the fluorochromes. In fact, biofilms are 3-Dimensional structures wherein oxygen is consumed faster than it can diffuse, creating sharp gradients of oxygen that can be absent in the deepest layers where organisms can exhibit anaerobic metabolisms (de Beer, Stoodley, Roe, & Lewandowski, 1994; Karampatzakis et al., 2017). Fluorescence of these proteins can also be limited in mature biofilms by low microbial metabolism associated with low protein synthesis (Monmeyran et al., 2018). Another limitation is the energetic cost they burden the producing cells with by their large weight (27 kb for GFP and mCherry). This important size can also be disadvantageous in the observation of fusion proteins, increasing the risk of functional interference with the fused protein. Finally, their use is limited to pH above 5 which can be in specific conditions, an important limiting factor. Hence, the development of new fluorescent reporters, overcoming these constraints has been necessary as discussed in the next section.

2.2.2.2 FMN-binding proteins

FMN-binding proteins were developed to overcome the sensitivity of GFP and RFP to environmental conditions. This method relies on the Light Oxygen Voltage (LOV) domain present in the phototropin proteins found in certain bacteria and plants. This domain, under blue light excitation, binds the flavin mononucleotide protein (FMN) which induces a green fluorescence in the bacteria. In 2007, Drepper et al. engineered several of these proteins to enhance their fluorescence and created new fluorescent markers called BsFbFP, EcFbFP (derived from the YtvA protein in *B. subtilis*) and PpFbFP (derived from the SB2 protein in *P. putida*) (Drepper et al., 2007). Other markers including iLOV (Chapman et al., 2008) and creiLOV (Mukherjee et al., 2015) were developed later from other phototropins and consequently adapted to more photostable versions, such as phiLOV (Christie et al., 2012). The main advantage of these markers is that they do not require oxygen, making them a more efficient tool in biofilm studies. They are also smaller molecules than GFP and are not sensitive to pH (Christie et al., 2012). However, their use is limited by the very weak fluorescent signal they produce, thus often being difficult to differentiate from the fluorescent background. In addition, all these dyes emit fluorescence in the same wavelength range, limiting their use to one species studies or to the requirement of other markers.

2.2.3 Fluorogenic reporting systems

2.2.3.1 Self-labelling proteins

Fluorogenic systems consist of a non-fluorescent protein encoded in the genome that can bind various ligands, called fluorogens, which are able to fluoresce at different wavelengths. Several fluorogenic complexes were developed such as SNAP-Tag (Keppler et al., 2003) and HALO-Tag (Los et al., 2008). These new markers are

eliminating most of the disadvantages of the methods cited before. Indeed, they are not dependent on oxygen and have fluorescence levels comparable to the ones of GFP or mCherry. SNAP-Tag is relatively small (19 kDa) and HALO-Tag relatively fast to mature (15 min), enabling the choice to select the ideal method depending on the experiment. Nevertheless, most of the existing fluorogens are fluorescing even when not bound to the protein, requiring an additional washing step to eliminate free molecules. However, new fluorogens, notably for HALO-Tag, have been developed, in which fluorescence is only activated when bound to the protein (Streett, Charubin, & Papoutsakis, 2021). These fluorogenic systems have been used successfully in multispecies biofilms, such as for example SNAP-Tag, which was used in a dual-species biofilm model composed of *S. gordonii* and *Porphyromonas gingivalis* (Nicolle et al., 2010) and allowed an efficient differentiation thanks to the collection of fluorogens available. A possible limitation of these systems is that the diffusion of fluorogen molecules is not always efficient in the biofilm. Of note, the costs of these fluorogens can be an issue, particularly in flowcell systems.

2.2.3.2 FAST (fluorescence-activating and absorption-shifting-tag)

Recently, a new fluorogenic system, called "Fluorescence-Activating and absorption-Shifting-Tag" (FAST), has been developed by Plamont et al. (2016). Derived from the Blue-light receptor PYP of *Halorhodospira halophila*, this system works slightly differently from the previously described ones. First, the fluorogen only fluoresces when bound to the FAST protein tag, avoiding any extra washing step. Then, its fixation with its fluorogen is reversible, when other fluorogenic systems usually bind their ligands irreversibly. Its 14 kDa size makes it very useful in the construction of fusion proteins. Finally, a big advantage of FAST is its instantaneous maturation. Thus, its immediate fluorescence allows the study of transitory conditions while other fluorochromes can take a considerable amount of time to maturate and miss early transient phenomena. FAST available ligands are increasing quickly and are already covering a large part of the visible spectrum (Benaissa et al., 2021). FAST has already been tested in biofilm conditions and shown to be more efficient in displaying the biofilm growth than GFP or mCherry, whose signals quickly saturate (Monmeyran et al., 2018). FAST has also been used successfully with SNAP-Tag and HALO-Tag in multi-species cultures (Charubin, Streett, & Papoutsakis, 2020), without any cross-reactivity, demonstrating that it is an interesting complementary tool for multispecies biofilm studies.

2.2.4 Combining different families of fluorophores

To differentiate several species inside of a biofilm, a combination of chemical and genetic approaches can be done as described by the protocol proposed in Section 3. The association of a genetically labelled strain with other bacterial species marked with nonspecific chemicals was performed here using an *E. coli* GFP and *Bacillus* spp. In this case, the specific spatial organization of the pathogen inside the

community was studied. In our example, there is only one species background member. Therefore, the subtraction of the red signal from the green signal gives the localization of the *Bacillus*. The same approach can be used for environmental or defined mixed-species background communities.

2.3 Imaging biofilms

Imaging micro-organisms is a challenging field for optical microscopy systems, due to the small cell size but also due to delicate mounting strategies, such as for live cells, for instance. Between 10 and 100 µm into the biofilm, the analysis of biofilm spatial organization can be limited by its opacity and thickness that limits light penetration.

In this part, we compare different strategies of optical microscopy that can be applied to image biofilms or that need further development to be applied to biofilm imaging.

Individual bacterial cells range roughly from 0.5 µm large to a couple of microns long, so microscopes with good optical sectioning capabilities are needed to obtain information at single cell resolution. We refer here to Confocal Laser Scanning Microscopy (CLSM) systems, two or multi-photon confocal systems, light sheet microscopes, structured illumination (SIM), stimulated-emission-depletion (STED), super-resolution technologies that use Total Internal Reflection Fluorescence (TIRF) approaches, with respect to conventional wide field epi-fluorescence microscopy.

Since the invention of the confocal microscope by Marvin Minsky in the 1950s (Minsky, 1988) and the first commercial laser scanning confocal systems in the late 1980s, CLSM has become one of the most widely used optical sectioning approaches for fluorescence microscopy in biology during the last 20 years.

The CLSM uses a pinhole system, an opening of about 100 µm large in front of the light detectors, that eliminates out of focus emitted light, when a fluorescent sample undergoes laser excitation (Batt & Tortorello, 2014). The micrograph image is formed when the laser beam scans point by point the sample, and the photons are transformed into an electrical signal by a photomultiplier (PMT) detector or an avalanche photodiode, that is a more sensitive detector, such as the Hybrid system (HyD) from Leica Microsystems or the GaAsP produced by Zeiss. CLSM systems allow a good penetration of the light through the sample and a slightly increased lateral and mostly axial resolution, when the pinhole opening is not more than 1 AU (Airy Unit) (Batt & Tortorello, 2014). The micro-morphologies of microbe interaction within a porous material was achieved at a depth of around 50 µm without incising samples (Munir et al., 2021). Scanning the sample with the laser beam implies rather slow acquisition of large images (i.e. more than 512×512 pixels). To acquire images faster, the use of a resonant scanner coupled to the CLSM, that allows high frequency scanning is possible but the obtained images can be very noisy so less informative to answer biological questions. Another solution would be the spinning-disc confocal, that enables faster imaging as it uses a camera like widefield systems. The optical sectioning is generated when the emitted light is filtered through

a fast spinning Nipkow disc. A major drawback for this kind of confocal technology is the poor penetration depth of the light, but recent commercial systems have implemented different pinhole sizes to overcome this limitation.

Conventional commercial CLSM systems allow functional measures for live samples such as precise decaging or photoconversion of fluorophores to follow a subpopulation (Costache et al., 2017) or FRAP (fluorescence recovery after photobleaching) to measure a flux, drift or protein turn-over (Hauth, Chodorski, Wirsen, & Ulber, 2020; Schulmeister et al., 2008).

If phototoxicity to the cells, photobleaching of fluorophores or the penetration depth of the light becomes an issue when imaging a biofilm with a conventional CLSM, this may be overcome by using a two-photon (2P) or a multi-photon (MP) excitation laser (Olpe, Glatt, Laszlo, & Schellenberg, 1980; Tran et al., 2021). 2P microscopy uses femtosecond pulsed lasers. Compared to a conventional monophoton laser, 2P lasers deliver twice the wavelength of the desired excitation wavelength in a non-linear way. For instance, to excite a GFP at 488 nm, the 2P laser generates photons of 976 nm that travel at different speeds, so two photons of 976 nm meet exactly at the focal plane, where the excitation light will become 488 nm. The advantage of this technique is that longer wavelength photons, i.e., near infrared light, produce less photodamage, as they display lower energy than blue and UV photons. The penetration depth of 2P lasers is greater, for instance 143 µm for a Kombucha biofilm (Schulmeister et al., 2008). MP like 2P lasers induce the excitation wavelength at the focal plane. Two or more photons with long wavelengths are generated in a more stochastic manner, to restore the desired excitation light at the focal plane (Thomsen, Graf, Farewell, & Ericson, 2018). Thus, 2P and MP illumination induces an optical sectioning that is limited by the size of the point spread function (PSF) in z at the focal plane, even though most of the commercial microscopes couple the MP excitation laser to a CLSM system, to benefit also from the pinhole optical sectioning. Another advantage of MP lasers is that they can be used for precise laser ablation experiments while acquiring images on the microscope and this can be useful for functional imaging of live cells, for instance, to measure force generation at the cell wall or within the matrix of a biofilm.

When analysing many samples, high content screening modules (HCS) within CLSM systems allow 5D imaging (3D+multi-position+time-lapse) of multiple conditions for live biofilms that develop on 2D support, such as the coverslip glass bottom of a multi-well plate.

Studying biofilms that develop on a 3D support would enhance understanding of biofilm formation, dynamics and functioning mechanisms. To overcome this technical challenge, light sheet microscopy is a well adapted optical sectioning approach that illuminates only the focal plane using a second objective rather than the whole sample as in CLSM (Fig. 2). This approach has low phototoxicicity and is very fast, as the image is formed on one or two cameras, like for widefield conventional microscopes. The optical sectioning in common commercial light sheet solutions does not perform as well as CLSM and the detection objective needs greater working distance, but the illumination techniques allow very fast imaging of large samples

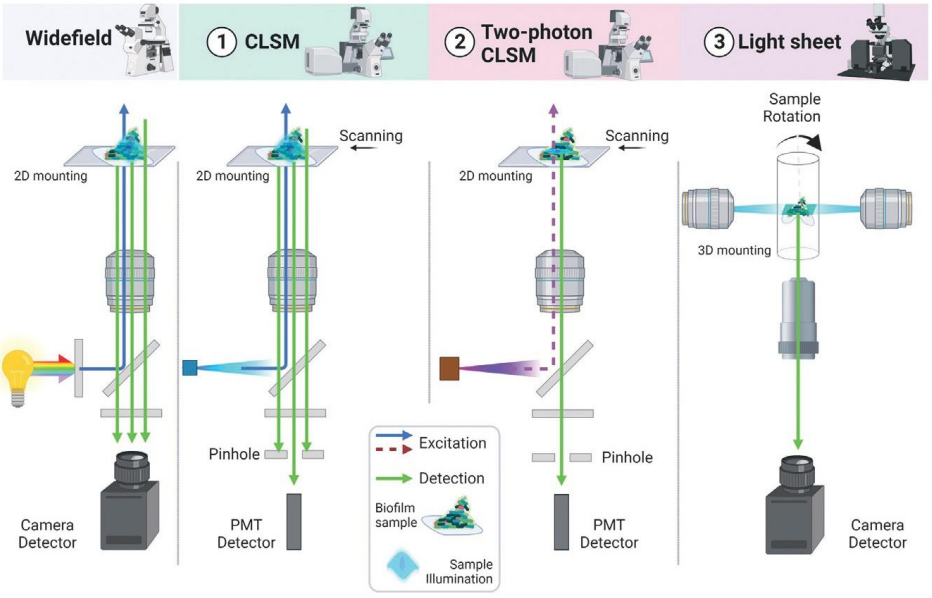

FIG. 2

Comparison of microscopy excitation strategies to detect fluorescence emission of a biofilm, using three optical sectioning approaches: Confocal Laser Scanning Microscopy (CLSM), Two-photon (2P) and Lightsheet (LS) microscopy, with respect to widefield epifluorescence (left). Here, the light from a multichromatic halogene lamp is filtered (grey rectangles), illuminates the whole sample and the signal is detected by a camera. The excitation optical trajectory is in blue and the emission signal in green. (1) CLSM often uses monochromatic laser excitation and the emission signal is filtered through a pinhole that eliminates out of focus blur. Thus, the PMT detects only signal coming from the focal plane. (2) 2P CLSM uses pulsed laser, often in the infrared domain. The excitation wavelength (twice lower) is reached only at the focal plane, which diminishes the photoxicity. See the sample illumination (at the desired excitation wavelength) that is less than in widefield and conventional CLSM. (3) LS microscope allows mounting on large 3D supports that can be rotated while imaging the sample. This is useful to overcome shaded areas comparing to conventional 2D mounting with a cover slip. Excitation light often comes from two objectifs, each one illuminating as a light sheet at the focal plane only. The excitation lightpath is orthogonal and fast camera detectors can be used, as for widefield microscopy. Figure created with https://biorender.com/.

and biofilms or cultures in 3D (Qin et al., 2020). This is mostly thanks to the alternative mounting strategies, i.e., within agarose cylinders or directly suspended in front of the objective with the possibility of rotating the sample for different view angles. Thus, the advantage of light sheet imaging is that the sample is more homogeneously illuminated as most commercial microscopes use two light sheets, on each side of the sample. This favours more precise volume reconstruction during 3D segmentation of the acquired images.

A milestone in optical imaging is the development of super resolution techniques bringing down lateral resolution to about 50 nm with respect to the light diffraction limited resolution that is about 200 nm. A major challenge for biofilm imaging is to better adapt super resolution techniques to help biofilm assessment at the nanoscale by using structured illumination (SIM), stimulated-emission-depletion (STED), and blinking strategies (PALM, STORM) (Berk et al., 2012; Billaudeau et al., 2017; Neu & Lawrence, 1999).

SIM uses several acquired images (3–7) on a camera through differently oriented grids that produce Moiré patterns enabling the enhancement of lateral resolution up to 150 nm, after image processing.

STED technology is coupled to CLSM and uses specific fluorescent dyes and a supplementary laser for emission-depletion as a donut shape during scanning to diminish the dimensions of each PSF to about 80 nm (xy). The laser power used is often too high for living cells, but there is no need for image processing to obtain the super-resolved image at the end of the acquisition.

The STORM/PALM strategies need the acquisition of many images, i.e., 2500–5000 frames, each one having only several fluorophores that emit, and that their precise localization allows to obtain a lateral resolution of the final image of about 10–30 nm (Altinoglu, Merrifield, & Yamaichi, 2019). These stochastic blinking methods are implemented in a TIRF microscope (Total Internal Reflection Fluorescence) that is one of the best optical sectioning strategies, illuminating only about 100 nm in thickness (z), but this illumination section has to be next to a coverslip. So, it is impossible to acquire images deeper than a couple of microns, even when near-TIRF or HILO (Highly Inclined Laminated Optics) are used.

Biofilm imaging would greatly benefit from super-resolved acquired images, but further development and adaptation of these technologies are needed to efficiently provide biological information, mostly for time-lapse of live biofilms.

2.4 Image analysis

Following acquisition, image analysis constitutes a crucial step enabling the extraction of meaningful qualitative and quantitative data from raw fluorescence microscopy image series. Recent advances in image analysis techniques open novel opportunities for spatial and temporal characterization of cells inside biofilms, and tremendous effort has been put into the development of powerful software tools for this purpose as recently reviewed (Jeckel & Drescher, 2021). Technically, several steps are required from pre-processing of raw images to spatial statistic extraction and object detection.

First, raw images from microscopic acquisition, which can be single 2D-images, 3D- or even 4D-image confocal series, should often be filtered to enable background noise reduction and enhance fluorescence signal contrast. Then, in the case of biofilms, 3D reconstructions, volumetric or isosurface projections or sections are mostly performed after filtering using dedicated commercial or freely available software

from confocal z-stack series to visualize 3D structure (Canette et al., 2019). In the example of Section 3, we used Imaris 9.31 (Bitplane).

Filtered images can also be quantified to extract numeric structural descriptors of biofilm and cell morphology that mostly require an upstream segmentation step. Segmentation is a critical step because it governs downstream analyses and greatly depends on image quality and resolution. The goal of segmentation is the partition of raw images into multiple regions to facilitate its quantitative analysis through the detection of objects (for instance, bacteria) and their separation from the background. Different methods of segmentation can be considered: semantic segmentation, instance segmentation or their combination (panoptic segmentation (Petrovai & Nedevschi, 2022). Semantic segmentation assigns a class label to each pixel, whereas instance segmentation detects and segments each object individually. With regards to biofilms, biovolume detection is an illustration of semantic segmentation as multiple objects identified as bacteria are treated as a single entity, and biofilm biomass can be quantified. Likewise, other global descriptors of biofilm architecture can be extracted as roughness, mean and maximum thickness, surface area, etc. Otherwise, instance segmentation treats multiple objects identified as bacteria as distinct individual instances. These features make instance segmentation a relevant approach for single-cell scale downstream analyses (Jeckel & Drescher, 2021). Recently, the concept of biofilm image cytometry was proposed in the BiofilmQ tool (Hartmann et al., 2021). BiofilmQ typically divides biofilm volume into cubes with user-defined size (which can correspond to the volume occupied by a single bacterium, i.e., *pseudo-cell* cubes), and fluorescence data and other cytometric properties in each cube are measured. This allows computing local spatio-temporal data in the biofilm as fluorescence intensity, the local density of cells, local porosity, local structure and texture, the spatial distribution of different markers, etc.

When using different fluorescent markers and reporters or working with differentially labelled bacterial strains, it is possible to analyse multi-channel fluorescent images to better decipher how the different fluorescent signals spatially interact. Focusing on multispecies bacterial biofilms is especially relevant for studying the nature of interactions in the 3D structure by analysing the spatial distribution patterns of bacterial species. Different methods can be applied to analyse colocalization from fluorescence images and can be divided into pixel-based methods and object-based methods (Lagache, Sauvonnet, Danglot, & Olivo-Marin, 2015). In pixel-based methods, individual pixels are analysed by the spectral information that they contain for the different channels and the overlap between fluorescence signals is measured. In object-based methods, the upstream segmentation of bacterial/cluster spots enables their representation as objects and the subsequent analysis of spatial distributions (Lagache et al., 2015).

The point-pattern analysis is classically used in spatial organization studies to extract quantitative spatial area-based or distance-based statistics (Lagache, Lang, Sauvonnet, & Olivo-Marin, 2013). Different coefficients such as Ripley's K function and derivative, pair-correlation or nearest neighbour functions for

instance constitute reference tools in this perspective (Lagache et al., 2015). Numerous studies have applied such analysis to bacterial communities to test if bacteria (points) are randomly distributed or colocalized, and therefore help to better understand interspecies microscale interactions (Esser, Leveau, Meyer, & Wiegand, 2015; Steinberg et al., 2021). The daime image analysis programme (Daims, Lücker, & Wagner, 2006) has been widely used for quantifying spatial arrangement patterns and relations between different species in FISH images using co-localization/co-aggregation and pair cross-correlation functions in mixed biofilms (Almstrand, Daims, Persson, Sörensson, & Hermansson, 2013; Ramírez-Puebla et al., 2022; Schillinger et al., 2012). These approaches enable a better understanding of the link between the spatial organization of strains and the biological activities of the community (Liu et al., 2016). The recent BiofilmQ tool also offers various parameters to quantify correlation and separation distances between species clusters in multispecies biofilm through comparisons of their respective biovolumes and other descriptors such as the Mander's or the Pearson's correlation coefficients (see examples in Section 3) (Hartmann et al., 2021). Complex bacterial 3D organization can thereby be quantitatively characterized including data on bacterial interactions based on spatial distribution. Both these coefficients have also been widely used to quantify probe co-localization in biological microscopy including to elucidate molecule functions in subcellular processes for instance (Dunn, Kamocka, & McDonald, 2011; Lagache et al., 2015).

The rise of artificial intelligence (AI) with machine and deep learning using convolutional neural networks (CNN) has provided an unprecedented opportunity to increase the flow and the power of image analysis. Therefore, the building and use of AI-driven automated workflows stand out as promising approaches for structural analysis of bacterial communities and complex biofilms from microscopy images (Ragi et al., 2021). Recently, a new deep-learning based 2D segmentation tool called Misic that is able to perform automatic semantic and instance segmentation of bacteria inside of bacterial communities images was proposed (Panigrahi et al., 2021). As a major advantage, this tool can be applied for the analysis of species interactions in 2D multispecies bacterial communities images using an interaction model, at a very high throughput independently from imaging modalities. Likewise, using an agent-based model combined with deep learning from both *in silico* and experimental microscopic data, a new network inference method was developed that allows prediction of interspecies interactions from self-organized spatiotemporal patterns (Lee et al., 2020). Toolboxes for studying 3D biofilms are also emerging as BCM3D or the already mentioned BiofilmQ (Hartmann et al., 2021; Zhang et al., 2020). These software tools enable automated morphometric cell classifications in multispecies biofilms and the deciphering of cell-to-cell interactions within the 3D structure.

Furthermore, the increase of computing power makes it possible to directly optimize images during acquisition through adaptive microscopy relying on feedback between acquisition, live AI-based image analysis, and microscope control (Jeckel & Drescher, 2021). All-in-one solutions are being proposed by microscope manufacturers in commercial systems (e.g. MICA from Leica) that will really extend our ability to explore biofilms at the single-cell scale and bacterial interactions within the 3D structure.

3 Experimental protocol

The objective of this experimental protocol is to study the spatial bacterial interactions within a mixed bi-species biofilm. The experimental protocol described here was used to generate the multispecies biofilm images presented Fig. 3 and the

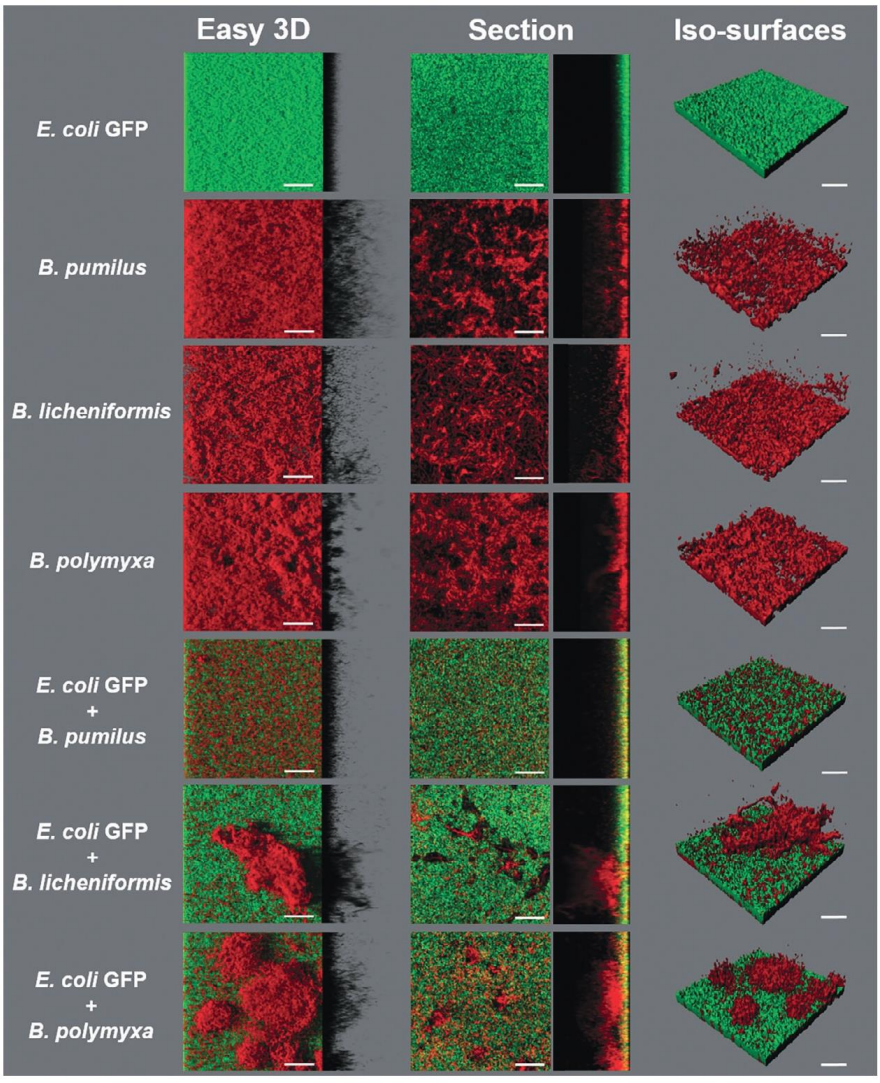

FIG. 3

Biofilm visualization using CLSM images with different modes of representation. *Bacillus* spp. strains were observed alone, or in a mixture with an *E. coli* strain that expresses GFP constitutively. SYTO 61 was used as a nonspecific marker to label in red all the cells. 3D projections of stacks using easy 3D mode are shown. The section mode allows the visualization of a fine (x,y) section of the base of the biofilm with a (z,y) section. 3D observation of isosurfaces of the mixed biofilm after binarization of both channels was made. All images were analysed using IMARIS software. The white scale bar represents 40 μm.

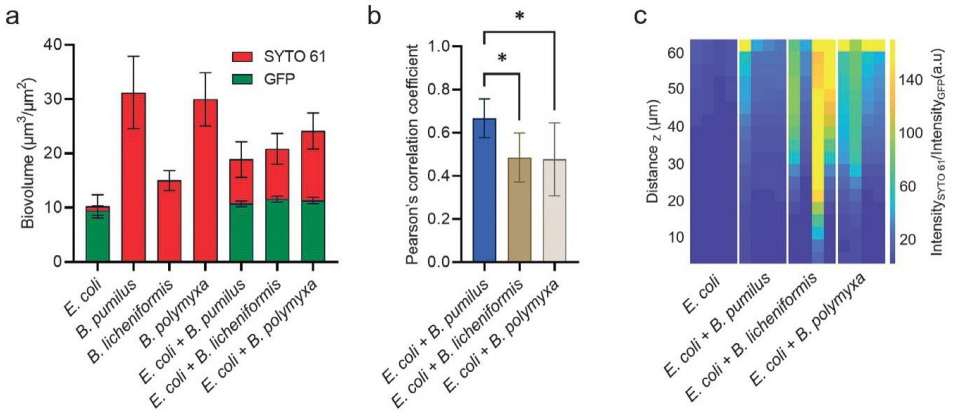

FIG. 4

Spatial analysis of mixed *E. coli* and *Bacillus* spp. biofilms. (A) Biovolume of each partner in mixed biofilms. The entire biofilm was labelled with SYTO 61 which targets nucleic acids and penetrates the cells allowing the labelling of the entire population (red). The monitoring of each partner is possible because *E. coli* expressed constitutively the GFP. The green bars in the graph correspond to the *E. coli* biovolume values in the total biofilm corresponding to the red bar values ($n=4$). (B) Pearson's correlation coefficient of mixed biofilms ($n=12$). (C) Kymographs of mixed biofilms fluorescence ratio intensity as a function of the distance to the substrate. A ratio value >1 means that there is more red intensity than green, so the higher the value, the more *Bacillus* spp. there are compared to *E. coli*. The yellow in the mixed biofilms of *E. coli* with *B. licheniformis* or *B. polymyxa* is consistent with the clusters of *Bacillus* spp. on the top of *E. coli* biofilm (Fig. 3). Each column corresponds to a replicate ($n=4$). The image stacks were taken with a CLSM. Error bars correspond to standard deviation and the asterisks correspond to $P< 0.05$. Statistical analysis were performed using two-way ANOVA and the uncorrected Fisher's least with PRISM software (GraphPad, San Diego, California, USA).

associated quantitative spatial analysis presented in Fig. 4. *E. coli* and *Bacillus* spp. biofilms were used as an example of multi-species biofilms to illustrate the experimental protocol.

3.1 Before you begin

Using fluorescent imaging to visualize spatial patterns of colonization in a multispecies biofilm is feasible only when it is possible to contrast both species with specific fluorophores. Having one partner expressing a fluorescent reporter (i.e. GFP) is enough as it can be combined with a second dye (i.e. nucleic acid probe SYTO 61) to label all the population in a second colour. The contrast between strains can be obtained with Gram staining, fluorescently labelled antibody or DNA probe (see Section 2.2).

All bacterial strains do not exhibit a similar adhesion rate on a specific surface. Hence to obtain a target initial ratio of adhering cells, it is necessary to calibrate the

relation between the number of planktonic cells added in the well and the number of adherent cells after incubation and rinsing.

In our example, we target a ratio of 0.50 ± 0.25 of each bacterial partner as estimated by quantifying the biovolume of adherent cells by CLSM using their respective fluorescent signatures (GFP or SYTO 61). If the value is not in the range, adjust the relative proportion of *Bacillus* spp. and *E. coli* to perform the adhesion phase. The protocol for this step is described below.

3.2 Materials

Equipment

- Laboratory incubator at 30 °C
- Polystyrene 96-well microtiter plate with a μclear® base (Greiner Bio-one, France)
- Leica SP8 AOBS inverted confocal laser scanning microscope (CLSM, LEICA Microsystems, Germany) equipped with a water immersion X63 objective (Numerical aperture = 1.2), a water pump, high-content screening module, two next-generation ultrasensitive detectors (HyD®)
- Leica Application Suite X (LAS X) software (LEICA Microsystems, Germany)
- IMARIS® 9.3.1 software (Bitplane, Zürich, Switzerland) with the batch option
- BiofilmQ software (Hartmann et al., 2021)

Chemicals and media

- SYTO 61 (Invitrogen, Carlsbad, CA, USA)
- Tryptic Soy Broth (TSB)
- TSB agar (1.5%) plate supplemented with ampicillin at 100 μg/mL (TSA Amp 100)

Strains

- A strain that constitutively expresses GFP. Here, we used *E. coli* CIRMBP 0248 isolated from a chick intestine that contains the pCM11 plasmid carrying the *gfp* expression system and *amp* gene encoding ampicillin (Amp) resistance for its selection (Malone et al., 2009).
- Non-labelled strains. Here, we used *B. pumilus* 1273, *B. licheniformis* 1218, and *B. polymyxa* 1167.

3.3 Methods

Growth of multi-species biofilms

1. From a −80 °C cryotube, plate the *E. coli* strain on a TSA Amp 100 Petri dish and incubate it for 24 h at 30 °C
2. Transfer a representative clone into a tube containing 5 mL of TSB without antibiotics. Scrape the surface of the −80 °C cryotubes containing the *Bacillus* spp. strains and inoculate tubes containing 5 mL of TSB. Incubate the cultures over night (~16 h) at 30 °C without agitation

3. Vortex the overnight cultures 3 s to homogenize the cell suspensions, and dilute at 1:100 in TSB for all the strains. For mixed biofilms, do the same but dilute in the same tube at 1:100 *E. coli* and one of the *Bacillus* spp. cultures
   Note: Read part "Quantification to make the ratio of the initial adhesion". If the ratio GFP/SYTO 61 is not between 0.25 and 0.75 with 1:100 dilution, adjust the proportion of *Bacillus* spp. in this step.
4. Adhesion phase: load 200 µL of the diluted solution in 2 different wells as technical replicates in polystyrene 96-well microtiter plates with a µclear® base. Incubate the plate for 90 min at 30 °C
5. Replace the medium in each well with 200 µL of fresh TSB. The plate is ready for labelling to verify initial adhesion. Once the ratio check has been performed, incubate the plate for 24 h at 30 °C for observation of the mixed biofilm.

Fluorescence labelling

1. Add SYTO 61 in 1 mL of TSB to obtain 15 µM final. Vortex the solution for 5 s
2. Load 50 µL of the SYTO 61 solution into each well
3. Protect from light and incubate for 10 min at room temperature. The plate is ready for image acquisition

Image acquisition

1. Turn on the confocal microscope with all the necessary components for its use (water pump, computer, microscope stand, controller, scan head, laser power and security)
2. Open LAS X software to set up the confocal microscope. Set the intensity of the 488 nm argon laser to 30% and switch on the HeNe 633 nm laser. Wait for 15 min to reach the power stability
3. Set one HyD detector photon collection between 500 and 550 nm to detect the fluorescence emitted by GFP. Use a second HyD detector to collect the fluorescence emitted by SYTO 61 between 650 and 750 nm. For both detectors, use the gain of 10%
4. Use the 63× water immersion lens. Turn on the water pump to get a drop of water on the lens. Remove air bubbles if needed. Carefully place the 96-well plate on the confocal platform and check the stability of the plate. Open shutter or brightfield and find the right well with the light intensity. Position the lens in the centre of the well
5. Set the image acquisition parameters. Set image definition at 512 × 512 pixels (pixel size = 360 nm). Choose a scan frequency value of 600 Hz for acquisition with the bidirectional scanning mode (image rate = 1.90/s). Use 1 as the pinhole value (value calculated with the Airy algorithm that optimizes the pinhole size for the acquisition parameters). Each image is taken by choosing a z-step of 1 µm for bacterial biofilms
6. Set the 488 nm laser intensity at 70% and the 633 nm at 40% with the acousto optical tunable filter (AOTF)
7. Raise the objective to find the base of the well
8. Create a new project for each well where the different stacks of images will be saved

9. Select the area to be imaged, in our case from the bottom of the well to the top of the biofilm and acquire the stack. In our example, two stacks of images per well were taken (4 zones per condition as there were two identical wells per plate)
10. Save image stacks in ".LIF" format

Image analysis

Visualization of the biofilms

(1) Open IMARIS and create a new "observed file" with the stacks in LIF format

(2) A background substraction with a threshold automatically calculated by the software is applied manually before each image stack observation

Notes: A batch can be created to do this step automatically if all images are in the same observed file.

(3) Open an image stack in the file to be analysed

(4) Select the easy 3D visualization with the blend mode, the section mode or 3D mode to visualize the mixed-species biofilm. The blend mode allows to obtain a reconstruction of the biofilm seen from above by the compilation of the stack images with a projection of the yz axis given by the shadow on the right of the image to obtain a representation of the relief. Thin sections of the biofilm along the xy, xz and yz axes are given by the section mode which allows a more precise visualization of the species between them. In the 3D mode, you have the possibility to binarize fluorescence signals of the two channels to perform isosurfaces. To do that, select the surface option and follow the steps indicated.

Notes: For all different representations, adjust the range of fluorescence of the two channels for optimized visualization.. For iso-surface, the binarization threshold can be adjusted manually.

(5) Take a snapshot to save the processed image projection

Quantification of the ratio of the initial adhesion

(1) Open BiofilmQ software and browse the LIF image stacks. In the folder where all the images are located, a new folder per project is created

(2) With BiofilmQ, open one newly created folder content and load the image stacks in the software

Notes: If there are a lot of images (i.e. confocal project), you have the possibility to make batches to analyse everything in the same way. To do this, create new files and copy the contents of each new folder into it. Set all desired parameters of "image preparation", "segmentation", "parameter calculation", "time-series analysis" and "data export" before going to "processe shortcuts" and select task that you want to batch. Click on "perform selected tasks on current experiment folder" to start the batch.

(3) Select channel 1 that corresponds to the GFP in the segmentation option. Set thresholding using OTSU class 2 with a sensitivity of 0.5. Segment image stacks using other default parameters of the segmentation option window. Check every image stack if the two segmentations correspond to the raw

image stack without background noise and over- or under-interpreting the size of the biofilm. Do the same with channel 2, which corresponds to SYTO 61

Notes: If the segmentation is not good, all the following steps must be restarted: adjust the segmentation sensitivity if needed.

(4) In parameter calculation, check the "global biofilm properties" option. Click on "Calculate object parameter" for both channels

(5) In data export, extract .csv files for both channels. One file is created per channel

(6) In every .csv file, extract the biovolume value. Calculate the GFP/SYTO 61 ratio with the control (*E. coli* alone). If the ratio is between 0.95 and 1.05, go to the next step. If not, check that the segmentations are correct with the segmentation preview option and adjust if necessary

(7) Calculate the GFP/SYTO 61 ratio with all images using the biovolume value of the csv files. The ratio must be between 0.25 and 0.75. If not, adjust the amount of *Bacillus* spp. in the 96-well plate and repeat all steps to be within the range.

Spatial analysis of the 24 h mix species biofilms

1. As in the above steps, images of 24 h mixed biofilms are loaded into BiofilmQ. The segmentation using thresholding OTSU class 2 with a sensitivity of 0.5 and a dissection method using cubes of 10 voxels side length (3.61 μm) is performed

   Notes: As above, a good segmentation is needed for the next steps. Adjust the sensitivity if needed.
2. In parameter calculation, check "Global biofilm properties", "Distance to surface", and "Fluorescence properties" withfor the last, "Mean intensity ratio per object channel 1 and channel 2" and the "Pearson coefficient calculation"
3. Export .csv files as previously described and extract values to graph biovolume and Pearson coefficient
4. Kymographs are made using the visualization window in BiofilmQ. One channel is loaded and in the Options window, choose "3D Heatmap/kymograph as calculated per title according method" as graph type. In the parameter choose "Frame" for X-axis, "Distance_From substrate" for Y_axis and "Intensity_Mean_Ch2_Ch1" for the colour code.

Arrange the range and Bins as needed to get the desired graph size (i.e. column size and sensitivity of the column split) and plot to obtain the Kymograph.

Summary of the analysis

The example analysis that was done to illustrate the experimental protocol has the objective to study the bacterial interaction inside a mixed bi-species biofilm. First, the structure of mono-specie biofilm was generated with IMARIS software and compared to mixed bi-species biofilm of *E. coli* GFP and the *Bacillus* spp. (Fig. 3). All mono-specie biofilm covered the surface, very densely for *E. coli* GFP. The *Bacillus* spp. strains formed 3D structured biofilms filamentous for *B. licheniformis* and clusters for *B. pumilus* and *B. polymyxa*.

Bi-species mixed biofilms showed different phenotypes in comparaison to mono-specie biofilms. Large clusters of *B. licheniformis* or *B. polymyxa* with a dense and flat biofilm of *E. coli* GFP around them are observed in mixed biofilm. These clusters seems to be on the biofilm of *E. coli* GFP.

To validate these observations, quantitative analysis were performed using BiofilmQ software with 4 images for each conditions (Fig. 4). The total biovolume of mono- and bi-species biofilms were calculated with the *E. coli* GFP and *Bacillus* spp. fractions (Fig. 4A). The biovolume of *E. coli* GFP was lower than the *Bacilus* spp. and *B. pumilus* and *B. polymyxa* had more biovolume in comparaison to *B. licheniformis*. The biovolume of *E. coli* GFP in bi-species biofilms were the same as the mono-specie biofilm of *E. coli* GFP unlike *Bacillus* spp. which decrease their biovolume in the presence of *E. coli* GFP. To quantify the organization of one partner in relation to the other within the mixed biofilm, the calculation of the Pearson's correlation coefficient was done (Fig. 4B). The value of *E. coli* GFP with *B. pumilus* was higher compared to the other two mixed biofilms, showing a more homogeneous organization of both partners in this case. To completment these analysis, a kymograph showing ratio of the $\text{intensity}_{\text{SYTO61}}/\text{Intensity}_{\text{GFP}}$ was performed to further investigate the stratification of bi-species biofilms (Fig. 4C). The results showed more SYTO61 intensity values on the top of the biofilm for *B. licheniformis* and *B. polymyxa* with *E. coli* GFP, corresponding to the clusters observed previously. All quantitative analyses confirmed the observations.

Acknowledgements

V.G. doctoral fellowship was funded by the "Association Nationale de la Recherche et de la Technologie" (contract 2020/0548) in the framework of a collaboration between INRAE and LALLEMAND SAS. R.C. was a recipient of an Anses-INRAE doctoral fellowship. This work was also supported by ANR JCJC BAoBAb (ANR-21-35CE-0001). Biofilm imaging was done at the INRAE MIMA2 imaging platform https://doi.org/10.15454/1.5572348210007727E12. Some figures were created with https://biorender.com/.

References

Almstrand, R., Daims, H., Persson, F., Sörensson, F., & Hermansson, M. (2013). New methods for analysis of spatial distribution and coaggregation of microbial populations in complex biofilms. *Applied and Environmental Microbiology*, *79*(19), 5978–5987. https://doi.org/10.1128/AEM.01727-13.

Altinoglu, I., Merrifield, C. J., & Yamaichi, Y. (2019). Single molecule super-resolution imaging of bacterial cell pole proteins with high-throughput quantitative analysis pipeline. *Scientific Reports*, *9*(1), 6680. https://doi.org/10.1038/s41598-019-43051-7.

Amieva, M., & Peek, R. M. (2016). Pathobiology of *Helicobacter pylori*-induced gastric cancer. *Gastroenterology*, *150*(1), 64–78. https://doi.org/10.1053/j.gastro.2015.09.004.

Arnaouteli, S., Bamford, N. C., Stanley-Wall, N. R., & Kovács, Á. T. (2021). *Bacillus subtilis* biofilm formation and social interactions. *Nature Reviews. Microbiology*, *19*(9), 600–614. https://doi.org/10.1038/s41579-021-00540-9.

Azeredo, J., Azevedo, N. F., Briandet, R., Cerca, N., Coenye, T., Costa, A. R., et al. (2017). Critical review on biofilm methods. *Critical Reviews in Microbiology*, *43*(3), 313–351. https://doi.org/10.1080/1040841X.2016.1208146.

Barnes, A. M. T., Dale, J. L., Chen, Y., Manias, D. A., Greenwood Quaintance, K. E., Karau, M. K., et al. (2017). *Enterococcus faecalis* readily colonizes the entire gastrointestinal tract and forms biofilms in a germ-free mouse model. *Virulence*, *8*(3), 282–296. https://doi.org/10.1080/21505594.2016.1208890.

Barraud, N., Hassett, D. J., Hwang, S.-H., Rice, S. A., Kjelleberg, S., & Webb, J. S. (2006). Involvement of nitric oxide in biofilm dispersal of *Pseudomonas aeruginosa*. *Journal of Bacteriology*, *188*(21), 7344–7353. https://doi.org/10.1128/JB.00779-06.

Bassères, E., Endres, B. T., Montes-Bravo, N., Pérez-Soto, N., Rashid, T., Lancaster, C., et al. (2021). Visualization of fidaxomicin association with the exosporium layer of *Clostridioides difficile* spores. *Anaerobe*, *69*, 102352. https://doi.org/10.1016/j.anaerobe.2021.102352.

Batt, C. A., & Tortorello, M. L. (Éds.). (2014). Encyclopedia of food microbiology (2nd ed.). AP, Academic Press/Elsevier.

Béchon, N., Mihajlovic, J., Lopes, A.-A., Vendrell-Fernández, S., Deschamps, J., Briandet, R., et al. (2022). *Bacteroides thetaiotaomicron* uses a widespread extracellular DNase to promote bile-dependent biofilm formation. *Proceedings of the National Academy of Sciences of the United States of America*, *119*(7), e2111228119. https://doi.org/10.1073/pnas.2111228119.

Benaissa, H., Ounoughi, K., Aujard, I., Fischer, E., Goïame, R., Nguyen, J., et al. (2021). Engineering of a fluorescent chemogenetic reporter with tunable color for advanced live-cell imaging. *Nature Communications*, *12*(1), 6989. https://doi.org/10.1038/s41467-021-27334-0.

Berk, V., Fong, J. C. N., Dempsey, G. T., Develioglu, O. N., Zhuang, X., Liphardt, J., et al. (2012). Molecular architecture and assembly principles of *Vibrio cholerae* biofilms. *Science (New York, N.Y.)*, *337*(6091), 236–239. https://doi.org/10.1126/science.1222981.

Billaudeau, C., Chastanet, A., Yao, Z., Cornilleau, C., Mirouze, N., Fromion, V., et al. (2017). Contrasting mechanisms of growth in two model rod-shaped bacteria. *Nature Communications*, *8*, 15370. https://doi.org/10.1038/ncomms15370.

Billaudeau, C., Yao, Z., Cornilleau, C., Carballido-López, R., & Chastanet, A. (2019). MreB forms subdiffraction nanofilaments during active growth in *Bacillus subtilis*. *MBio*, *10*(1). e01879-18 https://doi.org/10.1128/mBio.01879-18.

Blanchard, A. E., & Lu, T. (2015). Bacterial social interactions drive the emergence of differential spatial colony structures. *BMC Systems Biology*, *9*, 59. https://doi.org/10.1186/s12918-015-0188-5.

Bonicoli, F., Angelini, S., Riela, A., & Taiani, V. (1987). Anteposition of the tibial tuberosity in femoral-patellar arthrosis (4 to 7-year results). *La Chirurgia Degli Organi Di Movimento*, *72*(4), 327–332.

Bowler, P., Murphy, C., & Wolcott, R. (2020). Biofilm exacerbates antibiotic resistance: Is this a current oversight in antimicrobial stewardship? *Antimicrobial Resistance and Infection Control*, *9*(1), 162. https://doi.org/10.1186/s13756-020-00830-6.

Bridier, A., & Briandet, R. (2022). Microbial biofilms: Structural plasticity and emerging properties. *Microorganisms*, *10*(1), 138. https://doi.org/10.3390/microorganisms10010138.

Bridier, A., Briandet, R., Bouchez, T., & Jabot, F. (2014). A model-based approach to detect interspecific interactions during biofilm development. *Biofouling*, *30*(7), 761–771. https://doi.org/10.1080/08927014.2014.923409.

Bridier, A., Briandet, R., Thomas, V., & Dubois-Brissonnet, F. (2011). Resistance of bacterial biofilms to disinfectants: A review. *Biofouling*, *27*(9), 1017–1032. https://doi.org/10.1080/08927014.2011.626899.

Bridier, A., Dubois-Brissonnet, F., Boubetra, A., Thomas, V., & Briandet, R. (2010). The biofilm architecture of sixty opportunistic pathogens deciphered using a high throughput CLSM method. *Journal of Microbiological Methods*, *82*(1), 64–70. https://doi.org/10.1016/j.mimet.2010.04.006.

Bridier, A., Meylheuc, T., & Briandet, R. (2013). Realistic representation of *Bacillus subtilis* biofilms architecture using combined microscopy (CLSM, ESEM and FESEM). *Micron (Oxford, England: 1993)*, *48*, 65–69. https://doi.org/10.1016/j.micron.2013.02.013.

Bridier, A., Piard, J. C., Briandet, R., & Bouchez, T. (2020). Emergence of a synergistic diversity as a response to competition in *Pseudomonas putida* biofilms. *Microbial Ecology*, *80*(1), 47–59. https://doi.org/10.1007/s00248-019-01470-z.

Bridier, A., Piard, J.-C., Pandin, C., Labarthe, S., Dubois-Brissonnet, F., & Briandet, R. (2017). Spatial organization plasticity as an adaptive driver of surface microbial communities. *Frontiers in Microbiology*, *8*, 1364. https://doi.org/10.3389/fmicb.2017.01364.

Canette, A., Deschamps, J., & Briandet, R. (2019). High content screening confocal laser microscopy (HCS-CLM) to characterize biofilm 4D structural dynamic of foodborne pathogens. *Methods in Molecular Biology (Clifton, N.J.)*, *1918*, 171–182. https://doi.org/10.1007/978-1-4939-9000-9_14.

Chapman, S., Faulkner, C., Kaiserli, E., Garcia-Mata, C., Savenkov, E. I., Roberts, A. G., et al. (2008). The photoreversible fluorescent protein iLOV outperforms GFP as a reporter of plant virus infection. *Proceedings of the National Academy of Sciences of the United States of America*, *105*(50), 20038–20043. https://doi.org/10.1073/pnas.0807551105.

Charubin, K., Streett, H., & Papoutsakis, E. T. (2020). Development of strong anaerobic fluorescent reporters for *Clostridium acetobutylicum* and *Clostridium ljungdahlii* using HaloTag and SNAP-tag proteins. *Applied and Environmental Microbiology*, *86*(20), e01271-20. https://doi.org/10.1128/AEM.01271-20.

Chitlapilly Dass, S., Bosilevac, J. M., Weinroth, M., Elowsky, C. G., Zhou, Y., Anandappa, A., et al. (2020). Impact of mixed biofilm formation with environmental microorganisms on *E. coli* O157:H7 survival against sanitization. *NPJ Science of Food*, *4*, 16. https://doi.org/10.1038/s41538-020-00076-x.

Choong, F. X., Huzell, S., Rosenberg, M., Eckert, J. A., Nagaraj, M., Zhang, T., et al. (2021). A semi high-throughput method for real-time monitoring of curli producing Salmonella biofilms on air-solid interfaces. *Biofilms*, *3*, 100060. https://doi.org/10.1016/j.bioflm.2021.100060.

Christie, J. M., Hitomi, K., Arvai, A. S., Hartfield, K. A., Mettlen, M., Pratt, A. J., et al. (2012). Structural tuning of the fluorescent protein iLOV for improved photostability. *The Journal of Biological Chemistry*, *287*(26), 22295–22304. https://doi.org/10.1074/jbc.M111.318881.

Clevers, H. (2016). Modeling development and disease with organoids. *Cell*, *165*(7), 1586–1597. https://doi.org/10.1016/j.cell.2016.05.082.

Connell, J. L., Ritschdorff, E. T., Whiteley, M., & Shear, J. B. (2013). 3D printing of microscopic bacterial communities. *Proceedings of the National Academy of Sciences of the United States of America*, *110*(46), 18380–18385. https://doi.org/10.1073/pnas.1309729110.

Costache, V., Hebras, C., Pruliere, G., Besnardeau, L., Failla, M., Copley, R. R., et al. (2017). Kif2 localizes to a subdomain of cortical endoplasmic reticulum that drives asymmetric spindle position. *Nature Communications*, *8*(1), 917. https://doi.org/10.1038/s41467-017-01048-8.

Daims, H., Lücker, S., & Wagner, M. (2006). Daime, a novel image analysis program for microbial ecology and biofilm research. *Environmental Microbiology*, *8*(2), 200–213. https://doi.org/10.1111/j.1462-2920.2005.00880.x.

Dar, D., Dar, N., Cai, L., & Newman, D. K. (2021). Spatial transcriptomics of planktonic and sessile bacterial populations at single-cell resolution. *Science (New York, N.Y.)*, *373*(6556), eabi4882. https://doi.org/10.1126/science.abi4882.

Day, R. N., & Davidson, M. W. (2009). The fluorescent protein palette: Tools for cellular imaging. *Chemical Society Reviews*, *38*(10), 2887–2921. https://doi.org/10.1039/b901966a.

de Beer, D., Stoodley, P., Roe, F., & Lewandowski, Z. (1994). Effects of biofilm structures on oxygen distribution and mass transport. *Biotechnology and Bioengineering*, *43*(11), 1131–1138. https://doi.org/10.1002/bit.260431118.

Dekkers, J. F., Alieva, M., Wellens, L. M., Ariese, H. C. R., Jamieson, P. R., Vonk, A. M., et al. (2019). High-resolution 3D imaging of fixed and cleared organoids. *Nature Protocols*, *14*(6), 1756–1771. https://doi.org/10.1038/s41596-019-0160-8.

Deshmukh, R. A., Joshi, K., Bhand, S., & Roy, U. (2016). Recent developments in detection and enumeration of waterborne bacteria: A retrospective minireview. *MicrobiologyOpen*, *5*(6), 901–922. https://doi.org/10.1002/mbo3.383.

Díaz-Pascual, F., Lempp, M., Nosho, K., Jeckel, H., Jo, J. K., Neuhaus, K., et al. (2021). Spatial alanine metabolism determines local growth dynamics of *Escherichia coli* colonies. *eLife*, *10*, e70794. https://doi.org/10.7554/eLife.70794.

Doiron, K., Linossier, I., Fay, F., Yong, J., Abd Wahid, E., Hadjiev, D., et al. (2012). Dynamic approaches of mixed species biofilm formation using modern technologies. *Marine Environmental Research*, *78*, 40–47. https://doi.org/10.1016/j.marenvres.2012.04.001.

Douterelo, I., Jackson, M., Solomon, C., & Boxall, J. (2016). Microbial analysis of in situ biofilm formation in drinking water distribution systems: Implications for monitoring and control of drinking water quality. *Applied Microbiology and Biotechnology*, *100*(7), 3301–3311. https://doi.org/10.1007/s00253-015-7155-3.

Drepper, T., Eggert, T., Circolone, F., Heck, A., Krauss, U., Guterl, J.-K., et al. (2007). Reporter proteins for in vivo fluorescence without oxygen. *Nature Biotechnology*, *25*(4), 443–445. https://doi.org/10.1038/nbt1293.

Dubois, T., Tremblay, Y. D. N., Hamiot, A., Martin-Verstraete, I., Deschamps, J., Monot, M., et al. (2019). A microbiota-generated bile salt induces biofilm formation in Clostridium difficile. *NPJ Biofilms and Microbiomes*, *5*(1), 14. https://doi.org/10.1038/s41522-019-0087-4.

Dunn, K. W., Kamocka, M. M., & McDonald, J. H. (2011). A practical guide to evaluating colocalization in biological microscopy. *American Journal of Physiology. Cell Physiology*, *300*(4), C723–C742. https://doi.org/10.1152/ajpcell.00462.2010.

Elias, S., & Banin, E. (2012). Multi-species biofilms: Living with friendly neighbors. *FEMS Microbiology Reviews*, *36*(5), 990–1004. https://doi.org/10.1111/j.1574-6976.2012.00325.x.

Esser, D. S., Leveau, J. H. J., Meyer, K. M., & Wiegand, K. (2015). Spatial scales of interactions among bacteria and between bacteria and the leaf surface. *FEMS Microbiology Ecology*, *91*(3), fiu034. https://doi.org/10.1093/femsec/fiu034.

Fagerlund, A., Langsrud, S., & Møretrø, T. (2021). Microbial diversity and ecology of biofilms in food industry environments associated with *Listeria monocytogenes* persistence. *Current Opinion in Food Science*, *37*, 171–178. https://doi.org/10.1016/j.cofs.2020.10.015.

Farasin, J., Koechler, S., Varet, H., Deschamps, J., Dillies, M.-A., Proux, C., et al. (2017). Comparison of biofilm formation and motility processes in arsenic-resistant *Thiomonas* spp. strains revealed divergent response to arsenite. *Microbial Biotechnology*, *10*(4), 789–803. https://doi.org/10.1111/1751-7915.12556.

Flemming, H.-C., Neu, T. R., & Wingender, J. (Eds.). (2017). *The perfect slime: Microbial extracellular polymeric sibstances (EPS)*. IWA Publishing.

Flemming, H.-C., Wingender, J., Szewzyk, U., Steinberg, P., Rice, S. A., & Kjelleberg, S. (2016). Biofilms: An emergent form of bacterial life. *Nature Reviews. Microbiology*, *14*(9), 563–575. https://doi.org/10.1038/nrmicro.2016.94.

Frickmann, H., Zautner, A. E., Moter, A., Kikhney, J., Hagen, R. M., Stender, H., et al. (2017). Fluorescence in situ hybridization (FISH) in the microbiological diagnostic routine laboratory: A review. *Critical Reviews in Microbiology*, *43*(3), 263–293. https://doi.org/10.3109/1040841X.2016.1169990.

Giaouris, E., Heir, E., Desvaux, M., Hébraud, M., Møretrø, T., Langsrud, S., et al. (2015). Intra- and inter-species interactions within biofilms of important foodborne bacterial pathogens. *Frontiers in Microbiology*, *6*, 841. https://doi.org/10.3389/fmicb.2015.00841.

Grand, I., Bellon-Fontaine, M.-N., Herry, J.-M., Hilaire, D., Moriconi, F.-X., & Naïtali, M. (2011). Possible overestimation of surface disinfection efficiency by assessment methods based on liquid sampling procedures as demonstrated by in situ quantification of spore viability. *Applied and Environmental Microbiology*, *77*(17), 6208–6214. https://doi.org/10.1128/AEM.00649-11.

Guéneau, V., Rodiles, A., Piard, J.-C., Frayssinet, B., Castex, M., Plateau-Gonthier, J., et al. (2021). Capture and ex-situ analysis of environmental biofilms in livestock buildings. *Microorganisms*, *10*(1), 2. https://doi.org/10.3390/microorganisms10010002.

Guilbaud, M., Piveteau, P., Desvaux, M., Brisse, S., & Briandet, R. (2015). Exploring the diversity of *listeria monocytogenes* biofilm architecture by high-throughput confocal laser scanning microscopy and the predominance of the honeycomb-like morphotype. *Applied and Environmental Microbiology*, *81*(5), 1813–1819. https://doi.org/10.1128/AEM.03173-14.

Guilini, C., Baehr, C., Schaeffer, E., Gizzi, P., Rufi, F., Haiech, J., et al. (2015). New fluorescein precursors for live bacteria detection. *Analytical Chemistry*, *87*(17), 8858–8866. https://doi.org/10.1021/acs.analchem.5b02100.

Habimana, O., Guillier, L., Kulakauskas, S., & Briandet, R. (2011). Spatial competition with *Lactococcus lactis* in mixed-species continuous-flow biofilms inhibits *Listeria monocytogenes* growth. *Biofouling*, *27*(9), 1065–1072. https://doi.org/10.1080/08927014.2011.626124.

Hall, D. C., Palmer, P., Ji, H.-F., Ehrlich, G. D., & Król, J. E. (2021). Bacterial biofilm growth on 3D-printed materials. *Frontiers in Microbiology*, *12*, 646303. https://doi.org/10.3389/fmicb.2021.646303.

Han, X., Mslati, M. A., Davies, E., Chen, Y., Allaire, J. M., & Vallance, B. A. (2021). Creating a more perfect union: Modeling intestinal Bacteria-epithelial interactions using organoids. *Cellular and Molecular Gastroenterology and Hepatology*, *12*(2), 769–782. https://doi.org/10.1016/j.jcmgh.2021.04.010.

Hartmann, R., Jeckel, H., Jelli, E., Singh, P. K., Vaidya, S., Bayer, M., et al. (2021). Quantitative image analysis of microbial communities with BiofilmQ. *Nature Microbiology*, *6*(2), 151–156. https://doi.org/10.1038/s41564-020-00817-4.

Hautefort, I., Proença, M. J., & Hinton, J. C. D. (2003). Single-copy green fluorescent protein gene fusions allow accurate measurement of *Salmonella* gene expression in vitro and during infection of mammalian cells. *Applied and Environmental Microbiology*, *69*(12), 7480–7491. https://doi.org/10.1128/AEM.69.12.7480-7491.2003.

Hauth, J., Chodorski, J., Wirsen, A., & Ulber, R. (2020). Improved FRAP measurements on biofilms. *Biophysical Journal*, *118*(10), 2354–2365. https://doi.org/10.1016/j.bpj.2020.03.017.

Hernández-Galán, L., Cattenoz, T., Le Feunteun, S., Canette, A., Briandet, R., Le-Guin, S., et al. (2017). Effect of dairy matrices on the survival of *Streptococcus thermophilus*, *Brevibacterium aurantiacum* and *Hafnia alvei* during digestion. *Food Research International (Ottawa, Ont.)*, *100*(Pt 1), 477–488. https://doi.org/10.1016/j.foodres.2017.07.044.

Heumann, A., Assifaoui, A., Da Silva Barreira, D., Thomas, C., Briandet, R., Laurent, J., et al. (2020). Intestinal release of biofilm-like microcolonies encased in calcium-pectinate beads increases probiotic properties of *Lacticaseibacillus paracasei*. *NPJ Biofilms and Microbiomes*, *6*(1), 44. https://doi.org/10.1038/s41522-020-00159-3.

Høiby, N., Bjarnsholt, T., Givskov, M., Molin, S., & Ciofu, O. (2010). Antibiotic resistance of bacterial biofilms. *International Journal of Antimicrobial Agents*, *35*(4), 322–332. https://doi.org/10.1016/j.ijantimicag.2009.12.011.

Huang, Y., Xia, A., Yang, G., & Jin, F. (2018). Bioprinting living biofilms through optogenetic manipulation. *ACS Synthetic Biology*, *7*(5), 1195–1200. https://doi.org/10.1021/acssynbio.8b00003.

Jeckel, H., & Drescher, K. (2021). Advances and opportunities in image analysis of bacterial cells and communities. *FEMS Microbiology Reviews*, *45*(4), fuaa062. https://doi.org/10.1093/femsre/fuaa062.

Jo, J., Price-Whelan, A., & Dietrich, L. E. P. (2022). Gradients and consequences of heterogeneity in biofilms. *Nature Reviews. Microbiology*. https://doi.org/10.1038/s41579-022-00692-2.

Johnson, M. B., & Criss, A. K. (2013). Fluorescence microscopy methods for determining the viability of bacteria in association with mammalian cells. *Journal of Visualized Experiments: JoVE*, *79*. https://doi.org/10.3791/50729.

Karampatzakis, A., Sankaran, J., Kandaswamy, K., Rice, S. A., Cohen, Y., & Wohland, T. (2017). Measurement of oxygen concentrations in bacterial biofilms using transient state monitoring by single plane illumination microscopy. *Biomedical Physics & Engineering Express*, *3*(3), 035020. https://doi.org/10.1088/2057-1976/aa6db7.

Karygianni, L., Ren, Z., Koo, H., & Thurnheer, T. (2020). Biofilm Matrixome: Extracellular components in structured microbial communities. *Trends in Microbiology*, *28*(8), 668–681. https://doi.org/10.1016/j.tim.2020.03.016.

Keppler, A., Gendreizig, S., Gronemeyer, T., Pick, H., Vogel, H., & Johnsson, K. (2003). A general method for the covalent labeling of fusion proteins with small molecules in vivo. *Nature Biotechnology*, *21*(1), 86–89. https://doi.org/10.1038/nbt765.

Kim, D., Barraza, J. P., Arthur, R. A., Hara, A., Lewis, K., Liu, Y., et al. (2020). Spatial mapping of polymicrobial communities reveals a precise biogeography associated with human dental caries. *Proceedings of the National Academy of Sciences of the United States of America*, *117*(22), 12375–12386. https://doi.org/10.1073/pnas.1919099117.

Krishna Kumar, R., Meiller-Legrand, T. A., Alcinesio, A., Gonzalez, D., Mavridou, D. A. I., Meacock, O. J., et al. (2021). Droplet printing reveals the importance of micron-scale structure for bacterial ecology. *Nature Communications*, *12*(1), 857. https://doi.org/10.1038/s41467-021-20996-w.

Kristensen, M. F., Leonhardt, D., Neland, M. L. B., & Schlafer, S. (2020). A 3D printed microfluidic flow-cell for microscopy analysis of in situ-grown biofilms. *Journal of Microbiological Methods*, *171*, 105876. https://doi.org/10.1016/j.mimet.2020.105876.

Kühbacher, A., Cossart, P., & Pizarro-Cerdá, J. (2021). Internalization assays for *Listeria monocytogenes*. *Methods in Molecular Biology (Clifton, N.J.)*, *2220*, 189–200. https://doi.org/10.1007/978-1-0716-0982-8_15.

Lagache, T., Lang, G., Sauvonnet, N., & Olivo-Marin, J.-C. (2013). Analysis of the spatial organization of molecules with robust statistics. *PLoS One*, *8*(12), e80914. https://doi.org/10.1371/journal.pone.0080914.

Lagache, T., Sauvonnet, N., Danglot, L., & Olivo-Marin, J.-C. (2015). Statistical analysis of molecule colocalization in bioimaging. *Cytometry. Part A: The Journal of the International Society for Analytical Cytology*, *87*(6), 568–579. https://doi.org/10.1002/cyto.a.22629.

Lagendijk, E. L., Validov, S., Lamers, G. E. M., de Weert, S., & Bloemberg, G. V. (2010). Genetic tools for tagging Gram-negative bacteria with mCherry for visualization in vitro and in natural habitats, biofilm and pathogenicity studies. *FEMS Microbiology Letters*, *305*(1), 81–90. https://doi.org/10.1111/j.1574-6968.2010.01916.x.

Lee, K. W. K., Periasamy, S., Mukherjee, M., Xie, C., Kjelleberg, S., & Rice, S. A. (2014). Biofilm development and enhanced stress resistance of a model, mixed-species community biofilm. *The ISME Journal*, *8*(4), 894–907. https://doi.org/10.1038/ismej.2013.194.

Lee, J.-Y., Sadler, N. C., Egbert, R. G., Anderton, C. R., Hofmockel, K. S., Jansson, J. K., et al. (2020). Deep learning predicts microbial interactions from self-organized spatiotemporal patterns. *Computational and Structural Biotechnology Journal*, *18*, 1259–1269. https://doi.org/10.1016/j.csbj.2020.05.023.

Li, Q., Liu, L., Guo, A., Zhang, X., Liu, W., & Ruan, Y. (2021). Formation of multispecies biofilms and their resistance to disinfectants in food processing environments: A review. *Journal of Food Protection*, *84*(12), 2071–2083. https://doi.org/10.4315/JFP-21-071.

Liu, W., Røder, H. L., Madsen, J. S., Bjarnsholt, T., Sørensen, S. J., & Burmølle, M. (2016). Interspecific bacterial interactions are reflected in multispecies biofilm spatial organization. *Frontiers in Microbiology*, *7*, 1366. https://doi.org/10.3389/fmicb.2016.01366.

Los, G. V., Encell, L. P., McDougall, M. G., Hartzell, D. D., Karassina, N., Zimprich, C., et al. (2008). HaloTag: A novel protein labeling technology for cell imaging and protein analysis. *ACS Chemical Biology*, *3*(6), 373–382. https://doi.org/10.1021/cb800025k.

Lu, M., Wang, X., Sun, G., Qin, B., Xiao, J., Yan, S., et al. (2014). Fine structure of Tibetan kefir grains and their yeast distribution, diversity, and shift. *PLoS One*, *9*(6), e101387. https://doi.org/10.1371/journal.pone.0101387.

Malone, C. L., Boles, B. R., Lauderdale, K. J., Thoendel, M., Kavanaugh, J. S., & Horswill, A. R. (2009). Fluorescent reporters for Staphylococcus aureus. *Journal of Microbiological Methods*, *77*(3), 251–260. https://doi.org/10.1016/j.mimet.2009.02.011.

Mark Welch, J. L., Rossetti, B. J., Rieken, C. W., Dewhirst, F. E., & Borisy, G. G. (2016). Biogeography of a human oral microbiome at the micron scale. *Proceedings of the National Academy of Sciences of the United States of America*, *113*(6), E791–E800. https://doi.org/10.1073/pnas.1522149113.

Minsky, M. (1988). Memoir on inventing the confocal scanning microscope: Memoir on inventing the confocal scanning microscope. *Scanning*, *10*(4), 128–138. https://doi.org/10.1002/sca.4950100403.

Monmeyran, A., Thomen, P., Jonquière, H., Sureau, F., Li, C., Plamont, M.-A., et al. (2018). The inducible chemical-genetic fluorescent marker FAST outperforms classical fluorescent proteins in the quantitative reporting of bacterial biofilm dynamics. *Scientific Reports*, *8*(1), 10336. https://doi.org/10.1038/s41598-018-28643-z.

Mukherjee, A., Weyant, K. B., Agrawal, U., Walker, J., Cann, I. K. O., & Schroeder, C. M. (2015). Engineering and characterization of new LOV-based fluorescent proteins from *Chlamydomonas reinhardtii* and *Vaucheria frigida*. *ACS Synthetic Biology*, *4*(4), 371–377. https://doi.org/10.1021/sb500237x.

Munir, M. T., Maneewan, N., Pichon, J., Gharbia, M., Oumarou-Mahamane, I., Baude, J., et al. (2021). Confocal spectral microscopy, a non-destructive approach to follow contamination and biofilm formation of mCherry *Staphylococcus aureus* on solid surfaces. *Scientific Reports*, *11*(1), 15574. https://doi.org/10.1038/s41598-021-94939-2.

Neu, T. R., & Lawrence, J. R. (1999). Lectin-binding analysis in biofilm systems. *Methods in Enzymology*, *310*, 145–152. https://doi.org/10.1016/s0076-6879(99)10012-0.

Nicolle, O., Rouillon, A., Guyodo, H., Tamanai-Shacoori, Z., Chandad, F., Meuric, V., et al. (2010). Development of SNAP-tag-mediated live cell labeling as an alternative to GFP in *Porphyromonas gingivalis*. *FEMS Immunology and Medical Microbiology*, *59*(3), 357–363. https://doi.org/10.1111/j.1574-695X.2010.00681.x.

Ning, E., Turnbull, G., Clarke, J., Picard, F., Riches, P., Vendrell, M., et al. (2019). 3D bioprinting of mature bacterial biofilms for antimicrobial resistance drug testing. *Biofabrication*, *11*(4), 045018. https://doi.org/10.1088/1758-5090/ab37a0.

Noirot-Gros, M.-F., Shinde, S. V., Akins, C., Johnson, J. L., Zerbs, S., Wilton, R., et al. (2020). Functional imaging of microbial interactions with tree roots using a microfluidics setup. *Frontiers in Plant Science*, *11*, 408. https://doi.org/10.3389/fpls.2020.00408.

O'Donnell, A. G., Young, I. M., Rushton, S. P., Shirley, M. D., & Crawford, J. W. (2007). Visualization, modelling and prediction in soil microbiology. *Nature Reviews. Microbiology*, *5*(9), 689–699. https://doi.org/10.1038/nrmicro1714.

Oliveira, N. M., Oliveria, N. M., Martinez-Garcia, E., Xavier, J., Durham, W. M., Kolter, R., et al. (2015). Biofilm formation as a response to ecological competition. *PLoS Biology*, *13*(7), e1002191. https://doi.org/10.1371/journal.pbio.1002191.

Olpe, H. R., Glatt, A., Laszlo, J., & Schellenberg, A. (1980). Some electrophysiological and pharmacological properties of the cortical, noradrenergic projection of the locus coeruleus in the rat. *Brain Research*, *186*(1), 9–19. https://doi.org/10.1016/0006-8993(80)90251-6.

Pamp, S. J., Sternberg, C., & Tolker-Nielsen, T. (2009). Insight into the microbial multicellular lifestyle via flow-cell technology and confocal microscopy. *Cytometry. Part A: The Journal of the International Society for Analytical Cytology*, *75*(2), 90–103. https://doi.org/10.1002/cyto.a.20685.

Pandin, C., Darsonval, M., Mayeur, C., Le Coq, D., Aymerich, S., & Briandet, R. (2019). Biofilm formation and synthesis of antimicrobial compounds by the biocontrol agent *Bacillus velezensis* QST713 in an Agaricus bisporus compost micromodel. *Applied and Environmental Microbiology*, *85*(12). e00327-19 https://doi.org/10.1128/AEM.00327-19.

Panigrahi, S., Murat, D., Le Gall, A., Martineau, E., Goldlust, K., Fiche, J.-B., et al. (2021). Misic, a general deep learning-based method for the high-throughput cell segmentation of complex bacterial communities. *eLife*, *10*, e65151. https://doi.org/10.7554/eLife.65151.

Petrovai, A., & Nedevschi, S. (2022). Fast panoptic segmentation with soft attention Embeddings. *Sensors (Basel, Switzerland)*, *22*(3), 783. https://doi.org/10.3390/s22030783.

Plamont, M.-A., Billon-Denis, E., Maurin, S., Gauron, C., Pimenta, F. M., Specht, C. G., et al. (2016). Small fluorescence-activating and absorption-shifting tag for tunable protein imaging in vivo. *Proceedings of the National Academy of Sciences of the United States of America*, *113*(3), 497–502. https://doi.org/10.1073/pnas.1513094113.

Pouget, C., Dunyach-Remy, C., Pantel, A., Schuldiner, S., Sotto, A., & Lavigne, J.-P. (2021). New adapted in vitro technology to evaluate biofilm formation and antibiotic activity using live imaging under flow conditions. *Diagnostics (Basel, Switzerland)*, *11*(10), 1746. https://doi.org/10.3390/diagnostics11101746.

Qin, B., Fei, C., Bridges, A. A., Mashruwala, A. A., Stone, H. A., Wingreen, N. S., et al. (2020). Cell position fates and collective fountain flow in bacterial biofilms revealed by light-sheet microscopy. *Science (New York, N.Y.)*, *369*(6499), 71–77. https://doi.org/10.1126/science.abb8501.

Ragi, S., Rahman, M. H., Duckworth, J., Kalimuthu, J., Chundi, P., & Gadhamshetty, V. (2021). Artificial intelligence-driven image analysis of bacterial cells and biofilms. *IEEE/ACM Transactions on Computational Biology and Bioinformatics*. https://doi.org/10.1109/TCBB.2021.3138304.

Ramírez-Puebla, S. T., Weigel, B. L., Jack, L., Schlundt, C., Pfister, C. A., & Mark Welch, J. L. (2022). Spatial organization of the kelp microbiome at micron scales. *Microbiome*, *10*(1), 52. https://doi.org/10.1186/s40168-022-01235-w.

Reuter, A., Virolle, C., Goldlust, K., Berne-Dedieu, A., Nolivos, S., & Lesterlin, C. (2020). Direct visualisation of drug-efflux in live *Escherichia coli* cells. *FEMS Microbiology Reviews*, *44*(6), 782–792. https://doi.org/10.1093/femsre/fuaa031.

Romani, M., Carrion, C., Fernandez, F., Lebaron, P., & Lami, R. (2021). Methyl potassium Siliconate and siloxane inhibit the formation of multispecies biofilms on ceramic roof tiles: Efficiency and comparison of two common water repellents. *Microorganisms*, *9*(2), 394. https://doi.org/10.3390/microorganisms9020394.

Sadiq, F. A., Burmølle, M., Heyndrickx, M., Flint, S., Lu, W., Chen, W., et al. (2021). Community-wide changes reflecting bacterial interspecific interactions in multispecies biofilms. *Critical Reviews in Microbiology*, *47*(3), 338–358. https://doi.org/10.1080/1040841X.2021.1887079.

Saint Martin, C., Darsonval, M., Grégoire, M., Caccia, N., Midoux, L., Berland, S., et al. (2022). Spatial organisation of *Listeria monocytogenes* and *Escherichia coli O157:H7* cultivated in gel matrices. *Food Microbiology*, *103*, 103965. https://doi.org/10.1016/j.fm.2021.103965.

Sanchez-Vizuete, P., Dergham, Y., Bridier, A., Deschamps, J., Dervyn, E., Hamze, K., et al. (2022). The coordinated population redistribution between *Bacillus subtilis* submerged biofilm and liquid-air pellicle. *Biofilms*, *4*, 100065. https://doi.org/10.1016/j.bioflm.2021.100065.

Sanchez-Vizuete, P., Orgaz, B., Aymerich, S., Le Coq, D., & Briandet, R. (2015). Pathogens protection against the action of disinfectants in multispecies biofilms. *Frontiers in Microbiology*, *6*, 705. https://doi.org/10.3389/fmicb.2015.00705.

Schillinger, C., Petrich, A., Lux, R., Riep, B., Kikhney, J., Friedmann, A., et al. (2012). Co-localized or randomly distributed? Pair cross correlation of in vivo grown subgingival biofilm bacteria quantified by digital image analysis. *PLoS One*, *7*(5), e37583. https://doi.org/10.1371/journal.pone.0037583.

Schulmeister, S., Ruttorf, M., Thiem, S., Kentner, D., Lebiedz, D., & Sourjik, V. (2008). Protein exchange dynamics at chemoreceptor clusters in *Escherichia coli*. *Proceedings of the National Academy of Sciences of the United States of America*, *105*(17), 6403–6408. https://doi.org/10.1073/pnas.0710611105.

Shaner, N. C., Campbell, R. E., Steinbach, P. A., Giepmans, B. N. G., Palmer, A. E., & Tsien, R. Y. (2004). Improved monomeric red, orange and yellow fluorescent proteins derived from *Discosoma* sp. red fluorescent protein. *Nature Biotechnology*, *22*(12), 1567–1572. https://doi.org/10.1038/nbt1037.

Shank, E. A., Klepac-Ceraj, V., Collado-Torres, L., Powers, G. E., Losick, R., & Kolter, R. (2011). Interspecies interactions that result in *Bacillus subtilis* forming biofilms are mediated mainly by members of its own genus. *Proceedings of the National Academy of Sciences of the United States of America*, *108*(48), E1236–E1243. https://doi.org/10.1073/pnas.1103630108.

Shimomura, O., Johnson, F. H., & Saiga, Y. (1962). Extraction, purification and properties of aequorin, a bioluminescent protein from the luminous hydromedusan, *Aequorea*. *Journal of Cellular and Comparative Physiology*, *59*, 223–239. https://doi.org/10.1002/jcp.1030590302.

Silva, T. S. O., Freitas, A. R., Pinheiro, M. L. L., do Nascimento, C., Watanabe, E., & Albuquerque, R. F. (2018). Oral biofilm formation on different materials for dental implants. *Journal of Visualized Experiments: JoVE*, *136*. https://doi.org/10.3791/57756.

Steinberg, S., Grinberg, M., Beitelman, M., Peixoto, J., Orevi, T., & Kashtan, N. (2021). Two-way microscale interactions between immigrant bacteria and plant leaf microbiota as revealed by live imaging. *The ISME Journal*, *15*(2), 409–420. https://doi.org/10.1038/s41396-020-00767-z.

Streett, H., Charubin, K., & Papoutsakis, E. T. (2021). Anaerobic fluorescent reporters for cell identification, microbial cell biology and high-throughput screening of microbiota and genomic libraries. *Current Opinion in Biotechnology*, *71*, 151–163. https://doi.org/10.1016/j.copbio.2021.07.005.

Tawakoli, P. N., Al-Ahmad, A., Hoth-Hannig, W., Hannig, M., & Hannig, C. (2013). Comparison of different live/dead stainings for detection and quantification of adherent microorganisms in the initial oral biofilm. *Clinical Oral Investigations*, *17*(3), 841–850. https://doi.org/10.1007/s00784-012-0792-3.

Thomsen, H., Graf, F. E., Farewell, A., & Ericson, M. B. (2018). Exploring photoinactivation of microbial biofilms using laser scanning microscopy and confined 2-photon excitation. *Journal of Biophotonics*, *11*(10), e201800018. https://doi.org/10.1002/jbio.201800018.

Tolker-Nielsen, T., & Sternberg, C. (2011). Growing and analyzing biofilms in flow chambers. *Current Protocols in Microbiology*. *Chapter 1*, Unit 1B.2 https://doi.org/10.1002/9780471729259.mc01b02s21.

Tolker-Nielsen, T., & Sternberg, C. (2014). Methods for studying biofilm formation: Flow cells and confocal laser scanning microscopy. *Methods in Molecular Biology (Clifton, N.J.)*, *1149*, 615–629. https://doi.org/10.1007/978-1-4939-0473-0_47.

Tran, T., Grandvalet, C., Winckler, P., Verdier, F., Martin, A., Alexandre, H., et al. (2021). Shedding light on the formation and structure of Kombucha biofilm using two-photon fluorescence microscopy. *Frontiers in Microbiology*, *12*, 725379. https://doi.org/10.3389/fmicb.2021.725379.

van Tatenhove-Pel, R. J., Rijavec, T., Lapanje, A., van Swam, I., Zwering, E., Hernandez-Valdes, J. A., et al. (2021). Microbial competition reduces metabolic interaction distances to the low µm-range. *The ISME Journal*, *15*(3), 688–701. https://doi.org/10.1038/s41396-020-00806-9.

Wu, B. C., Haney, E. F., Akhoundsadegh, N., Pletzer, D., Trimble, M. J., Adriaans, A. E., et al. (2021). Human organoid biofilm model for assessing antibiofilm activity of novel agents. *NPJ Biofilms and Microbiomes*, *7*(1), 8. https://doi.org/10.1038/s41522-020-00182-4.

Xu, J.-G., Hu, H.-X., Han, B.-Z., & Chen, J.-Y. (2022). Interactions between *Salmonella enteritidis* and food processing facility isolate *Bacillus paramycoides* B5 in dual-species biofilms. *LWT*, *156*, 113053. https://doi.org/10.1016/j.lwt.2021.113053.

Yarwood, J. M., Bartels, D. J., Volper, E. M., & Greenberg, E. P. (2004). Quorum sensing in *Staphylococcus aureus* biofilms. *Journal of Bacteriology*, *186*(6), 1838–1850. https://doi.org/10.1128/JB.186.6.1838-1850.2004.

Yuan, L., de Haan, P., Peterson, B. W., de Jong, E. D., Verpoorte, E., van der Mei, H. C., et al. (2020). Visualization of bacterial colonization and cellular layers in a gut-on-a-chip system using optical coherence tomography. *Microscopy and Microanalysis: The Official Journal of Microscopy Society of America, Microbeam Analysis Society, Microscopical Society of Canada*, *26*(6), 1211–1219. https://doi.org/10.1017/S143192762002454X.

Zaborskytė, G., Wistrand-Yuen, E., Hjort, K., Andersson, D. I., & Sandegren, L. (2021). Modular 3D-printed peg biofilm device for flexible setup of surface-related biofilm studies. *Frontiers in Cellular and Infection Microbiology*, *11*, 802303. https://doi.org/10.3389/fcimb.2021.802303.

Zhang, M., Zhang, J., Wang, Y., Wang, J., Achimovich, A. M., Acton, S. T., et al. (2020). Non-invasive single-cell morphometry in living bacterial biofilms. *Nature Communications*, *11*(1), 6151. https://doi.org/10.1038/s41467-020-19866-8.

Zijnge, V., van Leeuwen, M. B. M., Degener, J. E., Abbas, F., Thurnheer, T., Gmür, R., et al. (2010). Oral biofilm architecture on natural teeth. *PLoS One*, *5*(2), e9321. https://doi.org/10.1371/journal.pone.0009321.

Résultats

1. Criblage et données préliminaires

Une première étape de criblage destinée à évaluer la capacité à former des biofilms du panel de 64 souches (cf Stratégie expérimentale 1.1) a été réalisée dans l'objectif de sélectionner une dizaine de souches pertinentes pour étudier l'adaptation aux biocides en mode de vie biofilm, toutes les souches n'étant pas nécessairement de grandes productrices de biofilms (1.1.). Une fois le criblage effectué, les souches sélectionnées ont été caractérisées afin de pouvoir définir les conditions expérimentales pour l'expérience d'évolution dirigée. La CMI des souches aux biocides a été quantifiée (1.2), tout comme la concentration d'antibiotiques nécessaire pour inhiber leur croissance sur gélose (1.3.).

1.1. Criblage sur Crystal Violet

Le criblage initial a été effectué sur les 64 souches afin d'identifier celles présentant des capacités significatives à former des biofilms. Celui-ci a été effectué à l'aide de la méthode quantitative du crystal violet. La distribution des souches formant des biofilms importants et moins importants est plus ou moins équitable selon la filière dans laquelle elles ont été isolées (les années 2014, 2016 et 2018 correspondent aux filières volailles, tandis que les années 2015, 2017 et 2019 sont liées aux filières porcines, en raison de l'alternance d'échantillonnage des filières définie dans les plans de surveillance) (Figure 8). De manière intéressante, une part plus importante des souches isolées en 2018 semblent former des biofilms conséquents, contrairement à celles de 2019 où la formation de biofilms est moindre. Toutefois, il est difficile de conclure sur une éventuelle corrélation entre l'année de prélèvement et la formation de biofilms sans tester si cette tendance se confirme sur une quantité plus importante de souches. N'étant pas l'objectif principal de la thèse, cette piste n'a pas été poursuivie.
Afin de conserver une répartition équitable entre les années et les filières, les souches formant des biofilms importants ont été choisies de manière équilibrée entre les différentes années. La souche de collection Ec223 répondant bien au crible a également été choisie, tout comme la souche Ec1655 qui forme des biofilms moins importants mais pouvant servir de référence. Les souches conservées sont présentées dans le tableau 2.

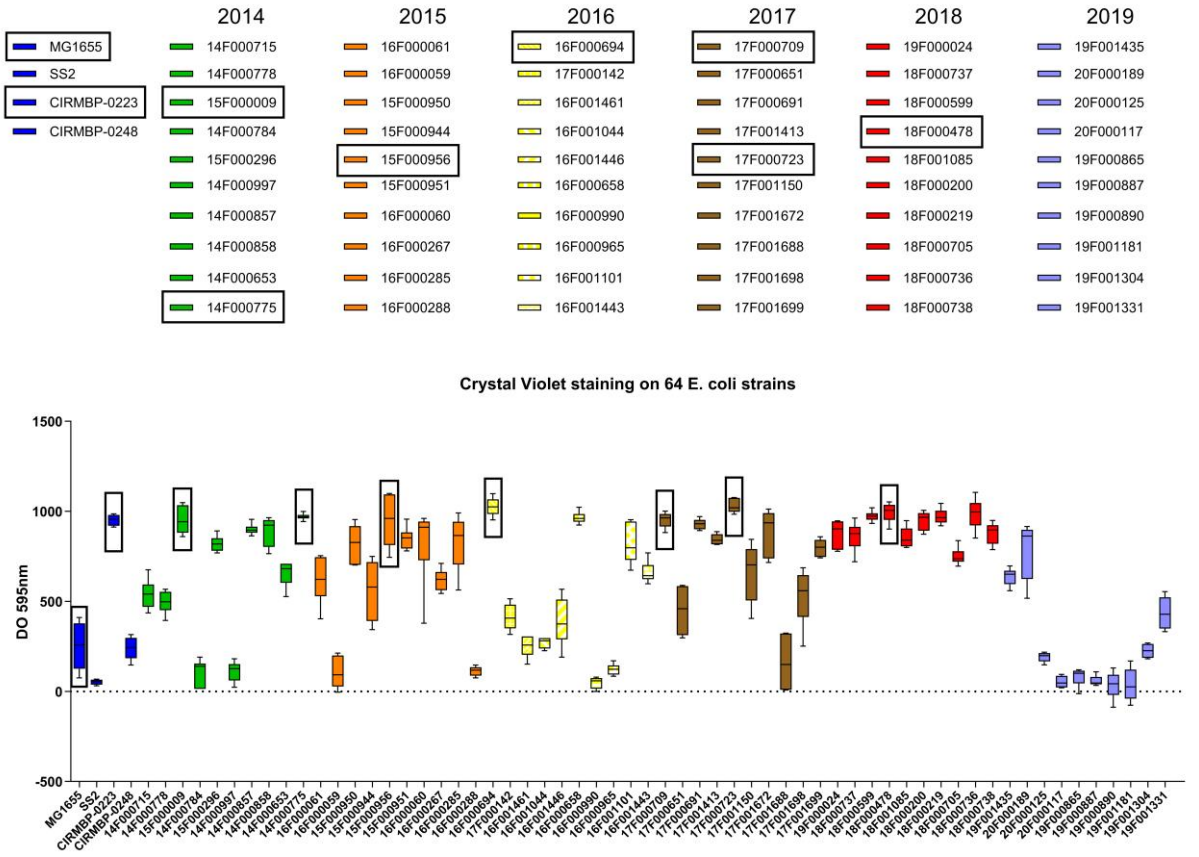

Figure 8 : Analyse au crystal violet des 64 souches. Les 9 souches conservées pour la suite de l'étude sont encadrées en noir.

Souche	Nom dans la thèse	Année de prélèvement	Résistance aux antibiotiques
MG1655	Ec1655		
CIRMBP-0223	Ec223	1977	
14F000775	Ec775	2014	
15F0000009	Ec009	2014	Gentamicine, Sulfaméthoxazole
15F000956	Ec956	2015	Tétracycline
16F000694	Ec694	2016	Ampicilline
17F000709	Ec709	2017	Ampicilline
17F000723	Ec723	2017	
18F000478	Ec478	2019	Tétracycline

Tableau 2 : Présentation des 9 souches conservées après le crible au crystal violet, avec leur abréviation dans la thèse, leur année de prélèvement et leur résistance aux antibiotiques.

1.2. Analyse de la CMI des biocides

Des analyses ont été effectuées pour déterminer la concentration appropriée à laquelle exposer les bactéries. Dans l'ensemble, sous forme planctonique, les 9 souches possédaient approximativement les mêmes niveaux de résistances aux biocides utilisés (Tableau 3). Pour les expériences ultérieures, il a été décidé d'exposer les biofilms de toutes les souches à la CMI la plus basse parmi les 10 souches, excepté pour le PHMB où la concentration de 2,5 mg/L a été choisie, afin que la souche Ec223 ne soit pas trop faiblement impactée, en considérant qu'en biofilms, Ec1655 serait capable de survivre à un stress plus élevé.

	Ec1655	Ec223	Ec775	Ec009	Ec694	Ec956	Ec709	Ec723	Ec478
BAC	12,5	12,5	12,5	12,5	12,5	6,25	12,5	12,5	12,5
PHMB	1,25	5	2,5	2,5	2,5	2,5	2,5	2,5	2,5
TMN	13,2	13,2	6,6	13,2	13,2	13,2	13,2	6,6	13,2
SHY	100	100	100	100	100	100	100	100	100

Tableau 3 : Analyse de la CMI des souches aux différents biocides utilisés dans l'étude (en mg/L).

1.3. Vérification de la sélectivité des géloses

La sélectivité des géloses TSA supplémentées en antibiotiques a été vérifiée vis-à-vis de leur capacité à discriminer une souche sensible d'une souche résistante et ainsi discriminer une souche parentale sensible d'un variant résistant émergeant. Les concentrations minimales pour inhiber toute croissance des souches parentales étaient de 10 mg/L pour la gentamicine, correspondant à 5 fois l'Ecoff, 1,2 mg/L pour la ciprofloxacine, correspondant à 20 fois l'Ecoff, et 20 mg/L pour la rifampicine (aucune donnée n'est disponible pour l'Ecoff de *E. coli* avec la rifampicine). La souche Ec009 possédant déjà une résistance à la gentamicine, a pu croître à ces concentrations et n'a donc pas été prise en compte pour ce test.

2. Le biofilm : une structure adaptative et promotrice de la résistance

Dans cette partie, sont présentés les effets du mode de vie biofilm et des biocides sur la résistance à la gentamicine. Ces antibiotiques font respectivement partie de la famille des aminoglycosides. Leur étude est essentielle, en témoignent les rapports de l'organisation mondiale de la santé (OMS), qui les classent parmi la liste des antibiotiques d'intérêt critique (World Health Organization, 2019). Les aminoglycosides ciblent la sous-unité 30S du ribosome (Smith and Baker, 2002), impliquée dans la traduction de l'ARN en protéines. Des résistances croisées avec le PHMB ont déjà été observées au sein du laboratoire (Cuzin et al., 2021) et se caractérisent notamment par des réductions d'activité métabolique de la bactérie, limitant les effets toxiques sur la cellule (Allison et al., 2011; Ibacache-Quiroga et al., 2018). Une résistance par baisse de l'activité métabolique est particulièrement pertinente dans le cadre des études sur les biofilms, où les gradients de nutriments et d'oxygène provoquent aussi un ralentissement de l'activité cellulaire (Jo et al., 2022a).
Dans cette étude, une première partie a révélé que le nombre de variants GenR était significativement plus élevé dans les conditions de biofilm, comparé aux conditions en surnageant et en phase planctonique (2.1). Les variants GenR se définissent ici comme les variants ayant poussé sur les géloses supplémentées avec 10 mg/L de gentamicine, sans distinction entre ceux avec résistances stables et ceux avec résistances transitoires (identifiés après le test de stabilité de la résistance). Ils ne comprennent pas non plus de variants ayant poussé sur des géloses avec 20 mg/L de gentamicine, car aucun variant n'a poussé à ces concentrations. Les analyses phénotypiques ont révélé que ces variants résistants avaient une croissance plus lente que les souches parentales dont ils étaient issus. Les analyses génotypiques ont confirmé que des cibles dans la respiration cellulaire étaient préférentiellement mutées chez les souches issues de l'industrie agro-alimentaire. En revanche, le mécanisme de résistance chez Ec1655 était différent, impliquant de larges délétions du génome.
En présence de biocides (2.2.1.), une augmentation du nombre de variants GenR a été identifiée au cours des dernières semaines de l'exposition au PHMB. Cependant, après analyse des variants émergeants dans cette condition, la plupart ne possédaient pas de résistances stables, ce qui signifie qu'ils émergeaient préférentiellement avec l'activation de réponses physiologiques temporaires. Cette observation, corrélée au fait que les variants GenR émergent préférentiellement en biofilms, nous a conduits à explorer le lien entre le PHMB et la formation de biofilms. Les analyses ont montré qu'en présence de PHMB, les souches formaient des clusters au sein du biofilm, créant potentiellement des microenvironnements induisant un métabolisme réduit, et favorisant la survie à la gentamicine. Des analyses par CLSM sur des expérimentations de longue durée (2.2.2.) ont également confirmé que le PHMB induisait la formation de matrice, modulant sa structure spatiale. *De facto*, la structuration induite par le PHMB associée à une réduction de l'accès aux nutriments et à l'oxygène favorise l'apparition de souches à la croissance réduite, étant capables de survivre à des expositions à la gentamicine.

2.1. Article 4 : L'émergence de variants résistants à la gentamicine est favorisée par le mode de vie biofilms

« Strain-dependent emergence of aminoglycoside resistance in *Escherichia coli* biofilms »

Raphaël Charron, Pierre Lemée, Antoine Huguet, Ornella Minlong, Marine Boulanger, Paméla Houée, Christophe Soumet, Romain Briandet, Arnaud Bridier

Strain-dependent emergence of aminoglycoside resistance in *Escherichia coli* biofilms

Raphaël Charron[1,2], Pierre Lemée[1], Antoine Huguet[1], Ornella Minlong[1], Marine Boulanger[1], Paméla Houée[1], Christophe Soumet[1], Romain Briandet[2], Arnaud Bridier[1]

1 Antibiotics, Biocides, Residues and Resistance Unit, Fougères Laboratory, Anses, 35300 Fougères, France

2 Université Paris-Saclay, INRAE, AgroParisTech, Micalis Institute, 78350, Jouy-en-Josas, France

Acknowledgments:
ANR JCJC BAoBAb (ANR-21-CE35-0001) supported financially this work. RC was also recipient of an ANSES-INRAE doctoral fellowship. Thanks to the MIMA 2 Imaging Core Facility (MIMA2, 2018) for the use of the Leica HCS-SP8 CLSM and especially to Vlad Costache for the useful advises. Thanks also to the French AntibioDEAL network of the Promise PPR antibioresistance ANR program for the useful scientific exchanges.

Declaration of Interest statement:
The authors declare that the research was conducted in the absence of any commercial or financial relationships that could be construed as a potential conflict of interest.

Corresponding author:
Arnaud Bridier
ANSES Laboratoire de Fougères
10b, rue Claude Bourgelat, 75133 Javené

Corresponding author email address:
arnaud.bridier@anses.fr

Abstract:
In most environments on Earth, bacteria predominantly exist in communities known as biofilms, where they are embedded in an extracellular matrix. These structures play a crucial role on physiology and significantly influence their evolutionary trajectories. Biofilms are particularly important in the emergence of antimicrobial resistance and the resilience of bacteria to treatments, with serious implications for public health. In this work, the impact of the growth and evolution in biofilms on the emergence of resistance to the aminoglycoside gentamicin was explored in eight *Escherichia coli* strains. During the one month-experiment, we observed that the emergence of gentamicin-resistant variants in some strains was significantly stimulated in biofilms in comparison to their planktonic counterparts. Genomic and phenotypic analysis of these variants revealed diverse resistance mechanisms, which varied depending on the *E. coli* strain. These findings underscore the complexity of adaptive evolution in biofilms and highlight the necessity of studying multiple strains to fully understand the diversity present in natural bacterial populations.

Keywords: Biofilms, Antibiotics, Resistance, Evolution, Aminoglycoside

Highlights:

- Biofilms favor the emergence of gentamicin-resistant variants but in a strain-dependent process
- Global bacterial gene expression severely decreased overtime during 31-days biofilm maturation
- Genotypical analysis on the variants revealed different strategies of adaptation among strains involving large genomic deletions for reference MG1655 strain and rather SNPs/indels in food chain isolates strains
- Variants with large deletions were more severely impacted in their fitness than variants with SNPs and indels

Introduction:

The discovery of antibiotics has revolutionized both human and veterinary medicine, preventing millions of deaths. Nevertheless, this success is now jeopardized by the propagation of antibiotic-resistant bacteria. Misuse of antibiotics, whether through improper medical applications or practices like their use as growth promoters in agriculture (Aslam et al., 2021b), has accelerated the selection of bacteria able to survive to these therapeutic agents. A wide diversity of mechanisms driving the emergence and the selection of antibiotic resistances has been identified in various bacterial species, including pathogens (Davies and Davies, 2010; Reygaert, 2018).
In natural environments, bacteria predominantly don’t exist in the free-floating planktonic form typically studied, but rather in fixed communal populations, called biofilms (Flemming et al., 2016). Microorganisms in biofilms are spatially organized through the formation of an extracellular matrix, mainly composed of polysaccharides, lipids, extracellular DNA or proteins (Karygianni et al., 2020). This lifestyle promotes the emergence of multiple heterogeneous populations, potentially including antibiotic-tolerant subpopulations (Jo et al., 2022b). The extracellular matrix and resource consumption by bacteria in the outer layers limit nutrients and oxygen diffusion to the deeper layers (Jo et al., 2022b), competing bacteria to adapt by entering in slow or non-growing lifestyles in response to nutrient scarcity (Yan

and Bassler, 2019). Such physiological shifts can enhance bacterial survival under antimicrobial stresses, as inactive metabolic pathways may shield the cells from antimicrobial toxicity (Lewis, 2010). The biofilm environment is however stressful for the cells, often triggering the activation of stress responses such as the stringent and the SOS response (Charron et al., 2023a). The use of error-prone polymerases in these responses, induced by the bacteria to favor a rapid DNA repair, can elevate mutation rates (Crane et al., 2021). In general, these properties are considered to be important for the development of mutations. Resistance mutations are moreover often reducing bacterial fitness (Melnyk et al., 2015). However, biofilms can provide a "protective cocoon" to the bacteria (Charron et al., 2023a), enabling resistant bacteria to survive long enough for enabling the rise of compensatory mutations, finally mitigating the fitness cost (Penesyan et al., 2021).
These biofilm-specific characteristics make this lifestyle a potent driver of bacterial evolution, contributing to the emergence of antibiotic-resistant clones, even in the absence of external stresses. In this study, we investigated how the biofilm lifestyle influence the emergence of gentamicin-resistant (GenR) bacteria, an aminoglycoside antibiotic classified as critically important by the World Health Organization (World Health Organization, 2019). Resistance to gentamicin is often associated with mutations in metabolic pathways (Allison et al., 2011; Ibacache-Quiroga et al., 2018), making it a valuable model for studying variant emergence in biofilms. Here, we characterized the biofilm profiles of eight different *E. coli* strains, including strains recently isolated from food industries, and their ability to generate GenR variants. Further characterization revealed a wide variability in the production of GenR variants, depending on strains and a wide diversity in the genotypical and phenotypical profiles of the produced variants.

Material and Methods:

1. Bacterial strains

Eight *E. coli* strains were used in this study. The strain MG1655, referred hereafter as Ec1655, was used as a reference. Another strain, CIRMBP-0223 (Ec223), was obtained from the CIRM collection at INRAE and originates from a chick. The remaining six strains (Ec478; Ec694; Ec709; Ec723; Ec775; Ec956) belong to the collection of the National Reference Laboratory for Antimicrobial Resistance, hosted in the laboratory of Fougères. These strains were isolated from the pork and poultry industries between 2014 and 2019. All strains were stored at -80°C in cryotubes (Mast Group, Bootle, UK).

2. Biofilm structure analysis by Confocal Laser Scanning Microscopy (CLSM)

Strains were first streaked from cryotubes onto Tryptone Soja Agar (TSA) plates and incubated overnight at 37 °C. A colony was suspended in ten-fold diluted Tryptone Soja Broth (TSB 1/10) and incubated overnight at 37 °C. The next day, cultures were diluted to reach a final $OD_{600\ nm}$ of 0.2. A microplate was prepared with 10 µL of the diluted suspensions and 190 µL of TSB 1/10 in each well. The plate was incubated at 19 °C for 1 h, followed by a medium change with fresh TSB 1/10. Biofilms were then incubated at 19°C for 72 h under static conditions. After the 72-hour incubation, biofilms were stained with SYTO™9 green fluorescent permeant nucleic acid stain (Invitrogen, USA) combined either with DeepRed Concanavalin A (Invitrogen, USA) (ConA) or red Wheat Germ Agglutinin (Invitrogen, USA) (WGA). Images were acquired using a Leica HCS-SP8 CLSM at the INRAE MIMA2

Imaging Core Facility (MIMA2, 2018). Fluorophores were excited at 488 nm for SYTO™9, 561 nm for WGA and 633 nm for ConA, and emission was collected was detected using photomultiplier tubes (PMT) at 500-550 nm for SYTO™9, 600-750 nm for WGA and 650-750 nm for ConA. A 63x water objective lens (numerical aperture: 1.2) was used to scan the biofilms, with a resolution of 512x512 and a 1 µm Z-step. Two wells were observed for each condition, with two images taken per well. Biofilm 3D reconstructions were generated using Imaris 9.3.1 software (Bitplane, AG-Zürich, Switzerland) and quantitative ConA and WGA biovolumes were extracted using BiofilmQ 0.2.2 (Hartmann et al., 2021)**.**

3. Congo red fluorescence assay

Biofilms of the parental strains were prepared at 24 h and 72 h as previously described. A solution of 50 µL of TSB 1/10 supplemented with Congo red (Sigma-Aldrich, France) was added to each well to achieve a final concentration of 40 µg/mL. The plates were incubated in the dark for 15 minutes. Fluorescence was quantified using a Biotek SynergyH1 microplate reader, with excitation at 525 nm and emission at 625 nm. Three biological replicates with three technical replicates were performed for each strain under each condition.

4. RT-q-PCR analysis in Ec1655 biofilms

Gene expression levels were quantified in Ec1655 biofilms over one month (Table S1). The medium was renewed daily with fresh TSB 1/10. Biofilms from eight wells were pooled on days 3 (the day after the 72-hour initial incubation), 10, 17 and 31. Total RNA was isolated using the NucleoSpin RNA kit according to manufacturer's instructions (Macherey-Nagel, Hoerd, France) with modifications. Enzymatic lysis was first performed using 25 µL of a 1 mg/mL lysozyme, Tris 10 mM and EDTA 1 mM mix for 10 min at 37 °C. RNA concentration and purity were assessed using a Biospec-Nano spectrophotometer (Shimadzu, Marne la Vallée, France). Reverse transcription, qPCR, primers design and analyses were performed as described in Reale *et al*. (Reale et al., 2019) with modifications. Reverse transcription was performed with 1.3 µg of total RNA, and quantitative PCR reactions were carried out with 2.6 ng cDNA. Primers were purchased from Sigma-Aldrich (Saint-Quentin Fallavier, France), and additional information on oligonucleotide primers are provided in Table S1. The *hcat* gene, identified using NormFinder software, was chosen as a reference gene due to its stable expression across samples. Three independent experiments were performed.

5. Biofilm and planktonic experimental evolution

Biofilms were prepared as previously described with eight wells per strain. Planktonic culture plates were prepared by adding 10 µL of bacterial suspensions adjusted to $OD_{600\ nm}$ of 0.2 into 190 µL of TSB 1/10, and incubated at 19 °C with shaking at 200 rpm for 72 h. The medium was renewed daily with fresh TSB 1/10. On days 3, 10, 17, 24 and 31, 5 µL of biofilm supernatants were plated on agar plates containing 10 mg/L gentamicin. Supernatants were then removed and 40 µL of fresh 1/10 TSB were added. Biofilms were resuspended and 5 µL of the biofilm suspension were dropped on the gentamicin plates. In parallel, 5 µL of the planktonic plates were also plated. Gentamicin-supplemented plates were incubated for 48 hours at 37 °C. Biofilm wells were filled to 200 µL. 10 µL of the planktonic culture were

transferred in 190 µL of fresh TSB 1/10 medium. Plates were incubated at 19°C and 200 rpm, for the planktonic cultures and static conditions for the biofilm cultures.

6. Mutation stability assay

The stability of the resistance phenotype of variants was evaluated as described in Charron *et al*. (Charron et al., 2023b)**.** Briefly, variants were streaked on TSA plates and incubated at 37 °C for 24 hours. This step was repeated four times. On the fifth passage, variants were plated on TSA containing 10 mg/L gentamicin to confirm resistance.

7. Enterobacterial Repetitive Intergenic Consensus – PCR (ERIC-PCR)

ERIC-PCR was performed to confirm that variants originated from the parental strain, following the method from Charron *et al.* (Charron et al., 2023b)**.** Briefly, parental and variant DNA was extracted using an InstaGene kit (Bio-Rad, Marnes-la-Coquette, France). ERIC-1 (ATGTAAGCTCCTGGGGATTCAC) and ERIC-2 (AAGTAAGTGACTGGGGTGAGCG) primers were used to amplify specific bands with the GoTaq Flexi polymerase (Promega, Charbonnières-les-Bains, France) in a LightCycler 480 thermocycler (Roche Diagnostics, Meylan, France) with the following parameters: a first cycle of 2 min at 95 °C; then 30 cycles at 95 °C for 1 min, 54 °C for 1 min, 72 °C for 4 min; and a final step at 72 °C for 8 min followed by an unlimited 4 °C cooldown.

8. DNA extraction and sequencing

Whole genome sequencing of all *E. coli* strains was performed using paired-end short-reads sequencing. Bacterial cultures were grown on Thermo Scientific™ Tryptone Soya Agar with 5% Sheep Blood plates (Reference: Thermo Fisher Scientific, PB5012A), overnight at 37 °C. A single colony was inoculated in 5 mL of a 1/10 Tryptone Soja Broth (TSB) solution and incubated overnight at 37 °C. Total DNA was isolated using the Nucleospin Tissue kit according to the manufacturer's instructions (Macherey-Nagel, Düren, Germany). DNA was quantified with the Qubit dsDNA BR HS assay kit according to the manufacturer's instructions and using a Qubit 4 (Thermo Fisher Scientific, Courtaboeuf, France). Illumina sequencing was performed at Institut du Cerveau et de la Moelle Epinière (Paris, France) on a Novaseq 6000 SP. Nextera XT kit was used to prepare Illumina libraries. The whole process of sequence analysis is described in Lemée *et al*. (Lemée et al., 2025). Reads were trimmed using fastp (0.23.4) (Chen, 2023) and genomes assembled using Unicycler (v0.5.0) (Wick et al., 2017), with only contigs longer than 200nt retained. Bakta (v1.8.2) (Schwengers et al., 2021) was used to annotate assembled genomes. Variant calling was carried out using Snippy (v4.6.0) (https://github.com/tseemann/snippy) for each variant, with the parental strain genome as the genome reference. Analysis pipelines are available on GitHub: https://github.com/AB2R/WGS_pipeline.git

9. Minimal inhibitory concentration (MIC) determination for 15 antibiotics

MIC values for 15 different antibiotics were determined as described in Cuzin et al. (Cuzin et al., 2021). Bacteria were streaked on TSA + 5% Sheep blood plate and incubated at 37 °C overnight. The following day, colonies were suspended in 5 mL sterile water to reach 0.5 Mac Farland (≈ 10^8 CFUs/mL). A 10 µL aliquot was transferred into 11 mL of Mueller Hinton Broth (MHB). 50 µL of the MHB suspension were transferred into a standardized microplate (EUVSEC, Sensititre®, TREK Diagnostic Systems Ltd., Thermo Fisher Scientific, East Grinstead, UK) containing lyophilized antibiotics. Plates were incubated for 24 h at 35 °C and read on the next day. MIC values were determined as the median value of three replicates.

10. Bacterial growth kinetics analysis

Growth kinetics of bacteria were analyzed during 18 hours. Subcultures of the strains were grown overnight in 1/10 TSB at 37 °C. The next day, OD_{600nm} of the cultures were adjusted to 0.2, and 10 µL of the culture was transferred in 190 µL of 1/10 TSB to reach a 0.01 OD_{600nm}. The cultures were incubated at 20 °C (± 1 °C) for 18 h in a FLUOstar OPTIMA (BMG Labtech, Champigny-sur-Marne, France). ODs were measured every 30 minutes. Growth rates (µmax) were extracted using the MARS Data analysis software (BMG Labtech, Champigny-sur-Marne, France).

11. Crystal Violet quantification of biofilm production

Crystal violet staining of biofilms was performed as described by Merritt et al. (Merritt et al., 2005)**.** Variants and wild-type strains were grown overnight at 37 °C in 5 mL of TSB 1/10. Biofilms were prepared as previously described. After 72 h, supernatants were removed, and wells were washed with 200 µL of a sterile NaCl 150 mM solution. Biofilms were stained with 125 µL of 0.1% Crystal Violet solution for 10 min. Excess Crystal Violet was removed and the well washed twice with 200 µL of sterile NaCl 150 mM solution. To solubilize the bound crystal violet, 200 µL of a Ethanol 80% / Acetone 20% solution was added and the wells were incubated for 15 min. Supernatants were transferred to a new plate, and OD_{590nm} was measured using a FLUOstar OPTIMA (BMG Labtech, Champigny-sur-Marne, France) to quantify biofilm formation.

12. Statistical analysis

Statistical analyses were performed using Graphpad Prism software. A Kruskal-Wallis test combined with a Dunn's multiple comparison test was used for: the comparison of the characterized parental strains (ConA and WGA biovolume values and congo red fluorescence values), the comparison of each timepoint of the RT-q-PCR analysis, and the comparison, for each strain and each week, of the biofilms, supernatants and planktonic conditions. Growth parameters and Crystal Violet assays were compared with the Mann-Whitney test, between variants and parental strains. P values are represented as follows: * = [0.05-0.01]; ** = [0.01-0.001]; *** = <0.001.

Results:

1. Biofilms promote the emergence of stable GenR variants in Ec1655

The biofilms formed by the Ec1655 reference strain were first characterized. Concanavalin A (ConA) staining, which targets polysaccharides with α-D-mannosyl and α-D-glucosyl residues, showed minimal staining of the biofilm matrix, both at 24 h (Fig. 1A and C) and at 72 h (Fig. 1B and C). Similarly, the congo red fluorescence assay (Fig. 1E), which detect amyloid fibers and cellulose, revealed a negligible amount of matrix staining at 24 hours, and only a few replicates showing some staining at 72 h. This weak congo red signal was also observed in one-week-old Ec1655 macrocolonies, which exhibited a SAW (Smooth and White) phenotype, associated with a deficit in curli and cellulose production (Fig. S1). In contrast, wheat germ agglutinin (WGA) staining which detects N-acetylglucosamine, revealed significant biofilm structures in which cells were embedded (Fig. 1A, B and D).

A one-month gene expression analysis of Ec1655 biofilms (Fig. 1F) revealed that biofilm formation genes showed the most stable expression profile. Notably, *pgaA*, which encodes poly-β-1,6-*N*-acetylglucosamine (PNAG) production, exhibited a tendancy for increased expression towards the end of the experiment, coherently with the WGA staining. Conversely, *csgA* and *csgB*, which encode curli proteins involved in adhesion, showed a marked decrease in expression after one week. Other genes involved in cell metabolism, stress responses and resistance showed a strong decrease in expression throughout time. Of the 26 tested genes, 17 showed significant expression decreases between the first and the last week of the experiment (*csgA, csgB, fimB, cpxR, dksA, hfq, recA, relA, rpoS, aceE, ackA, arcA, atpG, cydA, acrA, ompC, ompF*) (Table S4).

Concomitantly, biofilms, supernatants and planktonic cultures were sampled weekly over the course of one month and plated on gentamicin-supplemented agar to access the emergence of GenR variants (Fig. 1G). A significant difference was observed between biofilm and planktonic lifestyles, with most GenR variants isolated emerging from biofilms. This effect was mostly pronounced along biofilm maturation after a few weeks of evolution, and was significant at the 24 and 31-days timepoints (Table S3). No variants were isolated from the biofilm supernatants, suggesting a biofilm-specific emergence of resistance. The supernatants also had lower cell concentrations compared to biofilms, which may partly explain the lower frequency of GenR variants (Fig. S2). Analysis of resistance stability (Fig. 1H) revealed that most isolated clones conserved their resistance after several passages in non-selective conditions, illustrating a stable resistance phenotype.

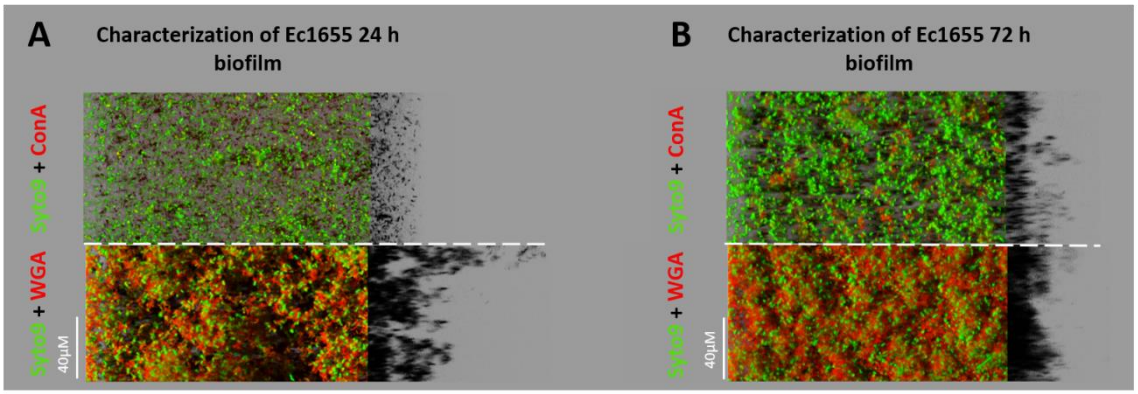
A
Characterization of Ec1655 24 h biofilm
Syto9 + ConA
Syto9 + WGA
40µM
B
Characterization of Ec1655 72 h biofilm
Syto9 + ConA
Syto9 + WGA
40µM

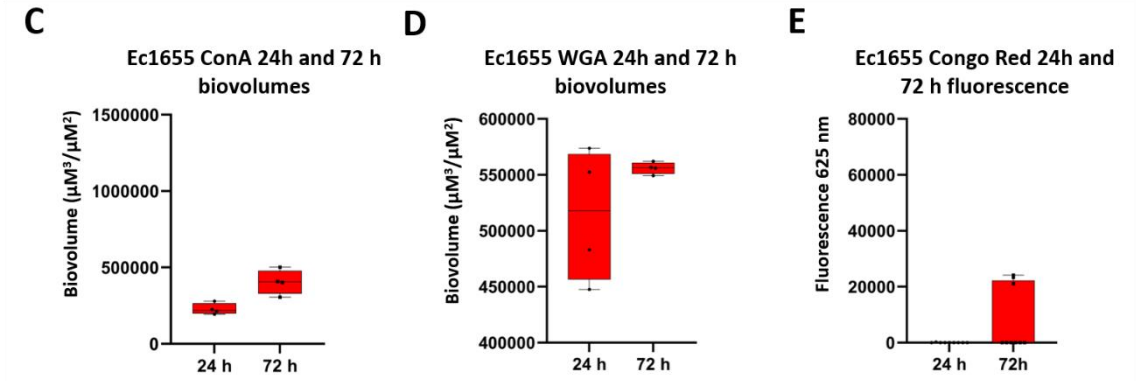
C
Ec1655 ConA 24h and 72 h biovolumes
Biovolume (µM³/µM²)
1500000
1000000
500000
0
24 h
72 h
D
Ec1655 WGA 24h and 72 h biovolumes
Biovolume (µM³/µM²)
600000
550000
500000
450000
400000
24 h
72 h
E
Ec1655 Congo Red 24h and 72 h fluorescence
Fluorescence 625 nm
80000
60000
40000
20000
0
24 h
72h

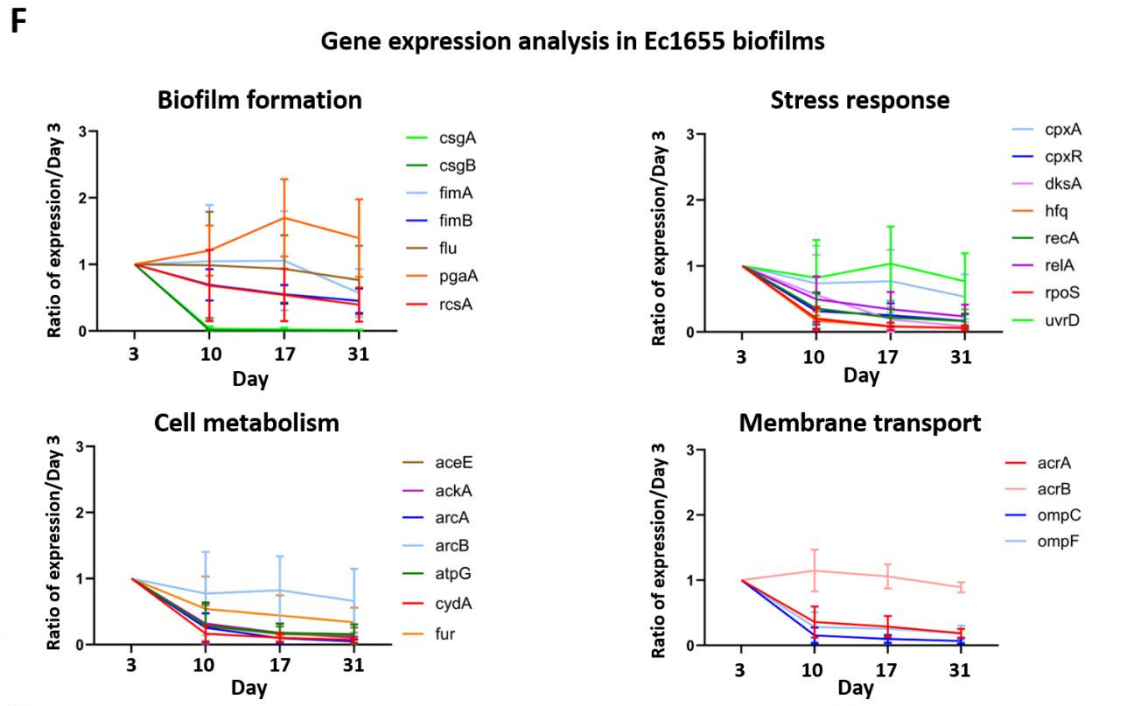
F
Gene expression analysis in Ec1655 biofilms
Biofilm formation
Ratio of expression/Day 3
Day
csgA
csgB
fimA
fimB
flu
pgaA
rcsA
Stress response
cpxA
cpxR
dksA
hfq
recA
relA
rpoS
uvrD
Cell metabolism
aceE
ackA
arcA
arcB
atpG
cydA
fur
Membrane transport
acrA
acrB
ompC
ompF

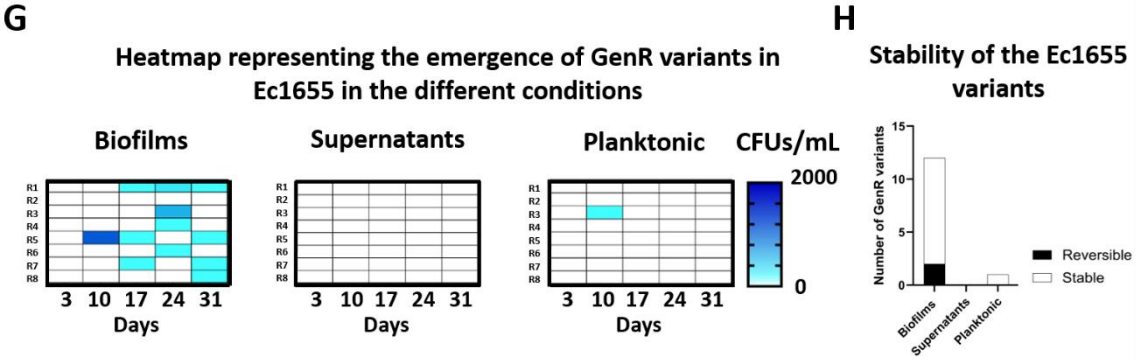
G
Heatmap representing the emergence of GenR variants in Ec1655 in the different conditions
Biofilms
Supernatants
Planktonic
CFUs/mL
2000
0
Days
H
Stability of the Ec1655 variants
Number of GenR variants
Reversible
Stable
Biofilms
Supernatants
Planktonic

Figure 1: Characterization of the Ec1655 biofilm dynamic and its influence on the evolution of GenR variants emergence. Representative CLSM images of 24 h (A) and 72 h (B) Ec1655 biofilms stained respectively with Syto9 (in green) and ConA (in red) in the upper part and Syto9 (in green) and WGA (in red) in the below part. Quantitative biovolume parameters of ConA (C) and WGA (D) in the Ec1655 biofilms at 24 h and 72 h, and congo red fluorescence quantification in Ec1655 biofilms at 24 h and 72 h (E). Analysis of gene expression in Ec1655 biofilms during one month (F). Quantification of the emergence of Ec1655 GenR variants in biofilms, supernatants and planktonic conditions over a month (G) and stability of the resistance phenotype of the emerging variants (H). Kruskal-wallis test combined with a Dunn's multiple comparison test were performed on RT-q-PCR values to compare each timepoint. The same tests were also performed to evaluate the variants emergence differences between biofilms, supernatants and planktonic cells at every timepoint. P-values are available in Table S4.

2. Strain-dependent diversity of biofilm phenotypes and GenR emergence

The study was extended to seven additional *E. coli* strains isolated from the food-processing industries, revealing variations of biofilm features and GenR emergence (Fig. 2A and B). ConA staining highlighted different matrix composition in the environmental strains compared to Ec1655, particularly at 72 hours. However, WGA staining revealed that Ec1655 produced more PNAG residues than the other strains (Fig. 2C, D, F and G). Congo red staining (Fig. 2E and H) showed that Ec1655 contained fewer amyloid fibers and cellulose than the environmental strains, which was corroborated by macrocolony analyses, where most environmental strains exhibited a RDAR (red, dry and rough) phenotype (Fig. S1).

Interesting strain-specific differences emerged from the biofilm analysis. For instance, Ec709 had a higher propensity to form biofilms, with significant higher ConA, WGA and Congo red signals at 24 h. At 72 hours, Ec723 had the largest polysaccharidic structures stained by ConA. Ec223 also displayed high levels of ConA-stained matrix but low WGA-staining, highlighting specificities of biofilm matrix composition, depending from the strain.

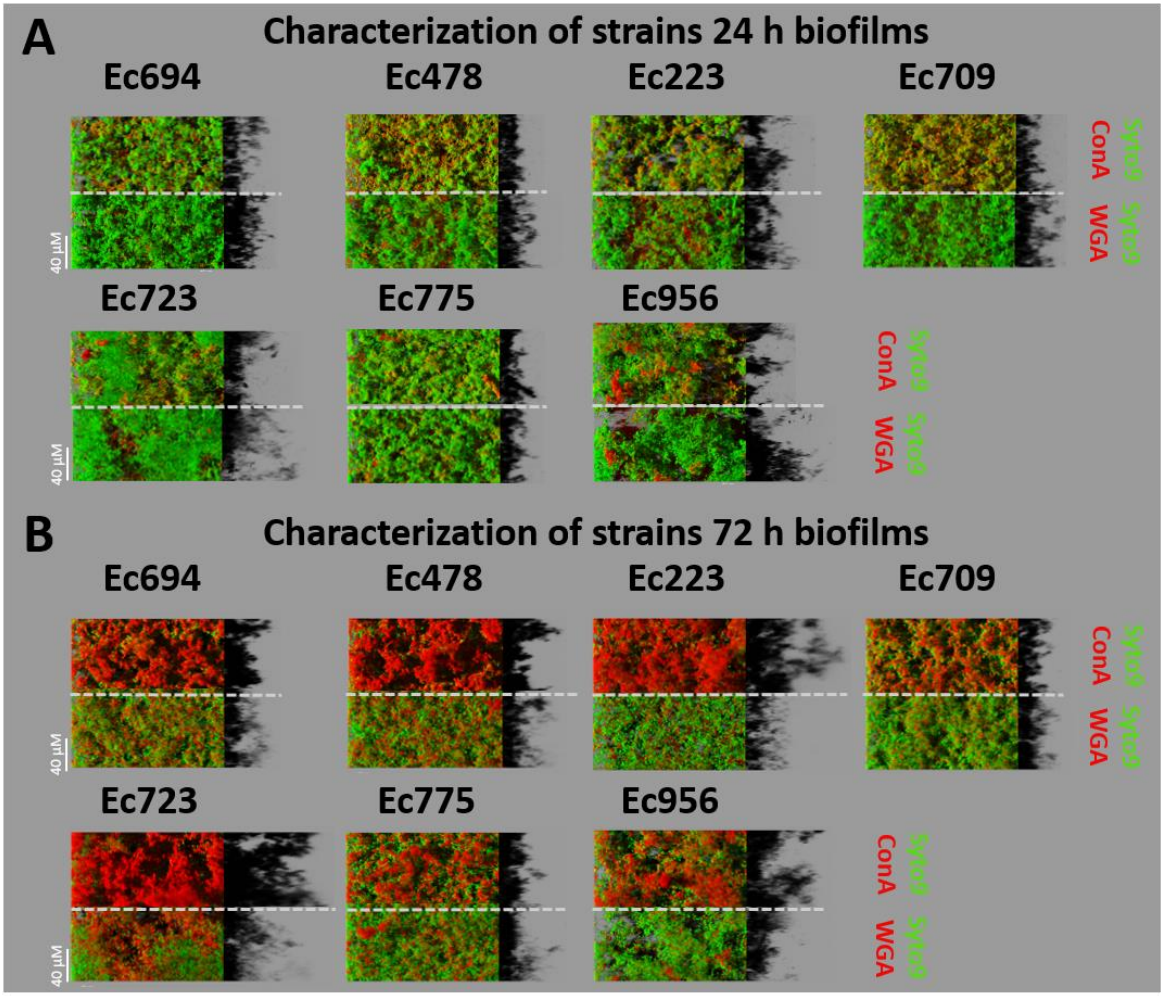
A
Characterization of strains 24 h biofilms
Ec694
Ec478
Ec223
Ec709
Ec723
Ec775
Ec956
ConA WGA Syto9
40 µM
B
Characterization of strains 72 h biofilms
Ec694
Ec478
Ec223
Ec709
Ec723
Ec775
Ec956
ConA WGA Syto9
40 µM

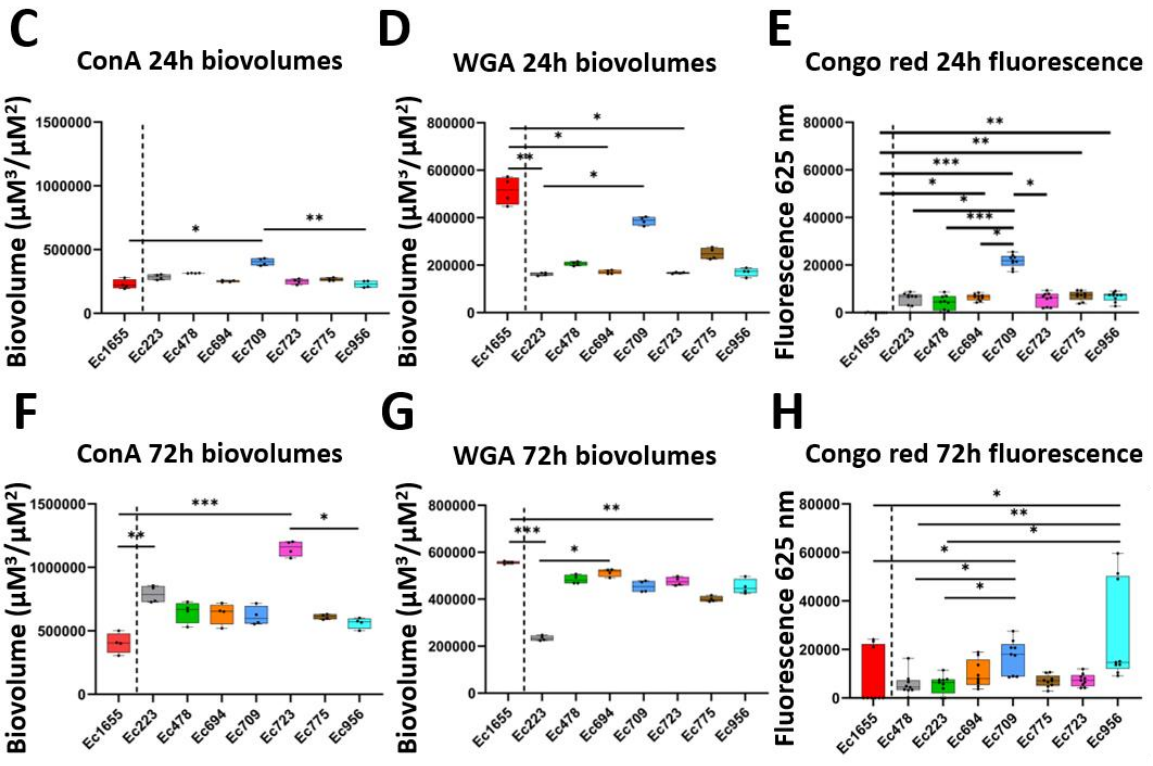
C
ConA 24h biovolumes
Biovolume (µM³/µM²)
D
WGA 24h biovolumes
Biovolume (µM³/µM²)
E
Congo red 24h fluorescence
Fluorescence 625 nm
F
ConA 72h biovolumes
Biovolume (µM³/µM²)
G
WGA 72h biovolumes
Biovolume (µM³/µM²)
H
Congo red 72h fluorescence
Fluorescence 625 nm
Ec1655
Ec223
Ec478
Ec694
Ec709
Ec723
Ec775
Ec956

*Figure 2: Characterization of the 7 environmental strains biofilm dynamics and their influence on the evolution of GenR variants emergence. Representative CLSM images of 24 h (A) and 72 h (B) biofilms stained respectively with Syto9 (in green) and ConA (in red) in the upper part and Syto9 (in green) and WGA (in red) in the below part. Quantitative biovolume parameters of ConA at 24h (C) and 72 h (F) and WGA at 24 h (D) and 72 h (G), and congo red fluorescence quantifications in the strains biofilms at 24 h (E) and 72 h (H), next to the Ec1655 values which were added as reference values. Kruskal-Wallis test combined with a Dunn's multiple comparison test were performed between every strain for the quantitative measurements of ConA, WGA and congo red (P value: * = [0.05-0.01]; ** = [0.01-0.001]; *** = <0.001)*

The emergence of GenR variants over one month was quantified for these strains (Fig. 3A). For strain Ec709, biofilm growth was associated with a higher frequency of GenR variants compared to supernatants or planktonic cultures. Ec709 strain, as Ec1655, showed a clear increase in the number of GenR in biofilms over time, with significant differences after 24 and 31 days (Table S3). Among the other strains, Ec478 and Ec694 also produced GenR variants repeatedly in different replicates or time points. Ec694 produced a majority of variants in biofilm, but Ec478 had variants emerging in both the biofilm and the planktonic condition, without any variants in the biofilm supernatants. As for the Ec1655 strain, the strains had a slightly lower concentration in the supernatants (Fig. S2). The other strains (Ec223, Ec723, Ec775, Ec956) did not produced GenR variants in any condition or in only one replicate and time point, demonstrating the variability of the evolution in the different strains. Further analysis on the stability of the resistance also showed differences with the Ec1655 strain (Fig. 3B). In the different strains, the majority of the phenotypes were unstable and lost after spread on non-selective medium. Ec709 and Ec478 were the only strain producing stable GenR variants. Interestingly, all the stable GenR variants came from the biofilms, while all variants coming from the supernatants and the planktonic conditions lost the resistance phenotype after subcultures without gentamicin.

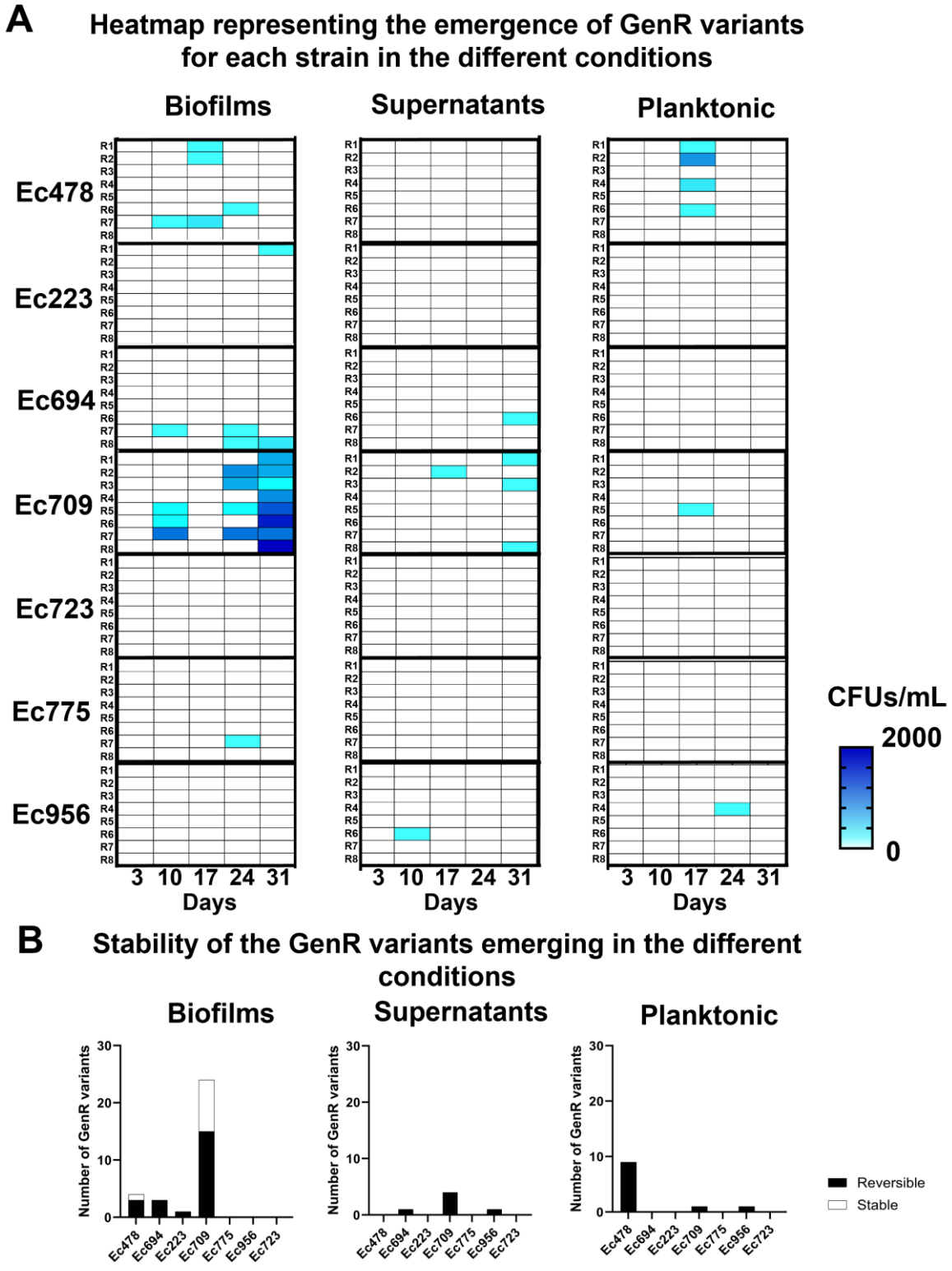

Figure 3: *Analysis of the emergence of GenR variants in biofilms, supernatants and planktonic cells in 7 strains isolated in food-processing industries (A). Stability of the resistance phenotype in the isolated variants (B). Kruskal-Wallis test combined with a Dunn's multiple comparison test were performed to evaluate the variants emergence differences between biofilms, supernatants and planktonic cells at every timepoint, p-values are presented in Table S3.*

3. Distinct genetic mutations associated with GenR emergence

Genetic analysis of the stable GenR variants revealed distinct mutational profiles between food isolates and reference strain Ec1655 (Fig. 4). The Ec478 and Ec709 GenR variants frequently carried point mutations in genes involved in the respiratory chain (Fig. 4), particularly *cydA*, which encodes a cytochrome oxidase. This gene was mutated in the Ec478 variant and in four out of nine Ec709 variants. Additionally, some Ec709 variants carried mutation in intergenic regions between *trxB* and *cydD*, and further analysis revealed that the mutations were located between the *cydCD* operon promoter and the *cydD* gene, potentially affecting gene regulation. Most of the Ec478 and Ec709 variants carried a second mutation in another gene with metabolic properties. The Ec478 variant carried a mutation in the folate-binding protein *ygfZ*, and the *cydA*-mutated Ec709 variants had mutations in the flavin reductase *fre*, in an intergenic region between *ampG* and *cyoA*, in the cell respiration regulator *arcB* and the pyruvate dehydrogenase *aceE*. Finally, two other Ec709 variants were not mutated in *cydA* and were mutated in other targets. Ec709_B_10_1 was mutated in the ATP synthase gene *atpG* and Ec709_B_31_2 was mutated in the elongation factor *fusA* and in the threonylcarbamoyladenosine synthase *tsaB*. One variant, Ec709_B_24_3 did not carry any point mutation in any gene.

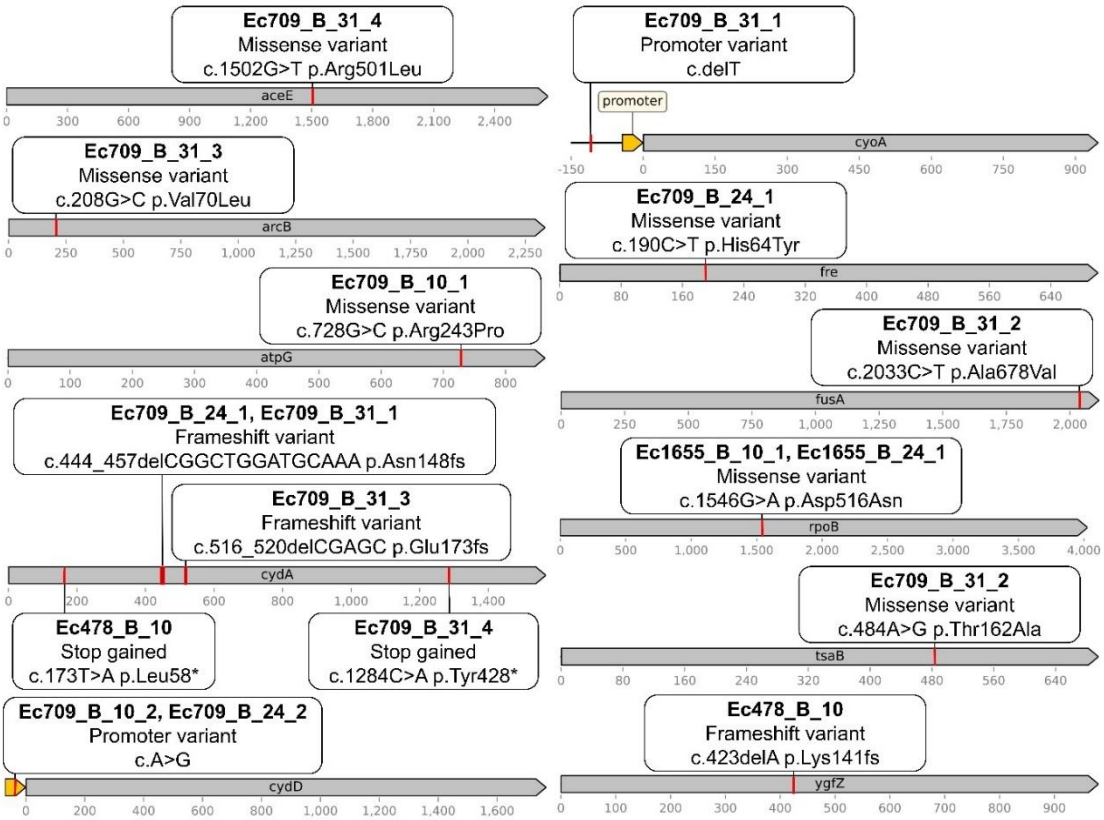

Figure 4: *Genetic modification identified in GenR variants with each mutated gene and its corresponding mutations.*

These genetic profiles were markedly different from those observed in the Ec1655 GenR variants. Of the ten Ec1655 GenR variants, only two displayed point mutations, neither of which were found in genes related to cellular respiration. Instead, both mutations occurred in the gene *rpoB,* which encodes an RNA polymerase subunit (Fig. 4). The remaining eight variants did not carry point mutations but rather exhibited large genomic deletions (Fig. 5). Interestingly, while these deletions occurred within the same genomic region, they vary in size across the different variants, suggesting independent deletion events. Among the genes found in the deleted region, the peptide transporter *sbmA,* was deleted in every strain, and is known to be involved in gentamicin resistance. Other genes found in the deleted region were mainly involved in diverse metabolic processes, including *iprA*, whose deletion confers high resistance to oxidative stress. Three strains (Ec1655_B_17_3, Ec1655_B_24_2, Ec1655_B_31_3) exhibited even larger deletions extending upstream, leading to the loss of genes encoding ferric transporters, fimbriae and other metabolism-related proteins.

While Ec709 variants did not exhibit large genomic deletions, the Ec478_B_10 variant did lose a genomic region. Analysis using the MobileOG software (Fig. 5) revealed that the majority of the Ec478 deleted region consisted of phage-related genes. In contrast, the deleted region in Ec1655 variants contained few mobile genetic elements, suggesting different mechanisms underlying these genomic alterations.

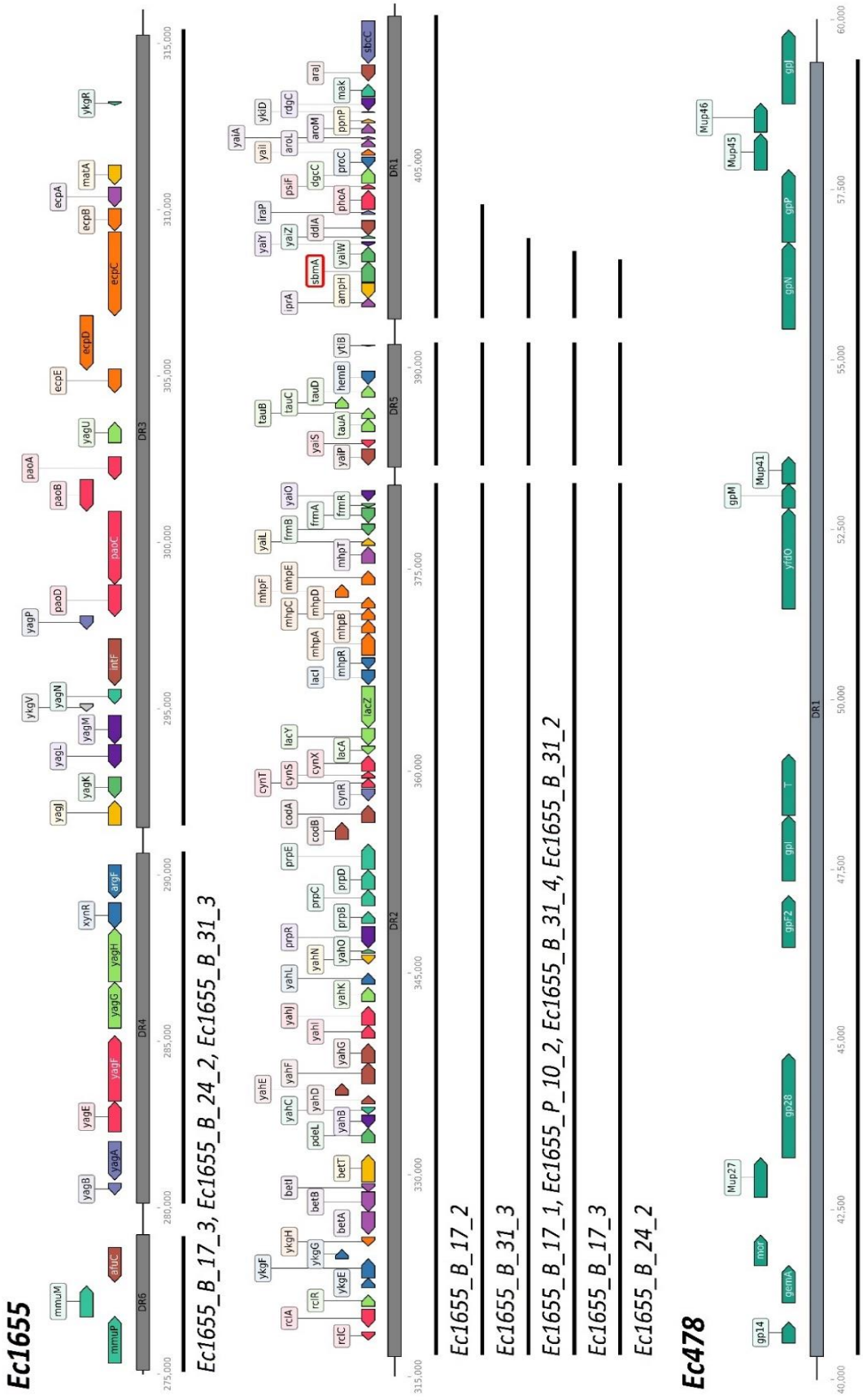

Figure 5: *Large genomic modifications identified in GenR variants with the corresponding deleted regions (DR).*

4. Broad aminoglycoside resistance in GenR variants

Profiles of resistance to 15 relevant antibiotics for *E. coli* were obtained through MIC value determination, to evaluate if the resistance mutation conferred cross-resistances to other antibiotics (Table 1). Among the tested antibiotics, two were part of the aminoglycoside family, gentamicin and amikacin. The resistance to gentamicin was first confirmed in all the variants. Moreover, amikacin MIC values showed that the mechanism of resistance was general to the aminoglycoside family. Interestingly, Ec1655 and Ec709 variants showed decreased susceptibility to sulfamethoxazole and trimethoprim, while the Ec478 variant did not. Regarding the level of resistance, the Ec1655 GenR variants were in general resistant to higher concentrations than the Ec709 and Ec478 variants. Interestingly, the Ec1655 and Ec478 variants became also slightly more sensitive to ampicillin, suggesting that the resistance mutations may have pleiotropic effects on other antibiotics.

	AMI	AMP	AZI	CFX	CFZ	CHL	CIP	COL	GEN	MER	NAL	SMX	TET	TIG	TMP
Ec1655	≤ 4	4	≤2	≤0.25	≤0.25	≤8	≤0.015	≤1	≤0.5	≤0.03	≤4	≤8	≤2	≤0.25	≤0.25
Ec1655_B_10_1	64	2	≤2	≤0.25	≤0.25	≤8	≤0.015	≤1	8	≤0.03	≤4	512	≤2	≤0.25	4
Ec1655_P_10_2	32	2	≤2	≤0.25	≤0.25	≤8	≤0.015	≤1	8	≤0.03-	≤4	128	≤2	≤0.25	2
Ec1655_B_17_1	64	2	≤2	≤0.25	≤0.25	≤8	≤0.015	≤1	8	≤0.03	≤4	128	≤2	≤0.25	1
Ec1655_B_17_2	32	1	≤2	≤0.25	≤0.25	≤8	≤0.015	≤1	8	≤0.03	≤4	128	≤2	1	≤0.25
Ec1655_B_17_3	64	4	≤2	≤0.25	≤0.25	≤8	≤0.015	≤1	8	≤0.03	≤4	512	≤2	≤0.25	4
Ec1655_B_24_1	16	2	≤2	≤0.25	≤0.25	≤8	≤0.015	≤1	8	≤0.03	≤4	64	≤2	≤0.25	1
Ec1655_B_24_2	64	2	≤2	≤0.25	≤0.25	≤8	≤0.015	≤1	8	≤0.03	≤4	128	≤2	≤0.25	1
Ec1655_B_31_1	64	2	≤2	≤0.25	≤0.25	≤8	≤0.015	≤1	8	≤0.03	≤4	512	≤2	≤0.25	1
Ec1655_B_31_2	64	4	≤2	≤0.25	≤0.25	≤8	≤0.015	≤1	8	≤0.03	≤4	512	≤2	≤0.25	1
Ec1655_B_31_3	64	4	4	≤0.25	≤0.25	≤8	≤0.015	≤1	8	≤0.03	≤4	256	≤2	≤0.25	2
Ec478	≤4	4	≤2	≤0.25	≤0.25	≤8	≤0.015	≤1	≤0.5	≤0.03	≤4	≤8	32	≤0.25	≤0.25
Ec478_B_10	8	2	≤2	≤0.25	≤0.25	≤8	≤0.015	≤1	4	≤0.03	≤4	≤8	32	≤0.25	≤0.25
Ec709	≤4	32	≤2	≤0.25	≤0.25	≤8	≤0.015	≤1	≤0.5	≤0.03	≤4	16	≤2	≤0.25	<0.25
Ec709_B_10_1	32	32	≤2	≤0.25	≤0.25	≤8	≤0.015	≤1	8	≤0.03	≤4	32	≤2	≤0.25	0,5
Ec709_B_10_2	32	32	≤2	≤0.25	≤0.25	≤8	≤0.015	≤1	4	≤0.03	≤4	512	≤2	≤0.25	0,5
Ec709_B_24_3	16	32	≤2	≤0.25	≤0.25	≤8	≤0.015	≤1	4	≤0.03	≤4	512	≤2	≤0.25	0,5
Ec709_B_24_2	32	32	≤2	≤0.25	≤0.25	≤8	≤0.015	≤1	4	≤0.03	≤4	128	≤2	≤0.25	0,5
Ec709_B_24_1	16	32	≤2	≤0.25	≤0.25	≤8	≤0.015	≤1	2	≤0.03	≤4	16	≤2	≤0.25	0,5
Ec709_B_31_1	8	32	≤2	≤0.25	≤0.25	≤8	≤0.015	≤1	2	≤0.03	≤4	16	≤2	≤0.25	0,5
Ec709_B_31_2	16	32	≤2	≤0.25	≤0.25	≤8	≤0.015	≤1	4	≤0.03	≤4	32	≤2	≤0.25	1
Ec709_B_31_3	8	32	≤2	≤0.25	≤0.25	≤8	≤0.015	≤1	2	≤0.03	≤4	32	≤2	≤0.25	0,5
Ec709_B_31_4	16	32	≤2	≤0.25	≤0.25	≤8	≤0.015	≤1	4	≤0.03	≤4	32	≤2	≤0.25	1

Table 1: Resistance to 15 antibiotics was evaluated for every variant and compared to the resistance of their parental strains. More than two-fold increase in resistance are represented in red, two-fold increase is represented in orange, two-fold decrease is represented in yellow and more than two-fold decrease are represented in green. (AMI = Amikacin; AMP = Ampicillin; AZI = Azithromycin; CFX = Cefotaxime; CFZ = Ceftazidime; CHL = Chloramphenicol; CIP = Ciprofloxacin; COL = Colistin; GEN = Gentamicin; MER = Meropenem; NAL = Nalidixic Acid; SMX = Sulfamethoxazole; TET = Tetracycline; TIG = Tigecycline; TMP = Trimethoprim)

5. Variants are impacted in their recolonization properties

Phenotypic analyses were performed on the GenR variants to characterize their ability relative to dissemination and colonization of new environments (Fig. 6). First, growth curves were performed in the absence of selective pressure and variant growths were compared to the growth of their respective parental strains (Fig. 6A). Overall, GenR variants exhibited growth rate decreases compared to their parents, but with disparities between strains. Ec1655 variants were severely impacted in their growth. No specific differences were observed between the variants with point mutations in *rpoB* and variants with large genomic deletions.

Ec478_B_10, the GenR variant of Ec478, was also severely impacted. Even though most of the Ec709 variants did also show some growth rate decrease, the reduction was lower than for the variants from strains Ec478 and Ec1655, some variants having close growth rates to the parental strain. Crystal Violet biofilm quantification (Fig. 6B) revealed that Ec1655 variants were unable to produce biofilms compared to their parental strain. In contrast, Ec478 and Ec709 variants produced similar biofilm biomass as their respective parental strains.

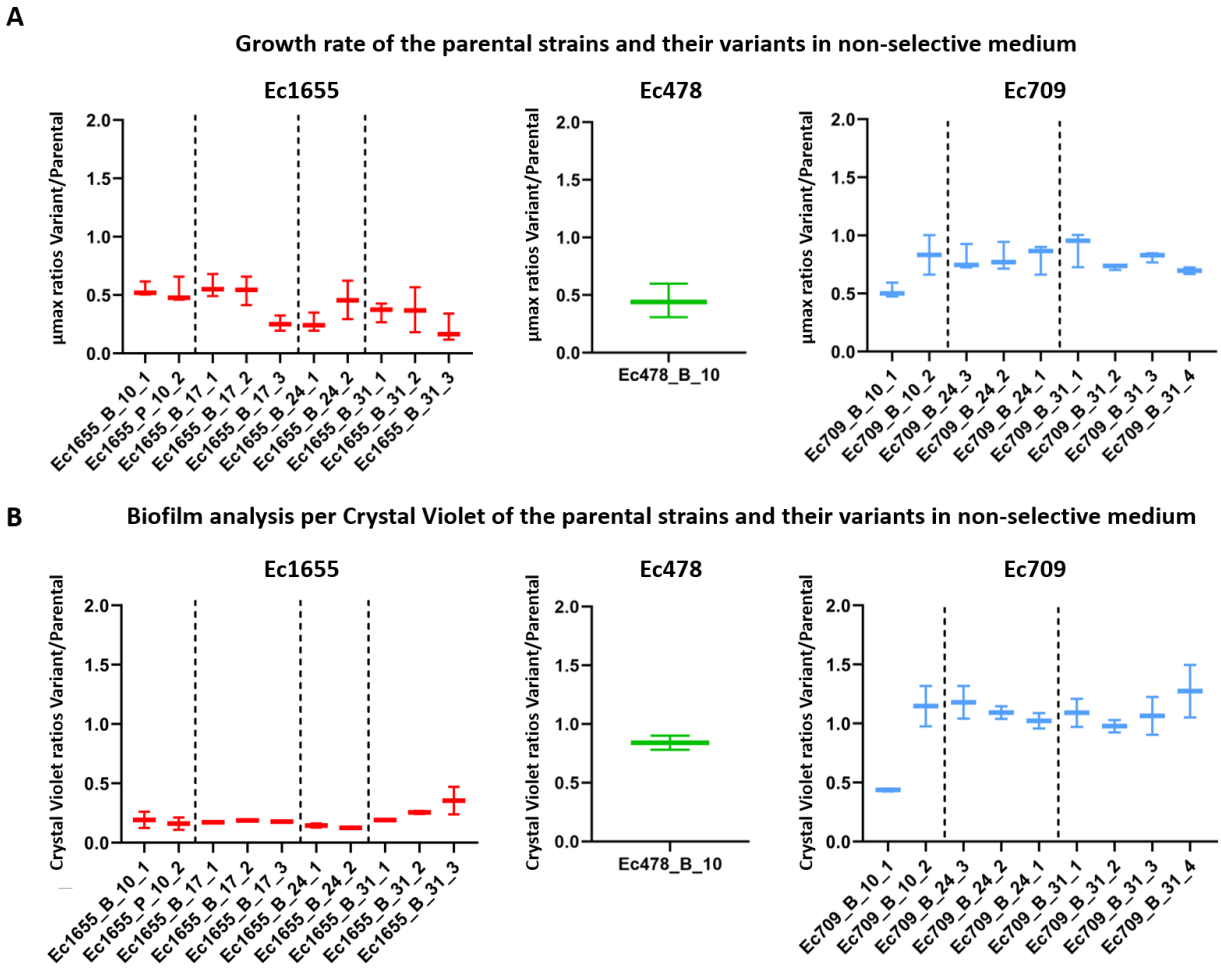

Figure 6: Graph representing the parental strain and the variants, separated by the day they were collected, with their maximum growth rate (A) and under crystal violet assay (B). Mann-Whitney test was performed between every variant and their corresponding parental strain, p-values are presented in Table S4.

Discussion:

Among the many factors influencing bacterial adaptation strategies, biofilms are known to play a crucial role in microbial evolution. As the predominant lifestyle of bacteria on Earth (Flemming and Wuertz, 2019), understanding how biofilms contribute to the emergence of antibiotic resistances is essential for addressing this significant public health threat. In this study, we explored the dynamics of spontaneous emergence of GenR variants in biofilms, supernatants and planktonic conditions using the *E. coli* reference strain Ec1665 and seven food isolates.

In the Ec1655 strain, cellular activity decreased over time as the biofilm matured. Even if some genes remained relatively stable, or even showed slight increased activity, like *pgaA*, gene expression analysis revealed a continuous decline in most of the genes involved in metabolism, stress responses, resistance mechanisms and some biofilm components producing genes, including the curli operon *csgAB*. Biofilms resilience to antimicrobial treatments is often linked to the emergence of specific subpopulations in a dormancy-like state, characterized by reduced cellular activity (Wood et al., 2013). These dormant cells can evade the effects of antimicrobials without acquiring resistance, by reducing the activity of drug targets (Jayaraman, 2008). Gentamicin, which relies on active cellular metabolism to exert its antimicrobial effect, is known to be less effective against cells with reduced metabolic activity (Mogre et al., 2014; Ibacache-Quiroga et al., 2018).

Our results showed that GenR variant emergence was privileged in biofilms compared to planktonic cultures, particularly after three to four weeks of evolution. This increase of resistance could be associated with the graduated decrease of cell activity observed in Ec1655 biofilms, potentially selecting variants with reduced activities. The biofilm development and maturation throughout the weeks could increase the gradients generated by the matrix establishment (Jo et al., 2022b). Thereby, the settlement of specific microenvironments influencing metabolic activities and potentially favorable to GenR emergence could appear.

Data collected in this work especially highlighted the diversity of responses and adaptation strategies depending on strains. While the GenR variants emergence was generally promoted in biofilms compared to other lifestyles, only few strains, notably Ec1655 and Ec709, recurrently produced GenR variants. Ec1655 had a distinct matrix profile, characterized by low levels of cellulose and curli but the highest levels of PNAG. Ec709, in contrast, displayed rapid biofilm formation, with the highest cellulose and curli and the second highest PNAG level at 24 h compared to other strains, but no particular differences were observable after 72 h. Moreover, despite its fast biofilm formation, Ec709 GenR variants emerged relatively late, suggesting that biofilm velocity alone cannot fully explain the emergence of resistance. In contrast, Ec723 formed biofilm with the thickest biofilm after 72 h, but did not produce GenR variants during the whole evolution experiment, underscoring the complexity of the relationship between biofilm biovolume, matrix production and resistance emergence. Naparstek *et al*. observed previously that susceptible *Klebsiella pneumoniae* strains did not show increased resistance to gentamicin in biofilms, and this with low and with high biofilm biovolumes (Naparstek et al., 2014). Resistance was only observed in strains that were already resistant to gentamicin, demonstrating the complexity of the link between gentamicin resistance and biofilm formation (Naparstek et al., 2014). Here, the strain-specific GenR emergence could be related to the large varieties in the genetic background of the strains, which would drive differently the selection of the variants. *E. coli* is known to be one of the species with the largest intra-species diversity (Touchon et al., 2009). The genetic backgrounds of each strain can significantly influence their capacity for evolutionary adaptation, with strains that develop and survive not necessarily being the ones with the highest initial fitness (Barrick et al., 2010; Woods et al., 2011). The interactions between background genes, their targets and other genetic factors, can determine whether a mutation is beneficial and will be selected (Mullis et al., 2018; Nucci et al., 2023).

Phenotypic characterization of the GenR variants revealed that the gentamicin resistance is often associated with a fitness cost, as already described with aminoglycosides in *E. coli* (France et al., 2019). The protective environment of the biofilm may have helped maintain the Ec1655 variants, which showed high fitness decreases compared to the parental strain (Penesyan et al., 2021; Charron et al., 2023a).

Genotypically, Ec1655 variants showed differences compared to Ec709 and Ec478. The GenR variants from Ec709 and Ec478 mostly carried SNPs or small indels in genes known for their

effect on bacterial resistance to gentamicin, which are mostly related to cell respiration such as *cydA*, *cydD*, *atpG*, *arcB* and *cyoA* (Mogre et al., 2014; Ibacache-Quiroga et al., 2018; Charron et al., 2023b). Other mutated genes, like *fusA* (Usui et al., 2023), or *aceE* (Cuzin et al., 2021) have also been directly associated to gentamicin resistance. In contrast, the Ec1655 GenR variants predominantly exhibited large genomic deletions rather that point mutations. Interestingly, the gene *sbmA*, encoding a peptide transporter involved in the internalization of gentamicin (Slotboom et al., 2020), was systematically deleted in Ec1655 GenR variants. The *sbmA* loss could therefore explain Ec1655 GenR resistance phenotypes. The varying size of the deletions support that independent genetic events occurred leading to the loss of this region. Analysis of the mobile genetic elements in the region also revealed that most of the region was stably anchored in the genome, in contrast to the Ec478 deleted region which was most likely due to a phage excision.

An analysis of the other deleted genes revealed a lot of genes involved in diverse metabolic functions. The *iprA* gene was also systematically deleted in Ec1655 GenR variants and a link between its deletion and resistance to oxidative stress was already shown (Herman et al., 2016). It is known that important oxidative stresses can be present in the biofilm matrix (Ryder et al., 2012). Consequently, the deletion of this region could thereby be an adaptation to the biofilm lifestyle, with an adaptation to oxidative stress and a reduction of cell activity. Being located next to these genes, *sbmA* would have been consequently deleted and gentamicin resistance would have occurred as a side effect. Phenotypic analysis of the Ec1655 variants confirmed that they were heavily impacted in their fitness, with severe growth decreases and an alteration of biofilm-producing abilities. In contrast, the Ec709 and Ec478 variants were still able to produce biofilms, despite being also impacted in their growth. This supports a reorientation of the variants towards biofilm production, as their growth was inhibited but not their biofilm biomass.

All variants had a broad resistance to aminoglycosides, with an increase in amikacin and gentamicin resistance. Most of the variants also had an increase in sulfamethoxazole and trimethoprim resistance. In general, Ec1655 variants exhibited higher MIC values compared to Ec478 and Ec709, which aligns with the common pattern that higher resistance levels often come with greater fitness cost (Melnyk et al., 2015). This supports the hypothesis that Ec1655 variants emerged in biofilms because they were too severely impaired to compete in a planktonic lifestyle.

Conclusion:

This study delved into the mechanisms leading to the selection of GenR variants in *E. coli* populations, highlighting the critical role of biofilm lifestyles in promoting genetic diversity. Our findings support the complexity of this selection process, which is highly strain-dependent and influenced by both genetic and environmental factors. The study provides valuable insights into how biofilm development contributes to the emergence of antimicrobial resistance, with implications for public health. By enhancing our understanding of these dynamics, this work lays the groundwork for developing more effective strategies to combat biofilm-associated infections and mitigate the spread of resistance.

Data availability
All sequencing data were deposit in NCBI under the BioProject accession number PRJNA947807. Detailed of accession numbers for assembled genomes of parental strains and sequence reads of variant strains were provided in table S2. Raw data in excel files are presented in Source data section.

Author contributions:
RC: Conceptualization, Formal analysis, Investigation, Visualization, Writing – original draft, Writing – review & editing. PL: Data curation, Formal analysis, Investigation, Methodology, Software, Writing – original draft. AH: Formal analysis, Investigation. OM: Investigation. MB: Investigation. PH: Investigation. CS: Project administration, Resources. RB: Conceptualization, Funding acquisition, Supervision, Writing – original draft, Writing – review & editing. AB: Conceptualization, Funding acquisition, Project administration, Resources, Supervision, Visualization, Writing - original draft, Writing – Review & editing

References:

Allison, K.R., Brynildsen, M.P., Collins, J.J., 2011. Metabolite-enabled eradication of bacterial persisters by aminoglycosides. Nature 473, 216–220. https://doi.org/10.1038/nature10069

Aslam, B., Khurshid, M., Arshad, M.I., Muzammil, S., Rasool, M., Yasmeen, N., Shah, T., Chaudhry, T.H., Rasool, M.H., Shahid, A., Xueshan, X., Baloch, Z., 2021. Antibiotic Resistance: One Health One World Outlook. Front Cell Infect Microbiol 11, 771510. https://doi.org/10.3389/fcimb.2021.771510

Barrick, J.E., Kauth, M.R., Strelioff, C.C., Lenski, R.E., 2010. *Escherichia coli* rpoB mutants have increased evolvability in proportion to their fitness defects. Mol Biol Evol 27, 1338–1347. https://doi.org/10.1093/molbev/msq024

Boles, B.R., Thoendel, M., Singh, P.K., 2004. Self-generated diversity produces “insurance effects” in biofilm communities. Proc. Natl. Acad. Sci. U.S.A. 101, 16630–16635. https://doi.org/10.1073/pnas.0407460101

Charron, R., Boulanger, M., Briandet, R., Bridier, A., 2023a. Biofilms as protective cocoons against biocides: from bacterial adaptation to One Health issues. Microbiology (Reading) 169. https://doi.org/10.1099/mic.0.001340

Charron, R., Lemée, P., Huguet, A., Minlong, O., Boulanger, M., Houée, P., Soumet, C., Briandet, R., Bridier, A., 2023b. Polyhexamethylene biguanide promotes adaptive cross-resistance to gentamicin in *Escherichia coli* biofilms. Front Cell Infect Microbiol 13, 1324991. https://doi.org/10.3389/fcimb.2023.1324991

Chen, S., 2023. Ultrafast one-pass FASTQ data preprocessing, quality control, and deduplication using fastp. Imeta 2, e107. https://doi.org/10.1002/imt2.107

Crane, J.K., Alvarado, C.L., Sutton, M.D., 2021. Role of the SOS Response in the Generation of Antibiotic Resistance In Vivo. Antimicrob Agents Chemother 65, e0001321. https://doi.org/10.1128/AAC.00013-21

Cuzin, C., Houée, P., Lucas, P., Blanchard, Y., Soumet, C., Bridier, A., 2021. Selection of a Gentamicin-Resistant Variant Following Polyhexamethylene Biguanide (PHMB) Exposure in *Escherichia coli* Biofilms. Antibiotics (Basel) 10, 553. https://doi.org/10.3390/antibiotics10050553

Davies, J., Davies, D., 2010. Origins and evolution of antibiotic resistance. Microbiol Mol Biol Rev 74, 417–433. https://doi.org/10.1128/MMBR.00016-10

Flemming, H.-C., Wingender, J., Szewzyk, U., Steinberg, P., Rice, S.A., Kjelleberg, S., 2016. Biofilms: an emergent form of bacterial life. Nat Rev Microbiol 14, 563–575. https://doi.org/10.1038/nrmicro.2016.94

Flemming, H.-C., Wuertz, S., 2019. Bacteria and archaea on Earth and their abundance in biofilms. Nat Rev Microbiol 17, 247–260. https://doi.org/10.1038/s41579-019-0158-9

France, M.T., Cornea, A., Kehlet-Delgado, H., Forney, L.J., 2019. Spatial structure facilitates the accumulation and persistence of antibiotic-resistant mutants in biofilms. Evol Appl 12, 498–507. https://doi.org/10.1111/eva.12728

Hartmann, R., Jeckel, H., Jelli, E., Singh, P.K., Vaidya, S., Bayer, M., Rode, D.K.H., Vidakovic, L., Díaz-Pascual, F., Fong, J.C.N., Dragoš, A., Lamprecht, O., Thöming, J.G., Netter, N., Häussler, S., Nadell, C.D., Sourjik, V., Kovács, Á.T., Yildiz, F.H., Drescher, K., 2021. Quantitative image analysis of microbial communities with BiofilmQ. Nat Microbiol 6, 151–156. https://doi.org/10.1038/s41564-020-00817-4

Herman, A., Serfecz, J., Kinnally, A., Crosby, K., Youngman, M., Wykoff, D., Wilson, J.W., 2016. The Bacterial iprA Gene Is Conserved across Enterobacteriaceae, Is Involved in Oxidative Stress Resistance, and Influences Gene Expression in *Salmonella enterica* Serovar Typhimurium. J Bacteriol 198, 2166–2179. https://doi.org/10.1128/JB.00144-16

Ibacache-Quiroga, C., Oliveros, J.C., Couce, A., Blázquez, J., 2018. Parallel Evolution of High-Level Aminoglycoside Resistance in *Escherichia coli* Under Low and High Mutation Supply Rates. Front Microbiol 9, 427. https://doi.org/10.3389/fmicb.2018.00427

Jayaraman, R., 2008. Bacterial persistence: some new insights into an old phenomenon. J Biosci 33, 795–805. https://doi.org/10.1007/s12038-008-0099-3

Jo, J., Price-Whelan, A., Dietrich, L.E.P., 2022. Gradients and consequences of heterogeneity in biofilms. Nat Rev Microbiol. https://doi.org/10.1038/s41579-022-00692-2

Karygianni, L., Ren, Z., Koo, H., Thurnheer, T., 2020. Biofilm Matrixome: Extracellular Components in Structured Microbial Communities. Trends Microbiol 28, 668–681. https://doi.org/10.1016/j.tim.2020.03.016

Lemée, P., Charron, R., Bridier, A., 2025. Genomic Pipeline for Analysis of Mutational Events in Bacteria, in: Bridier, A. (Ed.), Foodborne Bacterial Pathogens, Methods in Molecular Biology. Springer US, New York, NY, pp. 211–222. https://doi.org/10.1007/978-1-0716-4100-2_15

Lewis, K., 2010. Persister cells. Annu Rev Microbiol 64, 357–372. https://doi.org/10.1146/annurev.micro.112408.134306

Melnyk, A.H., Wong, A., Kassen, R., 2015. The fitness costs of antibiotic resistance mutations. Evol Appl 8, 273–283. https://doi.org/10.1111/eva.12196

Merritt, J.H., Kadouri, D.E., O'Toole, G.A., 2005. Growing and analyzing static biofilms. Curr Protoc Microbiol Chapter 1, Unit 1B.1. https://doi.org/10.1002/9780471729259.mc01b01s00

MIMA2, 2018. Microscopy and Imaging Facility for Microbes, Animals and Foods. https://doi.org/10.15454/1.5572348210007727E12

Mogre, A., Sengupta, T., Veetil, R.T., Ravi, P., Seshasayee, A.S.N., 2014. Genomic analysis reveals distinct concentration-dependent evolutionary trajectories for antibiotic resistance in *Escherichia coli*. DNA Res 21, 711–726. https://doi.org/10.1093/dnares/dsu032

Mullis, M.N., Matsui, T., Schell, R., Foree, R., Ehrenreich, I.M., 2018. The complex underpinnings of genetic background effects. Nat Commun 9, 3548. https://doi.org/10.1038/s41467-018-06023-5

Naparstek, L., Carmeli, Y., Navon-Venezia, S., Banin, E., 2014. Biofilm formation and susceptibility to gentamicin and colistin of extremely drug-resistant KPC-producing *Klebsiella pneumoniae*. J Antimicrob Chemother 69, 1027–1034. https://doi.org/10.1093/jac/dkt487

Nucci, A., Rocha, E.P.C., Rendueles, O., 2023. Latent evolution of biofilm formation depends on life-history and genetic background. npj Biofilms Microbiomes 9, 53. https://doi.org/10.1038/s41522-023-00422-3

Penesyan, A., Paulsen, I.T., Kjelleberg, S., Gillings, M.R., 2021. Three faces of biofilms: a microbial lifestyle, a nascent multicellular organism, and an incubator for diversity. NPJ Biofilms Microbiomes 7, 80. https://doi.org/10.1038/s41522-021-00251-2

Reale, O., Huguet, A., Fessard, V., 2019. Novel Insights on the Toxicity of Phycotoxins on the Gut through the Targeting of Enteric Glial Cells. Mar Drugs 17, 429. https://doi.org/10.3390/md17070429

Reygaert, W.C., 2018. An overview of the antimicrobial resistance mechanisms of bacteria. AIMS Microbiol 4, 482–501. https://doi.org/10.3934/microbiol.2018.3.482

Ryder, V.J., Chopra, I., O'Neill, A.J., 2012. Increased mutability of Staphylococci in biofilms as a consequence of oxidative stress. PLoS One 7, e47695. https://doi.org/10.1371/journal.pone.0047695

Schwengers, O., Jelonek, L., Dieckmann, M.A., Beyvers, S., Blom, J., Goesmann, A., 2021. Bakta: rapid and standardized annotation of bacterial genomes via alignment-free sequence identification. Microb Genom 7, 000685. https://doi.org/10.1099/mgen.0.000685

Slotboom, D.J., Ettema, T.W., Nijland, M., Thangaratnarajah, C., 2020. Bacterial multi-solute transporters. FEBS Lett 594, 3898–3907. https://doi.org/10.1002/1873-3468.13912

Touchon, M., Hoede, C., Tenaillon, O., Barbe, V., Baeriswyl, S., Bidet, P., Bingen, E., Bonacorsi, S., Bouchier, C., Bouvet, O., Calteau, A., Chiapello, H., Clermont, O., Cruveiller, S., Danchin, A., Diard, M., Dossat, C., Karoui, M.E., Frapy, E., Garry, L., Ghigo, J.M., Gilles, A.M., Johnson, J., Le Bouguénec, C., Lescat, M., Mangenot, S., Martinez-Jéhanne, V., Matic, I., Nassif, X., Oztas, S., Petit, M.A., Pichon, C., Rouy, Z., Ruf, C.S., Schneider, D., Tourret, J., Vacherie, B., Vallenet, D., Médigue, C., Rocha, E.P.C., Denamur, E., 2009. Organised genome dynamics in the *Escherichia coli* species results in highly diverse adaptive paths. PLoS Genet 5, e1000344. https://doi.org/10.1371/journal.pgen.1000344

Usui, M., Yoshii, Y., Thiriet-Rupert, S., Ghigo, J.-M., Beloin, C., 2023. Intermittent antibiotic treatment of bacterial biofilms favors the rapid evolution of resistance. Commun Biol 6, 275. https://doi.org/10.1038/s42003-023-04601-y

Wick, R.R., Judd, L.M., Gorrie, C.L., Holt, K.E., 2017. Unicycler: Resolving bacterial genome assemblies from short and long sequencing reads. PLOS Computational Biology 13, e1005595. https://doi.org/10.1371/journal.pcbi.1005595

Wood, T.K., Knabel, S.J., Kwan, B.W., 2013. Bacterial persister cell formation and dormancy. Appl Environ Microbiol 79, 7116–7121. https://doi.org/10.1128/AEM.02636-13

Woods, R.J., Barrick, J.E., Cooper, T.F., Shrestha, U., Kauth, M.R., Lenski, R.E., 2011. Second-order selection for evolvability in a large *Escherichia coli* population. Science 331, 1433–1436. https://doi.org/10.1126/science.1198914

World Health Organization, 2019. Critically important antimicrobials for human medicine, 6th rev. ed. World Health Organization, Geneva.

Yan, J., Bassler, B.L., 2019. Surviving as a Community: Antibiotic Tolerance and Persistence in Bacterial Biofilms. Cell Host Microbe 26, 15–21. https://doi.org/10.1016/j.chom.2019.06.002

Supplementary Data:

Supplementary Material and Method:

1. Macrocolony observation

Strains were streaked on TSA plates and grown overnight at 37 °C. On the second day, a colony of each strain was suspended in TSB 1/10 and grown overnight at 37 °C. On the following day, cultures were diluted to reach a final $OD_{600\ nm}$ of 0.2. 10 µL of the bacterial diluted suspensions were dropped on TSA plates supplemented with 40 µg/mL congo red and 20 µg/mL of brilliant blue. Plates were then incubated at 19°C or 37 °C during 7 days, where they were photographed using a Canon EOS R10 camera.

2. Colony forming unit (CFUs) quantification

Cells coming from 72 h biofilms, their supernatants and planktonic suspensions were counted to observe if differences could be observed in the cell quantities and densities between the conditions in the different parental strains. 72 h biofilms were prepared as in the section 2.1 of the material and method and planktonic cultures as in the section 3. 20 µL of the planktonic cultures were suspended in 180 µL TSB 1/10 medium. Serial dilutions were performed to reach a 10^{-8} dilution. 10 µL of the different dilutions were dropped on TSA plates. The same steps were repeated with the supernatants. For the biofilms, the supernatants were first removed and replaced with 100 µL of fresh TSB 1/10 medium. The biofilms were scratched and resuspended. The 100 µL were transferred in 900 µL of TSB 1/10 medium. Tubes were vortexed thoroughly during 30 s to separate the biofilm aggregates. Serial dilutions were then performed with 20 µL suspensions in 180 µL TSB 1/10 medium and 10 µL of the dilutions were dropped on TSB 1/10 medium. Finally, plates were incubated at 37 °C overnight and counted on the following day. Three biological replicates were performed for each strain.

Figure S1:

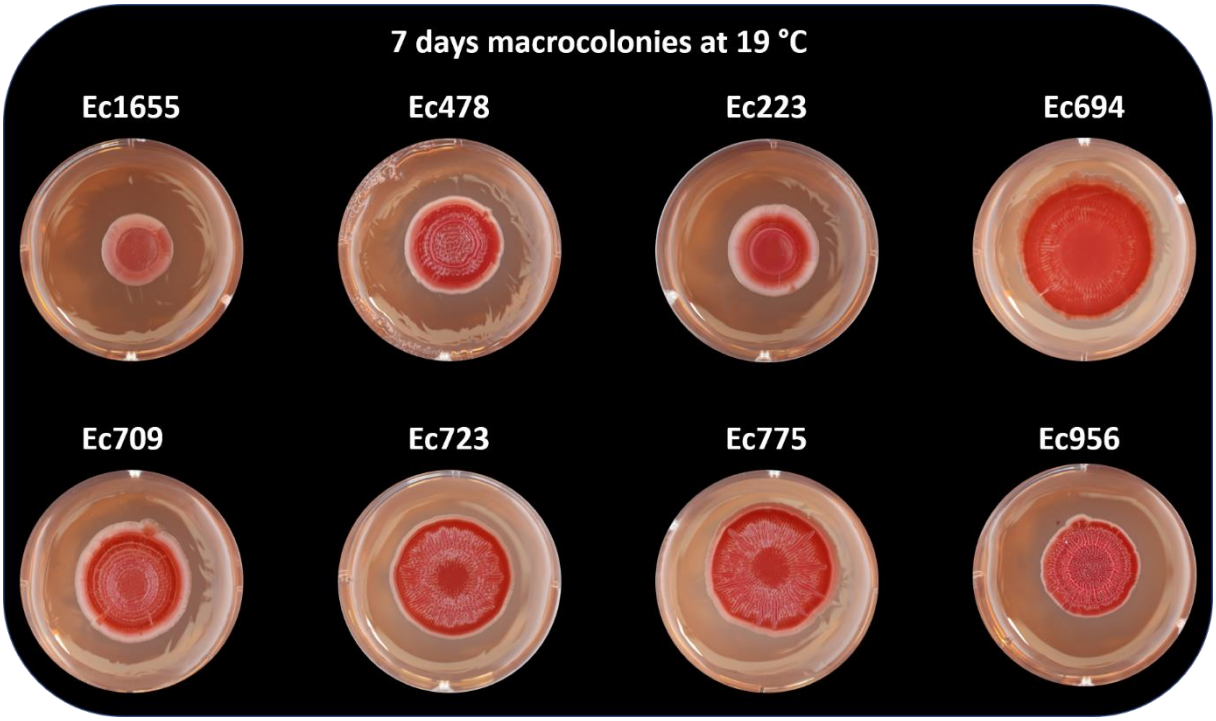

Figure S1: Macrocolonies of the tested strains can be observed after 7 days of incubation, at 19°C

Figure S2:

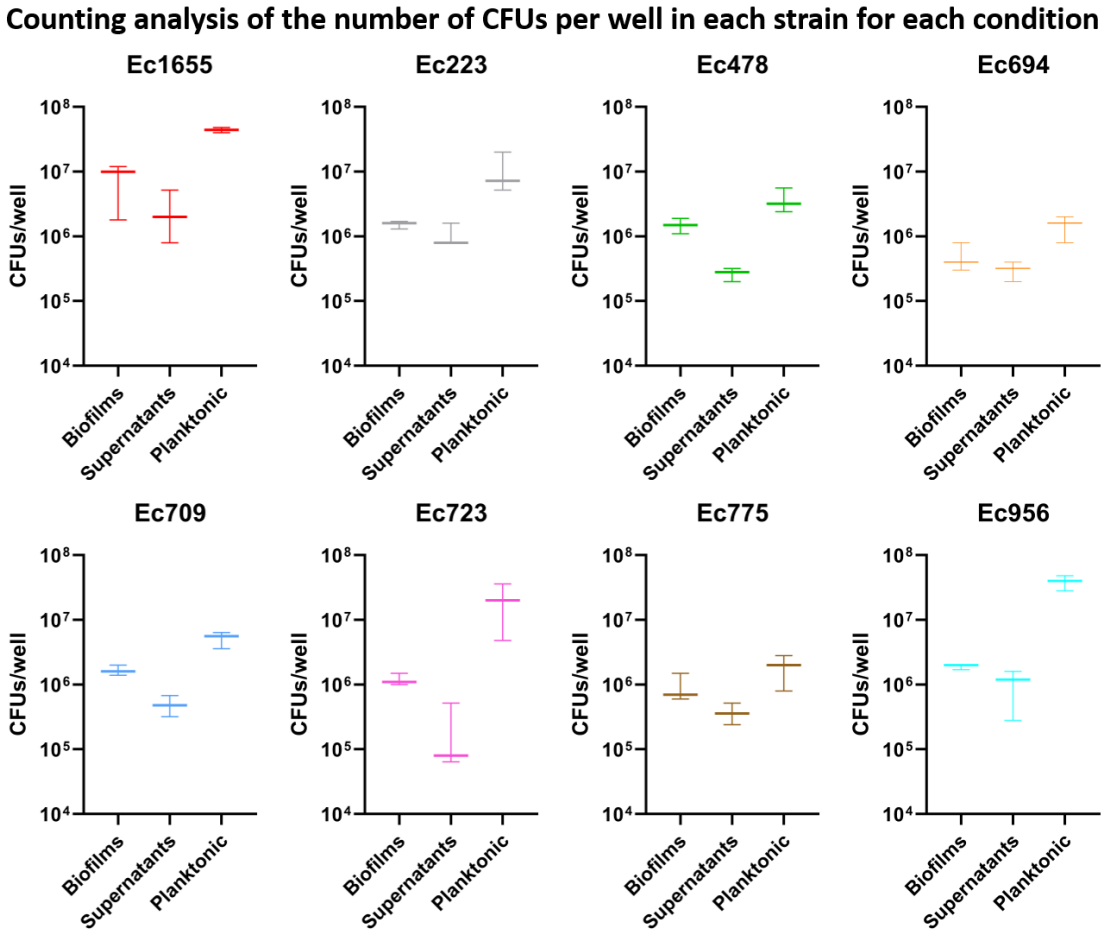

Figure S2: Number of CFUs/well in biofilms, supernatants and planktonic cultures, at 72 h, for each strain

Table S1: Table of every gene tested per RT-q-PCR with their oligonucleotides primers
Table S2: Detailed information on the genetic modifications
Table S3: NCBI accession number for every sequenced genome
Table S4: P-values of the differences between biofilms, supernatants and planktonic cultures observed in every strain for every week, per Kruskal-Wallis analysis and Dunn's Multiple Comparison Test

Supplementary files can be found on this link:

https://drive.google.com/drive/folders/1uJLVCO6PvYOODHoB_R-QTsapI7gOSPNz?usp=drive_link

2.2. Le PHMB induit la formation de biofilms et l'apparition de variants GenR

2.2.1. Article 5 : Le PHMB induit l'apparition de variants GenR non-stables

« Polyhexamethylene biguanide promotes adaptive cross-resistance to gentamicin in *Escherichia coli* biofilms », *Frontiers in Cellular and Infection Microbiology*, 2023

Raphaël Charron, Pierre Lemée, Antoine Huguet, Ornella Minlong, Marine Boulanger, Paméla Houée, Christophe Soumet, Romain Briandet, Arnaud Bridier

frontiers | Frontiers in Cellular and Infection Microbiology

TYPE Original Research
PUBLISHED 11 December 2023
DOI 10.3389/fcimb.2023.1324991

OPEN ACCESS

EDITED BY
Adline Princy Solomon,
SASTRA University, India

REVIEWED BY
Tahereh Navidifar,
Shoushtar Faculty of Medical Sciences, Iran
Jordy Evan Sulaiman,
University of Wisconsin-Madison,
United States

*CORRESPONDENCE
Arnaud Bridier
arnaud.bridier@anses.fr

RECEIVED 20 October 2023
ACCEPTED 16 November 2023
PUBLISHED 11 December 2023

CITATION
Charron R, Lemée P, Huguet A, Minlong O, Boulanger M, Houée P, Soumet C, Briandet R and Bridier A (2023) Polyhexamethylene biguanide promotes adaptive cross-resistance to gentamicin in *Escherichia coli* biofilms.
Front. Cell. Infect. Microbiol. 13:1324991.
doi: 10.3389/fcimb.2023.1324991

Polyhexamethylene biguanide promotes adaptive cross-resistance to gentamicin in *Escherichia coli* biofilms

Raphaël Charron[1,2], Pierre Lemée[1], Antoine Huguet[1], Ornella Minlong[1], Marine Boulanger[1], Paméla Houée[1], Christophe Soumet[1], Romain Briandet[2] and Arnaud Bridier[1]*

[1]Antibiotics, Biocides, Residues and Resistance Unit, Fougères Laboratory, French Agency for Food, Environmental and Occupational Health & Safety (ANSES), Fougères, France, [2]Université Paris-Saclay, National Research Institute for Agriculture, Food and the Environment (INRAE), AgroParisTech, Micalis Institute, Jouy-en-Josas, France

Antimicrobial resistance is a critical public health issue that requires a thorough understanding of the factors that influence the selection and spread of antibiotic-resistant bacteria. Biocides, which are widely used in cleaning and disinfection procedures in a variety of settings, may contribute to this resistance by inducing similar defense mechanisms in bacteria against both biocides and antibiotics. However, the strategies used by bacteria to adapt and develop cross-resistance remain poorly understood, particularly within biofilms –a widespread bacterial habitat that significantly influences bacterial tolerance and adaptive strategies. Using a combination of adaptive laboratory evolution experiments, genomic and RT-qPCR analyses, and biofilm structural characterization using confocal microscopy, we investigated in this study how *Escherichia coli* biofilms adapted after 28 days of exposure to three biocidal active substances and the effects on cross-resistance to antibiotics. Interestingly, polyhexamethylene biguanide (PHMB) exposure led to an increase of gentamicin resistance (GenR) phenotypes in biofilms formed by most of the seven *E. coli* strains tested. Nevertheless, most variants that emerged under biocidal conditions did not retain the GenR phenotype after removal of antimicrobial stress, suggesting a transient adaptation (adaptive resistance). The whole genome sequencing of variants with stable GenR phenotypes revealed recurrent mutations in genes associated with cellular respiration, including cytochrome oxidase (*cydA*, *cyoC*) and ATP synthase (*atpG*). RT-qPCR analysis revealed an induction of gene expression associated with biofilm matrix production (especially curli synthesis), stress responses, active and passive transport and cell respiration during PHMB exposure, providing insight into potential physiological responses associated with adaptive crossresistance. In addition, confocal laser scanning microscopy (CLSM) observations demonstrated a global effect of PHMB on biofilm architectures and compositions formed by most *E. coli* strains, with the appearance of dense cellular clusters after a 24h-exposure. In conclusion, our

results showed that the PHMB exposure stimulated the emergence of an adaptive cross-resistance to gentamicin in biofilms, likely induced through the activation of physiological responses and biofilm structural modulations altering gradients and microenvironmental conditions in the biological edifice.

KEYWORDS

biofilm, biocide, antibiotic resistance, aminoglycoside, biguanide, bacterial adaptation, tolerance, experimental evolution

1 Introduction

Antimicrobial resistance (AMR) of bacteria stands as a significant threat to human health in the coming decades. Although resistant strains have existed for millions of years prior to the development of clinical drugs, their (mis)use has accelerated the rapid selection and spread of multidrug resistant bacteria (Davies and Davies, 2010). Among the different bacterial families, concerns on multidrug resistance are particularly high in *Enterobacteriaceae* (Iovleva and Doi, 2017; Alkofide et al., 2020; Atamna-Mawassi et al., 2021). Treatment against *Enterobacteriaceae* include several families of antibiotics, notably fluoroquinolones and aminoglycosides and understanding the mechanisms of bacterial resistance to these antibiotics is of primary importance (Krause et al., 2016; World Health Organization, 2019; Bodendoerfer et al., 2020; Zhu et al., 2020). Additional drivers can also promote the emergence and propagation of AMR in interconnected environments (Aslam et al., 2021), highlighting the importance of identifying these factors and understanding their actual role in AMR. Among these factors, biocides are widely used in various environments, such as food-processing industries to mitigate the risk of pathogenic bacteria dissemination through the food chain. Unlike antibiotics, which often have specific targets in the bacterial cell, biocides typically employ a multi-targeted mode of action. However, mechanisms developed by bacteria to resist biocides can be close or imply common cellular components to those involved in antibiotic resistance and multiple possible cross-resistances have already been identified in different bacterial species (Maillard, 2018; Charron et al., 2023). Schematically, when exposing bacteria to a biocide, cross-adaptations could result from two major types of mechanisms. First, bacteria can become cross-resistant if stable mutations occur in a genetic target involved in both biocide and antibiotic resistance (mutational resistance). Second, physiological adaptations and gene expression modulations in response to biocidal stresses can confer bacteria a greater ability to transiently withstand both biocide or antibiotic challenge (adaptive resistance) (Fernández et al., 2011; Fernández and Hancock, 2012; Sindeldecker and Stoodley, 2021; D'Aquila et al., 2023). The potential of some biocidal active susbtances such as triclosan (Chuanchuen et al., 2001; Sanchez et al., 2005; Karatzas et al., 2007; Tkachenko et al., 2007; Fernández-Cuenca et al., 2015; Lu et al., 2018; Sonbol et al., 2019) or quaternary ammonium compounds (Bore et al., 2007; Fernández-Cuenca et al., 2015; Soumet et al., 2016; Kim et al., 2018; Guérin et al., 2021; Douarre et al., 2022) to select cross-resistance to antibiotics have already been recurrently reported for instance. However, data regarding the antimicrobial resistance effects of biocides are still lacking for the majority of widely used molecules and the underlying mechanisms are unclear. Given their widespread and extensive usage, coupled with the potential for cross-resistance with antibiotics, it is imperative to investigate and comprehend the role of biocides in AMR selection and dissemination.

Numerous studies have examined the impact of biocide on AMR using planktonic bacteria, the most common lifestyle studied in laboratories. However, it is important to recognize that bacteria predominantly live in surface-associated communities, commonly known as biofilms (Römling, 2023). Biofilms represent intricate three-dimensional structures formed by bacterial communities, embedded within a self-produced extracellular matrix. This matrix is composed of a wide variety of substances including exopolysaccharides, lipids, proteins, amyloids and nucleic acids (Karygianni et al., 2020; Flemming et al., 2023). The composition and structure of biofilms depend on the bacterial species and microenvironmental conditions, significantly influencing bacterial metabolism in a reciprocal manner. The dense tridimensional structure creates chemical gradients, resulting in distinct microenvironments for bacteria residing in the periphery, exposed to the external medium, as opposed to those in the inner layers, typically with low access to nutrients and oxygen (Jo et al., 2022). This chemical heterogeneity favors varied physiological responses, giving rise to different populations, including persister cells or viable but non-culturable phenotypes, often characterized by a substantial growth slowdown (Charron et al., 2023). These metabolic states can confer a heightened tolerance to antimicrobials, thus enhancing bacterial survival and potential acquisition of genetic resistance (Levin-Reisman et al., 2017; Nordholt et al., 2021). Furthermore, the external matrix often acts as a barrier, restricting the entry and the diffusion of biocidal substances inside of the biofilm, further increasing bacterial survival (Davison et al., 2010; Bridier et al., 2011).

The combination of these intricate factors is likely to influence significantly how bacteria adapt to their environment. Understanding the potential interplay between biocide exposure, biofilm adaptation and the emergence of AMR is therefore crucial. In this study, we aimed to investigate the effect of the exposure to

10.3389/fcimb.2023.1324991

three commonly used biocidal active substances (benzalkonium chloride (BAC), polyhexamethylene biguanide (PHMB), and N-(3-aminopropyl)-N-dodecylpropane-1,3-diamine (TMN) on the emergence of resistance against two critically important antibiotics for human medicine, the aminoglycoside gentamicin and the fluoroquinolone ciprofloxacin in *Escherichia coli* biofilms (World Health Organization, 2019).

2 Materials and methods

2.1 Bacterial strains and growth conditions

Seven *E. coli* strains were used in this study. Six strains originated from the collection of the national reference laboratory (NRL) for Antimicrobial Resistance hosted in Anses Fougères laboratory composed of *E. coli* isolated in pork (Ec694; Ec709; Ec723; Ec956) and poultry industries (Ec775; Ec478) between 2014 and 2018. The Ec223 strain originated from the CIRM collection from INRAe and was initially isolated on a chicken. These strains were conserved at -80°C in cryotubes (Mast Group, Bootle, UK). The strains were grown at 37°C on trypticase soy agar (TSA) or in ten times diluted trypticase soy broth (1/10 TSB).

2.2 Biocidal substances used and minimal inhibitory concentration assay

Strains susceptibility to three biocides has been tested: BAC (Stepan France); PHMB (Matrix Scientific France) and TMN (Quaron SAS France). The minimal inhibitory concentration (MIC) is here defined as the lowest concentration where cells are unable to grow and were determined as previously described with slight modifications (Guérin et al., 2021). Strains were grown overnight in 1/10 TSB medium and then adjusted to 0.2 (+/− 0.02) optical density at 620 nm (OD620). Microplates were filled with 200 µL of biocides in line A at the highest challenging concentration. 100µL of 1/10 TSB were added in line B to H. A cascade dilution with 100µL of previous line was done from A to H. Finally, 10µL of adjusted bacterial preculture were added in each well. Microplates were incubated at 20°C overnight and MIC were determined after 24 and 48 h of incubation. Experiments were performed in duplicate.

2.3 Experimental evolution with three biocides

Strains were grown overnight in 5ml of 1/10 TSB medium from a colony picked on TSA. On the next day, strains were diluted in fresh 1/10 TSB to reach an OD of 0.2 (+/- 0.02). For each strain, 4 columns of 8 wells on a 96-wells flat-bottom microtiter plate (Greiner Bio-One 655161) were filled with 190µL of 1/10 TSB and 10µL of the adjusted subcultures were added to reach a final OD of 0.01 (with an empty column between each). Plates were incubated at 20°C during 1h to enable adhesion of bacteria. Supernatants were then removed and replaced with 200 µl of fresh 1/10 TSB medium and plates were then incubated during 72h at 20°C to enable biofilm development.

After initial biofilm formation, a first cycle began. On the first cycle day, supernatants were removed and 40µL of fresh 1/10 TSB were added. Biofilms were sampled by scratching a quarter of the well bottom surface using tips. 5µL of the biofilm suspension were dropped on TSA plates supplemented with 10 mg/L of the aminoglycoside gentamicin (Gen). This Gen concentration corresponds to 5x the Ecoff value for *E. coli* (https://mic.eucast.org). 5µL of the biofilm suspension were also dropped on TSA supplemented with 1.2 mg/L of the fluoroquinolone ciprofloxacin (Cip). This Cip concentration corresponds to 20x the Ecoff value for *E. coli*. Preliminary tests were done to confirm these concentrations were able to discriminate between a sensitive and a resistant *E. coli* strain. Antibiotic -supplemented TSA plates were then incubated 48 h at 37°C to enable growth of Gen resistant (GenR) and Cip resistant (CipR) variants. Concurrently, 200µL of fresh 1/10 TSB containing biocides were added in wells of the biofilm microtiter plate with each column (8 wells) corresponding to one condition: H_2O, BAC, TMN, PHMB. The exposure concentrations used were respectively 6.25 mg/L for BAC, 2.5 mg/L for PHMB, 6.6 mg/L for TMN and were chosen based on MIC values determined on planktonic cells of the 7 strains (Table S1). Then, used medium was daily renewed with 200 µL fresh 1/10 TSB medium supplemented with biocides for 4 days. On the last day, the used medium was renewed, and the biofilm microtiter plate was incubated 72h at 20°C. The full cycle (one week) was repeated 4 times to reach a total of 28 days of exposure.

2.4 Assessment of resistance phenotypic stability

The stability of resistance phenotype in variants collected on antibiotic-supplemented plates after biocide exposure was assessed by repeatedly subculturing resistant variants without selective pressure and then checking the persistence of antibiotic resistance. Concretely, GenR variants collected from biofilms were spread on TSA plates and incubated at 37°C during 24 h. This step was repeated 4 times. Finally, variants were spread a fifth time on Gen-supplemented TSA plates to confirm they still displayed GenR phenotypes.

2.5 Enterobacterial repetitive intergenic consensus – PCR

ERIC-PCR was used to compare the patterns observed for the variants and their parental strain to ensure that the different collected variants were not due to contamination as previously described (Cuzin et al., 2021). DNA was first extracted using an InstaGene kit (Bio-rad, Marnes-la-Coquette, France) and amplified using a LightCycler® 480 thermocycler (Roche Diagnostics, Meylan, France) with primers ERIC1-R (ATGTAAGCTCCTGGGGATTCAC) and ERIC2 (AAGTAAGTGACTGGGGTGAGCG) and GoTaq Flexi polymerase

(Promega, Charbonnières-les-bains, France) as follows: 95 °CC for 2 min for initial melting; 30 cycles at 95 °CC for 1 min, 54 °CC for 1 min, 72 °CC for 4 min; final extension at 72 °CC for 8 min followed by incubation at 4 °CC. PCR products were then checked on 1% agarose gel and migrated over 90 min at 110 V before being revealed using a GelRED stain (Biotium, Brumath, France).

2.6 DNA extraction, sequencing and genomic analyses

E. coli genomes were sequenced by paired-end short-reads WGS. Bacteria were first grown on Thermo Scientific™ Tryptone Soya Agar with 5% Sheep Blood plates (Thermo Fischer Scientific, PB5012A), overnight at 37°C. One colony was then inoculated in 5mL of a 1/10 Tryptone Soja Broth (TSB) solution and incubated overnight at 37°C. Total DNA was extracted from 1 ml of bacterial suspension using the Macherey-Nagel Nucleospin Tissue kit according to the manufacturer's instructions (Macherey-Nagel, Düren, Germany). The concentration and quality of DNA were checked using a BioSpec-nano spectrophotometer (Shimadzu, Marne la Vallée, France). Illumina sequencing was performed on the strains at Institut du Cerveau et de la Moelle épinière (Paris, France) using the Novaseq 6000 SP. Nextera XT kit was used to prepare Illumina libraries. Before analyzing the reads, their qualities were analyzed with FastQC software and filtered with Trimmomatic (v0.39, ILLUMINACLIP : NexteraPE-PE.fa:2:30:10:8: keepBothReads HEADCROP:15 SLIDINGWINDOW:4:25). *De novo* assembly of parental strains was performed with Unicycler (v0.4.8). Contigs smaller than 200nt were removed from the newly formed genomes and Prokka (v1.14.6) was used for annotation. Variant calling was carried out using Snippy (v4.6.0) using filter reads for each variant, using as reference the genome of variant's parental strain. The analysis pipelines are available on the following GitHub repository: https://github.com/Arnaud-Bridier/BAoBAb

2.7 RNA extraction and RT-qPCR

The levels of expression of various genes of interest were also assessed during adaptation to PHMB (list of genes available in Table S2). In that aim, Ec223 biofilms were prepared and exposed to H_2O or PHMB for 28 days as previously described in section 3. At 0 (before exposure), 7, 14, and 28 days, total RNA was isolated from 8 wells for each experimental condition using the NucleoSpin RNA kit according to the manufacturer's instructions (Macherey-Nagel, Hoerd, France) with the following modifications. A first enzymatic lyse was performed with per well 25 µL mix composed of lysozyme 1 mg/mL, Tris 10 mM and EDTA 1 mM for 10 minutes at 37°C. RNA was quantified, and its purity was assessed with the Biospec-Nano (Shimadzu, Marne la Vallée, France). Reverse transcription, qPCR, primers design and analyses were performed as previously described (Reale et al., 2019) with the following modifications. Reverse transcription was performed with 1.3 µg of total RNA, and quantitative PCR reactions were carried out with 2.6 ng cDNA. All primers were purchased from Sigma-Aldrich (Saint Quentin Fallavier, France), and additional information on oligonucleotide primers are listed in Table S2. Using NormFinder software, the gene hcaT was chosen as a reference gene since it did not exhibit any significant variation of expression among the samples. Three independent experiments were performed.

2.8 CLSM analysis of biofilm architectural modulations

Biofilm architectures were characterized using CLSM observations in microtiter plates compatible with high resolution imaging (Bridier et al., 2010). For the 7 strains, 72h-biofilms were first grown in 1/10 TSB as previously described and then challenged for 24 h by renewing the used biofilm growth medium with 200µL of 1/10 TSB medium supplemented with 1.25 mg/L of PHMB (or H_2O for controls). Plates were incubated during 24 h at 20°C. Plates were analyzed with a Leica HCS-SP8 CLSM at the INRAE MIMA2 Imaging Core Facility (Microscopie et Imagerie des Microorganismes, Animaux et Aliments, INRAE, Jouy-en-Josas, doi.org/10.15454/1.5572348210007727E12). Total bacterial cells were dyed using the SYTO™9 green fluorescent permeant nucleic acid stain (Invitrogen, USA) and matrix production was contrasted using 8 µg/ml Congo red staining (Sigma-Aldrich, France). Both markers were excited with an Argon Laser set at 488 nm for SYTO™9 and 514 nm for Congo red. Fluorescence emissions were collected using photomultiplier tubes (PMT) at wavelengths of 500-550nm for SYTO™9 and 600-750nm for Congo red. Biofilm three-dimensional structures were scanned with a 63x water objective lens (numerical aperture: 1.2), with a resolution of 512x512 and a 1 µm Z-step. For each strain, a total of 12 stacks per condition (PHMB-exposed or H_2O controls) was captured corresponding to 2 Z-stacks per well, with 6 different wells per strain on 2 different plates. Biofilm 3D reconstructions were performed using the Imaris 9.3.1 software (Bitplane, AG-Zürich, Switzerland) via the maximum intensity projection (MIP) section view. Quantitative biofilm biovolumes were extracted from CLSM images with BiofilmQ 0.2.2 (Hartmann et al., 2021).

2.9 Statistical analysis

Frequencies of occurrence of GenR variants in H_2O and in every biocide conditions were compared using the Kruskal-Wallis test (*P* value: * = [0.05-0.01]; ** = [0.01-0.001]; *** = <0.001).

RT-q-PCR data analysis was performed with the Graphpad Prism software. For each week, a Student t-test was performed between the PHMB and H_2O condition (*P* value: * = [0.05-0.01]; ** = [0.01-0.001]; *** = <0.001).

3 Results

3.1 Quantification of GenR variants during biofilm exposure to biocides

E. coli biofilms were exposed to BAC, PHMB and TMN for 28 days and bacterial cells collected and enumerated on antibiotic-

10.3389/fcimb.2023.1324991

supplemented TSA plates along biocide exposure to investigate how this stress could influence the emergence of resistant variants against two antibiotics: the fluoroquinolone Cip and the aminoglycoside Gen. We did not detect any resistant variants on Cip-supplemented plates (CipR variants) in the biofilm of the seven *E. coli* strains after exposure to the three different biocides or H_2O (data not shown). Conversely, Gen resistant (GenR) variants were detected in different strains and conditions with differences between biocides and the control group (H_2O) as displayed in Figure 1A, where the frequency of GenR variant occurrence corresponds to the proportion of replicates for each strain in which at least one GenR variant was detected. After the first week of exposure (day 7), GenR variants tended to emerge preferentially in the control group rather than in presence of biocides (without significative difference). However, upon PHMB exposure, the proportions of GenR-positive replicates variants progressively increased over time in all seven strains when compared to other biocides or in H_2O controls, revealing a similar effect of PHMB on different *E. coli* strains. After 28 days, the frequency of occurrence of GenR variants was significantly higher in the PHMB-exposed group than in the other conditions, including H_2O (p=0.008704). Conversely, in the H_2O control, the increase in GenR variants frequency after 28 days was mainly attributed to one strain (Ec709), where GenR variants were seen in every replicate.

Stability assays were performed for each GenR variant to differentiate the number of variants that acquired a stable GenR phenotype and those with a transitory response (Figure 1B). Proportions of unstable GenR variants (losing the GenR phenotype after 5 subcultures without Gen selective pressure and called hereafter transient GenR variants) were consistently higher than the stable ones in the different conditions with minor variations. Among the 31 variants isolated in H2O, 7 of them were stable (23%) and emerged in strain Ec478 and especially in strain Ec709. Notably, strain Ec709 was the only strain exhibiting a higher number of GenR variants in the H_2O control than in the PHMB condition after the 28 days exposure. Concerning the biocides, only 4 of the 60 variants isolated in the different biocide conditions had a stable resistance phenotype, with 3 of them emerging in the PHMB condition (strains Ec478 and Ec709) and another in the TMN condition (strain Ec709).

3.2 Genomic analysis of stable GenR variants

The genomes of 11 GenR variants with stable resistance phenotype (8 from Ec709 and 3 from Ec478) that were collected during the experimental evolution phase were sequenced and analyzed in comparison with their respective parental strain. Genetic events responsible for the emergence of GenR phenotype were identified and are displayed in Table 1. Genomic analysis of these variants revealed several genetic targets, mainly involved in the electron transport chain. Variants that emerged under biocide conditions exhibited similar affected pathways to those in the H_2O control group. Two genes were targeted in more than one variant: *cydA* and *atpG*. The most frequently targeted gene was *cydA*, which was mutated in 5 among the 11 variants and was found in both Ec478 and Ec709, as well as in both H_2O and PHMB conditions.

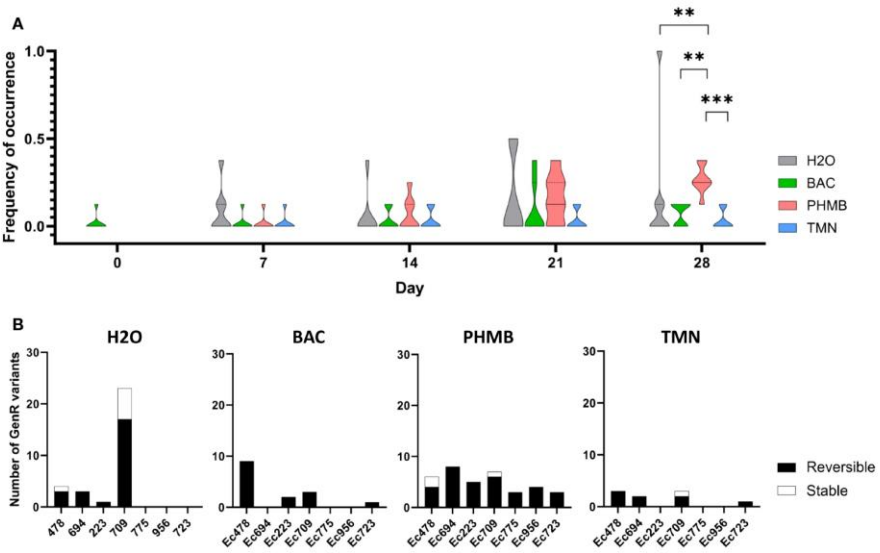

FIGURE 1
(A) Violin plots representing the dynamics of emergence of GenR variants (frequency of occurrence) in biofilms of the different strains in different conditions. Kruskal Wallis Tests were done for each week, comparing every condition, *P* value: *[0.05-0.01]; **[0.01-0.001]; ***<0.001 **(B)** Resistance phenotype stability of GenR variants collected for each of the seven (*E*) *coli* strains during experimental evolution (NB: Due to the high number of variants emerging in H_2O for the Ec709 strain, a previous selection was made, this graph is thus not showing the real quantity of emerging variants for this specific condition).

TABLE 1 GenR variants emerging in Ec478 and Ec709 in the control group, in PHMB and in TMN throughout the weeks and the associated mutations and aminoacid modifications.

Biocide	Variant name	Gene mutated	Nucleotide modifications	Aminoacid modifications
H_2O	Ec478_H2O_W1	*cydA*	c.173T>A	p.Leu58*
		ygfZ	c.423delA	p.Lys141fs
	Ec709_H2O_W1_1	*atpG*	c.728G>C	p.Arg243Pro
	Ec709_H2O_W3_1	*fre*	c.190C>T	p.His64Tyr
		cydA	c.444_457delCGGCTGGATGCAAA	p.Asn148fs
	Ec709_H2O_W4_1	*cydA*	c.444_457delCGGCTGGATGCAAA	p.Asn148fs
		Intergenic	c.delT	–
	Ec709_H2O_W4_2	*fusA*	c.2033>T	p.Ala678Val
		tsaB	c.484A>G	p.Thr162Ala
	Ec709_H2O_W4_3	*arcB*	c.208G>C	p.Val70Leu
		cydA	c.516_520delCGAGC	p.Glu173fs
	Ec709_H2O_W4_4	*aceE*	c.1502G>T	p.Arg501Leu
		cydA	c.1284C>A	p.Tyr428*
PHMB	Ec709_PHMB_W1	*atpG*	c.728G>C	p.Arg243Pro
		Intergenic	c.G>A	–
	Ec478_PHMB_W2	*cyoC*	c.302G>A	p.Trp101*
	Ec478_PHMB_W4	*fdx*	c.259T>A	p.Cys87Ser
		rpoS	c.562A>T	p.Lys188*
		cydA	c.331delG	p.Val111fs
TMN	Ec709_TMN_W1	*atpG*	c.728G>C	p.Arg243Pro

*, represent the classic annotation to illustrate a "stop codon" resulting in the stop of the aminoacid sequence.
-, not applicable.

This gene encodes a subunit of cytochrome bd-I, involved in the production of H+, that can be converted into energy for the cell. The *atpG* gene, which codes for a subunit of the ATP synthase, was mutated in 3 out of the 11 variants and was exclusively found in Ec709 strain. Other mutations were identified in similar target genes, including *cyoC*, which codes for another cytochrome subunit, as well as genes associated with ferric transport systems (*fdx* + *fre*), transcription regulators (*rpoS* + arcB), tRNA processing (*tsaB*), glycolysis (*aceE*) and an elongation factor, *fusA*, which is implicated in the translocation of the ribosome during protein synthesis.

3.3 Gene expression analysis in presence of PHMB

To gain better insights into biofilm adaptation and the bacterial response to PHMB, we examined changes in gene expression levels after 28 days of PHMB-exposure, comparing them to H_2O condition using RT-qPCR in the Ec223 strain (Figure 2). Efflux pumps (*acrAB*) and porins (*ompCF*) were explored because of their known effect against antimicrobials. Biofilm formation genes and stress responses were also investigated because of their relevance in the adaptation in a biofilm model. Finally, cellular metabolism genes were chosen to see if transient resistance was linked to the same genetic targets as the variants with acquired resistance. Globally, most of the pronounced variations occurred after one week of exposure and decreased over subsequent weeks, suggesting an initial response to the PHMB stress followed by a possible adaptation. Various genes were thus significantly overexpressed in the presence of PHMB after 1 week of exposure. Notably, *csgB* (fold change: 7.23) which is involved in curli biosynthesis and biofilm formation, showed a substantial increase, along with genes involved in stress response, such as *rpoS*, the activator of global stress response (fold change: 3.64) and *recA*, which mediates the SOS response (fold change: 5.46). Levels of expression of *csgB* and *recA* in the presence of PHMB remained elevated with regards to fold changes values compared to H_2O condition during the second part of experimental evolution at days 14 (3.40 and 3.78) and days 28 (7.58 and 3.56), although difference was not statistically significant. In a lesser extent, genes encoding proteins involved in passive transport *ompC/F (*fold changes: *ompC*: 2.77; *ompF*: 2.45) or active efflux *acrA* (fold change: 1.50) were also significantly up-regulated in PHMB compared to H_2O after 1 week of exposure. Finally, some

10.3389/fcimb.2023.1324991

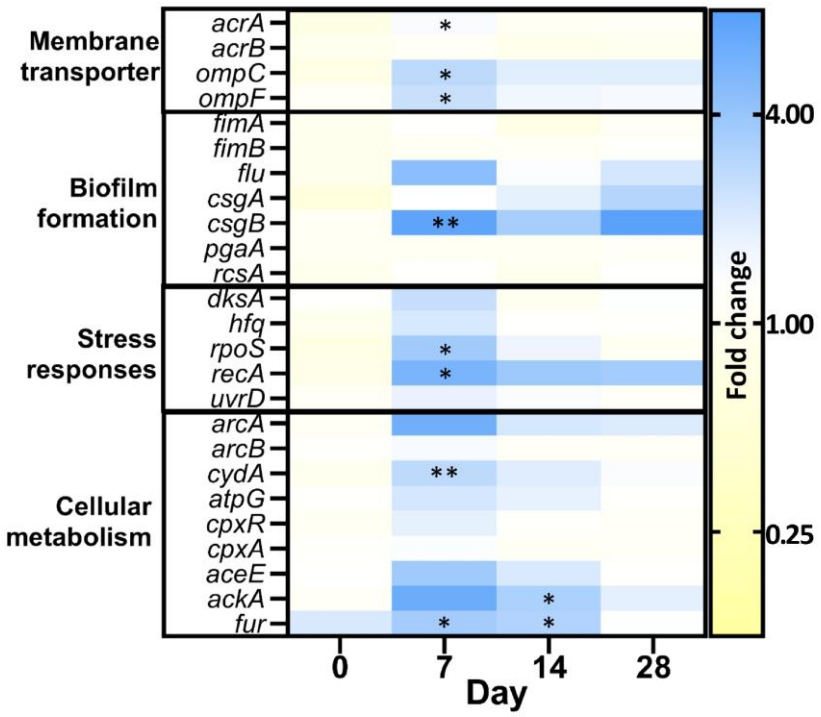

FIGURE 2
Gene expression differentiation in presence of PHMB, in the Ec223 strain. Fold changes were normalized on the *hcaT* gene and the H2O control. Values >1 indicate an increased expression in presence of PHMB and <1 a decreased expression in presence of PHMB. (*P* value: *[0.05-0.01]; **[0.01-0.001]).

cell metabolism genes such as *cydA* (fold change: 2.75) and fur (fold change: 3.52), a transcription regulator regulating the expression of several respiratory chain genes and ferric transporters, were also differentially expressed in the first week of PHMB exposure. Other genes showed an overexpression tendency without statistically significant difference, including *arcA*, the global regulator of the cell respiration process, *flu*, the gene involved in the synthesis of the auto-aggregation factor *Ag43*, and other metabolism genes such as *ackA*, an acetate kinase, and *aceE*, a pyruvate dehydrogenase.

3.4 Biofilm structural modulation after PHMB exposure

The impact of PHMB exposure on the architectural properties of biofilms formed by the seven *E. coli* strains was also investigated using CLSM to observe potential structural perturbations resulting from bacterial community adaptation. Bacterial cells were stained with SYTO^{TM}9 and part of the extracellular matrix was stained with Congo red, a dye known to stain amyloid fibers, including curli, which are essential components of the biofilm matrix. First, CLSM observations revealed that PHMB exposure provoked recurrent structural modifications among most *E. coli* strains, leading to the formation of dense clusters as shown on CLSM sections in Figure 3. The quantification of biofilm structures following both fluorescent staining (SYTO^{TM}9 and Congo red) provided complementary data showing that such architectural modulations in response to PHMB were related to slightly different processes depending on strains. One group composed of Ec223, Ec478, Ec709 and Ec775 had an induction of the matrix production and a reduction in cell biovolume after PHMB exposure. A second group comprising Ec694 and Ec723 also showed a reduction in cell biovolume but no induction of the biofilm matrix. Finally, Ec956 was the only strain with an increase in cell biovolume accompanied by an increase in biofilm matrix production after PHMB exposure.

4 Discussion

The escalating threat of antibiotic resistance challenges our understanding of bacterial adaptation mechanisms and the factors contributing to the emergence of resistant bacteria in our environments. Abundant evidence supported the central role of biofilm communities in bacterial adaptation to various antimicrobial substances (Uruén et al., 2020; Usui et al., 2023). However, the underlying mechanisms often remain ambiguous and are highly dependent on the molecules involved. In this contribution, we investigated the impacts of biocide exposures (BAC, TMN and PHMB) on aminoglycoside (Gen) and fluoroquinolone (Cip) resistance emergence in *E. coli* biofilms.

10.3389/fcimb.2023.1324991

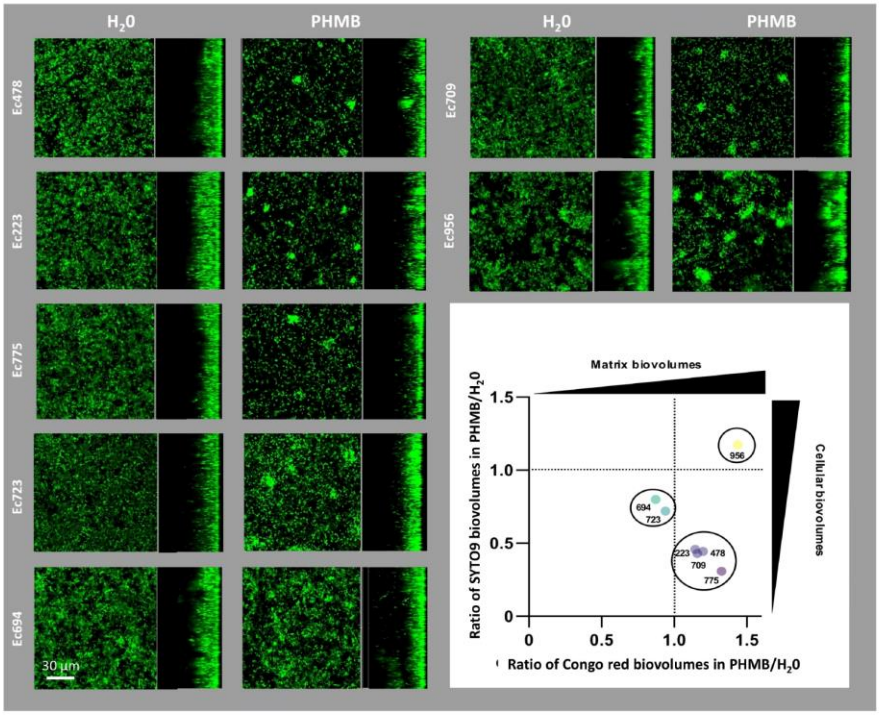

FIGURE 3
CLSM images of biofilms stained with SYTO^{TM}9 in presence or absence of sublethal concentrations of PHMB. On the bottom right, ratios between total cell biovolumes (SYTO^{TM}9, y-axis) and biofilm matrix (Congo red, x-axis) of biofilms exposed to PHMB or H_2O.

Gen and Cip are indeed considered as crucial antibiotics used in the treatment of several gram-negative infections notably involving *Enterobacteriaceae* like *E. coli* (Krause et al., 2016; Zhu et al., 2020).

Experimental evolution experiments revealed here that PHMB exposure resulted in a recurrent increase of transient GenR emergence in the biofilms formed by most of the seven *E. coli* strains compared to H_2O control. Only one strain, Ec709, showed a reduction in the quantity of variants in PHMB compared to H_2O (especially due to a high number of GenR variants emerging in H_2O). Such specific adaptive and mutability features of strain Ec709 would rely on its specific genetic background. Resistant variants appear naturally in bacterial populations and could be preferentially selected in Ec709 by the biofilm lifestyle itself rather than biocidal exposure. This can be related to particular chemical microenvironments in the three-dimensional structure of Ec709 biofilm that could participate in the induction of specific phenotypes and/or selection of genetic variants (Uruén et al., 2020; Charron et al., 2023). In addition, recent findings showed that hypermutator emergence rates are dependent of stress type in *E. coli* populations (Callens et al., 2023). It is therefore possible that in the case of Ec709, the presence of PHMB did not favor variant emergence and/or survival compared to H_20 condition.

Conversely, the other biocides BAC and TMN led to a slight decrease of GenR emergence in most *E. coli* strains emphasizing the specificity of exposure effects depending on biocide molecules and their mode of action. Importantly, most variants that emerged under biocidal conditions did not retain the GenR phenotype after removal of antimicrobial stress, suggesting a transient adaptation rather than stable mutation-based resistance. Contrarily to Gen, no Cip variant was detected in any condition during the time of experiment. One assumption is that CipR variants potentially emerging in biofilms were outcompeted here due to a decrease of their ability to survive under biofilm conditions and biocidal exposure. Fluoroquinolones act by inhibiting DNA Gyrase and Topoisomerase IV, enzymes involved in chromosome replication and RNA transcription, and high-level resistance to fluoroquinolones in *E. coli* indeed often requires multiple mutations which are associated with a high fitness cost (Marcusson et al., 2009).

Genomic analysis of the 11 stable GenR variants revealed mutations predominantly affecting the cell respiration pathway and indistinctly selected in H_2O or upon biocidal stress, showing unspecific evolutionary trajectories. Alteration of genes encoding components of the respiratory and electron transport chains was previously described to be associated with aminoglycoside resistance through the decrease of antibiotic uptake in *E. coli* and other gram-negative species including *Klebsiella pneumoniae* or *Salmonella enterica* for instance (Ibacache-Quiroga et al., 2018; Andersson et al., 2019). The *cydA* gene mutation was especially highly prevalent at the end of the experiment. Interestingly, most of the *cydA* variants had a second mutation, notably in *aceE*, *arcB* and *fre*. These genes are also linked to the cell respiration metabolism,

ArcB being known as the main regulator of the cell anoxic respiration process and regulating several of the other mutated genes, like *cydA* (Brown et al., 2022) and *atpG* (Salmon et al., 2005). Moreover, *aceE* has already been associated with a Gen-PHMB cross-resistance mutation (Cuzin et al., 2021). Hence, associations of different mutations in this pathway could strengthen the resistance phenotype and compensate for potential fitness defects caused by the *cydA* mutation. The last *cydA* variant had no other mutated gene, but a mutation in an intergenic region, which could possibly play a role in the fitness of the bacteria. The only variant found in the last two weeks without a *cydA* mutation exhibited two mutations, one in *fusA*, which is also an already-known GenR mutation (Ibacache-Quiroga et al., 2018; Usui et al., 2023) and the other one in *tsaB*. The selection of similar mutations in the H_2O control and upon biocidal exposure could result from the biofilm lifestyle itself, known to shape specifically adaptive trajectories due to the heterogeneity of microenvironments and associated stress in the three-dimensional structure (Bridier et al., 2017). In line with this, it was recently reported that *E. coli* biofilms upon aminoglycoside treatment favored specific resistance mutations otherwise counter-selected in planktonic cultures, illustrating such a specific biofilm-associated adaptive strategy (Usui et al., 2023).

Interestingly, we observed that PHMB promoted the emergence of transient GenR variants over subsequent weeks of exposure in most of the seven *E. coli* strains. This induction of transient variants upon PHMB exposure could rely on the activation of specific defensive responses to face biocide stress. Coherently, RT-qPCR gene expression analysis revealed the up-regulation of multiple genes linked to metabolic activity or membrane transport in response to PHMB in the first week of exposure, that could illustrate an attempt of bacteria to actively keep the biocide outside the cell. Previous researches reported the upregulation of efflux pumps in response to chlorhexidine digluconate (CHX), a biocide belonging, like PHMB, to the biguanide family (Morita et al., 2003; Fernández-Cuenca et al., 2015; Zhang et al., 2019; Tag ElDein et al., 2021). Interestingly, in another study performed on *Acinetobacter baumannii*, exposure to CHX reduced the resistance of one strain to Gen, while inducing several efflux pumps (Fernández-Cuenca et al., 2015). Here, efflux pumps (AcrA) were indeed slightly impacted by the PHMB pressure in the beginning of exposure. Additionally, general stress responses, like *rpoS*, and the SOS response through *recA* were globally overexpressed, affecting the expression of numerous genes playing a central role in the adaptation to suboptimal conditions and nucleic acid repair (Schellhorn, 2020). It has already been shown that PHMB can bind nucleic acids, which could explain why DNA repair systems are activated (Sowlati-Hashjin et al., 2020). Furthermore, the *csgB* gene involved in curli synthesis, a major amyloid proteinaceous component of extracellular matrix produced by many *Enterobacteriaceae* (Barnhart and Chapman, 2006), showed a prolonged overexpression in the presence of PHMB. Consequently, the denser biofilm matrix due to the overproduction of curli could thereby reinforce the biofilm structure and resistance by limiting PHMB diffusion. The role of curli in biofilm resistance to diverse molecules including biocides and antibiotics was indeed already shown in *E. coli* and other species (Ryu and Beuchat, 2005; Uhlich et al., 2006; Akbey and Andreasen, 2022). CLSM observations of biofilm here confirmed the overproduction of curli fibers after PHMB exposure illustrated by a modulation of the three-dimensional structure and the formation of dense clusters of bacteria associated with an increase in matrix biovolumes compared to H_20 controls in most *E. coli* strains tested (Figure 3). Interestingly, previous studies have also linked specific subpopulations of cells, also organized into clusters, with increased expression of *csgD*, regulating curli production, and with the production of other matrix components, like cellulose (Grantcharova et al., 2010). The densification of biofilm matrix and reshaping of three-dimensional structure resulting from PHMB-induced curli overproduction could therefore potentially participate to the creation of specific microenvironments (here the clusters) promoting a higher tolerance to Gen notably through slow growth phenotypes (Uhlich et al., 2006; Yan and Bassler, 2019). This could be part of the origin of the increased frequencies of transient GenR variants upon PHMB exposure observed here for the various *E. coli* strains tested.

In this study, Gen variants emerging in biocide conditions mainly exhibited reversible resistance phenotypes. Nevertheless, recent studies suggest a potential link between bacterial tolerance and the facilitated emergence of stable genetic resistances toward antibiotics (Levin-Reisman et al., 2017; Levin-Reisman et al., 2019; Nordholt et al., 2021). An explanation if that tolerant bacteria, capable of surviving longer treatment periods, increase the likelihood of acquiring genetic resistance and often have elevated mutation rates due to the stress they undergo (Windels et al., 2019; Crane et al., 2021). Exposure to PHMB induced stress responses here, such as the SOS response mediated by *recA* and the general stress response involving *rpoS*. The SOS response, typically utilized by bacteria to repair damaged DNA, can lead to the emergence of antibiotic resistant variants due to the use of error-prone polymerases for instance (Crane et al., 2021). As PHMB globally induces physiological responses in biofilms that enhance survival against Gen in most of the *E. coli* strains tested here, it may thereby potentialize the emergence of mutants carrying stables genetic resistance during extended exposures, heightening the risk of antibiotic resistances dissemination and raising public health concerns. Such hypothesis should nevertheless be mitigated regarding the behavior of specific strain as Ec709 here, for which PHMB exposure rather results in a decrease of frequency of GenR emergence, underlining the strain-dependent nature of adaptive strategies.

5 Conclusion

We showed in this work that PHMB could indirectly stimulate the emergence of transient Gen resistance in *E. coli* biofilms. Bacterial response to PHMB in biofilms is characterized by the induction of stress responses and architectural modulations, notably through the production of extracellular curlis. These structural rearrangements resulted in the formation of clusters that may constitute specific microenvironments favoring the emergence of slow-growing bacteria with Gen tolerant

phenotypes. Overall, this study provided valuable insights into the adaptive trajectories of biofilms exposed to biocidal stress and shed light on potential side effects on bacterial resistance to antibiotics. Further studies should be dedicated to deeply understanding collective biofilm adaptation to biocides and antimicrobial cross-resistance emergence.

Data availability statement

The datasets presented in this study can be found in online repositories. The names of the repository/repositories and accession number(s) can be found in the article/Supplementary Material.

Author contributions

RC: Conceptualization, Formal analysis, Investigation, Visualization, Writing – original draft, Writing – review & editing. PL: Data curation, Formal analysis, Investigation, Methodology, Software, Writing – original draft. AH: Investigation, Writing – review & editing. OM: Investigation, Writing – original draft. MB: Investigation, Writing – original draft. PH: Investigation, Writing – original draft. CS: Project administration, Resources, Writing – original draft. RB: Conceptualization, Funding acquisition, Supervision, Writing – review & editing, Writing – original draft. AB: Conceptualization, Funding acquisition, Project administration, Resources, Supervision, Visualization, Writing – review & editing, Writing – original draft.

Funding

The author(s) declare financial support was received for the research, authorship, and/or publication of this article. ANR JCJC BAoBAb (ANR-21-CE35-0001) financially supported this work. RC was also a recipient of an Anses-INRAE doctoral fellowship.

Acknowledgments

The authors express their gratitude to the French AntibioDEAL network of the Promise PPR antibioresistance ANR program for fostering valuable scientific exchanges.

Conflict of interest

The authors declare that the research was conducted in the absence of any commercial or financial relationships that could be construed as a potential conflict of interest.

The author(s) declared that they were an editorial board member of Frontiers, at the time of submission. This had no impact on the peer review process and the final decision.

Publisher's note

All claims expressed in this article are solely those of the authors and do not necessarily represent those of their affiliated organizations, or those of the publisher, the editors and the reviewers. Any product that may be evaluated in this article, or claim that may be made by its manufacturer, is not guaranteed or endorsed by the publisher.

Supplementary material

The Supplementary Material for this article can be found online at: https://www.frontiersin.org/articles/10.3389/fcimb.2023.1324991/full#supplementary-material

References

Akbey, Ü., and Andreasen, M. (2022). Functional amyloids from bacterial biofilms - structural properties and interaction partners. *Chem. Sci.* 13, 6457–6477. doi: 10.1039/d2sc00645f

Alkofide, H., Alhammad, A. M., Alruwaili, A., Aldemerdash, A., Almangour, T. A., Alsuwayegh, A., et al. (2020). Multidrug-resistant and extensively drug-resistant enterobacteriaceae: prevalence, treatments, and outcomes - A retrospective cohort study. *Infect. Drug Resist.* 13, 4653–4662. doi: 10.2147/IDR.S283488

Andersson, D. I., Nicoloff, H., and Hjort, K. (2019). Mechanisms and clinical relevance of bacterial heteroresistance. *Nat. Rev. Microbiol.* 17, 479–496. doi: 10.1038/s41579-019-0218-1

Aslam, B., Khurshid, M., Arshad, M. I., Muzammil, S., Rasool, M., Yasmeen, N., et al. (2021). Antibiotic resistance: one health one world outlook. *Front. Cell Infect. Microbiol.* 11. doi: 10.3389/fcimb.2021.771510

Atamna-Mawassi, H., Huberman-Samuel, M., Hershcovitz, S., Karny-Epstein, N., Kola, A., Cortés, L. E. L., et al. (2021). Interventions to reduce infections caused by multidrug resistant Enterobacteriaceae (MDR-E): A systematic review and meta-analysis. *J. Infect.* 83, 156–166. doi: 10.1016/j.jinf.2021.05.005

Barnhart, M. M., and Chapman, M. R. (2006). Curli biogenesis and function. *Annu. Rev. Microbiol.* 60, 131–147. doi: 10.1146/annurev.micro.60.080805.142106

Bodendoerfer, E., Marchesi, M., Imkamp, F., Courvalin, P., Böttger, E. C., and Mancini, S. (2020). Co-occurrence of aminoglycoside and β-lactam resistance mechanisms in aminoglycoside- non-susceptible *Escherichia coli* isolated in the Zurich area, Switzerland. *Int. J. Antimicrob. Agents* 56, 106019. doi: 10.1016/j.ijantimicag.2020.106019

Bore, E., Hébraud, M., Chafsey, I., Chambon, C., Skjæret, C., Moen, B., et al. (2007). Adapted tolerance to benzalkonium chloride in *Escherichia coli* K-12 studied by transcriptome and proteome analyses. *Microbiol. (Reading)* 153, 935–946. doi: 10.1099/mic.0.29288-0

Bridier, A., Dubois-Brissonnet, F., Boubetra, A., Thomas, V., and Briandet, R. (2010). The biofilm architecture of sixty opportunistic pathogens deciphered by a high-throughput CLSM method. *J. Microbiol. Methods* 82, 64–70. doi: 10.1016/j.mimet.2010.04.006

Bridier, A., Dubois-Brissonnet, F., Greub, G., Thomas, V., and Briandet, R. (2011). Dynamics of the action of biocides in Pseudomonas aeruginosa biofilms. *Antimicrob. Agents Chemother.* 55, 2648–2654. doi: 10.1128/AAC.01760-10

Bridier, A., Piard, J.-C., Pandin, C., Labarthe, S., Dubois-Brissonnet, F., and Briandet, R. (2017). Spatial organization plasticity as an adaptive driver of surface microbial communities. *Front. Microbiol.* 8. doi: 10.3389/fmicb.2017.01364

Brown, A. N., Anderson, M. T., Bachman, M. A., and Mobley, H. L. T. (2022). The arcAB two-component system: function in metabolism, redox control, and infection. *Microbiol. Mol. Biol. Rev.* 86, e0011021. doi: 10.1128/mmbr.00110-21

Callens, M., Rose, C. J., Finnegan, M., Gatchitch, F., Simon, L., Hamet, J., et al. (2023). Hypermutator emergence in experimental Escherichia coli populations is stress-type dependent. *Evol. Lett.* 7, 252–261. doi: 10.1093/evlett/qrad019

Charron, R., Boulanger, M., Briandet, R., and Bridier, A. (2023). Biofilms as protective cocoons against biocides: from bacterial adaptation to One Health issues. *Microbiol. (Reading)* 169. doi: 10.1099/mic.0.001340

Chuanchuen, R., Beinlich, K., Hoang, T. T., Becher, A., and Karkhoff-Schweizer, R. R. (2001). and schweizer, H Cross-resistance between triclosan and antibiotics in Pseudomonas aeruginosa is mediated by multidrug efflux pumps: exposure of a susceptible mutant strain to triclosan selects nfxB mutants overexpressing MexCD-OprJ. *P. Antimicrob. Agents Chemother.* 45, 428–432. doi: 10.1128/AAC.45.2.428-432.2001

Crane, J. K., Alvarado, C. L., and Sutton, M. D. (2021). Role of the SOS response in the generation of antibiotic resistance *in vivo*. *Antimicrob. Agents Chemother.* 65, e0001321. doi: 10.1128/AAC.00013-21

Cuzin, C., Houée, P., Lucas, P., Blanchard, Y., Soumet, C., and Bridier, A. (2021). Selection of a gentamicin-resistant variant following polyhexamethylene biguanide (PHMB) exposure in *escherichia coli* biofilms. *Antibiotics (Basel)* 10, 553. doi: 10.3390/antibiotics10050553

D'Aquila, P., De Rango, F., Paparazzo, E., Passarino, G., and Bellizzi, D. (2023). Epigenetic-based regulation of transcriptome in *escherichia coli* adaptive antibiotic resistance. *Microbiol. Spectr.* 11, e0458322. doi: 10.1128/spectrum.04583-22

Davies, J., and Davies, D. (2010). Origins and evolution of antibiotic resistance. *Microbiol. Mol. Biol. Rev.* 74, 417–433. doi: 10.1128/MMBR.00016-10

Davison, W. M., Pitts, B., and Stewart, P. S. (2010). Spatial and temporal patterns of biocide action against Staphylococcus epidermidis biofilms. *Antimicrob. Agents Chemother.* 54, 2920–2927. doi: 10.1128/AAC.01734-09

Douarre, P.-E., Sévellec, Y., Le Grandois, P., Soumet, C., Bridier, A., and Roussel, S. (2022). FepR as a central genetic target in the adaptation to quaternary ammonium compounds and cross-resistance to ciprofloxacin in listeria monocytogenes. *Front. Microbiol.* 13. doi: 10.3389/fmicb.2022.864576

Fernández, L., Breidenstein, E. B. M., and Hancock, R. E. W. (2011). Creeping baselines and adaptive resistance to antibiotics. *Drug Resist. Update* 14, 1–21. doi: 10.1016/j.drup.2011.01.001

Fernández, L., and Hancock, R. E. W. (2012). Adaptive and mutational resistance: role of porins and efflux pumps in drug resistance. *Clin. Microbiol. Rev.* 25, 661–681. doi: 10.1128/CMR.00043-12

Fernández-Cuenca, F., Tomás, M., Caballero-Moyano, F.-J., Bou, G., Martínez-Martínez, L., Vila, J., et al. (2015). Reduced susceptibility to biocides in Acinetobacter baumannii: association with resistance to antimicrobials, epidemiological behaviour, biological cost and effect on the expression of genes encoding porins and efflux pumps. *J. Antimicrob. Chemother.* 70, 3222–3229. doi: 10.1093/jac/dkv262

Flemming, H.-C., van Hullebusch, E. D., Neu, T. R., Nielsen, P. H., Seviour, T., Stoodley, P., et al. (2023). The biofilm matrix: multitasking in a shared space. *Nat. Rev. Microbiol.* 21, 70–86. doi: 10.1038/s41579-022-00791-0

Grantcharova, N., Peters, V., Monteiro, C., Zakikhany, K., and Römling, U. (2010). Bistable expression of CsgD in biofilm development of Salmonella enterica serovar typhimurium. *J. Bacteriol* 192, 456–466. doi: 10.1128/JB.01826-08

Guérin, A., Bridier, A., Le Grandois, P., Sévellec, Y., Palma, F., Félix, B., et al. (2021). Exposure to quaternary ammonium compounds selects resistance to ciprofloxacin in listeria monocytogenes. *Pathogens* 10, 220. doi: 10.3390/pathogens10020220

Hartmann, R., Jeckel, H., Jelli, E., Singh, P. K., Vaidya, S., Bayer, M., et al. (2021). Quantitative image analysis of microbial communities with BiofilmQ. *Nat. Microbiol.* 6, 151–156. doi: 10.1038/s41564-020-00817-4

Ibacache-Quiroga, C., Oliveros, J. C., Couce, A., and Blázquez, J. (2018). Parallel evolution of high-level aminoglycoside resistance in *escherichia coli* under low and high mutation supply rates. *Front. Microbiol.* 9. doi: 10.3389/fmicb.2018.00427

Iovleva, A., and Doi, Y. (2017). Carbapenem-resistant *enterobacteriaceae*. *Clin. Lab. Med.* 37, 303–315. doi: 10.1016/j.cll.2017.01.005

Jo, J., Price-Whelan, A., and Dietrich, L. E. P. (2022). Gradients and consequences of heterogeneity in biofilms. *Nat. Rev. Microbiol.* 20, 593–607. doi: 10.1038/s41579-022-00692-2

Karatzas, K. A. G., Webber, M. A., Jorgensen, F., Woodward, M. J., Piddock, L. J. V., and Humphrey, T. J. (2007). Prolonged treatment of Salmonella enterica serovar Typhimurium with commercial disinfectants selects for multiple antibiotic resistance, increased efflux and reduced invasiveness. *J. Antimicrob. Chemother.* 60, 947–955. doi: 10.1093/jac/dkm314

Karygianni, L., Ren, Z., Koo, H., and Thurnheer, T. (2020). Biofilm matrixome: extracellular components in structured microbial communities. *Trends Microbiol.* 28, 668–681. doi: 10.1016/j.tim.2020.03.016

Kim, M., Weigand, M. R., Oh, S., Hatt, J. K., Krishnan, R., Tezel, U., et al. (2018). Widely used benzalkonium chloride disinfectants can promote antibiotic resistance. *Appl. Environ. Microbiol.* 84, e01201–e01218. doi: 10.1128/AEM.01201-18

Krause, K. M., Serio, A. W., Kane, T. R., and Connolly, L. E. (2016). Aminoglycosides: an overview. *Cold Spring Harb. Perspect. Med.* 6, a027029. doi: 10.1101/cshperspect.a027029

Levin-Reisman, I., Brauner, A., Ronin, I., and Balaban, N. Q. (2019). Epistasis between antibiotic tolerance, persistence, and resistance mutations. *Proc. Natl. Acad. Sci. U.S.A.* 116, 14734–14739. doi: 10.1073/pnas.1906169116

Levin-Reisman, I., Ronin, I., Gefen, O., Braniss, I., Shoresh, N., and Balaban, N. Q. (2017). Antibiotic tolerance facilitates the evolution of resistance. *Science* 355, 826–830. doi: 10.1126/science.aaj2191

Lu, J., Jin, M., Nguyen, S. H., Mao, L., Li, J., Coin, L. J. M., et al. (2018). Non-antibiotic antimicrobial triclosan induces multiple antibiotic resistance through genetic mutation. *Environ. Int.* 118, 257–265. doi: 10.1016/j.envint.2018.06.004

Maillard, J. Y. (2018). Resistance of bacteria to biocides. *Microbiol. Spectr.* 6, 6.2.19. doi: 10.1128/microbiolspec.ARBA-0006-2017

Marcusson, L., Frimodt-Moller, N., and Hughes, D. (2009). Interplay in the selection of fluoroquinolone resistance and bacterial fitness. *PloS Pathog.* 5,8, e1000541. doi: 10.1371/journal.ppat.1000541

Morita, Y., Murata, T., Mima, T., Shiota, S., Kuroda, T., Mizushima, T., et al. (2003). Induction of mexCD-oprJ operon for a multidrug efflux pump by disinfectants in wild-type Pseudomonas aeruginosa PAO1. *J. Antimicrob. Chemother.* 51, 991–994. doi: 10.1093/jac/dkg173

Nordholt, N., Kanaris, O., Schmidt, S. B. I., and Schreiber, F. (2021). Persistence against benzalkonium chloride promotes rapid evolution of tolerance during periodic disinfection. *Nat. Commun.* 12. doi: 10.1038/s41467-021-27019-8

Reale, O., Huguet, A., and Fessard, V. (2019). Novel insights on the toxicity of phycotoxins on the gut through the targeting of enteric glial cells. *Mar. Drugs* 17, 429. doi: 10.3390/md17070429

Römling, U. (2023). Is biofilm formation intrinsic to the origin of life? *Environ. Microbiol.* 25, 26–39. doi: 10.1111/1462-2920.16179

Ryu, J. H., and Beuchat, L. R. (2005). Biofilm formation by *Escherichia coli* O157:H7 on stainless steel: effect of exopolysaccharide and Curli production on its resistance to chlorine. *Appl. Environ. Microbiol.* 71, 247–254. doi: 10.1128/AEM.71.1.247-254.2005

Salmon, K. A., Hung, S., Steffen, N. R., Krupp, R., Baldi, P., Hatfield, G. W., et al. (2005). Global gene expression profiling in *Escherichia coli* K12: effects of oxygen availability and ArcA. *J. Biol. Chem.* 280, 15084–15096. doi: 10.1074/jbc.M414030200

Sanchez, P., Moreno, E., and Martinez, J. L. (2005). The biocide triclosan selects Stenotrophomonas maltophilia mutants that overproduce the SmeDEF multidrug efflux pump. *Antimicrob. Agents Chemother.* 49, 781–782. doi: 10.1128/AAC.49.2.781-782.2005

Schellhorn, H. E. (2020). Function, evolution, and composition of the *rpoS* regulon in *escherichia coli*. *Front. Microbiol.* 11. doi: 10.3389/fmicb.2020.560099

Sindeldecker, D., and Stoodley, P. (2021). The many antibiotic resistance and tolerance strategies of Pseudomonas aeruginosa. *Biofilm* 3, 100056. doi: 10.1016/j.bioflm.2021.100056

Sonbol, F. I., El-Banna, T. E., Abd El-Aziz, A. A., and El-Ekhnawy, E. (2019). Impact of triclosan adaptation on membrane properties, efflux and antimicrobial resistance of *Escherichia coli* clinical isolates. *J. Appl. Microbiol.* 126, 730–739. doi: 10.1111/jam.14158

Soumet, C., Méheust, D., Pissavin, C., Le Grandois, P., Frémaux, B., Feurer, C., et al. (2016). Reduced susceptibilities to biocides and resistance to antibiotics in food-associated bacteria following exposure to quaternary ammonium compounds. *J. Appl. Microbiol.* 121, 1275–1281. doi: 10.1111/jam.13247

Sowlati-Hashjin, S., Carbone, P., and Karttunen, M. (2020). Insights into the polyhexamethylene biguanide (PHMB) mechanism of action on bacterial membrane and DNA: A molecular dynamics study. *J. Phys. Chem. B* 124, 4487–4497. doi: 10.1021/acs.jpcb.0c02609

Tag ElDein, M. A., Yassin, A. S., El-Tayeb, O., and Kashef, M. T. (2021). Chlorhexidine leads to the evolution of antibiotic-resistant Pseudomonas aeruginosa. *Eur. J. Clin. Microbiol. Infect. Dis.* 40, 2349–2361. doi: 10.1007/s10096-021-04292-5

Tkachenko, O., Shepard, J., Aris, V. M., Joy, A., Bello, A., Londono, I., et al. (2007). A triclosan-ciprofloxacin cross-resistant mutant strain of Staphylococcus aureus displays an alteration in the expression of several cell membrane structural and functional genes. *Res. Microbiol.* 158, 651–658. doi: 10.1016/j.resmic.2007.09.003

Uhlich, G. A., Cooke, P. H., and Solomon, E. B. (2006). Analyses of the red-dry-rough phenotype of an *Escherichia coli* O157:H7 strain and its role in biofilm formation and resistance to antibacterial agents. *Appl. Environ. Microbiol.* 72, 2564–2572. doi: 10.1128/AEM.72.4.2564-2572.2006

Uruén, C., Chopo-Escuin, G., Tommassen, J., Mainar-Jaime, R. C., and Arenas, J. (2020). Biofilms as promoters of bacterial antibiotic resistance and tolerance. *Antibiotics (Basel)* 10, 3. doi: 10.3390/antibiotics10010003

Usui, M., Yoshii, Y., Thiriet-Rupert, S., Ghigo, J.-M., and Beloin, C. (2023). Intermittent antibiotic treatment of bacterial biofilms favors the rapid evolution of resistance. *Commun. Biol.* 6, 275. doi: 10.1038/s42003-023-04601-y

Windels, E. M., Michiels, J. E., Fauvart, M., Wenseleers, T., Van den Bergh, B., and Michiels, J. (2019). Bacterial persistence promotes the evolution of antibiotic resistance by increasing survival and mutation rates. *ISME J.* 13, 1239–1251. doi: 10.1038/s41396-019-0344-9

World Health Organization. (2019). *Critically important antimicrobials for human medicine* (Geneva: World Health Organization). Available at: https://iris.who.int/handle/10665/312266 (Accessed November 10, 2023).

Yan, J., and Bassler, B. L. (2019). Surviving as a community: antibiotic tolerance and persistence in bacterial biofilms. *Cell Host Microbe* 26, 15–21. doi: 10.1016/j.chom.2019.06.002

Zhang, Y., Zhao, Y., Xu, C., Zhang, X., Li, J., Dong, G., et al. (2019). Chlorhexidine exposure of clinical Klebsiella pneumoniae strains leads to acquired resistance to this disinfectant and to colistin. *Int. J. Antimicrob. Agents* 53, 864–867. doi: 10.1016/j.ijantimicag.2019.02.012

Zhu, D. M., Li, Q.-H., Shen, Y., and Zhang, Q. (2020). Risk factors for quinolone-resistant *Escherichia coli* infection: a systematic review and meta-analysis. *Antimicrob. Resist. Infect. Control* 9, 11. doi: 10.1186/s13756-019-0675-3

2.2.2. Le PHMB induit des adaptations collectives en modulant la matrice

Des analyses supplémentaires ont été effectuées sur deux souches parentales, la souche de référence Ec1655 et la souche Ec223, afin de mieux comprendre comment ces souches s'adaptent collectivement et pour établir des liens entre l'apparition de variants et les modulations collectives de la population. Pour ce faire, l'expérience d'exposition des souches aux biocides (Figure 6) a été reproduite avec le PHMB, et les profils des biofilms de ces deux souches ont été observés chaque semaine au CLSM. Les biofilms ont été marqués avec du Syto9 permettant d'observer la totalité des cellules bactériennes, ainsi qu'avec de la ConA, une lectine se liant à l'α-D-Mannose et à l'α-D-Glucose, permettant de marquer certains polysaccharides présents dans la matrice des biofilms.
L'évolution effectuée a clairement confirmé la stimulation de la production de matrice en présence du biocide, manifestée de deux manières distinctes chez les deux souches. Pour la souche Ec1655 (Figure 9), une légère augmentation du biovolume de la ConA est observée quantitativement après exposition au PHMB, bien que les biovolumes soient déjà légèrement plus élevés avant exposition, en S0. En revanche, l'intensité de fluorescence de la ConA est largement supérieure après ajout de PHMB chez cette souche. Plusieurs hypothèses pourraient expliquer cette augmentation. Une densité plus élevée de matrice dans certaines régions du biofilm pourrait amplifier le signal fluorescent. La sécrétion spécifique de certains composés matriciels ayant une affinité plus forte pour la ConA pourrait également accroître le signal de la ConA (Goldstein et al., 1974). Il est cependant également possible que l'ajout de PHMB modifie les propriétés physico-chimiques du milieu, comme le pH, affectant ainsi le signal du fluorophore et donc que l'augmentation du signal ne soit pas causée par une augmentation de la matrice (Zand et al., 1971).
L'observation spatiale du marquage ConA en présence de PHMB montre que la matrice est augmentée dans les couches supérieures du biofilm, probablement pour se protéger du biocide, mais aussi dans les couches internes, où un « tapis » de matrice est formé à la surface du puit, en dessous des cellules. Ce phénomène pourrait être une conséquence indirecte de l'ajout de PHMB, les cellules stimulant leur production générale de polysaccharides, y compris ceux servant à l'adhésion (comme le poly-N-acétylglucosamine) et ceux composant la matrice des couches externes (comme la cellulose) (Beloin et al., 2008). Cette production accrue pourrait aussi permettre aux bactéries d'être totalement enchâssées dans la matrice, réduisant ainsi au maximum leur contact avec les molécules biocides. Ce confinement pourrait également limiter l'accès aux nutriments et à l'oxygène, créant des micro-environnements propices à l'émergence de variants résistants à la gentamicine de manière transitoire, en raison du ralentissement de la croissance des bactéries. Ici aussi, il n'est pas exclu que le « tapis » soit simplement causé par un artéfact lié au contact du PHMB avec le fond du puit.
L'observation du marquage ConA avec la souche Ec223 (Figure 10) démontre également une augmentation de la matrice, confirmée par la quantification et la comparaison des biovolumes. Toutefois, cette augmentation est limitée aux couches supérieures, sans formation du « tapis » observé avec Ec1655. L'intensité de fluorescence n'est également pas augmentée chez Ec223, ce qui suggère que l'augmentation de l'intensité de fluorescence chez Ec1655 est due à une modulation de la matrice chez cette souche plutôt qu'une interaction du PHMB avec le milieu. De même, l'absence du « tapis » chez Ec223 démontre que celui formé chez Ec1655 serait bien formé par la souche et pas par un artéfact lié au PHMB.

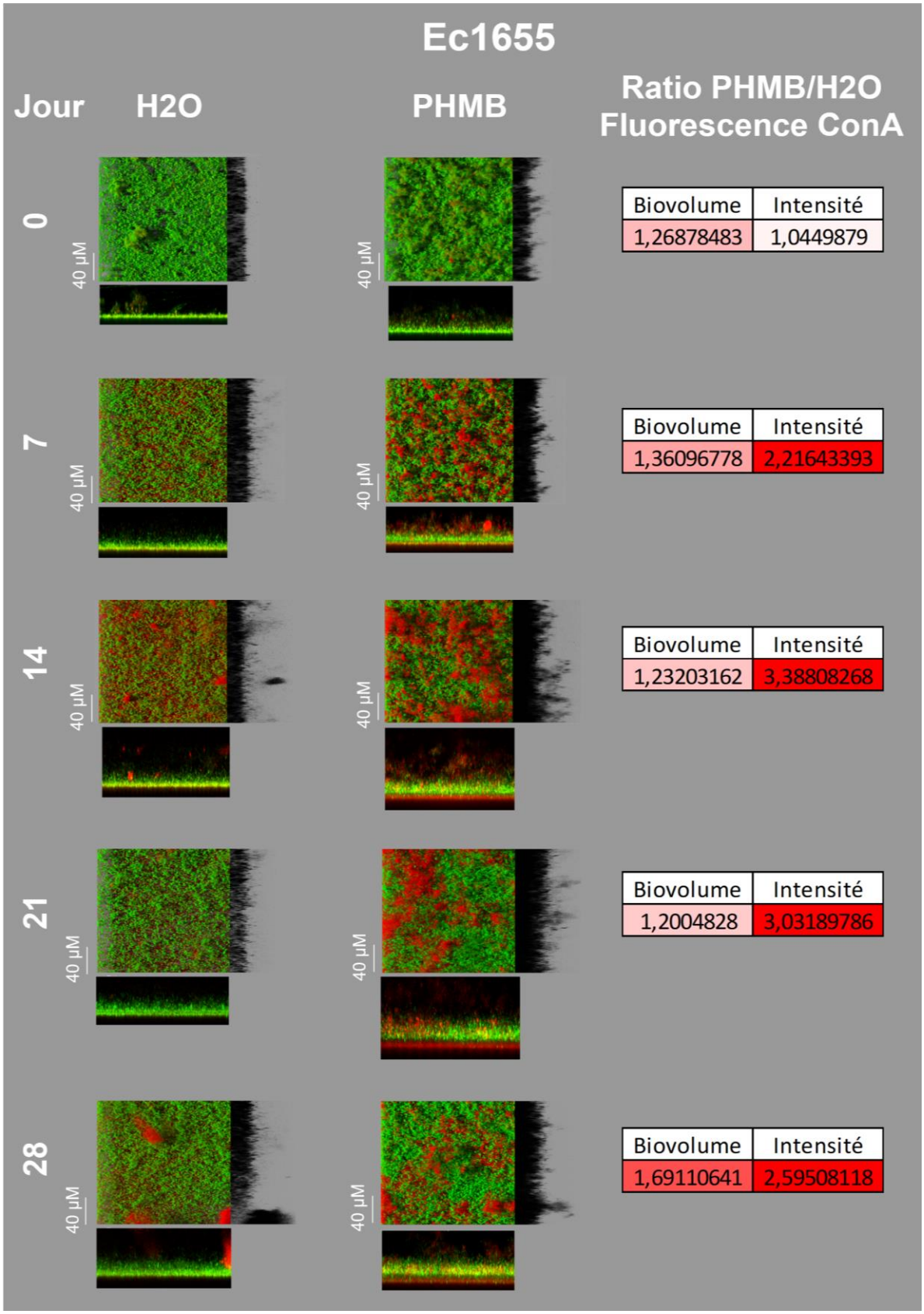

Figure 9 : Evolution du profil des biofilms de Ec1655 au CLSM, au fil de l'exposition au PHMB, avec le contrôle à l'H_2O à gauche et la condition PHMB à droite. Des ratios des biovolumes et de l'intensité de fluorescence de la ConA, en condition PHMB sur la condition H_2O, effectuées avec le logiciel Biofilm Q, ont également été ajoutés à droite.

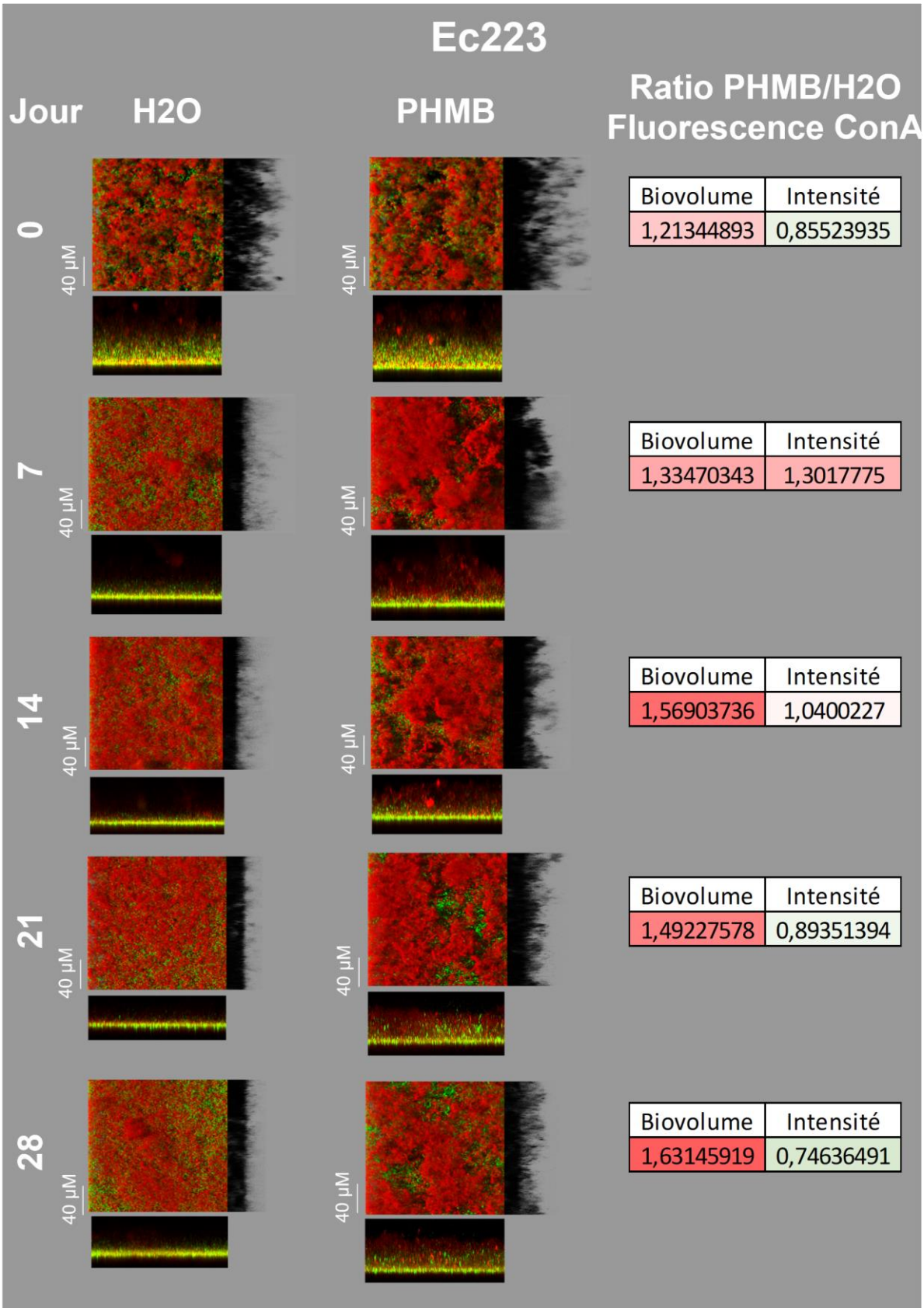

Figure 10 : Evolution du profil des biofilms de Ec223 au CLSM, au fil de l'exposition au PHMB, avec le contrôle à l'H_2O à gauche et la condition PHMB à droite. Des ratios des biovolumes et de l'intensité de fluorescence de la ConA, en condition PHMB sur la condition H_2O, effectuées avec le logiciel Biofilm Q, ont également été ajoutés à droite.

Une autre observation intéressante suite à l'ajout de PHMB chez les souches concerne la modification de la morphologie de la souche Ec1655 (Figure 11). En présence du biocide, la taille des bacilles de la souche Ec1655 a augmenté par rapport aux bactéries non exposées de la condition contrôle. Cette modification n'a pas été observée chez Ec223. La quantification de la taille des bactéries, effectuée à l'aide du logiciel ImageJ, sur un échantillon représentatif de cellules (20 bactéries aléatoires par image avec 3 images par semaine et par condition), a permis de préciser les variations de taille entre les conditions. Ainsi, les bactéries présentes dans la condition PHMB doublent de taille, par rapport à celles de la condition contrôle. Cette différence ne semble pas augmenter ou diminuer au fil des semaines mais rester stable de la semaine 1 à la semaine 4.
L'augmentation de la taille des cellules est une conséquence bien documentée de l'exposition aux antimicrobiens (Cylke et al., 2022). Selon la cible de l'antimicrobien, la morphologie de la cellule est différemment impactée. Les antibiotiques ciblant l'ADN et ceux ciblant la paroi cellulaire peuvent notamment induire des morphotypes plus allongés (Cylke et al., 2022). Certaines études ont montré que le PHMB pouvait avoir un effet sur l'ADN des cellules (Chindera et al., 2016; Sowlati-Hashjin et al., 2020), ce qui pourrait expliquer l'élongation du morphotype observé dans cette étude.

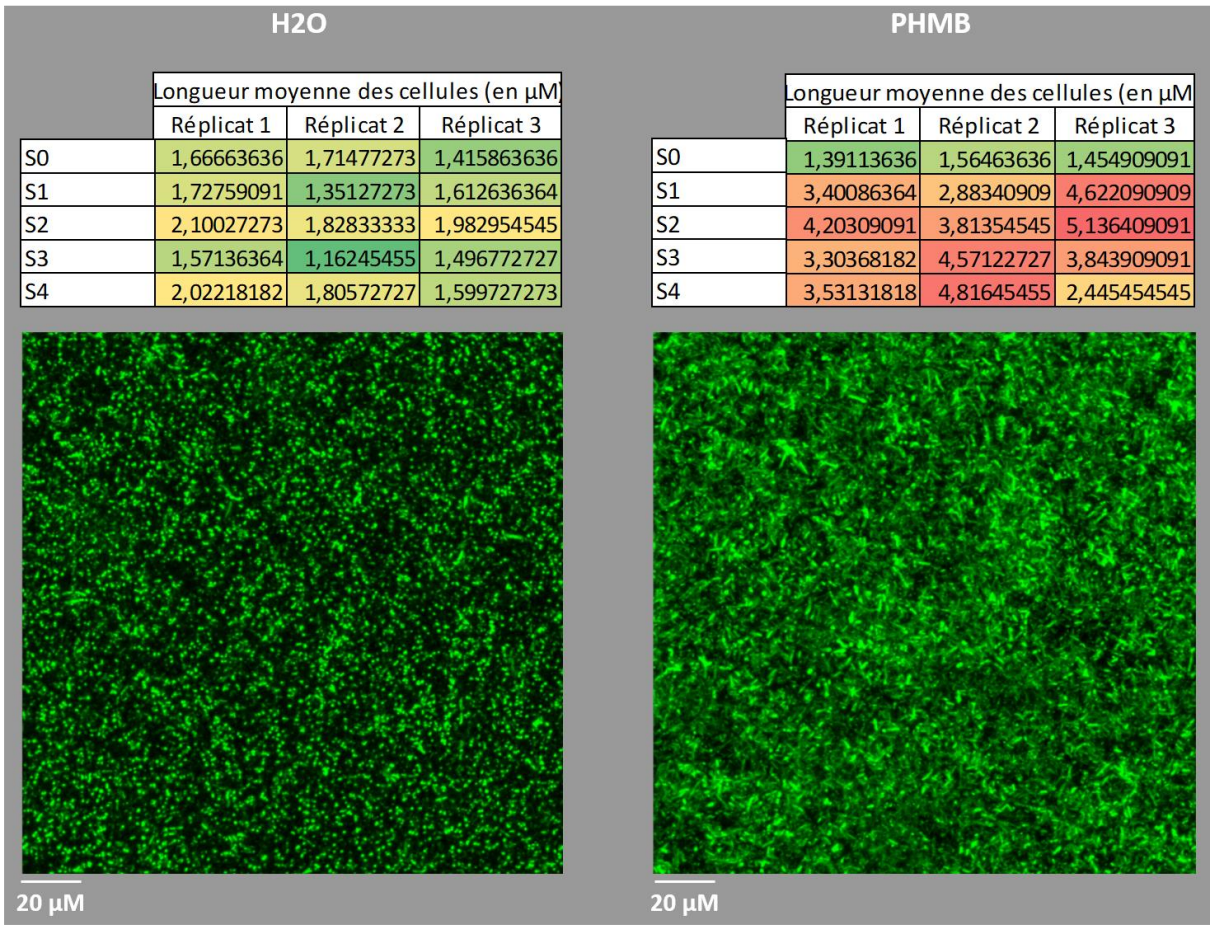

H2O

	Longueur moyenne des cellules (en µM)		
	Réplicat 1	Réplicat 2	Réplicat 3
S0	1,66663636	1,71477273	1,415863636
S1	1,72759091	1,35127273	1,612636364
S2	2,10027273	1,82833333	1,982954545
S3	1,57136364	1,16245455	1,496772727
S4	2,02218182	1,80572727	1,599727273

PHMB

	Longueur moyenne des cellules (en µM)		
	Réplicat 1	Réplicat 2	Réplicat 3
S0	1,39113636	1,56463636	1,454909091
S1	3,40086364	2,88340909	4,622090909
S2	4,20309091	3,81354545	5,136409091
S3	3,30368182	4,57122727	3,843909091
S4	3,53131818	4,81645455	2,445454545

Figure 11 : Représentation de la différenciation de la morphologie des cellules observées au CLSM chez Ec1655 en présence de PHMB comparé à la condition contrôle H_2O, avec des quantifications moyennes des longueurs cellulaires effectuées avec le logiciel ImageJ (moyenne de 20 longueurs mesurées aléatoirement pour chaque réplicat).

3. Article 6 : Le biofilm : une structure protectrice, favorisant l'émergence de variants aux résistances croisées

Cette deuxième partie se concentre sur les résultats obtenus avec le dernier antibiotique testé, la rifampicine, qui est également un antibiotique d'intérêt critique selon l'OMS, notamment pour le traitement d'infections à *Mycobacterium tuberculosis* (World Health Organization, 2019). Cet antibiotique fait partie de la famille des ansamycines et cible l'ARN polymérase, impliquée dans la transcription de l'ADN en ARN. Des rifamycines, telles que la rifaximine, sont utilisées dans le traitement de certaines infections à *E. coli*, notamment la diarrhée du voyageur (Steffen et al., 2018). L'intérêt de la rifampicine réside également dans son utilisation pour étudier l'évolution bactérienne, à travers leur taux de mutation (Majumdar et al., 2018). Dans ce travail de thèse, un lien entre la résistance à la rifampicine et l'exposition à deux biocides, le BAC et la TMN, a été identifié. Le BAC est l'un des biocides les plus étudiés pour son rôle dans l'induction de résistances croisées, tandis que la TMN, bien que largement utilisée dans diverses industries, reste très peu étudiée, notamment concernant ses effets sur les résistances aux antibiotiques. Ces deux biocides augmentaient significativement la proportion de variants RifR 20 mg/L dans les biofilms, comparativement à la condition H_2O, ce différentiel étant moins marqué dans les surnageants. Comme pour le terme GenR, RifR caractérise ici l'ensemble des variants ayant poussé sur les géloses, indépendamment de celles ayant des résistances stables et celles ayant des résistances transitoires. Des variants RifR 100 mg/L ont également été isolés, mais cette fois-ci sans aucune différence entre la condition H_2O et les conditions BAC et TMN. Les variants RifR présentaient généralement des résistances stables, dues à des mutations génétiques. L'analyse génomique de ces variants a révélé un nombre significatifs de mutations dans *rpoB*, la cible principale de la rifampicine (Alifano et al., 2015). Ces mutations étaient réparties de manière relativement équitable dans toutes les conditions, bien que légèrement moins fréquentes dans la condition TMN. Parmi les variants isolés à 100 mg/L de rifampicine, tous possédaient une mutation dans *rpoB*, indiquant que la mutation de ce gène est nécessaire pour des résistances élevées. Cependant, l'absence de différences quantitatives notables entre la condition H_2O et les conditions BAC et TMN, à la concentration 100 mg/L, ne nous a pas incité à poursuivre dans cette direction.

En revanche, de manière très intéressante, une récurrence des mutations survenant au sein de gènes codant pour la synthèse du lipopolysaccharide (LPS) a été observée parmi les variants de la condition TMN, avec 6 des 8 souches d'*E. coli* testées. L'analyse phénotypique de ces variants a révélé des différences structurelles dans le LPS en comparaison des souches parentales. Ces modifications du LPS engendraient une réduction du potentiel membranaire des variants résistants. Un potentiel membranaire plus faible peut améliorer la stabilité de la membrane, protégeant ainsi la cellule plus longtemps des biocides cationiques comme la TMN, qui peuvent déstabiliser la membrane en la dépolarisant, via leur charge positive (Halder et al., 2015). Des analyses supplémentaires ont révélé que ces variants possédaient principalement de faibles niveaux de résistance, à l'opposé des souches mutées dans *rpoB*. Cependant, plus une résistance est forte, plus les effets secondaires délétères sur la cellule peuvent limiter sa compétitivité. Ici, les variants LPS n'étaient pas impactés négativement par leur mutation. En présence de biocide, certains variants affichaient même un avantage, avec une phase de latence réduite avant d'atteindre la phase exponentielle de croissance, en comparaison de la souche parentale d'origine. En biofilms, les variants semblaient tous produire davantage de composés de la matrice et surpassaient parfois leur souche parentale dans des biofilms mixtes, témoignant de leur compétitivité et des risques de propagation associés.

« Pivotal role of lipopolysaccharide modulation in biofilm adaptation to triamine biocide and antibiotic cross-resistance »,

Raphaël Charron, Pierre Lemée, Paméla Houée, Patricia Le Grandois, Marine Boulanger, Antoine Huguet, Thibaut Léger, Christophe Soumet, Romain Briandet, Arnaud Bridier

Pivotal role of lipopolysaccharide modulation in biofilm adaptation to triamine biocide and antibiotic cross-resistance

Raphaël Charron[1,2], Pierre Lemée[1], Paméla Houée[1], Patricia Le Grandois[1], Marine Boulanger[1], Antoine Huguet[1], Thibaut Léger[3], Christophe Soumet[1], Romain Briandet[2], Arnaud Bridier[1*]

[1]*Antibiotics, Biocides, Residues and Resistance Unit, Fougères Laboratory, ANSES, 35300 Fougères, France*
[2]*Paris-Saclay University, INRAE, AgroParisTech, Micalis Institute, 78350, Jouy-en-Josas, France*
[3]*Toxicology of Contaminants Unit, Fougères Laboratory, ANSES, 35300 Fougères, France*
*corresponding author: arnaud.bridier@anses.fr

Abstract:
It is essential to identify the factors that drive the selection of antimicrobial resistance (AMR) so as to better control the emergence of resistance. Disinfectant biocides, massively used in food-processing industries, have already been associated with the cross-selection of antibiotic-resistant bacterial populations. However, very few studies have addressed this topic using a biofilm model, known to be the main lifestyle of bacteria in the food industry. We examined the adaptation of *Escherichia coli* biofilms to four biocides over one month, along with subsequent effects on antibiotic resistance. Exposure to N-(3-aminopropyl)-N-dodecylpropane-1,3-diamine (Triamine, TMN) and benzalkonium chloride (BAC) led to a significant increase in rifampicin-resistant (RifR) variants in biofilms compared with exposure to H_2O. Genomic analyses revealed that the RifR variants that emerged when exposed to TMN recurrently harboured mutations in genes related to lipopolysaccharide (LPS) biosynthesis. Resulting alterations in membrane potential and cell permeability were correlated with enhanced bacterial survival under antimicrobial stress. These findings suggested that LPS plays a central role in adaptation to TMN and subsequent rifampicin cross-resistance development. Additionally, LPS modifications also gave RifR variants competitive advantages over parental strains when exposed to TMN at both individual and collective biofilm level, supporting the likelihood of a higher risk of resistant variants being disseminated throughout the food chain.

Keywords: biofilm, adaptation, cross-resistance, biocides, antimicrobial resistance, LPS

Introduction:

Antimicrobial resistance (AMR) is one of the foremost challenges for public health in the coming decades. Recent years have seen a marked increase in antibiotic resistance among bacteria, including the emergence of multidrug-resistant strains that complicate therapeutic strategies[1]. Although natural resistance mechanisms have existed within bacterial communities for centuries, often deriving from natural substances produced by microorganisms, the selection of resistant clones has been accelerated not only by the use or misuse of antibiotics but also by other factors directly or indirectly related to human activities. The One Health concept further underscores the need for a multisectoral approach to tackle AMR, emphasising the interconnection of human, animal, and environmental health as a continuum in the propagation of resistance determinants[2] .Increasingly, attention is being paid to co-selectants, i.e. non-antibiotic agents, especially in light of recent studies[3]. Among these co-selectants, chemical disinfectants — a subclass of biocides — has been receiving more and more attention, especially since the COVID crisis[4]. Disinfectants are used massively in a wide variety of sectors, including the food industry, where they safeguard consumers from pathogenic bacteria. Disinfectant biocides differ from antibiotics by their use on inanimate surfaces, but can share similar cellular targets and related modes of action. A large number of publications have hence shown that bacteria often use the same mechanisms to adapt to both biocides and antibiotics[5,6]. However, the amount of knowledge available on the different biocide families differs greatly. Some of them have already been extensively studied[5], such as quaternary ammonium compounds (QACs) or chlorhexidine, and have been recurrently found to affect antibiotic resistance. Nevertheless, the effects of the vast majority of biocidal active substances have barely been characterised, despite their frequent use. N-(3-aminopropyl)-N-dodecylpropane-1,3-diamine (TMN) for example, is a biocidal active substance increasingly used in food-processing industries, particularly in an admixture with QACs or as an alternative[7]. Nevertheless, we need further insights into TMN modes of action and possible effects on antimicrobial (cross-)resistance.

Moreover, while current data predominantly focus on planktonic bacteria, most of the bacterial populations in food-processing environments exist within biofilms. Biofilms are three-dimensional structures that bacteria form on surfaces through the production of an extracellular matrix composed mostly of polysaccharides, lipids, proteins and extracellular DNA[8]. The 3D structuration of biofilms generates a variety of microenvironments, resulting in broad heterogeneity of metabolic states for embedded bacterial populations. The diffusion of molecules in the structure may be reduced, leading to oxygen and nutrient gradients. While bacteria around the periphery of the biofilms have access to every nutrient they need, bacteria in the centre do not. This heterogeneity has a strong effect on bacterial metabolism, with internal subpopulations often exhibiting slow growth and persister phenotypes. Such a collective and organised lifestyle generally enhances bacterial tolerance to environmental stresses, including disinfectant biocides, through both a physical barrier effect and by inducing physiological heterogeneity and resistant phenotypes[5,9]. Recently, we showed that modulation of the biofilm structure following exposure to a biguanide substance could promote the emergence of adaptive (physiological) cross-resistance to aminoglycoside[10].Biofilms are therefore dynamic edifices that evolve in response to internal and external signals, potentially influencing evolution towards antibiotic resistance[11]. These biological structures may not only enhance bacterial survival but could also facilitate the emergence of stable genetic resistance through mutational events, as already reported [5,12,13]. Additionally, the extracellular matrix has been shown to limit the penetration of biocides into the structure, as already reported for quaternary ammonium compounds[14]. Such an effect increases the possibility for bacteria to be exposed to sub-lethal doses, leading to variability in microenvironmental conditions between cells, which is a feature that cannot be observed in

planktonic populations, where biocide and bacteria are more homogeneously distributed and exposed. These factors collectively shape biofilms into unique ecosystems that could play a specific role in bacterial adaptation strategies and cross-resistance phenomenon. In this work, we investigate the effects of bacterial adaptation to biocidal molecules used in the food chain on the selection of rifampicin resistance, integrating the biofilm lifestyle through adaptive laboratory evolution.

Results:

1. **Exposure to TMN or BAC promotes the emergence of rifampicin-resistant (RifR) variants in biofilms**

The biofilms of eight *E. coli* strains were repeatedly exposed over one month to four biocidal active substances including BAC, TMN, sodium hypochlorite (SHY) and polyhexamethylene biguanide (PHMB) belonging to different families, at minimal concentrations determined to inhibit the growth of planktonic bacteria (MIC). Depending on the biocides, different effects on RifR variant emergence were observed (Figs. 1 and S1). Interestingly, TMN exposure consistently stimulated the emergence of RifR variants in biofilm with an increase in RifR variant quantity in seven out of the eight *E. coli* strains compared with the H_2O control (Fig. 1A). BAC exposure was also correlated with the selection of RifR variants in biofilms formed by five out of the eight strains for at least one time point during the exposure period. Conversely, exposure to PHMB and SHY did not significantly promote the emergence of resistance and even sometimes resulted in a decrease in the quantity of RifR variants isolated compared with the H_2O control (Fig. S1). It should be noted that three out of the eight strains (Ec1655, Ec223 and Ec956) were completely eradicated by the planktonic MIC of SHY after seven days of exposure, demonstrating that the biofilm's lifestyle did not result in higher cell survival with this biocide compared with the planktonic state. This also explains the small number of RifR variants isolated for SHY. The dynamics of RifR variant emergence varied greatly depending on the *E. coli* strain over the one-month exposure to biocides. In the Ec1655 strain exposed to TMN, RifR variants were selected quickly, reaching the maximal concentration of countable resistant clones after one week of exposure. Ec956 reacted differently, starting with many RifR variants from t0, but the effect of the biocides was reflected as a smaller decrease in variants over the exposure period compared with the H_2O control group. The effect of TMN was also more pronounced on some strains, such as Ec1655, Ec723 or Ec956, which displayed a significant difference in the number of RifR variants isolated compared with the H_2O control group throughout the experiment. In contrast, other strains like Ec775, Ec478 or Ec223 only showed differences at certain time points. Interestingly, the general effect of TMN and BAC on RifR variant emergence highlighted in biofilms was not observable when analysing supernatant populations, suggesting a specific adaptive response of biofilms to biocides (Fig. 1B). In three out of the eight strains (Ec223, Ec009, Ec478), neither BAC nor TMN exposure had any significant effect on RifR variant counts in supernatants compared with the H_2O control. Only Ec956 showed a significant and lasting increase in RifR variants in supernatants over the first two weeks of exposure to TMN compared with H_2O.

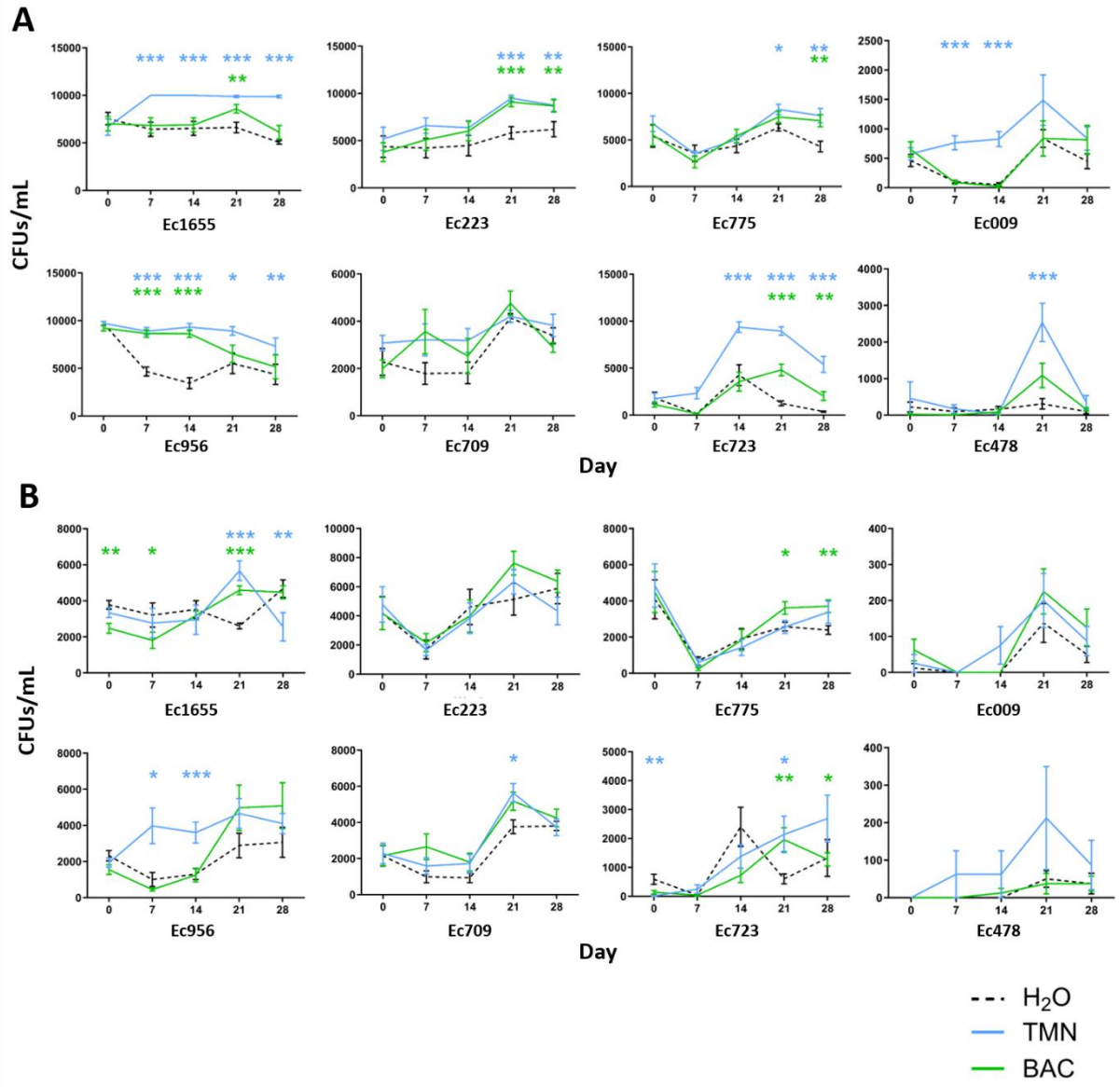

Figure 1. Effects of TMN and BAC on the quantity of RifR variants in E. coli biofilms. *Evolution curves representing the number of CFUs/mL of rifampicin-resistant variants enumerated on TSA plates supplemented with 20 mg/L of rifampicin and collected from biofilms (A) or supernatants (B) exposed to H_2O (dashed lines), BAC (in green) or TMN (in blue). Error bars represent the standard error of the mean. Statistical analysis was performed using a Mann-Whitney test for the biocide condition and the H_2O condition, separately, for each week. P-values are represented as follows:* * = [0.05-0.01]; ** =]0.01-0.001]; *** = <0.001

2. Adaptation to TMN and resistance to rifampicin are mainly mediated through alteration of LPS biosynthesis genes in variants

Illumina sequencing was performed and the genomes of RifR variants were analysed and compared with their corresponding parental strains to identify mutations underlying the adaptation and resistance phenotypes. Detailed information about the genetic modifications identified is presented in Table S1. Figure 2 displays the genetic targets carrying point mutations in RifR variants isolated from H_2O, TMN or BAC conditions, classified by their level of resistance to rifampicin (in mg/L). The most prevalently mutated gene was *rpoB*,

encoding the DNA-dependent RNA polymerase β-subunit, known as the primary target of rifampicin. However, the proportions of mutations in *rpoB* varied with each biocide. Among RifR variants selected after exposure to TMN, only 54% exhibited a mutation in *rpoB*, while this percentage reached 67% with H_2O. Although BAC has already been associated with *rpoB* mutations[15], it did not show a higher correlation in this study, with 65% of BAC-selected variants having *rpoB* mutations. Other mutations were observed in different global stress responses. The general stress response was impacted, with mutations in *rpoS*[16] and in *hfq*, a chaperone protein known to have a post-transcriptional effect on *rpoS*[17]. These mutations were not, however, clearly associated with exposure to a specific biocide, and some were also linked to *rpoB* mutations. Three variants exclusively from the BAC condition were mutated in genes relating to the stringent response (*dksA*[18]; *gppA*[19]), a stress response activated under nutrient depletion, which is consistent with the conditions within biofilms. Mutations were also recurrently observed in the rbs operon, involved in D-ribose transport and catabolism, and more specifically in *rbsR*, the repressor of the ribose operon[20]. This genetic target seemed particularly associated with the BAC condition, as four of the five *rbsR* variants emerged under BAC exposure and only one in the control condition (H_2O). Importantly, four of the five *rbsR* variants also carried a mutation in *rpoB*.

Interestingly, seven RifR variants from the TMN condition, originating from six different parental strains, had mutations in the LPS biosynthesis pathway, demonstrating a recurrent association between TMN exposure, RifR emergence, and adaptive modifications in this cellular target. Variants with mutations in LPS biosynthesis genes mostly carried single mutations compared with their parental strains. Only one of them (Ec723_TMN_2) had an additional mutation in *barA*, a gene encoding a sensor kinase involved in the regulation of several processes, including biofilm formation[21], and none had *rpoB* mutations. Mutations in LPS biosynthesis genes were mainly related to low levels of rifampicin resistance, in contrast to the stronger resistances observed in *rpoB*-mutated strains as shown in Figure 2. Beside the variants originating from the TMN condition, mutations in LPS biosynthesis genes were identified in only one variant isolated under the H_2O condition (Ec723_H_2O_1) and one under BAC conditions (Ec956_BAC_1), both in the *waaU* gene, which was also mutated once in the TMN condition in an Ec723_TMN_2 variant. This gene encodes a putative heptosyltransferase[22]. Mutations in the *rfbB* gene, encoding a dTDP-glucose 4,6-dehydratase 1 involved in rhamnose biosynthesis[23] was observed in two strains isolated after exposure to TMN (Ec223_TMN_5 and Ec775_TMN_5). Other LPS biosynthesis variants isolated under TMN conditions had mutations in genes such as *yfdI* (Ec1655_TMN_2), a glucosyltransferase[24], *wbbK* (Ec223_TMN_1) and *htrL* (Ec478_TMN_3)[25], both putative glycosyltransferases[26] and *wbbL* (Ec009_TMN_4) encoding a rhamnosyltransferase[27].

Major genomic modifications were also observed in three of the seven LPS biosynthesis variants selected under TMN conditions (Ec223_TMN_5, Ec775_TMN_5 and Ec723_TMN_2), often resulting from the genomic plasticity associated with mobile genetic elements (MGEs) (Table S1). In the Ec223_TMN_5 and Ec723_TMN_2 variants, these modifications corresponded to phage excisions. The analysis of Ec775_TMN_5 revealed that the MGEs in this strain were mostly related to transposon excisions. MGEs were found in many strains: 41% of TMN variants, 29% of BAC variants and 33% of H_2O variants. Some strains, like Ec723 and Ec956, displayed high genome plasticity, with more than 10 identified MGEs. Nevertheless, no correlation was observed between MGE excision and the conditions under which the variants were isolated.

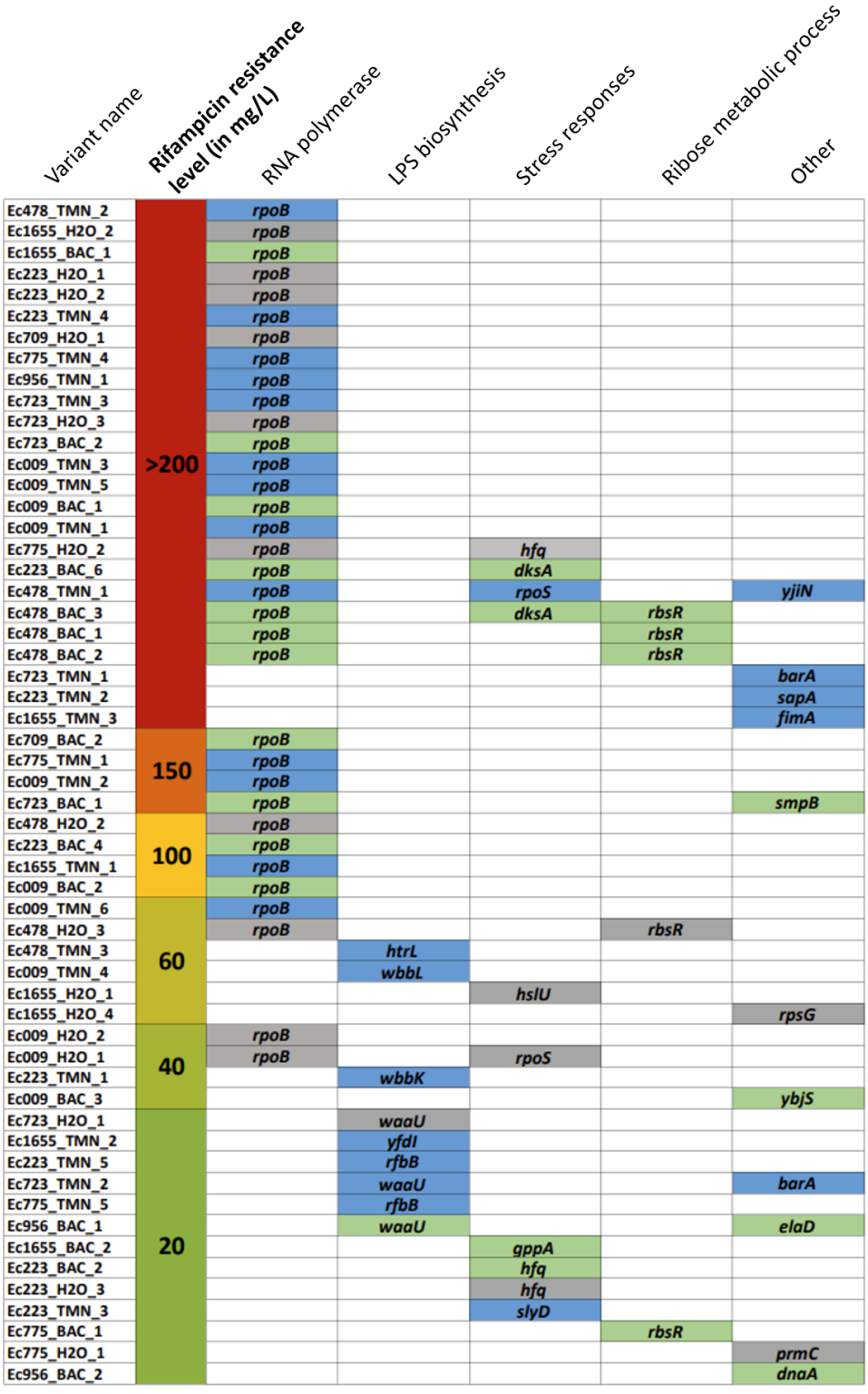

Variant name	Rifampicin resistance level (in mg/L)	RNA polymerase	LPS biosynthesis	Stress responses	Ribose metabolic process	Other
Ec478_TMN_2	>200	*rpoB*				
Ec1655_H2O_2		*rpoB*				
Ec1655_BAC_1		*rpoB*				
Ec223_H2O_1		*rpoB*				
Ec223_H2O_2		*rpoB*				
Ec223_TMN_4		*rpoB*				
Ec709_H2O_1		*rpoB*				
Ec775_TMN_4		*rpoB*				
Ec956_TMN_1		*rpoB*				
Ec723_TMN_3		*rpoB*				
Ec723_H2O_3		*rpoB*				
Ec723_BAC_2		*rpoB*				
Ec009_TMN_3		*rpoB*				
Ec009_TMN_5		*rpoB*				
Ec009_BAC_1		*rpoB*				
Ec009_TMN_1		*rpoB*				
Ec775_H2O_2		*rpoB*		*hfq*		
Ec223_BAC_6		*rpoB*		*dksA*		
Ec478_TMN_1		*rpoB*		*rpoS*		*yjiN*
Ec478_BAC_3		*rpoB*		*dksA*	*rbsR*	
Ec478_BAC_1		*rpoB*			*rbsR*	
Ec478_BAC_2		*rpoB*			*rbsR*	
Ec723_TMN_1						*barA*
Ec223_TMN_2						*sapA*
Ec1655_TMN_3						*fimA*
Ec709_BAC_2	150	*rpoB*				
Ec775_TMN_1		*rpoB*				
Ec009_TMN_2		*rpoB*				
Ec723_BAC_1		*rpoB*				*smpB*
Ec478_H2O_2	100	*rpoB*				
Ec223_BAC_4		*rpoB*				
Ec1655_TMN_1		*rpoB*				
Ec009_BAC_2		*rpoB*				
Ec009_TMN_6	60	*rpoB*				
Ec478_H2O_3		*rpoB*			*rbsR*	
Ec478_TMN_3			*htrL*			
Ec009_TMN_4			*wbbL*			
Ec1655_H2O_1				*hslU*		
Ec1655_H2O_4						*rpsG*
Ec009_H2O_2	40	*rpoB*				
Ec009_H2O_1		*rpoB*		*rpoS*		
Ec223_TMN_1			*wbbK*			
Ec009_BAC_3						*ybjS*
Ec723_H2O_1	20		*waaU*			
Ec1655_TMN_2			*yfdI*			
Ec223_TMN_5			*rfbB*			
Ec723_TMN_2			*waaU*			*barA*
Ec775_TMN_5			*rfbB*			
Ec956_BAC_1			*waaU*			*elaD*
Ec1655_BAC_2				*gppA*		
Ec223_BAC_2				*hfq*		
Ec223_H2O_3				*hfq*		
Ec223_TMN_3				*slyD*		
Ec775_BAC_1					*rbsR*	
Ec775_H2O_1						*prmC*
Ec956_BAC_2						*dnaA*

Figure 2. TMN selects for LPS-mediated variants with low-level rifampicin resistance. *Table representing the median level of rifampicin resistance in mg/L for every variant with its associated mutated genetic targets. The grey-coloured genes are mutated in strains isolated in the H_2O condition, the green ones are mutated in strains isolated in the BAC condition and the blue ones are mutated in strains isolated in the TMN condition*

3. LPS biosynthesis variants selected following TMN exposure displayed a lower membrane zeta potential and reduced cellular permeability

The specific association between TMN and LPS biosynthesis genes in RifR variants prompted us to further characterise the seven corresponding variants. Firstly, an SDS-PAGE analysis of the variants' LPS was performed to observe how the LPS structure was impacted by the mutations (Fig. 3A). Most of the variants exhibited pronounced perturbations in LPS structure, with clear differences in their band profiles compared with their corresponding parental strains (red boxes). Five out of the seven variants showed modifications indicated by the disappearance of bands between 10 kDa and 15 kDa. These variants also had modified profiles in the heavier bands, between 20 kDa and 35 kDa, with either reduced intensity or the disappearance of some bands. Conversely, the last two variants — Ec1655_TMN_2 and Ec009_TMN_4 — did not show a marked difference in LPS profiles compared with their parental strain after SDS-PAGE. It should be noted that the Ec1655 parental profile is already lighter than the other parental strains because the strain is known to have a transposon insertion in one LPS biosynthesis gene, leading to an O-antigen production defect, which explains the lack of bands above 15 kDa.

Given the negative charge carried by LPS molecules[28], we investigated whether the mutations impacted the membrane potential. A zeta potential analysis was performed on the variants and their parental cells to compare global membrane charge (Fig. 3B). Interestingly, four out of the seven variants were significantly different from their parental strain, with a more negative potential than their parents. The most notable difference was observed for the Ec223_TMN_1 variant, with a reduction from -19.6 mV (SD ± 0.70) in the parental strain to -24 mV (SD ± 1.30) in the variant. The two variants that did not reveal apparent LPS structural changes on gel (Ec1655_TMN_2 and Ec009_TMN_4) consistently did not exhibit zeta potential modifications either. Interestingly, these strains also displayed the most negative membrane potential among all the strains. Conversely, the Ec223_TMN_5 variant was the only strain that showed LPS structural modifications on the gel without also showing a modification in the membrane charge.

The negative charge of the LPS is known to help maintain cell structure through interactions with divalent cations of the LPS molecules[29]. Hence, a Crystal Violet permeability assay was performed with the seven LPS biosynthesis variants (Fig. 3C) to evaluate the impact of LPS modifications on cellular membrane permeability. Significant differences were observed in five out of the seven strains compared with their parental strains, showing significantly reduced cell membrane permeability. Particularly strong differences were observed for both variants of the Ec223 strain and the Ec478_TMN_3 variant. The only two variants that did not show any changes in permeability were again the Ec1655_TMN_2 and Ec009_TMN_4 variants, reinforcing the link between LPS structural changes, zeta potential and cell permeability.

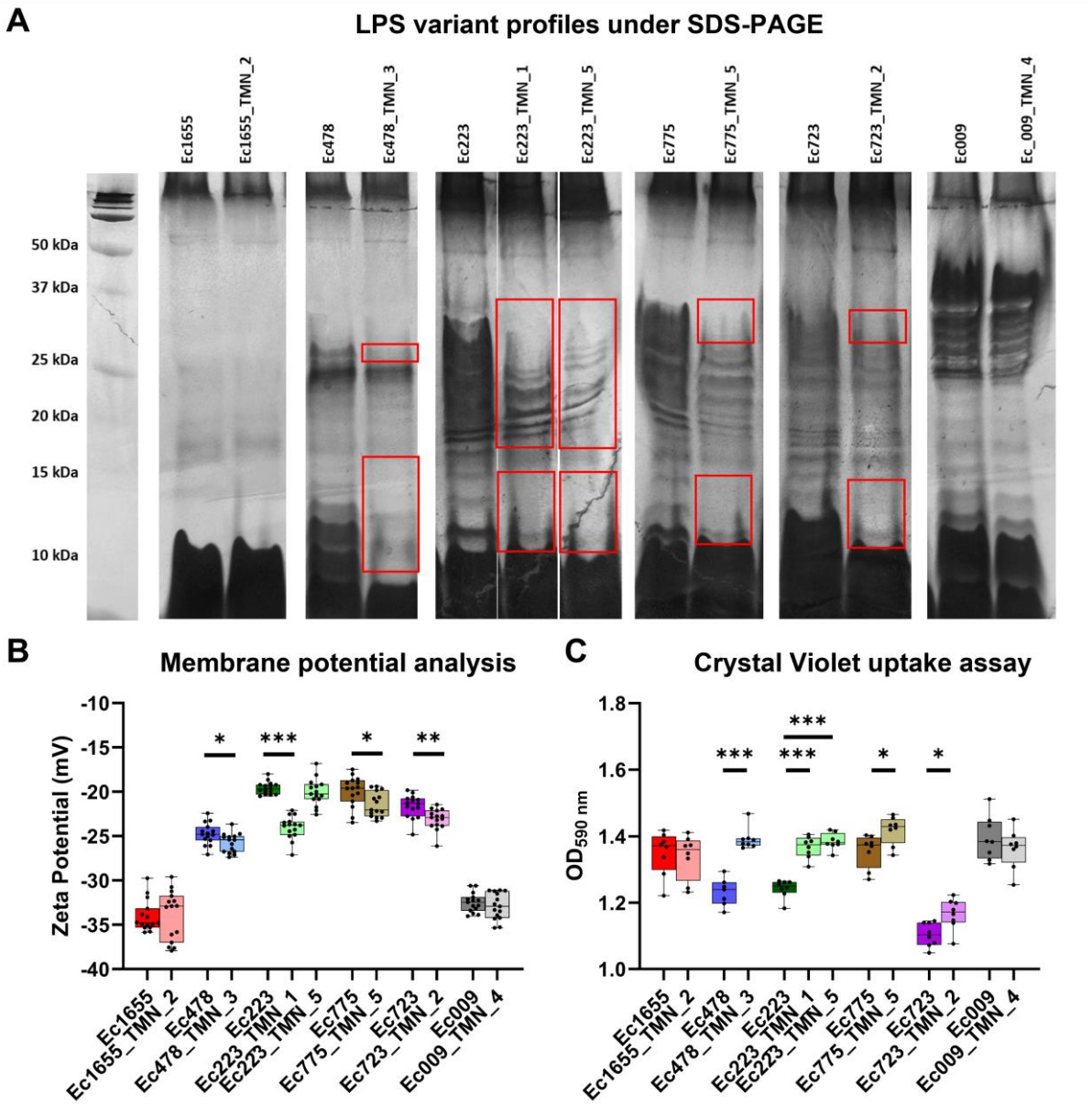

Figure 3. LPS biosynthesis variants have a lower membrane potential, which reduces global cell permeability. *SDS-PAGE representing the LPS profile of the parental strains and variants (A)* (red boxes show the difference between parents and variants)*; Membrane potential analysis of the LPS biosynthesis variants and their parental strains (B); Crystal Violet uptake assay of the LPS biosynthesis variants and their parental strains to assess their permeability (C). Statistical analysis was performed with a Mann-Whitney test comparing variants with their parental strains. P-values are represented as follows: * = [0.05-0.01]; ** =]0.01-0.001]; *** = <0.001. The P-values of the co-culture comparisons are shown in Figure S3*

4. Specific antibiotic susceptibility profiles of the LPS biosynthesis variants

Further analysis was performed on the LPS biosynthesis variants to precisely determine their level of resistance against antibiotics. First, their growth with or without rifampicin (5 mg/L) was analysed. Growth ratios are represented in Figures 4A and 4B, comparing their µmax and lag phases, respectively. Raw data and statistical analysis results can be seen in Figure S2.

Without rifampicin, parental strains and variants had similar growth rates and lag phase durations, except for Ec775_TMN_5 which grew faster and had a shorter lag phase than its parental strain. This demonstrates that LPS biosynthesis mutations did not impact the growth capacities of variants. Most of the variants showed a clear difference in their growth and their lag phase duration with rifampicin. Four out of the seven variants (Ec478_TMN_3; Ec223_TMN_1; Ec223_TMN_5; Ec009_TMN_4) showed marked differences from their parental strain, with faster growth and a reduced lag phase when exposed to 5 mg/L of rifampicin. Conversely, Ec1655_TMN_2 showed small variations and Ec775_TMN_5 and Ec723_TMN_2, despite the modifications in structural and cell properties previously observed, did not show better growth ability with rifampicin. However, their isolation on rifampicin-supplemented plates demonstrates that these variants are still able to grow when exposed to lethal concentrations of the antibiotic, suggesting that their resistance mechanism may be condition-specific.

Given that the resistance mechanism linked to cell permeability is often nonspecific, further analysis was conducted with 14 other antibiotics using the microdilution broth method to assess the global effect of LPS alteration in variants on antibiotic susceptibility profiles (Fig. 4C). Interestingly, a recurrent MIC modification was observed for the macrolide azithromycin in six out of seven variants with a modified phenotype. The five variants that showed structural LPS modifications displayed a two-fold MIC increase to azithromycin, while Ec009_TMN_4 exhibited a two-fold decrease. Both Ec223 variants showed two-fold MIC increases to chloramphenicol, ciprofloxacin (also observed for Ec478_TMN_3), tetracycline and also trimethoprim for Ec223_TMN_1 only.

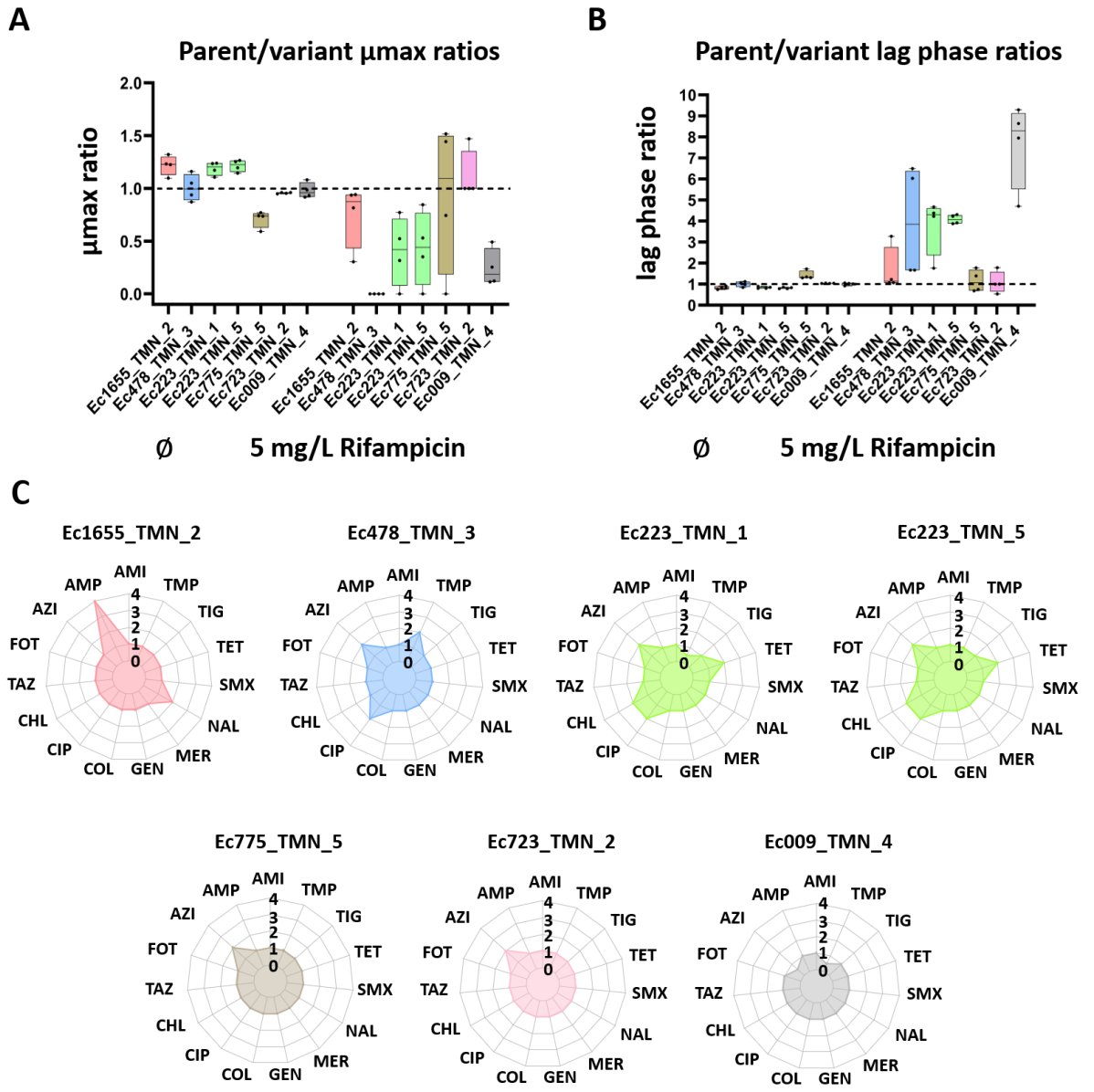

Figure 4. Antibiotic susceptibility modulations in LPS biosynthesis variants. *Ratios between the µmax (A) and lag phases (B) of the parental strains/variants with or without rifampicin (5 mg/L). MIC fold change between the variants and their parental strain for 15 antibiotics representative of the different families with a clinical interest for E. coli (AMI = Amikacin; AMP = Ampicillin; AZI = Azithromycin; FOT = Cefotaxime; TAZ = Ceftazidime; CHL = Chloramphenicol; CIP = Ciprofloxacin; COL = Colistin; GEN = Gentamicin; MER = Meropenem; NAL = Nalidixic Acid; SMX = Sulfamethoxazole; TET = Tetracycline; TIG = Tigecycline; TMP = Trimethoprim) (C). Statistical analysis was performed with a Mann-Whitney test comparing the variants and their parental strains. P-values are represented as follows: * = [0.05-0.01]; ** =]0.01-0.001]; *** = <0.001. The P-values of the co-culture comparisons are shown in Figure S2*

5. Competitive advantages of LPS variants exposed to TMN at individual and collective levels

The growth parameters of variants exposed to TMN were compared with those of their corresponding parental strains. Some variants appeared more adapted in planktonic conditions

(Fig. 5). Sub-lethal concentrations of TMN had no significant effects on their growth compared with their parental strains (Fig. 5A), except Ec223_TMN_5 which had a slightly faster growth rate. Three variants (Ec478_TMN_3, Ec223_TMN_5, Ec775_TMN_5) were able to leave the lag phase and enter the exponential growth phase faster than their parental strain (Fig. 5B), indicating an increased ability to grow when exposed to the biocide. Despite their previously observed structural modifications, Ec223_TMN_1, Ec723_TMN_2, Ec1655_TMN_2 and Ec009_TMN_4 variants did not show significant changes in their lag phases compared with their parental strains.

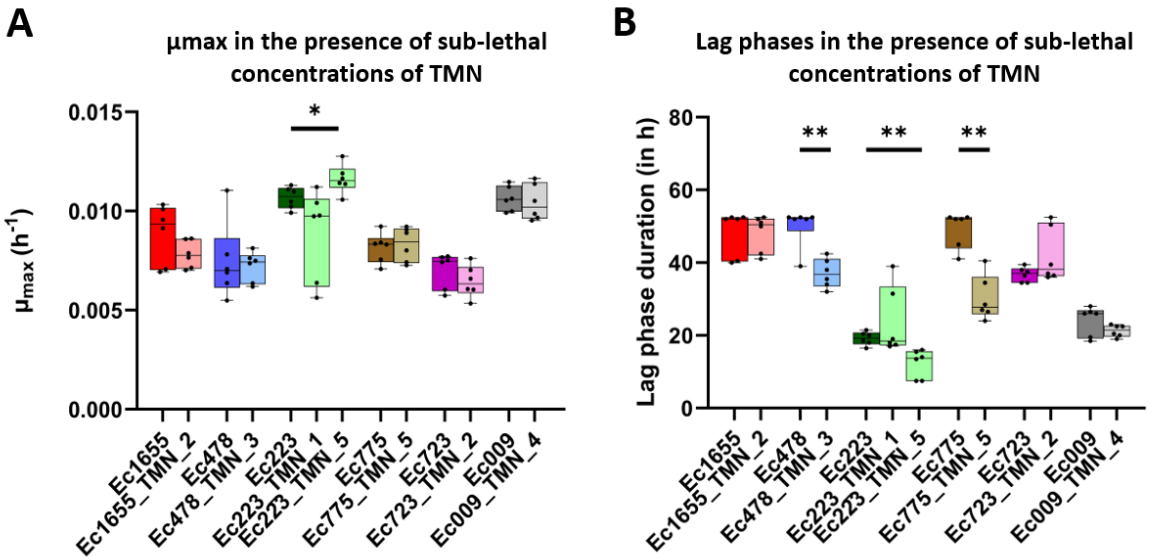

Figure 5. LPS biosynthesis variants show facilitated growth when exposed to TMN*. µmax (A) and Lag phases (B) of the LPS biosynthesis variants and their parental strains in planktonic condition with 2.2 mg/L of TMN. Statistical analysis was performed with a Mann-Whitney test comparing the variants and their parental strains. P-values are represented as follows: * = [0.05-0.01]; ** =]0.01-0.001]; *** = <0.001.*

To understand the mechanism of adaptation linked to the biofilm lifestyle, the variants' ability to produce matrix components was investigated. A Congo Red assay was performed on the variants to observe their matrix production (cellulose and amyloid fibres) (Fig. 6). All variants showed an increased production of matrix components without TMN, except Ec1655_TMN_2. The Ec223_TMN_1 strain was the one that induced biofilm growth the most. When exposed to TMN, most variants still showed increased matrix production, but Ec478_TMN_3 did not show significant differences compared with its parental strain under these conditions. To determine whether this increased ability to form biofilms impacted the competitiveness of the strains in biofilms, strains were transformed with a GFP plasmid and an mCherry plasmid (except for Ec723 and Ec723_TMN_2 due to transforming issues). Co-cultures of parental strains and variants were performed to assess which strain had a competitive advantage with or without the biocide. Co-cultures were conducted both ways: one with the parental strain tagged with GFP and variants with mCherry (Fig. 6) and the other vice versa (Fig. S3). The results of the statistical analyses of the differences observed between parental strains and variants are presented in Figure S4. Stability tests were performed to observe whether the variants maintained the plasmid in the absence of antibiotic selective pressure (Fig. S5) and other tests were performed to ensure the plasmid did not impact the strain's growth (Fig. S6). Most strains exhibited stable fluorescence, except for Ec1655 and its variant, which showed a slight reduction in fluorescence (Fig. S5). The Ec1655_TMN_2 variant also seemed slightly impacted in its growth with the plasmid (Fig. S6). Generally,

GFP had a weaker signal than mCherry across most strains, but the trends were observed in both conditions. Variants showed differential and interesting phenotypes. The Ec478_TMN_3 variant showed increased abundance compared with the parental strain with or without the biocide, with more pronounced differences with the biocide, as observed through the analysis of biovolumes and biofilm images (Fig. 6). The Ec1655_TMN_2 variant was the only other strain to have increased biofilm compared with its parental strain with the biocide, while most other strains showed either no changes or less pronounced differences. Ec1655_TMN_2 was, however, also the only variant with a smaller biovolume than its parental strain without the biocide, while three variants had a significatively higher biovolume than their associated parental strains (Ec478_TMN_3; Ec223_TMN_1; Ec775_TMN_5). The Ec223_TMN_1 strain differed the most from its parental strain, consistent with its enhanced matrix component production. Some images of the biofilm co-cultures are also shown in Figure 6.

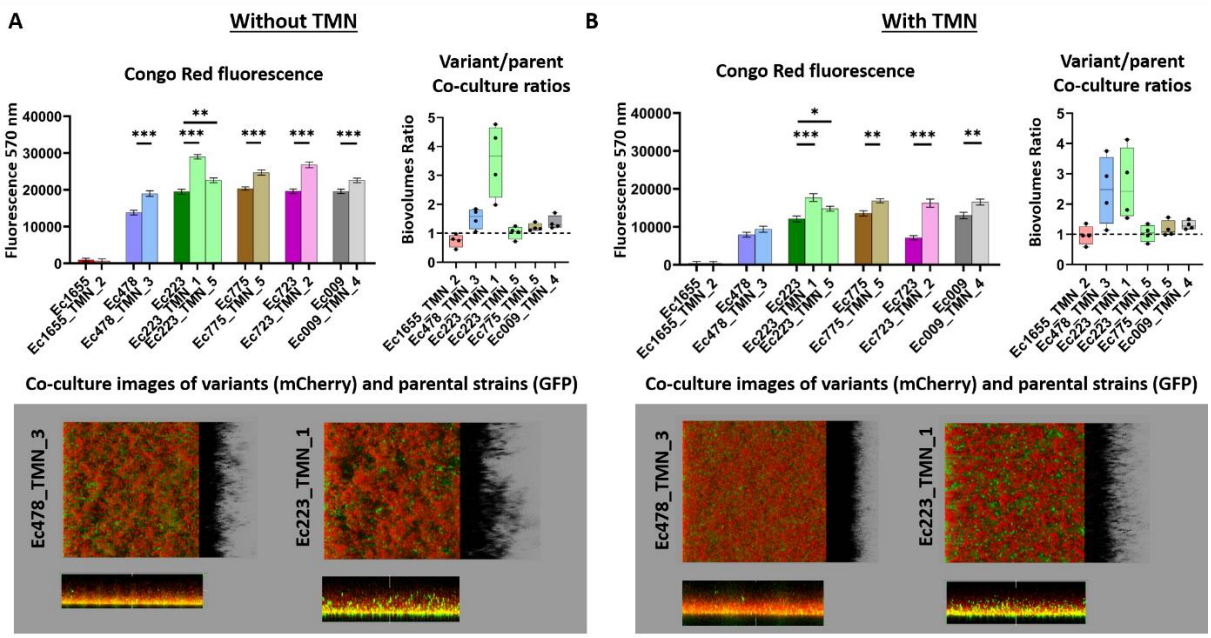

Figure 6. LPS variants show increased biofilm production. *Several experiments were performed to observe the ability of the variants to grow in biofilms, without (A) or with (B) TMN. Matrix production was quantified by the use of Congo Red through the analysis of the differences in fluorescence intensity of the biofilms of variants and parental strains after a 72-h pre-formation step without a biocide, and 24-h exposure to MIC concentrations of TMN (6.6 mg/L). mCherry-tagged variants and GFP-tagged parental strains were also co-cultured with or without 2.2 mg/L of TMN and biovolume ratios of the variants and parents are shown. One representative image of the co-cultures showing the two variants with the biggest difference from their parental strain is also presented, with the variants in red and the parental strains in green. Statistical analysis was performed with a Mann-Whitney test comparing the variants and their parental strains. P-values are represented as follows: * = [0.05-0.01]; ** =]0.01-0.001]; *** = <0?001. The P-values of the co-culture experiment are shown in Figure S3*

Discussion:

Antimicrobial resistance constitutes one of the major health challenges of the coming decades. One possible factor of risk promoting antibiotic resistance is the use of biocides, which could select for antibiotic cross-resistant variants through their effects[5,6]. In this study, four biocidal active substances (BAC, PHMB, TMN and SHY), representative of molecules used in food chain disinfection processes, were used to continuously expose *E. coli* biofilms for one

month, monitoring their effects on rifampicin resistance. Rifampicin is considered a critically important antibiotic for human health[30]. It is also widely used to study the evolutionary processes of bacterial populations[31,32], and is a useful tool for quantifying mutation rates through the rifampicin resistance assay[33].

In this study, recurrent mutational events were observed in the *rpoB* gene in RifR variants, which codes for the RNA Polymerase β subunit, the primary target of rifampicin in *E. coli* and other genera like *Mycobacterium*[34,35]. This observation aligns with the central role of *rpoB* mutations in the emergence of rifampicin resistance among *E. coli* as extensively described in previous works[36]. Mutations in *rpoB* conferred here the highest levels of rifampicin resistance, with MIC values ranging from 40 to 200 mg/L (Fig. 2), but they can sometimes have deleterious effects on bacterial fitness[37,38].

While PHMB and SHY presence did not induce RifR variants compared to H2O, BAC and TMN exposure significantly promoted RifR variants in various *E. coli* strains during exposure. Both biocides were associated with mutational events in specific pathways. First, BAC was associated with mutations in the *rbsR* gene and in stringent response genes (*dksA*; *gppA*). D-ribose — catabolised by the rbs operon — has already been associated with biofilm inhibition, hence the mutation could be a way for the bacteria to increase D-ribose degradation and thereby biofilm production[39]. Besides controlling the D-ribose metabolism, *rbsR* has also been associated with the control of purine synthesis, inhibiting de novo synthesis but activating the bacteria's salvage pathway[40]. The stringent response is activated in the event of nutrient depletion, and inhibits cell activity, notably purine nucleotide synthesis[41], suggesting a possible link between mutations in the stringent response genes and *rbsR* mutations under BAC conditions. However, the link between BAC and these mutations remains unclear. Moreover, these mutations were often associated with *rpoB*, reducing the likelihood of a specific cross-resistance mechanism with rifampicin.

Interestingly, TMN exposure was strongly associated with mutations in LPS biosynthesis pathways in RifR variants, suggesting a pivotal role of LPS modulation in TMN adaptation and cross-resistance development to rifampicin. LPS biosynthesis variants were selected in six of the eight tested strains when exposed to TMN, demonstrating the recurrence of this phenomenon despite the various genetic backgrounds of the bacterial strains. These LPS biosynthesis variants exhibited low-level rifampicin resistance (from 20 to 60 mg/L) and did not carry additional mutations in *rpoB* (Fig. 2). LPS biosynthesis variants were more frequently isolated in biofilms than in supernatants (Fig. 1). This is consistent with the potential of biofilms to maintain variants within the bacterial population, constituting a protective environment in which they can develop[5,42]. Several studies have reported a differential emergence in biofilms compared with planktonic cultures, with low-resistance variants emerging in biofilms (where the bacteria is exposed to reduced concentrations of antimicrobials), while high-resistance variants emerged preferentially in planktonic cultures[43,44]. Low-level resistances are favoured in less stringent environments because the side effects of mutations often have less impact on cell fitness than the deleterious effects of high-resistance mutations on cell growth[43].

In most of the RifR variants, the effect of mutations on the LPS structure and associated phenotype was clear, with modifications in the LPS SDS-PAGE profile, membrane charge and permeability. Only two variants, Ec1655_TMN_2 and Ec009_TMN_4, did not reveal any changes in their structural and membrane properties. TMN is a cationic biocide, and positively-charged biocides are known to affect membrane stability. BAC and PHMB interact with anionic phospholipids such as the lipid A part of the LPS, disrupting the equilibrium between these phospholipids and fixed divalent cations[45]. This depolarises and disrupts the membrane, leading to the release of cell components and cell lysis[46]. Some associations between mutations in lipid A synthesis genes and BAC, which is also positively charged, have

already been observed[12]. In our study, mutations were mainly found in genes involved in the synthesis of the saccharide part of the LPS, with most genes coding for glycosyltransferases. The core part of the LPS is also negatively charged, which could explain the effects of the *waaU* mutation in Ec723_TMN_2, coding for a heptosyltransferase involved in core oligosaccharide synthesis. However, other LPS biosynthesis variants carried mutations in genes involved in the synthesis of the O-antigen part, which is not charged. The modification of membrane Zeta potential reflects a modification in cell surface charge in LPS biosynthesis variants, which could help bacteria to overcome the stress from the biocide's positive charge. The O-antigen regulates membrane fluidity through indirect effects on the anionic part[47] and changes in the O-antigen chain length have been associated with decreased cell permeability[48]. Although rifampicin is not a charged antibiotic, the increased robustness brought by the more negative charge and the fixation of divalent cations could help the bacteria when it encounters other antimicrobial stresses. Murata et al.[49] demonstrated that modifications in LPS lipid A synthesis affect bacterial resistance to uncharged molecules, and that LPS was essential for the robustness of the membrane and survival against erythromycin, novobiocin and notably rifampicin. In our own study, among the 15 antibiotics tested, RifR variants with pronounced modifications in the LPS structure exhibited a slight increase in the MIC for azithromycin, an antibiotic belonging to the macrolide family, like erythromycin; this underlines effects that are similar to those reported by Murata et al.[49] Additionally, rifampicin and azithromycin are hydrophobic molecules, like ciprofloxacin, for which a two-fold increase in MIC was also observed in three of the seven LPS biosynthesis variants. This observation supports the recognised role of LPS in limiting permeability to hydrophobic compounds[50].

The ability of LPS biosynthesis variants to disseminate and recolonise new environments was then evaluated. Resistance mutations can often cause severe growth damage to the strains, impacting their competitiveness when there are no antimicrobials[51]. We found that mutations in LPS biosynthesis pathways did not lead to degradation in the variants' growth kinetics without TMN. Moreover, when exposed to TMN some variants displayed a shorter lag phase than their parental strain, which could help them to develop and disseminate more easily. Even though these resistances are low and biocides are usually used at higher concentrations, several factors can inhibit their efficiency (e.g. interfering substances, pH, wrong administration of the biocide[52]). It is known that surfaces are quickly re-colonised after a biocide treatment[53]. The presence of biofilms can also limit biocide efficiency[5]. In the present study, LPS biosynthesis variants exhibited similar or often higher competitiveness than their parental strain in mixed biofilms, as shown by biovolume ratios (Fig. 6) thus potentially indicating a higher risk of propagation. Coherently, Congo Red analysis demonstrated an overproduction of matrix components in most LPS biosynthesis variants. The reason for this overproduction is unclear. It could be due to an increased availability of ose precursors redirected from LPS biosynthesis to matrix polysaccharide synthesis. The increased availability of some precursors and the LPS-coding genes have previously been associated with colanic acid overproduction, a component of the *E. coli* extracellular matrix[54].

Although in our study mutations in LPS biosynthesis pathways did not lead to high phenotypic antibiotic resistances in the variants, they can help bacteria to survive longer under antimicrobial stresses, providing more time for the emergence of secondary high-level mutations. It has been demonstrated that low-resistance mutations often precede the emergence of higher resistance mutations[13,55].

Moreover, the antibiotics to which the variants became less susceptible are particularly relevant for *E. coli*. Rifaximin is a molecule close to rifampicin, azithromycin and ciprofloxacin, which are all used to treat travellers' diarrhoea[56,57]. Reduced susceptibilities could therefore reduce the treatments' effectiveness. Furthermore, these antibiotics are also

used in various treatments against other pathogens, opening up new avenues of research to investigate whether the effects observed in the present study could be extended to other bacterial species of interest.

Conclusion:

This work reports an association between exposure to biocidal active substances commonly used in the food industry and antibiotic resistance selection in *E. coli* biofilms. It also reveals the pivotal role of LPS in adaptation to TMN and the development of rifampicin cross-resistance. Interestingly, mutations occurring in LPS biosynthesis genes selected during TMN exposure resulted in benefits for RifR variants exposed to antimicrobials at both cellular and/or biofilm levels. These findings support the diversity of adaptive strategies among bacteria and their interplay, which together ultimately lead to the evolution and survival of bacterial populations under stress. Such insights are of prime interest for understanding how bacteria adapt to biocides and provide potential markers for cross-resistance monitoring in the food chain.

Methods:

1. Bacterial strains

The *E. coli* strains used in this study are listed in Table 1. Strain Ec1655 corresponds to the reference strain MG1655, Ec223 is a strain from the INRAE CIRM-BP collection of bacterial pathogens for humans and animals originally isolated from chickens, and the other six strains were from a collection belonging to the French National Reference Laboratory for Antimicrobial Resistance (NRL-AR) hosted in ANSES Fougères, and composed of *E. coli* strains isolated from the pork and poultry industries. Strains were conserved at -80 °C in cryoprotective solutions (Mast Group, Bootle, UK).

Name in the study	Origin (isolation date)
Ec1655	*E. coli* K-12 substr. MG1655 reference strain
Ec223	CIRM-BP Collection (1977)
Ec775	NRL-AR collection, Chicken (2014)
Ec009	NRL-AR collection, Chicken (2014)
Ec956	NRL-AR collection, Pork (2015)
Ec709	NRL-AR collection, Pork (2017)
Ec723	NRL-AR collection, Pork (2017)
Ec478	NRL-AR collection, Chicken (2018)

Table 1. E. coli strains used with their origin

2. Determination of susceptibility to biocides

The strains' susceptibility to four biocidal active substances was tested: BAC (BTC 50E, Stepan, France); TMN (Triameen Y12D.30, Quaron SAS, France); PHMB (Matrix scientific, France) and SHY (VWR Chemicals, France). Strains were grown overnight in 1/10 TSB medium. On the following day, strains were diluted in fresh 1/10 TSB to reach a 600 nm optical density (OD_{600nm}) of 0.2 (+/- 0.02). Microplates were filled with biocides in line A, with two wells per biocide. Then 100 µL of 1/10 TSB was added in lines B to H. A cascade dilution with 100 µL of the previous line was carried out from A to H. Finally, 10 µL of bacterial preculture was added to each well. Microplates were incubated at 22 °C overnight and MICs were read after 24 and 48 h.

Growth kinetics were investigated using sub-lethal concentrations of TMN (2.2mg/L). Bacterial strains were first streaked over fresh TSA + 5% sheep blood plate and incubated overnight at 37 °C. On the following day, colonies were resuspended in 1/10 TSB, reaching a final concentration of 0.2 OD_{600nm}. Next, 10 µL of the culture was added to 190 µL of 1/10 TSB supplemented with 2.2 mg/L TMN to reach 0.01 OD_{600nm}. Cultures were then grown at 22 °C for 48 h using a FLUOstar OPTIMA (BMG Labtech, Champigny-sur-Marne, France). The OD_{620nm} was measured every 30 minutes. The lag phase duration and maximal growth rate (µmax) were extracted using MARS data analysis software (BMG Labtech, Champigny-sur-Marne, France). There were three biological replicates and two technical replicates for each cycle.

3. Determination of susceptibility to antibiotics

The minimal inhibitory concentrations (MICs) of 15 different antibiotics were determined as previously described[58]. Briefly, bacteria were first grown on a fresh TSA + 5% sheep blood plate and incubated overnight at 37 °C. On the following day, some colonies were resuspended in 5 mL of sterile water to reach 0.5 Mac Farland (≈ 10^8 CFU/mL). Next, 10 µL of the suspension was added to 11 mL of Mueller Hinton Broth (MHB) then 50 µL of the MHB suspension was transferred into each well of a standard microplate (EUVSEC, Sensititre®, TREK Diagnostic Systems Ltd., Thermo Fisher Scientific, East Grinstead, UK). Plates were incubated for 24 h at 35 °C and read the next day. The figure was drawn up using the radarchart function in the fmsb package (https://minato.sip21c.org/). Three biological replicates were performed and MIC values displayed correspond to the median.
Growth kinetics were also investigated with 5 mg/L rifampicin. Bacterial strains were first streaked over a fresh TSA + 5% sheep blood plate and incubated overnight at 37 °C. On the following day, colonies were resuspended in MHB to reach a final concentration of 0.2 OD_{600nm}. Next, 10µL of the culture was added to 190 µL of MHB supplemented with 5 mg/L rifampicin to reach 0.01 OD_{600nm}. Cultures were then grown at 35 °C for 48 h using a FLUOstar OPTIMA (BMG Labtech, Champigny-sur-Marne, France). The OD_{620nm} was measured every 30 minutes. There were four biological replicates and two technical replicates for each cycle.

4. Experimental evolution with biocides and isolation of antibiotic-resistant variants

The exposure to biocides was performed as follows (Fig. 7). Strains were grown overnight in 1/10 TSB medium. On the following day, strains were diluted in fresh 1/10 TSB to reach an OD_{600nm} of 0.2 (+/- 0.02). For each strain, five columns of eight wells were filled with 190 µL of 1/10 TSB and 10 µL of the subcultures were then added to reach a final OD_{600nm} of 0.01. Plates were incubated at 20 °C for 1 h. Supernatants were then removed and replaced with fresh 1/10 TSB medium to keep only the fixed cells. Plates were incubated for 72 h at 20 °C.
After 72 h, the first cycle began. On the first cycle day, 5 µL of biofilm supernatants were first pipetted onto 20 mg/L rifampicin-supplemented plates, to evaluate RifR variants emerging in biofilm supernatants. Supernatants were then removed and 40 µL of fresh 1/10 TSB was added. Biofilms were resuspended and 5 µL of the biofilm suspension was pipetted onto the rifampicin plates, which were then incubated for 48 h at 37 °C. Finally, fresh media with planktonic MIC concentrations of biocides was added. Each column corresponded to one condition, Milli Q water being used as a control and the biocides being used separately for the other four conditions. Then, each day for 4 days, the medium was renewed with fresh 1/10 TSB medium supplemented with MIC concentrations of biocides (BAC = 6.25 mg/L; PHMB = 1.25 mg/L; TMN = 6.67 mg/L; SHY = 100 mg/L). Finally, on the last day, media were renewed but then they were not renewed for 72 h, until the new cycle began. The cycle was

repeated four times over the month. A first one-month experiment was performed with H_2O and all four biocides, then the experiment was repeated with only the H_2O control group and the BAC and TMN groups, the results of which are presented in Figure 1. The PHMB and SHY results are presented in Figure S1 with the results of H_2O that were obtained only in the first experiment.

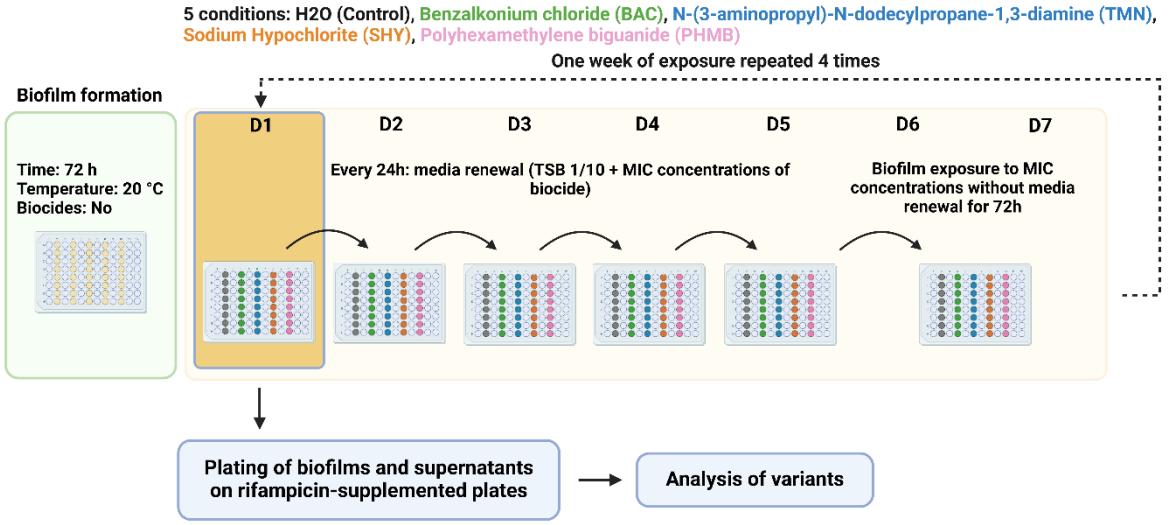

Figure 7. Description of the one-month experiment cycle to monitor strain evolution

5. Confirmation of variants and phenotypic resistance stability

After colonies development on rifampicin-supplemented plate, stability of resistance phenotypes was assessed by subculturing RifR variants on TSA plates without rifampicin every day for four days. On the 5th day, variants were streaked again over 20 mg/L rifampicin-supplemented TSA plates to observe whether the variant was still able to grow on antibiotic-supplemented medium after being spread over non-selective media.

Levels of rifampicin resistance were characterised using TSA plates supplemented with various rifampicin concentrations. Each variant and its parent were first grown on a fresh TSA + 5% sheep blood plate and incubated overnight at 37 °C. On the following day, variants were resuspended in TSB 1/10 to reach a final concentration of 0.2 OD_{600nm}. Next, 5 µL of each culture was pipetted onto TSA rifampicin-supplemented plates at different concentrations (20 mg/L; 40 mg/L; 60 mg/L; 80 mg/L; 100 mg/L; 150 mg/L; 200 mg/L) and on one antibiotic-free plate. Plates were incubated overnight at 37 °C. Experiment was performed from two to three times and median was displayed.

Enterobacterial repetitive intergenic consensus – PCR (ERIC-PCR) was performed as previously described[11] in order to check that variants were indeed derivatives of associated parental strains. DNA was extracted using the InstaGene kit (Bio-rad, Marnes-la-Coquette, France) and amplified using a LightCycler® 480 thermocycler (Roche Diagnostics, Meylan, France) with primers ERIC1-R (ATGTAAGCTCCTGGGGATTCAC) and ERIC2 (AAGTAAGTGACTGGGGTGAGCG) and GoTaq Flexi polymerase (Promega, Charbonnières-les-bains, France) as follows: 95 °C for 2 min for initial melting; 30 cycles at 95 °C for 1 min, 54 °C for 1 min, 72 °C for 4 min; final extension at 72 °C for 8 min followed by incubation at 4 °C. PCR products were then checked on 1% agarose gel and migrated over 90 min at 110 V before being revealed using a GelRED stain (Biotium, Brumath, France).

6. Genomic analysis of RifR variants

The whole genome of parental and variant strains was sequenced. First, DNA was extracted using the Macherey-Nagel Nucleospin Tissue kit (Düren, Germany) according to the manufacturer's instructions. DNA concentrations were then checked with BiospecNano quantification. Illumina sequencing was performed on the strains at the Institut du Cerveau et de la Moelle épinière (Paris, France) using the Novaseq 6000 SP. Data from the raw reads were analysed and filtered with the fastp tool (v0.23.4)[59] using --correction, --cut_front and --cut_right options with a threshold of 25. Adapters were automatically detected and removed from the reads with --detect_adapter_for_pe option. Unicycler (v0.5.0)[60] was then used to perform de novo assembly on the genome of parental strains, keeping only contigs longer than 200 bp. These newly reconstituted genomes were annotated using Bakta (v1.8.2)[61] with the full database and *Escherichia coli* as --genus and --species options. Afterwards, variant calling was performed with the variant strains exposed to a biocide and rifampicin using the annotated genomes of parental strains. Snippy (v4.6.0) was used to search for point mutations. The workflow described previously is available on the following GitHub repository: https://github.com/AB2R/WGS_pipeline.git. Mutated genes were analysed using the EcoCyc database[62]. The genomes of the variants and their parental strains were compared and the variants' genomes were assembled using Unicycler (v0.5.0)[60]. They were then compared against the genomes of the parental strains using BLAST[63]. Proksee[64] was used to generate the genome ring figures. A search for genes linked to mobile genetic elements was carried out on the genome of the parental strains using the mobileOG[65] database.

7. SDS-PAGE characterisation of LPS

LPSs were extracted using the Sigma-Aldrich lipopolysaccharide (LPS) isolation kit (Saint-Louis, USA), according to the manufacturer's instructions. LPS extracts were reduced with β-mercaptoethanol for 5 min at 95 °C and migrated by SDS-PAGE using mini-Protean tris-tricine precast gels (16.5% acrylamide, BIO-RAD) and a mini Protean 3 migration system (BIO-RAD). A Tris/Tricine/SDS buffer (16610744, BIO-RAD) and a Tricine sample buffer 10X (1610739, BIO-RAD) were used. Fixation was performed in a solution of EtOH 30% (Sigma-Aldrich) and acetic acid 10% (UN2789, VWR) for 1 h. The gel was then washed for 3x 5 min in ultrapure water (MilliQ, Millipore) before incubation in 0.7% metaperiodate (98%, 013798.22, Thermo Scientific) for 10 min. Another washing step of 3x 5 min in ultrapure water was performed before incubation in a 0.02% sodium thiosulfate solution (99%, 217263, Sigma-Aldrich) for 1 min. Yet another washing step of 2x 1 min in ultrapure water was performed, followed by incubation in 25 mM AgNO3 (>99%, 209139, Sigma-Aldrich) for 10 min. The final washing step using ultrapure water was for 15 s. The gel was revealed in 50 mL ultrapure water supplemented with 1.75 g of potassium carbonate (>99%, 209619, Sigma-Aldrich), 15 µL of formaldehyde (37 wt in water, 252549, Sigma-Aldrich) and 6.25 µL of thiosulfate 10% and incubated until the bands were revealed. Finally, the gel was incubated for 30 min in a stop solution composed of 4% Tris base (TG791, Sigma-Aldrich) and 2% acetic acid.

8. Determination of cell membrane surface charge

Bacteria were grown overnight on TSA plates at 37 °C. On the following day, bacteria were resuspended in 5 mL of TSB and grown overnight at 37 °C. On the third day, cultures were centrifuged at 2000 g / 10 min / 4 °C. Two washing steps were performed with 5 mL of 15 mM NaCl and 2000 g / 10 min / 4 °C centrifugations. Then the OD_{600nm} was adjusted to 0.02 in 15 mM NaCl. Zeta potential was measured using a Zetasizer Nano ZS90 (Malvern, UK). Next, 900 µL of the cell suspension was added to folded capillary Zeta cells (DTS 1070,

Malvern Panalytical). The following settings were used: equilibration time 50 s, auto mode, 3 measurement replicates, 30-s pause between replicates. Between each sample, the cuvette was rinsed three times with Milli Q water. At the end of the experiment, the cuvette was rinsed with 70% ethanol. There were five biological replicates for this experiment.

9. Assessment of membrane permeability modifications

Outer membrane permeability was evaluated using the Crystal Violet assay[66]. First, cells were grown on TSA plates overnight at 37 °C. On the following day, cells were resuspended in 5 mL of 1/10 TSB medium and incubated overnight at 37 °C. On the 3rd day, bacterial cultures were first normalised by their OD_{600nm} so that parental strains and variants would be at the same concentrations. The bacterial suspension was centrifuged at 4500 g / 5 min / 4 °C. Cells were then washed twice with 15 mM NaCl and centrifuged at 4500 g / 5 min / 4 °C. After the second centrifugation, cells were resuspended in 15 mM NaCl supplemented with 10 µg/mL of Crystal Violet. Suspensions were then incubated for 10 minutes at 37 °C followed by a centrifugation step at 13,400 g / 15 min / 4 °C. Finally, the OD_{590nm} was read. A solution of 15 mM NaCl was used as a blank. The OD_{590nm} represents the amount of Crystal Violet that was not internalised by the cells, so a higher OD_{590nm} represents a strain which is less permeable than one with a lower OD_{590nm}. There were eight biological replicates for this experiment.

10. Biofilm matrix quantification

Biofilms of the variants and their parents were prepared as in section 3 and grown for 72 h, without biocide. Then, in one condition, the medium was replaced with a fresh medium without biocide. In the other condition, the medium was replaced with a fresh medium supplemented with MIC concentrations of TMN. Plates were incubated for an additional 24 h. Finally, 50 µL of Congo Red at a concentration of 40 µg/mL was added to each biofilm. Fluorescence was quantified using a FLUOstar OPTIMA (BMG Labtech, Champigny-sur-Marne, France) with an excitation wavelength of 520 nm and an emission wavelength of 570 nm. There were 10 biological replicates with three technical replicates each time for this experiment.

11. Evaluation of the LPS biosynthesis variants' competitiveness in biofilms

Competent cells were prepared as in Chang et al.[68] with slight modifications (centrifuged at 6000 rpm instead of 4000 rpm; first icing step for 15 min instead of 20 min). Plasmids were transformed using the same protocol. The plasmids used were pCM11_sGFP or pCM11_mCherry[67]. Variants were selected on 100 µg/mL ampicillin-supplemented TSA plates. On the following day, transformants were identified on a UV plate. Transformants were then grown overnight at 37 °C in TSB 1/10 supplemented with 100 µg/mL ampicillin (AMP). On the following day, cryotubes were prepared with 500 µL of 40% glycerol and 500 µL of the overnight culture and stored at -80 °C.

Co-cultures were performed between tagged parental and variant strains. Strains were grown on TSA with 100 µg/mL AMP overnight at 37 °C. On the following day, strains were resuspended in TSB 1/10 with 100 µg/mL AMP overnight at 37 °C. On the third day, co-cultures were prepared either with parental strains tagged with GFP and variants with mCherry, or parental strains tagged with mCherry and variants with GFP, to avoid a fluorescence bias due to the fluorescent protein. Cultures were adjusted to 0.02 OD_{600nm}. Next, 10 µL of the parent and 10 µL of the variant were added to 180 µL TSB 1/10. After 1 h of adhesion, media was replaced with fresh TSB 1/10 or TSB 1/10 supplemented with MIC/3 TMN (2.22 mg/L) and plates were incubated for 72 h at 19 °C. They were then analysed with a Leica HCS-SP8 CLSM at the INRAE MIMA2 Imaging Core Facility (Microscopie et Imagerie des Microorganismes, Animaux et Aliments, INRAE, Jouy-en-Josas)[69]. GFP was

excited with an argon laser set at 488 nm, and mCherry with a DPSS laser set at 561 nm. Fluorescence emissions were collected using photomultiplier tubes (PMTs) at wavelengths of 500-550 nm for the GFP signal and 600-750 nm for the mCherry signal. The biofilms' three-dimensional structures were scanned with a 63x water objective lens (numerical aperture: 1.2), with a resolution of 512x512 and a 1 µm Z-step. Sixteen stacks were taken for each condition and strain with two images per well, and two wells per biological replicate (4). The biofilms' 3D structures were reconstructed using the Imaris 9.3.1 software (Bitplane, AG-Zürich, Switzerland) with the Blend Easy 3D and cross-section views. Quantitative biofilm biovolumes were extracted from CLSM images with BiofilmQ 0.2.2[70].

12. Statistical Analysis

Statistics were generated using Graphpad Prism. Throughout the current study, the Mann Whitney test was used to compare two groups. It was first used to compare the different biocides with the H_2O control group for each week, in both biofilms and supernatants. It was then used to compare the variants with their parental strain. The P values are represented in the study by the symbols: * = [0.05-0.01]; ** =]0.01-0.001]; *** = <0.001.

Data availability

All sequencing data were deposit in NCBI under the BioProject accession number PRJNA947807. Detailed of accession numbers for assembled genomes of parental strains and sequence reads of variant strains were provided in table S2. Raw data in excel files are presented in Source data section.

Author contributions:

RC: Conceptualisation, Formal analysis, Investigation, Visualisation, Writing – original draft, Writing – review & editing. PL: Data curation, Formal analysis, Investigation, Methodology, Software, Writing – original draft. PH: Investigation. PLG: Investigation. MB: Formal analysis, Investigation, Visualisation. AH: Methodology. TL: Methodology, Investigation. CS: Project administration, Resources. RB: Conceptualisation, Funding acquisition, Supervision, Writing – original draft, Writing – review & editing. AB: Conceptualisation, Funding acquisition, Project administration, Resources, Supervision, Visualisation, Writing - original draft, Writing – Review & editing

Funding:

Financial support was received from ANR JCJC BAoBAb (ANR-21-CE35-0001).
RC was also the recipient of an ANSES-INRAE doctoral fellowship.

Acknowledgements:

Financial support was received from ANR JCJC BAoBAb (ANR-21-CE35-0001).
RC was also recipient of an ANSES-INRAE doctoral fellowship.
Christophe Beloin was thanked for helpful discussions and his useful advices on the establishment of the SDS-PAGE experiment.
The MicrobAdapt team of the Micalis Institute was thanked for the use of the Zetasizer Nano ZS90 and especially Jasmina Vidic and Debora Pinamonti for their helpuf explanations and assistance.
Then, we would like to thank Vlad Costache and the MIMA 2 Imaging Core Facility for the use of the Leica HCS-SP8 CLSM.
We would also like to thank the French AntibioDEAL network of the Promise PPR antibioresistance ANR program for the useful scientific exchanges

Finally, we would like to thank Hugo Grandjean for his help on the R software for the production of the figure 4.
The figure 7 was realized on the Biorender website.

References:

1. Serra-Burriel, M. *et al.* Impact of multi-drug resistant bacteria on economic and clinical outcomes of healthcare-associated infections in adults: Systematic review and meta-analysis. *PLoS One* **15**, e0227139 (2020).

2. McEwen, S. A. & Collignon, P. J. Antimicrobial Resistance: a One Health Perspective. *Microbiol Spectr* **6**, (2018).

3. Murray, L. M. *et al.* Co-selection for antibiotic resistance by environmental contaminants. *npj Antimicrob Resist* **2**, 9 (2024).

4. Chen, B., Han, J., Dai, H. & Jia, P. Biocide-tolerance and antibiotic-resistance in community environments and risk of direct transfers to humans: Unintended consequences of community-wide surface disinfecting during COVID-19? *Environ Pollut* **283**, 117074 (2021).

5. Charron, R., Boulanger, M., Briandet, R. & Bridier, A. Biofilms as protective cocoons against biocides: from bacterial adaptation to One Health issues. *Microbiology (Reading)* **169**, (2023).

6. Kampf, G. Biocidal Agents Used for Disinfection Can Enhance Antibiotic Resistance in Gram-Negative Species. *Antibiotics (Basel)* **7**, 110 (2018).

7. Slimani, K., Pirotais, Y., Maris, P., Abjean, J.-P. & Hurtaud-Pessel, D. Liquid chromatography-tandem mass spectrometry method for the analysis of N-(3-aminopropyl)-N-dodecylpropane-1,3-diamine, a biocidal disinfectant, in dairy products. *Food Chem* **262**, 168–177 (2018).

8. Karygianni, L., Ren, Z., Koo, H. & Thurnheer, T. Biofilm Matrixome: Extracellular Components in Structured Microbial Communities. *Trends Microbiol* **28**, 668–681 (2020).

9. Bridier, A., Briandet, R., Thomas, V. & Dubois-Brissonnet, F. Resistance of bacterial biofilms to disinfectants: a review. *Biofouling* **27**, 1017–1032 (2011).

10. Charron, R. *et al.* Polyhexamethylene biguanide promotes adaptive cross-resistance to gentamicin in *Escherichia coli* biofilms. *Front Cell Infect Microbiol* **13**, 1324991 (2023).

11. Bridier, A. *et al.* Spatial Organization Plasticity as an Adaptive Driver of Surface Microbial Communities. *Front Microbiol* **8**, 1364 (2017).

12. Nordholt, N., Kanaris, O., Schmidt, S. B. I. & Schreiber, F. Persistence against benzalkonium chloride promotes rapid evolution of tolerance during periodic disinfection. *Nat Commun* **12**, 6792 (2021).

13. Levin-Reisman, I. *et al.* Antibiotic tolerance facilitates the evolution of resistance. *Science* **355**, 826–830 (2017).

14. Bridier, A., Dubois-Brissonnet, F., Greub, G., Thomas, V. & Briandet, R. Dynamics of the action of biocides in *Pseudomonas aeruginosa* biofilms. *Antimicrob Agents Chemother* **55**, 2648–2654 (2011).

15. Jia, Y., Lu, H. & Zhu, L. Molecular mechanism of antibiotic resistance induced by mono- and twin-chained quaternary ammonium compounds. *Sci Total Environ* **832**, 155090 (2022).

16. Weber, H., Polen, T., Heuveling, J., Wendisch, V. F. & Hengge, R. Genome-wide analysis of the general stress response network in *Escherichia coli*: sigmaS-dependent genes, promoters, and sigma factor selectivity. *J Bacteriol* **187**, 1591–1603 (2005).

17. Muffler, A., Fischer, D. & Hengge-Aronis, R. The RNA-binding protein HF-I, known as a host factor for phage Qbeta RNA replication, is essential for *rpoS* translation in *Escherichia coli*. *Genes Dev* **10**, 1143–1151 (1996).

18. Gourse, R. L. *et al.* Transcriptional Responses to ppGpp and DksA. *Annu Rev Microbiol* **72**, 163–184 (2018).

19. Rakshit, D., Dasgupta, S., Das, B. & Bhadra, R. K. Functional Insights Into the Role of *gppA* in (p)ppGpp Metabolism of *Vibrio cholerae*. *Front Microbiol* **11**, 564644 (2020).

20. Lopilato, J. E., Garwin, J. L., Emr, S. D., Silhavy, T. J. & Beckwith, J. R. D-ribose metabolism in *Escherichia coli* K-12: genetics, regulation, and transport. *J Bacteriol* **158**, 665–673 (1984).

21. Alvarez, A. F., Rodríguez, C., González-Chávez, R. & Georgellis, D. The *Escherichia coli* two-component signal sensor BarA binds protonated acetate via a conserved hydrophobic-binding pocket. *J Biol Chem* **297**, 101383 (2021).

22. Heinrichs, D. E., Monteiro, M. A., Perry, M. B. & Whitfield, C. The assembly system for the lipopolysaccharide R2 core-type of *Escherichia coli* is a hybrid of those found in *Escherichia coli* K-12 and *Salmonella enterica*. Structure and function of the R2 WaaK and WaaL homologs. *J Biol Chem* **273**, 8849–8859 (1998).

23. Stevenson, G. *et al.* Structure of the O antigen of *Escherichia coli* K-12 and the sequence of its rfb gene cluster. *J Bacteriol* **176**, 4144–4156 (1994).

24. Adams, M. M., Allison, G. E. & Verma, N. K. Type IV O antigen modification genes in the genome of *Shigella flexneri* NCTC 8296. *Microbiology (Reading)* **147**, 851–860 (2001).

25. Sirisena, D. M., MacLachlan, P. R., Liu, S. L., Hessel, A. & Sanderson, K. E. Molecular analysis of the *rfaD* gene, for heptose synthesis, and the *rfaF* gene, for heptose transfer, in lipopolysaccharide synthesis in *Salmonella typhimurium*. *J Bacteriol* **176**, 2379–2385 (1994).

26. Qin, J., Hong, Y., Morona, R. & Totsika, M. O antigen biogenesis sensitises *Escherichia coli* K-12 to bile salts, providing a plausible explanation for its evolutionary loss. *PLoS Genet* **19**, e1010996 (2023).

27. Rubirés, X. *et al.* A gene (wbbL) from *Serratia marcescens* N28b (O4) complements the rfb-50 mutation of *Escherichia coli* K-12 derivatives. *J Bacteriol* **179**, 7581–7586 (1997).

28. Adams, P. G., Lamoureux, L., Swingle, K. L., Mukundan, H. & Montaño, G. A. Lipopolysaccharide-induced dynamic lipid membrane reorganization: tubules, perforations, and stacks. *Biophys J* **106**, 2395–2407 (2014).

29. Clifton, L. A. *et al.* Effect of divalent cation removal on the structure of gram-negative bacterial outer membrane models. *Langmuir* **31**, 404–412 (2015).

30. Hardie, K. R. & Fenn, S. J. JMM profile: rifampicin: a broad-spectrum antibiotic. *J Med Microbiol* **71**, (2022).

31. Krašovec, R. *et al.* Mutation rate plasticity in rifampicin resistance depends on *Escherichia coli* cell-cell interactions. *Nat Commun* **5**, 3742 (2014).

32. France, M. T., Cornea, A., Kehlet-Delgado, H. & Forney, L. J. Spatial structure facilitates the accumulation and persistence of antibiotic-resistant mutants in biofilms. *Evol Appl* **12**, 498–507 (2019).

33. Majumdar, C., Nuñez, N. N., Raetz, A. G., Khuu, C. & David, S. S. Cellular Assays for Studying the Fe-S Cluster Containing Base Excision Repair Glycosylase MUTYH and Homologs. *Methods Enzymol* **599**, 69–99 (2018).

34. Zenkin, N., Kulbachinskiy, A., Bass, I. & Nikiforov, V. Different rifampin sensitivities of *Escherichia coli* and *Mycobacterium tuberculosis* RNA polymerases are not explained by the difference in the beta-subunit rifampin regions I and II. *Antimicrob Agents Chemother* **49**, 1587–1590 (2005).

35. Li, M.-C. *et al. rpoB* Mutations and Effects on Rifampin Resistance in *Mycobacterium tuberculosis*. *Infect Drug Resist* **14**, 4119–4128 (2021).

36. Jin, D. J. & Gross, C. A. Mapping and sequencing of mutations in the *Escherichia coli rpoB* gene that lead to rifampicin resistance. *J Mol Biol* **202**, 45–58 (1988).

37. Cutugno, L., Mc Cafferty, J., Pané-Farré, J., O'Byrne, C. & Boyd, A. *rpoB* mutations conferring rifampicin-resistance affect growth, stress response and motility in *Vibrio vulnificus*. *Microbiology (Reading)* **166**, 1160–1170 (2020).

38. Brandis, G., Pietsch, F., Alemayehu, R. & Hughes, D. Comprehensive phenotypic characterization of rifampicin resistance mutations in *Salmonella* provides insight into the evolution of resistance in *Mycobacterium tuberculosis*. *J Antimicrob Chemother* **70**, 680–685 (2015).

39. Liu, L., Wu, R., Zhang, J., Shang, N. & Li, P. D-Ribose Interferes with Quorum Sensing to Inhibit Biofilm Formation of *Lactobacillus paraplantarum* L-ZS9. *Front Microbiol* **8**, 1860 (2017).

40. Shimada, T., Kori, A. & Ishihama, A. Involvement of the ribose operon repressor RbsR in regulation of purine nucleotide synthesis in *Escherichia coli*. *FEMS Microbiol Lett* **344**, 159–165 (2013).

41. Irving, S. E., Choudhury, N. R. & Corrigan, R. M. The stringent response and physiological roles of (pp)pGpp in bacteria. *Nat Rev Microbiol* **19**, 256–271 (2021).

42. Penesyan, A., Paulsen, I. T., Kjelleberg, S. & Gillings, M. R. Three faces of biofilms: a microbial lifestyle, a nascent multicellular organism, and an incubator for diversity. *NPJ Biofilms Microbiomes* **7**, 80 (2021).

43. Santos-Lopez, A., Marshall, C. W., Scribner, M. R., Snyder, D. J. & Cooper, V. S. Evolutionary pathways to antibiotic resistance are dependent upon environmental structure and bacterial lifestyle. *Elife* **8**, e47612 (2019).

44. Ahmed, M. N., Porse, A., Sommer, M. O. A., Høiby, N. & Ciofu, O. Evolution of Antibiotic Resistance in Biofilm and Planktonic *Pseudomonas aeruginosa* Populations Exposed to Subinhibitory Levels of Ciprofloxacin. *Antimicrob Agents Chemother* **62**, e00320-18 (2018).

45. Wessels, S. & Ingmer, H. Modes of action of three disinfectant active substances: a review. *Regul Toxicol Pharmacol* **67**, 456–467 (2013).

46. Halder, S. *et al.* Alteration of Zeta potential and membrane permeability in bacteria: a study with cationic agents. *Springerplus* **4**, 672 (2015).

47. Nikaido, H. Molecular basis of bacterial outer membrane permeability revisited. *Microbiol Mol Biol Rev* **67**, 593–656 (2003).

48. Bryan, L. E., O'Hara, K. & Wong, S. Lipopolysaccharide changes in impermeability-type aminoglycoside resistance in *Pseudomonas aeruginosa*. *Antimicrob Agents Chemother* **26**, 250–255 (1984).

49. Murata, T., Tseng, W., Guina, T., Miller, S. I. & Nikaido, H. PhoPQ-mediated regulation produces a more robust permeability barrier in the outer membrane of *Salmonella enterica* serovar typhimurium. *J Bacteriol* **189**, 7213–7222 (2007).

50. Bertani, B. & Ruiz, N. Function and Biogenesis of Lipopolysaccharides. *EcoSal Plus* **8**, (2018).

51. Vogwill, T. & MacLean, R. C. The genetic basis of the fitness costs of antimicrobial resistance: a meta-analysis approach. *Evol Appl* **8**, 284–295 (2015).

52. Russell, A. D. Biocide use and antibiotic resistance: the relevance of laboratory findings to clinical and environmental situations. *Lancet Infect Dis* **3**, 794–803 (2003).

53. Luyckx, K. *et al.* A 10-day vacancy period after cleaning and disinfection has no effect on the bacterial load in pig nursery units. *BMC Vet Res* **12**, 236 (2016).

54. Wang, C. *et al.* Corrigendum to 'Colanic acid biosynthesis in *Escherichia coli* is dependent on lipopolysaccharide structure and glucose availability' [Microbiol. Res. 239 (October 2020) 126527]. *Microbiol Res* **243**, 126656 (2021).

55. Levin-Reisman, I., Brauner, A., Ronin, I. & Balaban, N. Q. Epistasis between antibiotic tolerance, persistence, and resistance mutations. *Proc Natl Acad Sci U S A* **116**, 14734–14739 (2019).

56. Steffen, R. *et al.* Rifamycin SV-MMX® for treatment of travellers' diarrhea: equally effective as ciprofloxacin and not associated with the acquisition of multi-drug resistant bacteria. *J Travel Med* **25**, tay116 (2018).

57. de la Cabada Bauche, J. & Dupont, H. L. New Developments in Traveler's Diarrhea. *Gastroenterol Hepatol (N Y)* **7**, 88–95 (2011).

58. Cuzin, C. *et al.* Selection of a Gentamicin-Resistant Variant Following Polyhexamethylene Biguanide (PHMB) Exposure in *Escherichia coli* Biofilms. *Antibiotics (Basel)* **10**, 553 (2021).

59. Chen, S., Zhou, Y., Chen, Y. & Gu, J. fastp: an ultra-fast all-in-one FASTQ preprocessor. *Bioinformatics* **34**, i884–i890 (2018).

60. Wick, R. R., Judd, L. M., Gorrie, C. L. & Holt, K. E. Unicycler: Resolving bacterial genome assemblies from short and long sequencing reads. *PLOS Computational Biology* **13**, e1005595 (2017).

61. Schwengers, O. *et al.* Bakta: rapid and standardized annotation of bacterial genomes via alignment-free sequence identification. *Microb Genom* **7**, 000685 (2021).

62. Karp, P. D. *et al.* The EcoCyc Database (2023). *EcoSal Plus* **11**, eesp00022023 (2023).

63. Altschul, S. F., Gish, W., Miller, W., Myers, E. W. & Lipman, D. J. Basic local alignment search tool. *J Mol Biol* **215**, 403–410 (1990).

64. Grant, J. R. *et al.* Proksee: in-depth characterization and visualization of bacterial genomes. *Nucleic Acids Res* **51**, W484–W492 (2023).

65. Brown, C. L. *et al.* mobileOG-db: a Manually Curated Database of Protein Families Mediating the Life Cycle of Bacterial Mobile Genetic Elements. *Appl Environ Microbiol* **88**, e0099122 (2022).

66. Vaara, M. & Vaara, T. Outer membrane permeability barrier disruption by polymyxin in polymyxin-susceptible and -resistant *Salmonella typhimurium*. *Antimicrob Agents Chemother* **19**, 578–583 (1981).

67. Lauderdale, K. J., Malone, C. L., Boles, B. R., Morcuende, J. & Horswill, A. R. Biofilm dispersal of community-associated methicillin-resistant *Staphylococcus aureus* on orthopedic implant material. *J Orthop Res* **28**, 55–61 (2010).

68. Chang, A. Y., Chau, V. W., Landas, J. A., & Pang, Y. Preparation of calcium-competent *Escherichia coli* and heat-shock transformation. *JEMI Methods* **1**, 22–25 (2017)

69. MIMA2. Microscopy and Imaging Facility for Microbes, Animals and Foods. (2018) doi:10.15454/1.5572348210007727E12.

70. Hartmann, R. *et al.* Quantitative image analysis of microbial communities with BiofilmQ. *Nat Microbiol* **6**, 151–156 (2021).

Supplementary Data:

Supplementary Materials and methods:

The plasmid's stability was evaluated to ensure that it would not be released by the strains in the absence of selective pressure. Strains were counted with and without selective pressure. Transformed cells were first plated on TSA using 100 µg/mL AMP-supplemented plates and incubated overnight at 37°C. On the following day, one fluorescent colony was resuspended in 5 mL TSB 1/10 with 100 µg/L AMP and grown overnight at 37°C. On the following day, biofilms were prepared as in section 3 and grown in TSB 1/10 with or without 100 µg/mL AMP for 72 hr. After 72 h, supernatants were first removed and replaced with 100 µL of fresh TSB 1/10. Biofilms were then totally resuspended in the 100 µL by scraping the well's surface. The 100 µL was added to 900 µL of TSB 1/10 and vortexed thoroughly for 30 s. After vortexing, 20 µL of the cell suspension was added to 180 µL of TSB 1/10. Serial dilutions were performed until reaching a dilution factor of 10^{-9}. A 10-µL dose of each dilution was then plated on TSA plates with or without 100 µg/mL AMP. The plates were incubated overnight at 37°C and counted the following day.

To evaluate the impact of the plasmid on cell growth, cells with or without plasmid were grown on TSA plates, respectively with or without 100 µg/mL AMP, overnight at 37°C. On the following day, a colony was resuspended in 5 mL of TSB with or without AMP and incubated overnight at 37°C. On the following day, cultures were adjusted to 0.2 OD_{600nm} and 10 µL was added to 190 µL of 1/10 TSB for cells without plasmid and 190 µL of 1/10 TSB with 100 µg/mL AMP for cells with plasmid to reach a 0.01 OD_{600nm} concentration. Cultures were then grown for 24 h and OD_{600nm} was measured every 30 minutes by a microplate reader (Biotek Synergy H1). Three biological replicates with two technical replicates were performed for each strain.

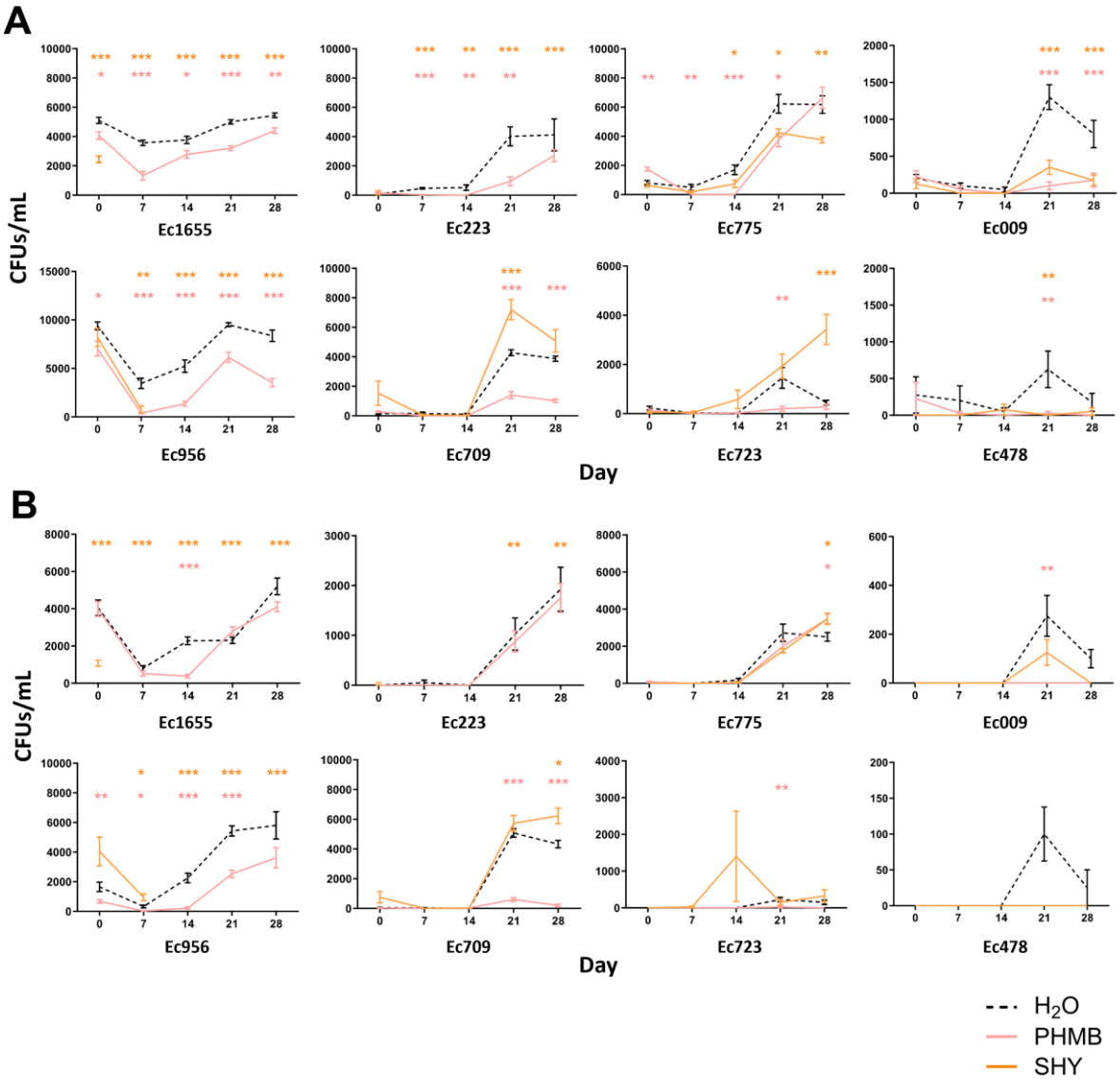

Figure S1. *Evolution curves representing the number of CFUs/mL of RifR variants enumerated on TSA plates supplemented with 20 mg/L of rifampicin and collected from biofilms (A) or supernatants (B) exposed to H_2O (black dashed lines), PHMB (in pink) or SHY (in orange). Error bars represent the standard error of the mean. Statistical analysis was performed with a Mann-Whitney test between the biocide condition and the H_2O condition, separately for each week. P-values are represented as following:* * = [0,05-0,01]; ** =]0,01-0,001]; *** = <0,001.

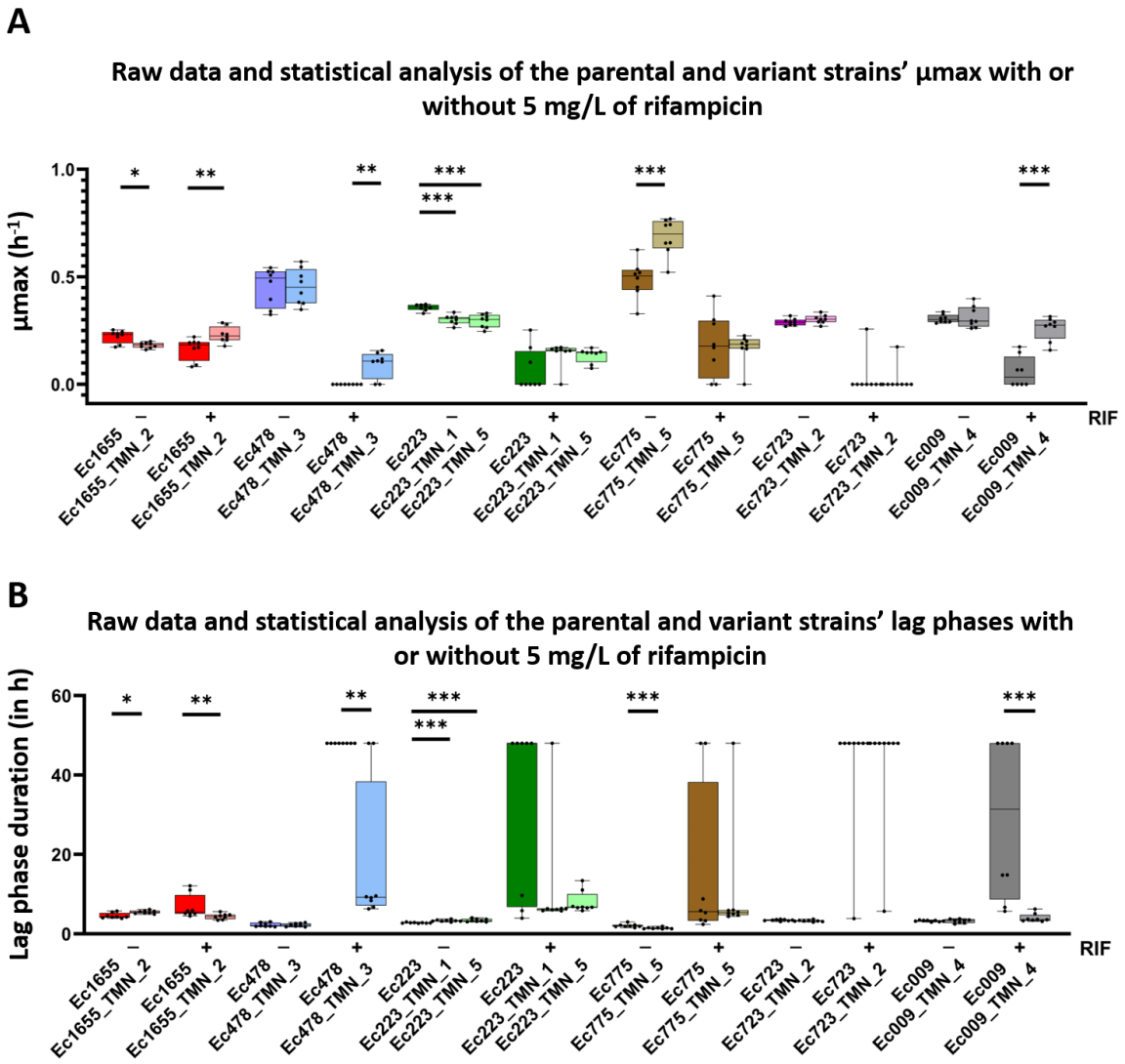

Figure S2. *Raw growth parameters of µmax (A) and lag phases (B) in absence or in presence of 5 mg/L of rifampicin, with a statistical analysis performed per Mann-Whitney test between variants and parental strains. P-values are represented as following: * = [0,05-0,01]; ** =]0,01-0,001]; *** = <0,001*

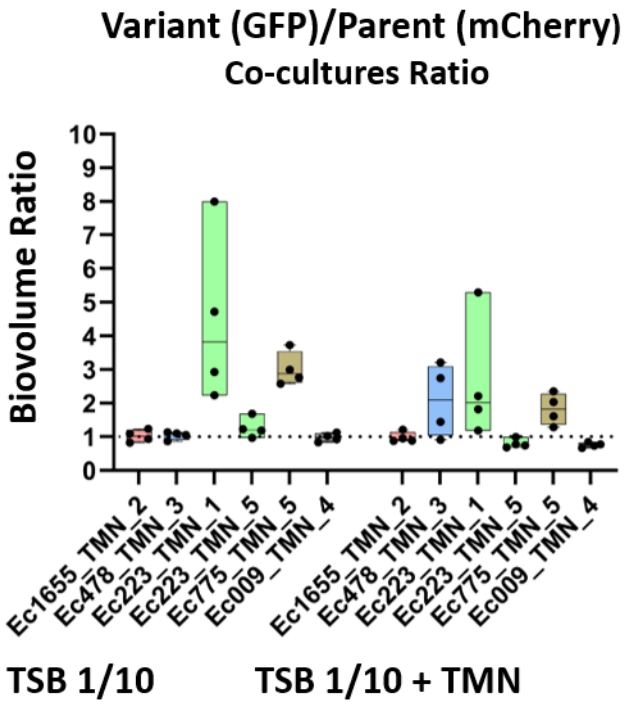

Figure S3. Representation of the biofilm co-cultures ratios for the GFP-tagged variants and their corresponding mCherry-tagged parental strains with or without 2.2 mg/L TMN.

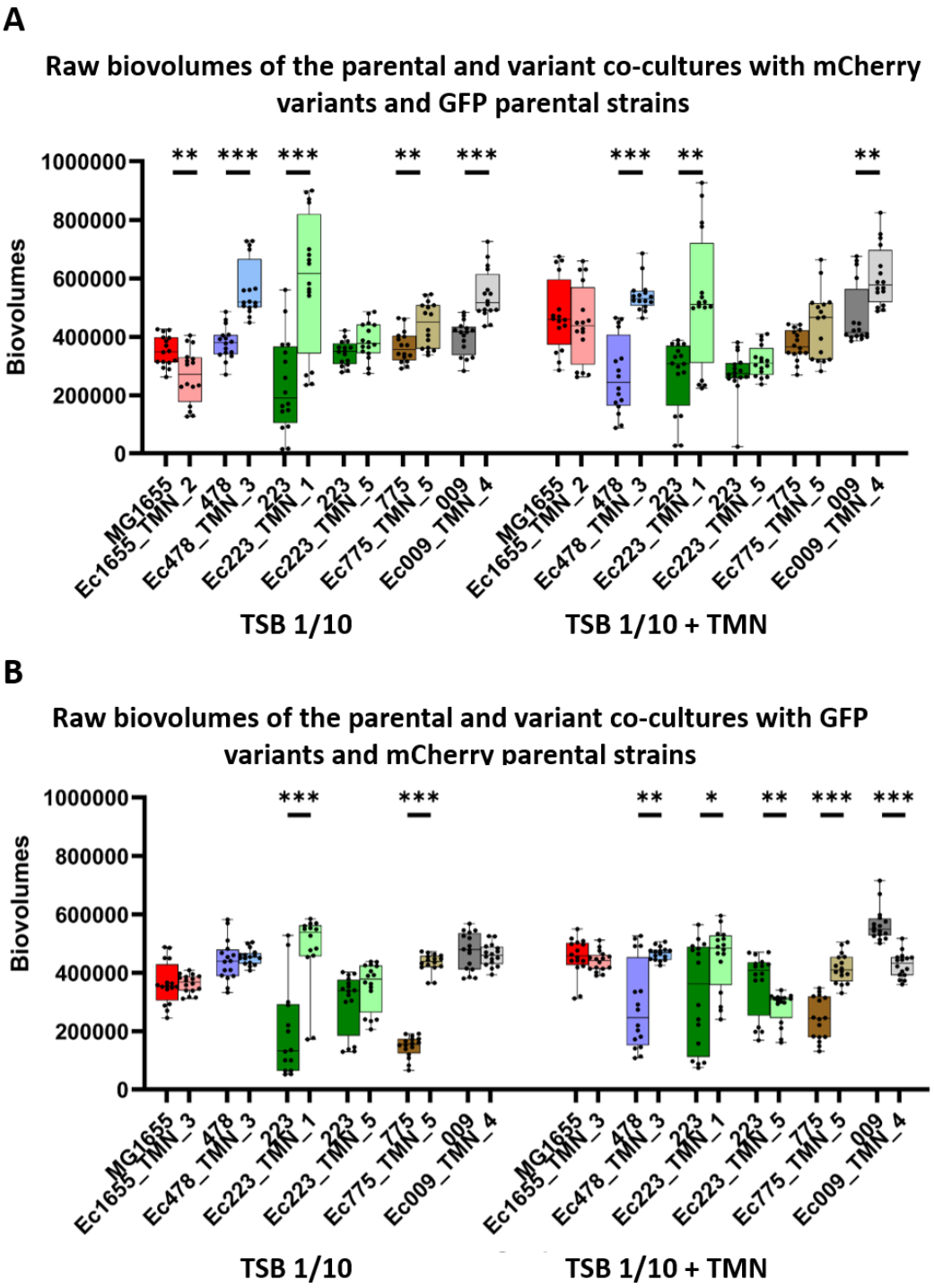

Figure S4. *Raw biovolumes of GFP-tagged parental strains and mCherry-tagged variants (A) and mCherry-tagged parental strains and GFP-tagged variants (B) with or without 2.2 mg/L TMN. Statistical analysis was performed with a Mann-Whitney test between variants and parental strains. P-values are represented as following: * = [0,05-0,01]; ** =]0,01-0,001]; *** = <0,001*

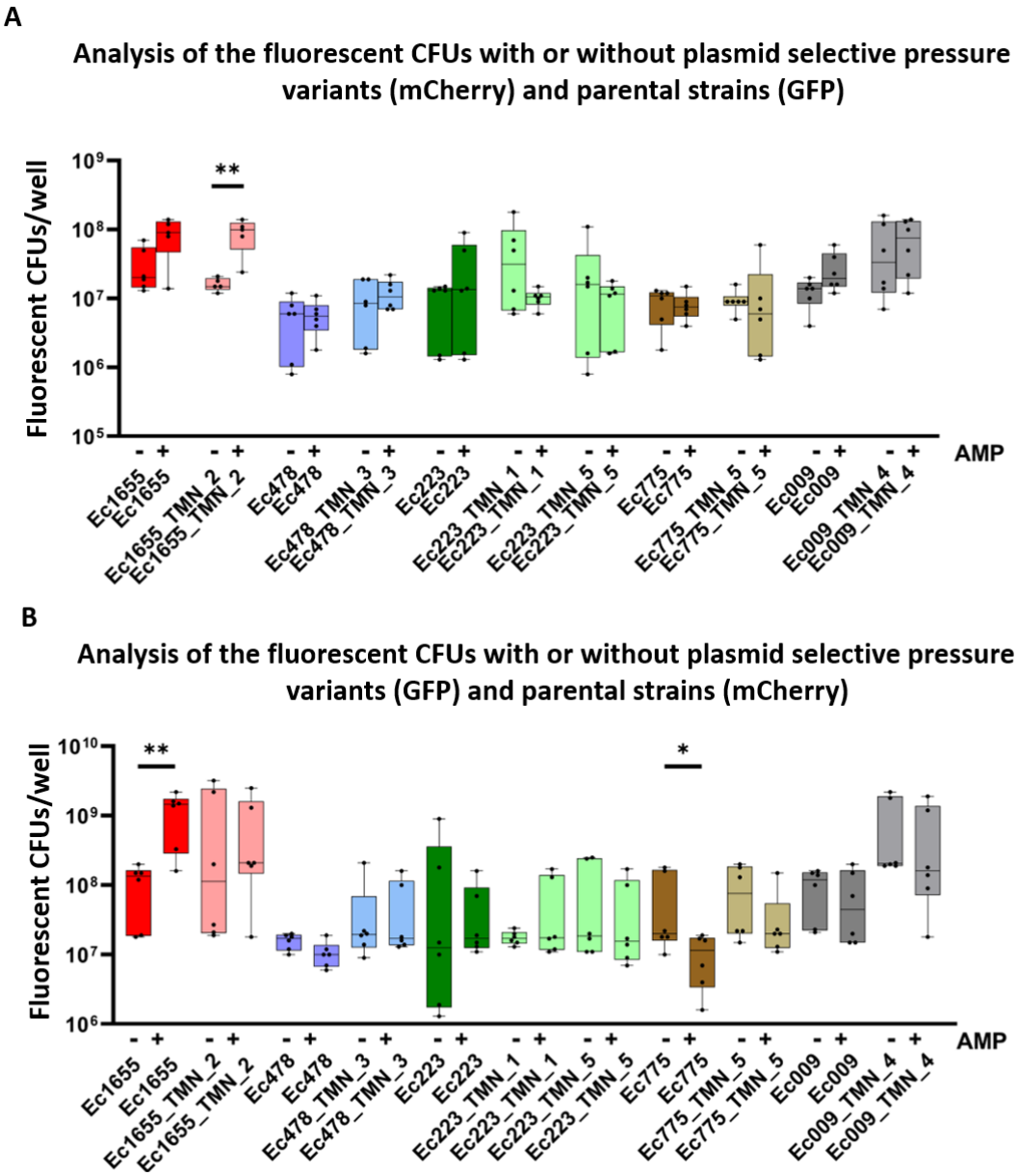

Figure S5. Stability of the plasmid after 72 h, with and without ampicillin selective pressure, in parental strains and variants. Stability was assessed per counting, comparing the CFUs for the mCherry-tagged variants and GFP-tagged parental strains (A) and GFP-tagged variants and mCherry-tagged parental strains (B)

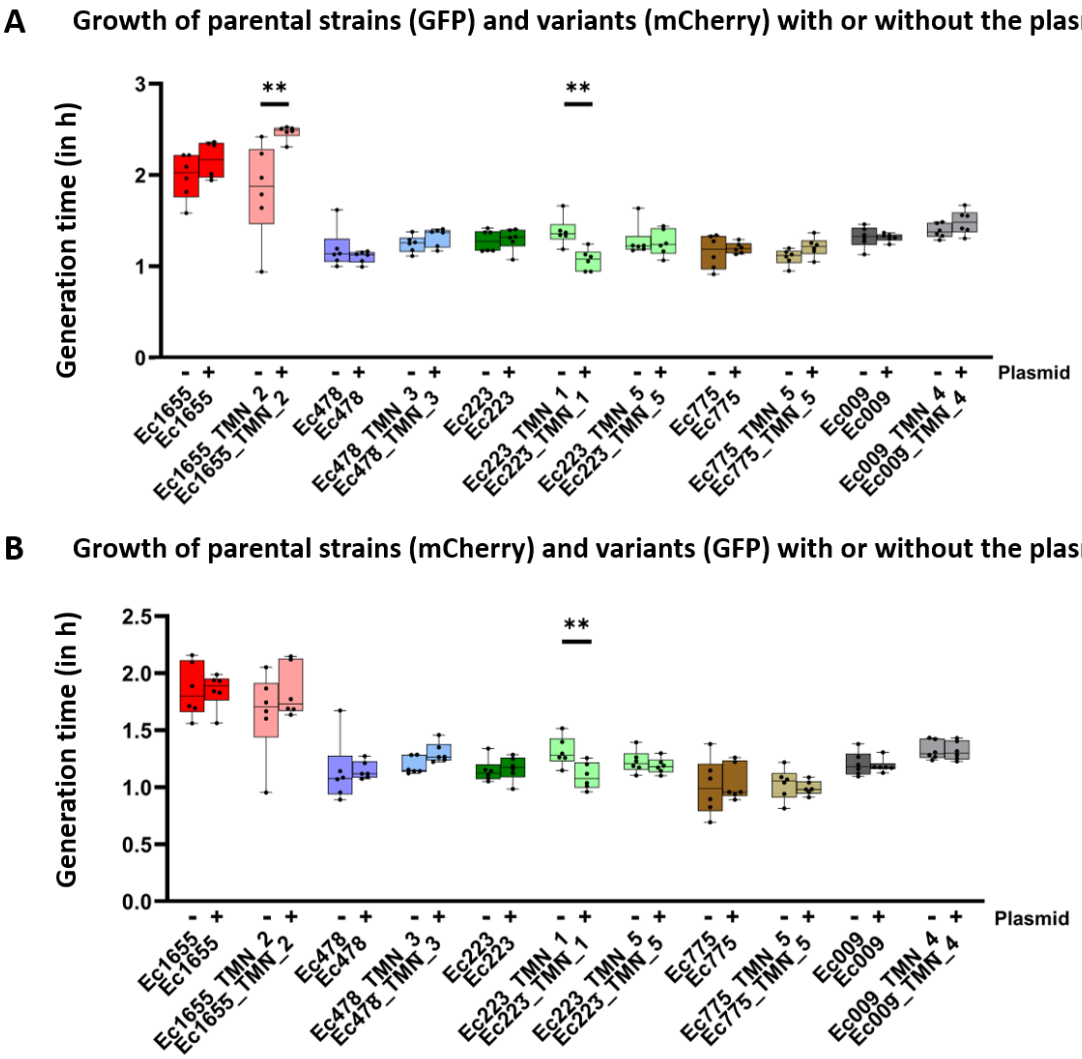

Figure S6. Growth of the strains with or without the GFP or mCherry plasmid in mCherry-tagged variants and GFP-tagged parental strains (A) and GFP-tagged variants and mCherry-tagged parental strains (B)

Table S1: List of all the mutations found in the sequenced variants
Table S2: NCBI accession number for every sequenced genome

Supplementary files can be found on this link:

https://drive.google.com/drive/folders/1uJLVCO6PvYOODHoB_R-QTsapI7gOSPNz?usp=drive_link

Discussion générale et perspectives

1. Rôle des biofilms dans la sélection de résistances

L'objectif central de cette thèse était de mieux comprendre comment le biofilm influence l'apparition de résistances aux antibiotiques en réponse à l'adaptation aux biocides. Deux mécanismes adaptatifs différents ont été mis en lumière :

- Le premier mécanisme implique l'induction de la production de biofilm en réponse à l'exposition au PHMB, favorisant l'émergence de résistances transitoires aux aminoglycosides (cf Résultats *2.*).

- Le second mécanisme concerne la sélection de mutants en présence de TMN présentant des résistances croisées faibles mais stables à la rifampicine et bénéficiant de la structure protectrice du biofilm (cf Résultats *3.*).

La première partie consacrée à l'étude des variants GenR a montré que ces derniers émergent préférentiellement en biofilms. Ce phénomène a été observé même sans pression de sélection, où la quantité de variants était plus importante dans les conditions de biofilm que dans les conditions de surnageant ou de phase planctonique, bien que ce phénomène soit fortement dépendant de la souche. Ces résultats sont en cohérence avec de précédents travaux démontrant la capacité des biofilms à favoriser l'évolution de la résistance aux antimicrobiens, et notamment aux aminoglycosides (Uruén et al., 2020; Usui et al., 2023). Les gradients de nutriments et d'oxygène présents dans les biofilms peuvent induire chez les cellules situées dans les couches profondes du biofilm des réponses à ces conditions sub-optimales (Høiby et al., 2010). L'activation de réponses au stress et le ralentissement de la croissance en résultant, peuvent augmenter la résilience des bactéries à des stress induits par les biocides et les antibiotiques, notamment par l'inactivation de voies métaboliques ciblées par les antimicrobiens (Ciofu et al., 2022) ou par la réduction de l'internalisation des molécules antimicrobiennes (Allison et al., 2011; Ibacache-Quiroga et al., 2018). De plus, une stimulation du taux de mutation est également observée dans les biofilms, en raison de l'activation de polymérases à taux d'erreur élevé dans des cellules en état de stress (Crane et al., 2021).

Dans cette étude, aucun biocide n'a significativement augmenté le nombre de variants présentant une résistance stable à la gentamicine. Toutefois, le PHMB a induit l'apparition de variants avec des résistances transitoires. Une augmentation générale de la quantité de variants GenR a été observée parmi les 8 souches en présence de PHMB dans les biofilms (alors qu'en l'absence de pression de sélection, l'effet était spécifique à certaines souches). En revanche, le nombre de variants émergeant dans les surnageants exposés au PHMB était comparable à celui observé dans les témoins traités à l'eau. Cette augmentation était graduelle, se révélant plutôt dans les deux dernières semaines de l'exposition. Des analyses supplémentaires ont démontré que le PHMB avait un effet sur la production de certains composés de la matrice du biofilm, tels que les polysaccharides, et que les souches s'organisaient au sein de clusters en présence de PHMB. L'hypothèse est donc qu'en réponse à ce stress biocide, les bactéries surproduisent certains composés matriciels, favorisant ainsi l'apparition de micro-environnements où la croissance est limitée, favorables à l'émergence de variants GenR (Figure 12).

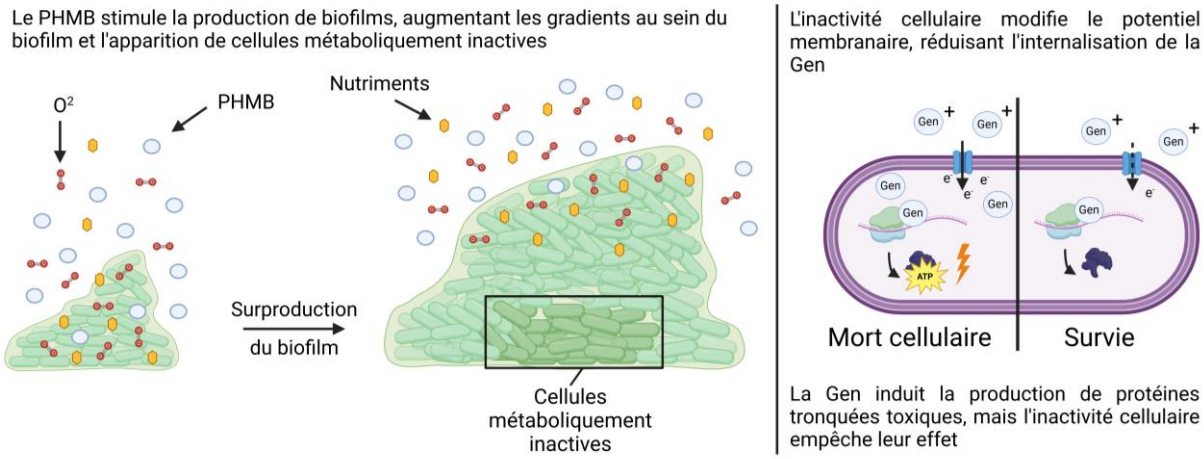

Figure 12 : Schéma bilan représentant l'effet du PHMB sur le biofilm et l'apparition indirecte de variants résistants à la gentamicine. Figure créée avec Biorender.com.

Dans une deuxième partie, une association entre l'exposition à deux biocides (le BAC et la TMN) et l'émergence de résistances croisées à la rifampicine a été observée dans les biofilms. Cet effet n'a pas été observé dans les surnageants. Les variants retrouvés avaient en revanche ici principalement des résistances stables ancrées dans le génome. Dans la condition TMN, l'augmentation du nombre de variants RifR, a pu être directement corrélée à des mutations spécifiques qui étaient absentes dans les souches provenant de la condition témoin (H_2O), liées à la synthèse du LPS. Ces variants étaient également moins sensibles à ce biocide. Ceci reflète un lien plus direct entre l'adaptation des bactéries en biofilm à la TMN et la résistance à l'antibiotique. La raison pour laquelle ces variants émergent plus facilement en biofilms pourrait être que les résistances sont ici faibles et donc que le variant profite de l'effet protecteur du biofilm (Figure 13). Il est notamment connu que les biofilms réduisent les concentrations d'exposition des bactéries, permettant à certains variants de survivre, là où les concentrations biocides plus élevées à l'extérieur du biofilm auraient pu empêcher leur développement (Penesyan et al., 2021; Charron et al., 2023a). De plus, plusieurs études montrent une émergence préférentielle en biofilms de variants avec des résistances plus faibles qu'en condition planctonique, mais avec un taux de compétitivité accru (Santos-Lopez et al., 2019). Certains variants isolés dans les surnageants ont également été séquencés, sans que des mutations dans les gènes de synthèse du LPS ne soient détectées. Cependant le nombre de variants séquencés dans la condition « surnageants » était également plus faible, réduisant *de facto* les chances de détecter de telles mutations.

L'émergence préférentielle des variants dans les biofilms peut également s'expliquer par les effets des mutations dans le LPS sur ce mode de vie. En effet, le LPS est connu pour moduler la structuration spatiale du biofilm, en intervenant dans l'adhésion et l'agrégation des cellules (Beloin et al., 2008; Nakao et al., 2012). Une altération de ces composants membranaires pourrait donc influencer les interactions entre les cellules au sein du biofilm, tout en modulant celles de la cellule avec les composés antimicrobiens. De plus, une augmentation de la production de matrice a été observée chez les variants RifR dans ce travail de thèse. Cette augmentation pourrait résulter d'une disponibilité plus élevée de certains précurseurs utilisés pour la formation de composants du biofilm, qui auraient normalement été utilisés dans la production de LPS (Wang et al., 2021). En effet, les sucres formant l'antigène O du LPS peuvent être utilisés pour la production de certains exopolysaccharides. Toutes ces modifications pourraient être à l'origine de la compétitivité accrue de certains variants au sein de biofilms mixtes vis-à-vis de leurs souches parentales.

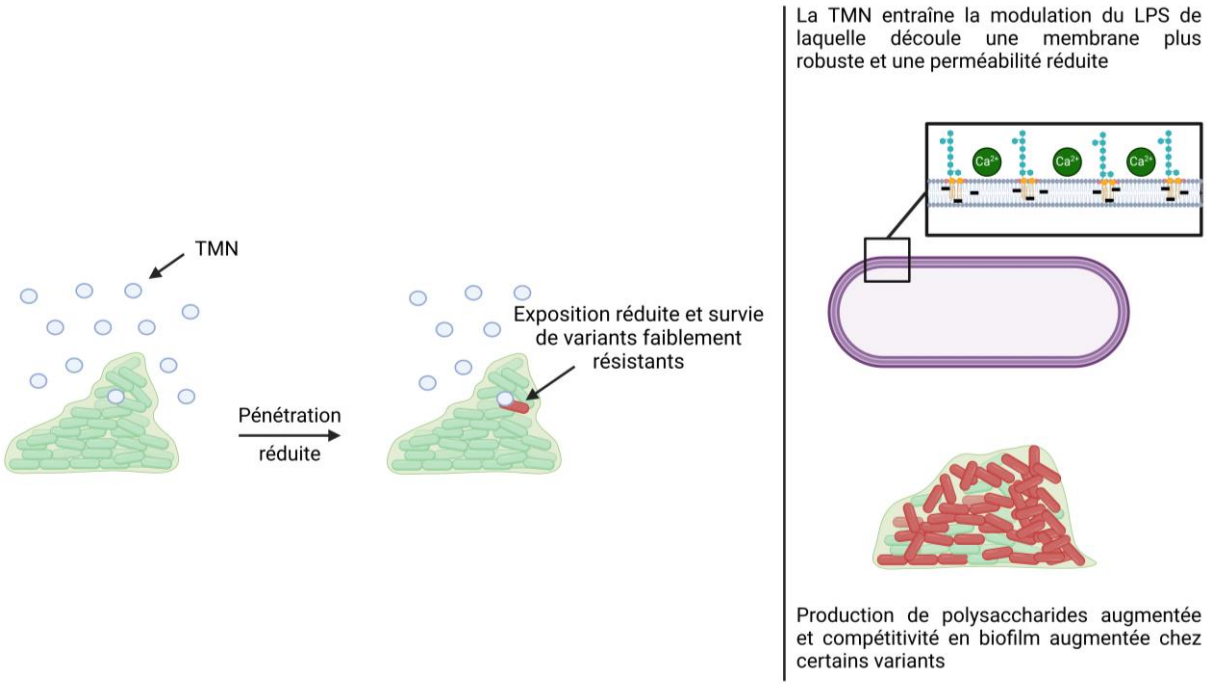

Figure 13 : Schéma bilan représentant comment le biofilm protège les cellules qui y sont enchâssées, modulant ainsi l'apparition de faibles résistances avec des mutations dans la voie de biosynthèse du LPS. Figure créée avec Biorender.com.

2. Caractérisation et compréhension de nouveaux mécanismes de résistance

Les résultats obtenus dans ce travail de thèse ont confirmé certains mécanismes déjà bien documentés et expliqués. Premièrement, les mutations dans les gènes codant la chaîne de respiration cellulaire observées chez les variants GenR sont des cibles connues pour la résistance à cet antibiotique (Ibacache-Quiroga et al., 2018). L'entrée des aminoglycosides dans la cellule nécessite une activité dans la chaîne de transport d'électrons (Krause et al., 2016). Par conséquent, les ralentissements de croissance, qu'ils soient dus à des modifications physiologiques ou génétiques, affectent la résistance des bactéries à la gentamicine.

De même, les mutations dans *rpoB*, qui représentent la majorité des résistances à la rifampicine identifiées dans cette thèse, sont bien connues et caractérisées (Alifano et al., 2015). Ce gène, codant pour la cible principale de la rifampicine, subit des mutations qui modifient la cible, empêchant ainsi la fixation de l'antibiotique (Alifano et al., 2015). Le gène *rpoB* est généralement la première cible analysée par défaut pour caractériser la résistance à la rifampicine (Huang et al., 2009; André et al., 2017). De nombreuses études ont déjà cartographié les sites nucléotidiques mutés en les liant au niveau de résistance à l'antibiotique (Huitric et al., 2006; Berrada et al., 2016; Li et al., 2021; Shea et al., 2021). Dans cette étude, ces mutations semblent émerger de manière stochastique, la quantité de variants mutés dans *rpoB* étant à peu près équivalente entre les conditions H_2O, BAC et TMN.

A l'inverse, les mutations dans les gènes impliqués dans la synthèse du LPS, observées, comme dit précédemment, principalement dans la condition TMN, sont moins bien

caractérisées et soulèvent de nombreuses nouvelles questions. Le LPS est connu pour avoir un rôle clé dans la résistance à plusieurs agents antimicrobiens. Les polymyxines, telles que la colistine (Sabnis et al., 2021), et de nombreux autres peptides antimicrobiens, comme les adhérines (Desriac et al., 2020), sont connus pour interagir directement avec le LPS, leur charge cationique leur permettant de se fixer à la partie négativement chargée du LPS. Cette fixation empêche la fixation de cations divalents stabilisant la membrane et perturbe ainsi l'intégrité cellulaire, amenant à la perte de composés cytoplasmiques et la lyse de la cellule (Sabnis et al., 2021). Certains biocides, comme le BAC et le PHMB, agissent de la même manière, et les résistances liées au lipide A, partie chargée du LPS, ont déjà été identifiées après exposition au BAC (Nordholt et al., 2021). Comme la TMN est également cationique et que les variants semblent subir des modifications de charge, il est probable que le mécanisme de résistance soit similaire. Cependant, les mutations dans les variants induits par la TMN se trouvent dans d'autres régions du LPS. En effet, elles sont principalement localisées dans des gènes codant pour des glycosyltransférases, qui codent pour la synthèse de la partie saccharidique du LPS (Figure 14). La partie « core » du LPS est saccharidique et également négativement chargée, ce qui pourrait expliquer la mutation de *waaU*, impliqué dans la synthèse de l'heptose dans le « core » (Heinrichs et al., 1998). En revanche, certaines mutations affectent la synthèse de l'antigène O, qui n'est pas chargé, soulevant la question du mécanisme de résistance et de l'effet de la TMN sur la bactérie. Les chaînes d'antigène O peuvent avoir un effet sur la partie anionique et donc un effet sur la fluidité de la membrane (Nikaido, 2003). Elles ont également déjà été associées à des réductions de perméabilité à des substances antimicrobiennes (Bryan et al., 1984).

Plusieurs caractérisations supplémentaires seront nécessaires pour élucider le mécanisme d'action de la TMN. Des études d'interactions peuvent être réalisées afin de voir si la TMN interagit directement avec le LPS, en utilisant des méthodes permettant de détecter la fixation d'une molécule à son récepteur, comme la résonance plasmonique de surface (Desriac et al., 2020). D'autres techniques pourraient permettre de préciser le mécanisme et l'interaction entre la TMN et le LPS, comme l'utilisation de la résonance magnétique nucléaire, permettant d'observer directement les zones d'interaction entre la molécule et le LPS. Ainsi, il serait possible de voir si la TMN se fixe directement au niveau des parties chargées du LPS et d'un potentiel lien avec la conformation de l'antigène O (Mares et al., 2009). Si la partie lipidique du LPS est généralement bien conservée, la création d'une banque de mutants avec des LPS ayant des profils d'antigène O diversifiés pourrait également permettre de tester l'effet d'une longueur plus ou moins élevée de la chaîne de l'antigène O sur la survie face à la TMN, afin de préciser le lien entre le LPS et cette molécule. L'utilisation d'autres espèces, telles que *Neisseria meningitidis* ou *Acinetobacter baumannii,* chez lesquelles le LPS n'est pas essentiel, pourrait également aider à caractériser les effets de la TMN sur des souches dépourvues de LPS (Zhang et al., 2013).

La question du mécanisme se pose également pour la résistance à la rifampicine. Contrairement aux biocides précédemment cités, la rifampicine n'est pas chargée, et son mécanisme d'action est bien connu. Une membrane plus structurée et rigide pourrait être à l'origine de la résistance observée. Il est établi que le LPS participe à l'exclusion de molécules hydrophobes hors de la cellule (Bertani and Ruiz, 2018), or la rifampicine est hydrophobe (Motiei et al., 2021). Des tests de diffusion avec des molécules fortement hydrophobes, comme la testostérone, pourraient être effectués sur les variants et leurs souches parentales, pour déterminer si des différences de pénétration sont observées (Plesiat et al., 1997).

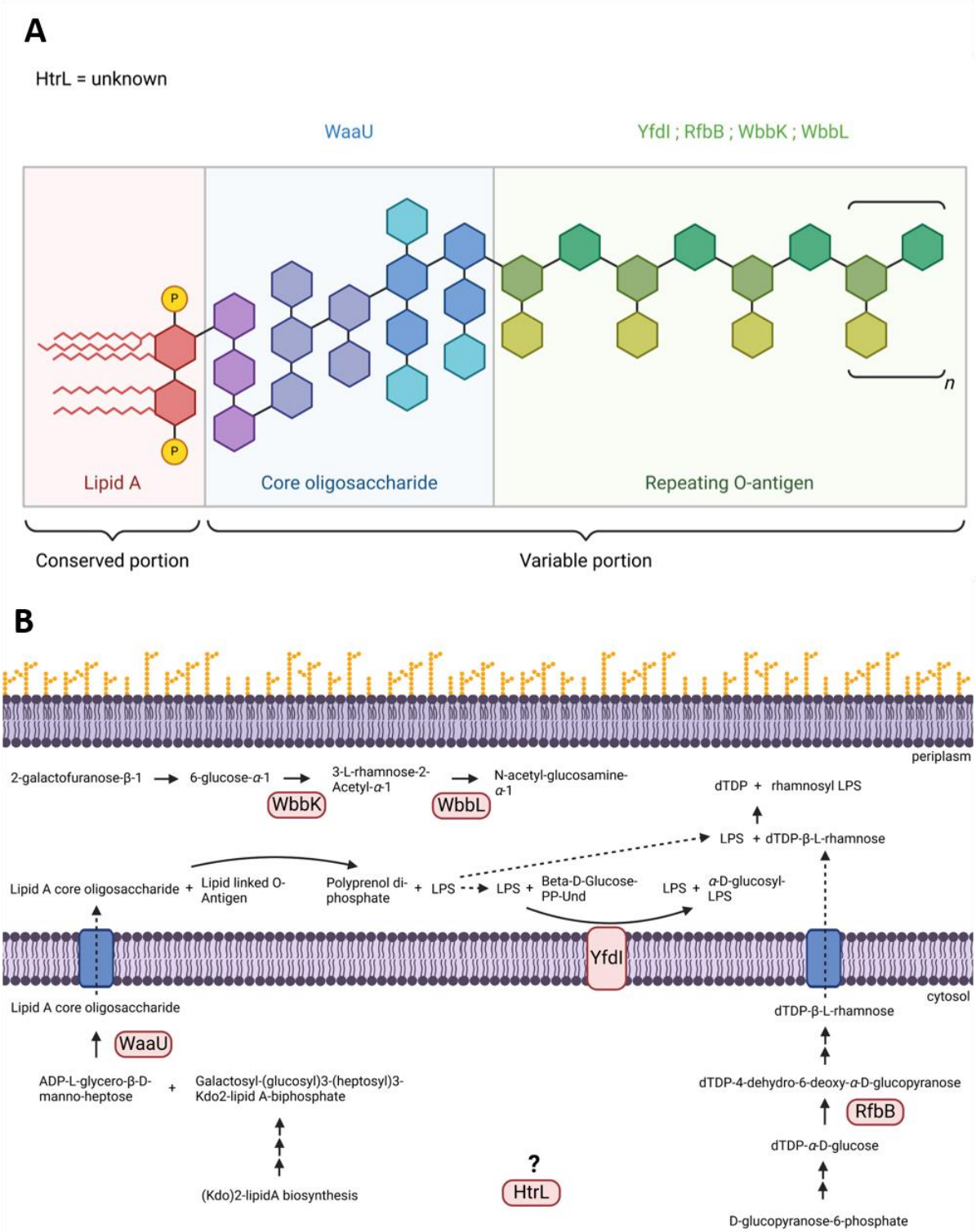

Figure 14 : Structure typique du LPS et association de chaque gène muté avec la partie du LPS pour laquelle ils participent à la synthèse (A). Détail des réactions enzymatiques associées à chacun des gènes ainsi que la localisation dans la cellule dans laquelle elles ont lieu (B). Figure créée avec Biorender.com.

3. Convergence adaptative des souches

Un des points forts de cette thèse réside dans le fait que les expériences d'évolution en présence de biocides ont été effectuées sur un panel de 9 souches, révélant des convergences évolutives malgré une diversité génétique initiale significative.

Premièrement, l'effet du PHMB a été global, avec une augmentation du nombre de variants GenR chez la majorité des 8 souches testées. La modulation de la structure tridimensionnelle du biofilm en réponse au PHMB, via la formation d'amas denses de bactéries et une augmentation de la production de matrice, a été observée chez la plupart des souches, suggérant une stratégie adaptative partagée. Ce constat est d'autant plus remarquable qu'en absence de biocides, les souches semblent évoluer de manière distincte. Par exemple, Ec709 et Ec1655 montrent une forte propension à produire un grand nombre de variants GenR en biofilms, sans pression de sélection, contrairement aux autres souches.

Deuxièmement, une modulation des LPS conférant une résistance à la rifampicine en présence de TMN a été observée chez 6 des 8 souches étudiées. Ici encore, la récurrence de cette réponse adaptative est d'autant plus intéressante que le fond génétique des souches et leur capacité à générer de la diversité génétique varie considérablement. Par exemple, les souches Ec1655 et Ec956 avaient un nombre élevé de variants RifR dès le début de l'expérience, tandis que celui-ci était très bas chez les souches Ec009 et Ec478 tout le long de l'exposition.

Mieux comprendre l'articulation entre la « mutabilité » spontanée des souches et leurs capacités adaptatives et évolutives face à un stress donné (biocide par exemple), notamment vis-à-vis du développement de résistances, est crucial. La forte capacité d'une souche à produire de la diversité génétique (comme les souches hypermutatrices) est souvent considérée comme un facteur clé dans le développement de résistances multiples (Maciá et al., 2005; Gifford et al., 2023). Une évaluation plus précise du taux de mutation des différentes souches étudiées pourrait être réalisée via le test de fluctuation de Luria-Delbrück (Rosche and Foster, 2000) pour approfondir ce lien. Un autre facteur pouvant expliquer cette différence dans la production de variants, est le fond génétique propre à chaque souche, qui influence le coût compétitif de certaines mutations, favorisant ou non la fixation de certains variants dans la population (Mullis et al., 2018; Nucci et al., 2023). Pour identifier les gènes ou mutations responsables des convergences ou divergences entre les souches, il serait intéressant de reproduire ces expériences d'évolution en présence de biocide sur un panel bien plus large de souches. La vaste collection du LNR-Résistance antimicrobienne du laboratoire de Fougères, qui regroupe des souches d'*E. coli* isolées de la chaîne alimentaire depuis 25 ans, pourrait être utilisée dans cet objectif. Une étude d'association pangénomique (Genome Wide Association Study, GWAS) permettrait alors de relier certains phénotypes adaptatifs à des déterminants génétiques spécifiques impliqués dans l'évolution (Chen and Shapiro, 2015).

La convergence évolutive observée ici chez *E. coli*, en réponse au PHMB et à la TMN, pose naturellement la question des mécanismes d'adaptation chez d'autres espèces bactériennes, étant donné l'influence de la variabilité génomique sur l'adaptation aux biocides. Dans le cas de l'adaptation dans la voie de biosynthèse du LPS, il est certain que ce mécanisme est restreint aux souches gram négatives, comme les souches gram positives ne possèdent pas de LPS (Silhavy et al., 2010). Il serait donc intéressant d'examiner les mécanismes d'adaptation spécifiques aux souches gram positives, notamment celles qui posent des problèmes de contamination alimentaire comme *Listeria monocytogenes* ou *Enterococcus faecium* (Farber and Peterkin, 1991; Giraffa, 2002).

4. Spécificité des mécanismes adaptatifs selon les biocides

Bien qu'une convergence des stratégies d'adaptation ait été observée parmi les souches pour certains biocides, des réponses adaptatives distinctes ont émergé en fonction du mode d'action spécifique de chaque biocide. Quatre substances actives biocides ont été testées dans ce travail de thèse, chacune associée à une spécificité des résistances croisées développées aux antibiotiques. Alors que le PHMB induisait plutôt des résistances transitoires à la gentamicine, la TMN et le BAC étaient associés au développement de résistance à la rifampicine, tandis que le SHY n'a pas entraîné, dans nos conditions, une résistance croisée à un antibiotique. Ces résultats soulignent que les effets des biocides varient et que les stratégies d'adaptation des bactéries diffèrent en conséquence.

Dans ce contexte, l'augmentation de variants résistants à la rifampicine en condition TMN et BAC pourrait s'expliquer par une certaine similarité entre ces deux molécules, même si les mutations retrouvées étaient ici différentes. Le LPS reste une cible potentiellement commune entre ces deux molécules, ayant déjà été identifié par le passé en réponse au BAC (Nordholt et al., 2021). Cependant, dans cette étude, le BAC n'a pas sélectionné de variants dans cette voie, peut-être en raison des concentrations utilisées, des souches ou bien du mode de vie. La TMN, quant à elle, est ici caractérisée pour la première fois en termes d'induction de résistances croisées aux antibiotiques, ce qui ne permet pas encore une comparaison solide avec la littérature. Néanmoins, cette thèse a permis de mieux comprendre son mécanisme d'action, et ouvre la voie à de nouvelles recherches sur cette substance active biocide, dont l'utilisation est en pleine expansion dans plusieurs filières agro-alimentaires (Bridier et al., 2021).

Les mécanismes d'adaptation aux biocides restent globalement encore peu décryptés. Cette thèse met en lumière l'importance de mener des études à grande échelle, en testant plusieurs biocides. Cela permet d'établir des corrélations plus précises et de limiter les effets des variations de protocole souvent observées entre différentes études menées dans différents laboratoires. Elle démontre aussi une nécessité de développer des protocoles standardisés, permettant la reproductibilité des résultats entre les laboratoires. Des premiers protocoles en ce sens ont déjà été développés (Wesgate et al., 2016). Cependant, ceux-ci se basent sur des cellules planctoniques, et, à ce jour, aucun protocole standardisé pour l'étude des biofilms n'a été adopté (Maillard and Centeleghe, 2023).

5. Transfert des résultats et application en filières industrielles

Les résultats de cette thèse soulèvent la question de l'émergence de variants résistants en dehors de conditions de laboratoire. Certains paramètres expérimentaux ont été spécifiquement établis pour se rapprocher des conditions industrielles. Tout d'abord, la température à laquelle les biofilms ont été exposés était, comme souvent en industrie, ambiante (Piras et al., 2015). Avant l'exposition aux biocides, les biofilms ont également eu une phase de pré-croissance de 72 heures, imitant ainsi les biofilms préétablis dans les chaînes de production. Enfin, le choix de travailler avec plusieurs souches, principalement isolées sur les chaînes de production alimentaire au cours des dix dernières années, permet de mieux refléter la diversité et la réalité industrielle de la chaîne alimentaire, en termes de modèles bactériens.

Néanmoins, dans les industries agro-alimentaires, les biofilms sont souvent bien plus complexes que ceux produits dans des conditions expérimentales de laboratoire, avec des espèces bactériennes coexistant les unes avec les autres (Yuan et al., 2022; Guéneau et al., 2023). Les interactions écologiques entre espèces, sont susceptibles de jouer un rôle important dans la survie et l'orientation de leur évolution adaptative (Sanchez-Vizuete et al., 2015; Yuan et al., 2022; Guéneau et al., 2023; Sadiq et al., 2023). La protection conférée par les biofilms multi-espèces à certaines souches bactériennes faiblement productrices de biofilms, y compris des pathogènes, face aux traitements de désinfection a, par exemple, déjà été documentée (Bridier et al., 2012; Sanchez-Vizuete et al., 2015). Il serait donc pertinent d'étudier l'évolution de plusieurs espèces simultanément et l'adaptation aux biocides de communautés bactériennes complexes prélevées directement en industrie, afin de mieux comprendre la dynamique des populations bactériennes au cours d'une exposition aux biocides.

Par ailleurs, le milieu de culture utilisé, du BTS dilué au dixième, ne reflète pas nécessairement les conditions dans lesquels poussent les bactéries dans les industries agro-alimentaires, où l'apport de nutriments est plus irrégulier, mais où les matières organiques présentes peuvent considérablement enrichir l'environnement bactérien. La dilution du BTS a été choisie pour limiter les risques d'interférence de certains composants du milieu avec les molécules biocides (Condell et al., 2012).

Le support de croissance utilisé pour les biofilms était des microplaques 96 puits, adaptées aux expériences à grande échelle nécessitant de multiple réplicats. Cependant, ce support n'est pas nécessairement représentatif des surfaces rencontrées en industrie. Pour simuler ces surfaces industrielles, il serait pertinent d'utiliser des coupons de matériaux couramment retrouvés dans les industries agro-alimentaires, tels que l'acier inoxydable (Leriche et al., 2003; Cuzin et al., 2021) ou le polytétrafluoroéthylène (Maifreni et al., 2023), afin d'étudier les capacités de colonisation des variants sur ces surfaces.

Enfin, une divergence importante entre les conditions utilisées dans cette étude et celles rencontrées en industrie concerne les biocides eux-mêmes. Les molécules choisies ici représentent les substances actives et ont été utilisées séparément afin d'étudier spécifiquement leur mécanisme d'action, et homogénéiser les résultats avec ceux de la littérature. Cependant, les solutions commerciales sont souvent composées d'un mélange de plusieurs substances actives ainsi que d'autres composés influant sur la texture, la stabilité ou encore les propriétés tensioactives du produit (Maillard, 2002; Forbes et al., 2017; Bridier et al., 2021). De plus, les concentrations d'utilisation dans cette étude diffèrent considérablement de celles retrouvées dans les industries. Dans ces dernières, les biocides sont souvent utilisés à des concentrations 100 à 1000 fois supérieures (Jones and Joshi, 2021; Maillard and Pascoe, 2024). Cela questionne la possibilité de l'émergence des mutations retrouvées ici en présence de concentrations aussi élevées. Ces concentrations n'ont pas pu être utilisées dans l'étude car elles auraient probablement éradiqué l'intégralité de la population dans notre modèle de laboratoire. Cependant, comme évoqué précédemment, de nombreux facteurs incluant la présence de matière organique et de substances interférentes, la topologie des chaînes de production et la présence de biofilms plus complexes, peuvent réduire localement les concentrations des biocides désinfectants auxquelles sont réellement exposées les bactéries en industrie agroalimentaire. Cela augmente la probabilité d'exposition des bactéries à des concentrations sub-inhibitrices similaires à celles utilisées dans cette thèse, favorisant ainsi les phénomènes adaptatifs qui en découlent.

Ce type d'étude pourrait néanmoins constituer une base pour le développement de marqueurs de résistance croisée qui pourraient, *in fine,* servir au développement d'outils de surveillance précoce dans la chaîne alimentaire. Par exemple, des PCR ciblant des mutations précises pourraient être mises en place pour identifier des variants présents dans les chaînes de production. L'identification sur BLAST de certaines mutations retrouvées dans l'étude, chez des souches environnementales, ouvre la possibilité que certains phénotypes puissent être sélectionnés dans la nature. Une analyse approfondie de ces souches, qui confirme qu'elles possèdent bien le phénotype de résistance, serait cependant nécessaire pour valider cette hypothèse.

A l'avenir, des recherches plus appliquées sur les effets de la TMN lors de son utilisation en agro-industrie pourraient permettre d'en préciser l'impact réel. Par exemple, des projets de métagénomique shotgun pourraient être effectués sur des échantillons prélevés dans des industries utilisant ou n'utilisant pas la TMN, pour déterminer si son utilisation est associée à la présence de certains gènes de résistance (Bridier, 2019). L'utilisation de coupons détachables pourrait également permettre de collecter des biofilms environnementaux et les observer dans leur état naturel, afin de voir l'effet de la TMN sur la structuration spatiale des biofilms (Guéneau et al., 2021). Enfin, au sein du laboratoire, des protocoles expérimentaux visant à simuler les conditions industrielles, notamment celles où des interférences avec le biocide réduisent son efficacité, pourraient être utilisés (Wesgate et al., 2016).

6. Impact sanitaire des adaptations et résistances révélées

Les résistances identifiées dans cette étude soulèvent naturellement des questions cruciales concernant leurs effets potentiels sur la santé publique, notamment dans le cadre de l'approche « One Health ». Parmi ces effets, les échecs thérapeutiques liés à ces résistances représentent un enjeu majeur. Les phénotypes de résistance à la gentamicine induits par le PHMB résultent principalement de modifications physiologiques transitoires. Une fois le stress éliminé, ces résistances ne sont généralement pas maintenues, ce qui réduit les risques d'une persistance du phénotype en cas d'infection humaine ultérieure. Des études récentes montrent cependant qu'une survie prolongée sous stress peut augmenter la probabilité de développer des mutations stabilisatrices favorisant une persistance face aux traitements et conduisant potentiellement à des résistances accrues (Bakkeren et al., 2020). En effet, la survie rallongée des bactéries et le taux de mutation accentué par l'état de stress, augmentent le risque de développement de mutations de résistance stables (Levin-Reisman et al., 2019).

Des études effectuées avec le BAC montrent qu'une exposition répétée à ce biocide entraîne une augmentation progressive de la quantité de cellules survivant au stress, menant à des mutations ancrées dans le génome (Nordholt et al., 2021). Des études similaires pourraient être effectuées avec le PHMB, pour déterminer si l'exposition répétée accroît la survie bactérienne et favorise l'émergence de mutations conférant une résistance au biocide, voire une résistance croisée aux antibiotiques, comme cela a été démontré pour la gentamicine (Cuzin et al., 2021).

En ce qui concerne les résistances associées au LPS, celles-ci sont bien ancrées dans le génome mais demeurent de faible niveau. Ces résistances pourraient toutefois favoriser la survie des souches, augmentant ainsi le risque de mutations supplémentaires. Leur faible coût de fitness est également favorable à une survie accrue dans certaines conditions et ainsi à une dissémination jusqu'à l'humain. Etant donné l'impact limité des mutations sur la résistance, il

serait pertinent de déterminer si celle-ci se restreint à une survie favorisée dans des conditions expérimentales ou si elle a un effet sur la survie à un traitement antibiotique *in vivo*. Dans ce but, une souche pathogénique d'*E. coli* pourrait être utilisée, dans laquelle les mutations identifiées dans l'étude pourraient être introduites par clonage moléculaire.

7. Effet des biocides sur la dissémination de résistances non-mutatoires

Au cours de cette thèse, les résistances étudiées se sont restreintes à celles dues à des mutations dans le génome. Certaines de ces mutations n'entrainent pas de coût compétitif significatif et ont déjà été identifiées dans des isolats cliniques (Munita and Arias, 2016). Cependant, cette tendance n'est pas générale, une majorité des mutations impactant la croissance des bactéries et donc leur capacité à se disséminer (Vanacker et al., 2023). Pour certaines classes d'antibiotiques comme les fluoroquinolones ou les rifamycines, il est courant d'observer des résistances dans des échantillons cliniques dues à des mutations (Zulfiana et al., 2021; An et al., 2023). Pour d'autres classes en revanche, les bactéries privilégient l'acquisition de gènes de résistance via des mécanismes de transfert horizontal de gènes (HGT), plutôt que par mutation. Par exemple, pour les céphalosporines de 3^{e} génération ou les carbapénèmes, les résistances résultent plus fréquemment de l'acquisition de gènes que de mutations (van Hoek et al., 2011).

En plus d'augmenter les risques de propagation, en n'étant pas restreints à des transmissions verticales comme les mutations, ces gènes de résistance sont d'autant plus inquiétants que les éléments génétiques mobiles (MGE) sur lesquels ils se trouvent (plasmides, intégrons, etc) possèdent en général plusieurs gènes et permettent donc la propagation simultanée de nombreuses résistances. Les MGE sont notamment connus pour porter des gènes de résistances aux biocides, tels que les gènes *qac*, codant pour des pompes d'efflux à large spectre. Ces pompes d'efflux tirent leur nom des ammoniums quaternaires (QAC = Quaternary Ammonium Compound), qu'elles peuvent rejeter hors de la cellule (Slipski et al., 2021). Elles peuvent donc à la fois être responsables de résistances croisées en étant capables de rejeter des biocides et des antibiotiques hors de la cellule, mais aussi de sélection croisée en se trouvant sur les mêmes MGE que d'autres gènes de résistance à d'autres molécules (von Wintersdorff et al., 2016).

Les biofilms sont souvent décrits comme des environnements privilégiés pour les transferts de gènes, en raison de la proximité cellulaire et des conditions micro-environnementales spécifiques qui peuvent jouer un rôle crucial dans ce processus (Lee et al., 2022). Par exemple, il a déjà été montré qu'en état de stress, les machineries de transfert horizontal de gènes peuvent être induites (Beaber et al., 2004). Le transfert de plasmides conjugatifs constitue un des mécanismes majeurs dans la dissémination des gènes de résistance (von Wintersdorff et al., 2016). Certaines études ont montré que la conjugaison peut être induite par certaines molécules biocides, notamment les QAC, le peroxyde d'hydrogène, la chlorhexidine ou le triclosan (Zhang et al., 2017; Jutkina et al., 2018; Han et al., 2019; Zhu et al., 2023). Toutefois, les données disponibles restent limitées, notamment dans le contexte des biofilms, et parfois contradictoires. Il est donc essentiel de déterminer si les biocides influencent réellement la dissémination des gènes de résistance dans les biofilms via HGT, ainsi que les concentrations impliquées.

L'impact des biocides sur le transfert de plasmides sera abordé dans un « work-package » dédié du projet ANR JCJC BAoBAb, auquel j'aurai l'occasion de participer lors de mon post-doctorat. Nous exploiterons des souches d'*E. coli* possédant un plasmide comportant des gènes de résistance aux antibiotiques, ainsi que, soit un gène codant pour la RFP (Red Fluorescent Protein) (bactérie « donneuse », fluorescence rouge), soit un gène codant pour la GFP (bactérie « receveuse », fluorescence verte). L'analyse et la quantification des souches donneuses, receveuses, et des transconjugants après une exposition à des résidus de biocides seront réalisées par cytométrie en flux et par dénombrement sur milieux sélectifs. Cette approche permettra de mieux comprendre l'impact des résidus de biocides sur le transfert de gènes de résistance au sein des biofilms.

Conclusion

Conclusion

Ce travail de thèse a permis de caractériser plusieurs stratégies d'adaptation des bactéries aux biocides et d'explorer leur rôle dans l'émergence de résistances aux antibiotiques. Les résultats montrent que les biofilms jouent un rôle clé dans la protection et l'adaptation des bactéries ainsi que dans l'émergence de variants résistants susceptibles de développer des résistances croisées aux antibiotiques. La relation étroite entre la structure du biofilm et sa modulation en réponse aux traitements biocides, l'hétérogénéité phénotypique, et l'émergence de résistance aux antibiotiques souligne l'importance cruciale d'intégrer cette notion d'adaptation collective pour mieux évaluer les risques liés à l'utilisation des biocides en lien avec l'antibiorésistance sur la chaîne alimentaire.

La méthodologie employée durant la thèse s'est avérée efficace pour identifier des associations entre biocides et résistances aux antibiotiques et pourra servir de modèle dans le futur pour de nouveaux cribles. Cette méthodologie a notamment permis de mettre en lumière la spécificité des réponses adaptatives aux substances actives biocides et souligne l'importance de multiplier les études sur différents couples substance-espèce/souche bactérienne représentatifs de la chaîne alimentaire. Cela permettra de mieux identifier la pluralité des voies d'adaptation bactérienne, en lien avec le développement de résistances croisées à des antibiotiques d'intérêt majeur dans une perspective One Health.

Ces découvertes interrogent donc sur l'impact de l'utilisation massive des biocides dans notre société, accentuée depuis la pandémie de Covid-19. Certaines substances biocides comme la TMN sont de plus en plus utilisées, notamment en guise de remplacement de substances comme les ammoniums quaternaires, mais sans que leurs effets sur les bactéries soient encore bien connus. Sans remettre en cause l'utilisation des biocides, cette thèse souligne l'importance de proposer de nouvelles perspectives de recherches tant au laboratoire qu'en milieu industriel, afin de caractériser en détail les effets de l'usage des biocides désinfectants sur les bactéries. A terme, cela pourrait amener à une utilisation plus éclairée et une régulation plus précise de ces molécules, qui demeurent des outils indispensables pour garantir l'hygiène des surfaces et éviter la transmission d'agents pathogènes.

Références bibliographiques

Références bibliographiques

Alifano, P., Palumbo, C., Pasanisi, D., and Talà, A. (2015). Rifampicin-resistance, rpoB polymorphism and RNA polymerase genetic engineering. *J Biotechnol* 202, 60–77. doi: 10.1016/j.jbiotec.2014.11.024

Allison, K. R., Brynildsen, M. P., and Collins, J. J. (2011). Metabolite-enabled eradication of bacterial persisters by aminoglycosides. *Nature* 473, 216–220. doi: 10.1038/nature10069

Alonso, M. Z., Lucchesi, P. M. A., Rodríguez, E. M., Parma, A. E., and Padola, N. L. (2012). Enteropathogenic (EPEC) and Shigatoxigenic *Escherichia coli* (STEC) in broiler chickens and derived products at different retail stores. *Food Control* 23, 351–355. doi: 10.1016/j.foodcont.2011.07.030

An, Q., Lin, R., Yang, Q., Wang, C., and Wang, D. (2023). Evaluation of genetic mutations associated with phenotypic resistance to fluoroquinolones, bedaquiline, and linezolid in clinical *Mycobacterium tuberculosis*: A systematic review and meta-analysis. *J Glob Antimicrob Resist* 34, 214–226. doi: 10.1016/j.jgar.2023.05.001

André, E., Goeminne, L., Colmant, A., Beckert, P., Niemann, S., and Delmee, M. (2017). Novel rapid PCR for the detection of Ile491Phe rpoB mutation of *Mycobacterium tuberculosis*, a rifampicin-resistance-conferring mutation undetected by commercial assays. *Clin Microbiol Infect* 23, 267.e5-267.e7. doi: 10.1016/j.cmi.2016.12.009

ANSES (2023a). Bilan du suivi de l'antibiorésistance en santé animale et de la vente des antibiotiques à usage vétérinaire. Available at: https://www.anses.fr/fr/system/files/Press2023DPA01.pdf

ANSES (2023b). Suivi des ventes de médicaments vétérinaires contenant des antimicrobiens en France en 2022. Available at: https://www.anses.fr/fr/system/files/ANMV-Ra-Antibiotiques2022.pdf

Aslam, B., Khurshid, M., Arshad, M. I., Muzammil, S., Rasool, M., Yasmeen, N., et al. (2021). Antibiotic Resistance: One Health One World Outlook. *Front Cell Infect Microbiol* 11, 771510. doi: 10.3389/fcimb.2021.771510

Aslam, M., Greer, G. G., Nattress, F. M., Gill, C. O., and McMullen, L. M. (2004). Genotypic analysis of *Escherichia coli* recovered from product and equipment at a beef-packing plant. *J Appl Microbiol* 97, 78–86. doi: 10.1111/j.1365-2672.2004.02277.x

Bakkeren, E., Diard, M., and Hardt, W.-D. (2020). Evolutionary causes and consequences of bacterial antibiotic persistence. *Nat Rev Microbiol* 18, 479–490. doi: 10.1038/s41579-020-0378-z

Ballén, V., Cepas, V., Ratia, C., Gabasa, Y., and Soto, S. M. (2022). Clinical *Escherichia coli*: From Biofilm Formation to New Antibiofilm Strategies. *Microorganisms* 10, 1103. doi: 10.3390/microorganisms10061103

Beaber, J. W., Hochhut, B., and Waldor, M. K. (2004). SOS response promotes horizontal dissemination of antibiotic resistance genes. *Nature* 427, 72–74. doi: 10.1038/nature02241

Beloin, C., Roux, A., and Ghigo, J. M. (2008). *Escherichia coli* biofilms. *Curr Top Microbiol Immunol* 322, 249–289. doi: 10.1007/978-3-540-75418-3_12

Berrada, Z. L., Lin, S.-Y. G., Rodwell, T. C., Nguyen, D., Schecter, G. F., Pham, L., et al. (2016). Rifabutin and rifampin resistance levels and associated rpoB mutations in clinical isolates of

Mycobacterium tuberculosis complex. *Diagn Microbiol Infect Dis* 85, 177–181. doi: 10.1016/j.diagmicrobio.2016.01.019

Bertani, B., and Ruiz, N. (2018). Function and Biogenesis of Lipopolysaccharides. *EcoSal Plus* 8. doi: 10.1128/ecosalplus.ESP-0001-2018

Bódi, Z., Farkas, Z., Nevozhay, D., Kalapis, D., Lázár, V., Csörgő, B., et al. (2017). Correction: Phenotypic heterogeneity promotes adaptive evolution. *PLoS Biol* 15, e1002607. doi: 10.1371/journal.pbio.1002607

Bridier, A. (2019). Exploring Foodborne Pathogen Ecology and Antimicrobial Resistance in the Light of Shotgun Metagenomics. *Methods Mol Biol* 1918, 229–245. doi: 10.1007/978-1-4939-9000-9_19

Bridier, A., Briandet, R., Thomas, V., and Dubois-Brissonnet, F. (2011a). Resistance of bacterial biofilms to disinfectants: a review. *Biofouling* 27, 1017–1032. doi: 10.1080/08927014.2011.626899

Bridier, A., Dubois-Brissonnet, F., Greub, G., Thomas, V., and Briandet, R. (2011b). Dynamics of the action of biocides in *Pseudomonas aeruginosa* biofilms. *Antimicrob Agents Chemother* 55, 2648–2654. doi: 10.1128/AAC.01760-10

Bridier, A., Sanchez-Vizuete, M. D. P., Le Coq, D., Aymerich, S., Meylheuc, T., Maillard, J.-Y., et al. (2012). Biofilms of a *Bacillus subtilis* hospital isolate protect *Staphylococcus aureus* from biocide action. *PLoS One* 7, e44506. doi: 10.1371/journal.pone.0044506

Bridier, A., Sanchez-Vizuete, P., Guilbaud, M., Piard, J.-C., Naïtali, M., and Briandet, R. (2015). Biofilm-associated persistence of food-borne pathogens. *Food Microbiol* 45, 167–178. doi: 10.1016/j.fm.2014.04.015

Bridier, A., Soumet, C., Attig, I., Brauge, T., Midelet, G., Fremaux, B., et al. (2021). “Chapitre 6 : Biocide désinfectants en agroalimentaire,” in *Agents antimicrobiens et sécurité sanitaire des aliments*, (Paris).

Brugère, H., Auvray, F., Mariani-Kurkdjian, P., King, L. A., and Loukiadis, E. (2012). E. coli producteurs de Shigatoxines (STEC) : définitions, virulence et propriétés des souches entérohémorragiques (EHEC).

Bryan, L. E., O’Hara, K., and Wong, S. (1984). Lipopolysaccharide changes in impermeability-type aminoglycoside resistance in *Pseudomonas aeruginosa*. *Antimicrob Agents Chemother* 26, 250–255. doi: 10.1128/AAC.26.2.250

Castanon, J. I. R. (2007). History of the use of antibiotic as growth promoters in European poultry feeds. *Poult Sci* 86, 2466–2471. doi: 10.3382/ps.2007-00249

Cerf, O., Carpentier, B., and Sanders, P. (2010). Tests for determining in-use concentrations of antibiotics and disinfectants are based on entirely different concepts: “resistance” has different meanings. *Int J Food Microbiol* 136, 247–254. doi: 10.1016/j.ijfoodmicro.2009.10.002

Charron, R., Boulanger, M., Briandet, R., and Bridier, A. (2023). Biofilms as protective cocoons against biocides: from bacterial adaptation to One Health issues. *Microbiology (Reading)* 169. doi: 10.1099/mic.0.001340

Références bibliographiques

Chen, C. Z., and Cooper, S. L. (2002). Interactions between dendrimer biocides and bacterial membranes. *Biomaterials* 23, 3359–3368. doi: 10.1016/s0142-9612(02)00036-4

Chen, L., Chavda, K. D., Fraimow, H. S., Mediavilla, J. R., Melano, R. G., Jacobs, M. R., et al. (2013). Complete nucleotide sequences of blaKPC-4- and blaKPC-5-harboring IncN and IncX plasmids from *Klebsiella pneumoniae* strains isolated in New Jersey. *Antimicrob Agents Chemother* 57, 269–276. doi: 10.1128/AAC.01648-12

Chen, P. E., and Shapiro, B. J. (2015). The advent of genome-wide association studies for bacteria. *Curr Opin Microbiol* 25, 17–24. doi: 10.1016/j.mib.2015.03.002

Chindera, K., Mahato, M., Sharma, A. K., Horsley, H., Kloc-Muniak, K., Kamaruzzaman, N. F., et al. (2016). The antimicrobial polymer PHMB enters cells and selectively condenses bacterial chromosomes. *Sci Rep* 6, 23121. doi: 10.1038/srep23121

Chokshi, A., Sifri, Z., Cennimo, D., and Horng, H. (2019). Global Contributors to Antibiotic Resistance. *J Glob Infect Dis* 11, 36–42. doi: 10.4103/jgid.jgid_110_18

Ciofu, O., Moser, C., Jensen, P. Ø., and Høiby, N. (2022). Tolerance and resistance of microbial biofilms. *Nat Rev Microbiol* 20, 621–635. doi: 10.1038/s41579-022-00682-4

Colello, R., Cáceres, M. E., Ruiz, M. J., Sanz, M., Etcheverría, A. I., and Padola, N. L. (2016). From Farm to Table: Follow-Up of Shiga Toxin-Producing *Escherichia coli* Throughout the Pork Production Chain in Argentina. *Front Microbiol* 7, 93. doi: 10.3389/fmicb.2016.00093

Condell, O., Iversen, C., Cooney, S., Power, K. A., Walsh, C., Burgess, C., et al. (2012). Efficacy of biocides used in the modern food industry to control *salmonella enterica*, and links between biocide tolerance and resistance to clinically relevant antimicrobial compounds. *Appl Environ Microbiol* 78, 3087–3097. doi: 10.1128/AEM.07534-11

Conibear, T. C. R., Collins, S. L., and Webb, J. S. (2009). Role of mutation in *Pseudomonas aeruginosa* biofilm development. *PLoS One* 4, e6289. doi: 10.1371/journal.pone.0006289

Crane, J. K., Alvarado, C. L., and Sutton, M. D. (2021). Role of the SOS Response in the Generation of Antibiotic Resistance In Vivo. *Antimicrob Agents Chemother* 65, e0001321. doi: 10.1128/AAC.00013-21

CRITT IAA (2015). Dossier Technique “Nettoyage et désinfection.” Available at: https://critt-iaa-paca.com/wp-content/uploads/2015/02/Guide-Effinet-ND.pdf

Cuzin, C., Houée, P., Lucas, P., Blanchard, Y., Soumet, C., and Bridier, A. (2021). Selection of a Gentamicin-Resistant Variant Following Polyhexamethylene Biguanide (PHMB) Exposure in *Escherichia coli* Biofilms. *Antibiotics (Basel)* 10, 553. doi: 10.3390/antibiotics10050553

Cylke, C., Si, F., and Banerjee, S. (2022). Effects of antibiotics on bacterial cell morphology and their physiological origins. *Biochem Soc Trans* 50, 1269–1279. doi: 10.1042/BST20210894

Davies, J., and Davies, D. (2010). Origins and evolution of antibiotic resistance. *Microbiol Mol Biol Rev* 74, 417–433. doi: 10.1128/MMBR.00016-10

Denamur, E., Clermont, O., Bonacorsi, S., and Gordon, D. (2021). The population genetics of pathogenic *Escherichia coli*. *Nat Rev Microbiol* 19, 37–54. doi: 10.1038/s41579-020-0416-x

Desriac, F., El Harras, A., Simon, M., Bondon, A., Brillet, B., Le Chevalier, P., et al. (2020). Alterins Produced by Oyster-Associated *Pseudoalteromonas* Are Antibacterial Cyclolipopeptides with LPS-Binding Activity. *Mar Drugs* 18, 630. doi: 10.3390/md18120630

Donaghy, J. A., Jagadeesan, B., Goodburn, K., Grunwald, L., Jensen, O. N., Jespers, A. D., et al. (2019). Relationship of Sanitizers, Disinfectants, and Cleaning Agents with Antimicrobial Resistance. *J Food Prot* 82, 889–902. doi: 10.4315/0362-028X.JFP-18-373

Dong, P., Xiao, T., Nychas, G.-J. E., Zhang, Y., Zhu, L., and Luo, X. (2020). Occurrence and characterization of Shiga toxin-producing *Escherichia coli* (STEC) isolated from Chinese beef processing plants. *Meat Sci* 168, 108188. doi: 10.1016/j.meatsci.2020.108188

Dourou, D., Beauchamp, C. S., Yoon, Y., Geornaras, I., Belk, K. E., Smith, G. C., et al. (2011). Attachment and biofilm formation by *Escherichia coli* O157:H7 at different temperatures, on various food-contact surfaces encountered in beef processing. *Int J Food Microbiol* 149, 262–268. doi: 10.1016/j.ijfoodmicro.2011.07.004

European Chemicals Agency (2012). Types de produits Biocides. Available at: https://echa.europa.eu/fr/regulations/biocidal-products-regulation/product-types

Farber, J. M., and Peterkin, P. I. (1991). *Listeria monocytogenes*, a food-borne pathogen. *Microbiol Rev* 55, 476–511. doi: 10.1128/mr.55.3.476-511.1991

Farrokh, C., Jordan, K., Auvray, F., Glass, K., Oppegaard, H., Raynaud, S., et al. (2013). Review of Shiga-toxin-producing *Escherichia coli* (STEC) and their significance in dairy production. *Int J Food Microbiol* 162, 190–212. doi: 10.1016/j.ijfoodmicro.2012.08.008

Flemming, H.-C., and Wingender, J. (2010). The biofilm matrix. *Nat Rev Microbiol* 8, 623–633. doi: 10.1038/nrmicro2415

Forbes, S., Cowley, N., Humphreys, G., Mistry, H., Amézquita, A., and McBain, A. J. (2017). Formulation of Biocides Increases Antimicrobial Potency and Mitigates the Enrichment of Nonsusceptible Bacteria in Multispecies Biofilms. *Appl Environ Microbiol* 83, e03054-16. doi: 10.1128/AEM.03054-16

Fox, L. J., Kelly, P. P., Humphreys, G. J., Waigh, T. A., Lu, J. R., and McBain, A. J. (2022). Assessing the risk of resistance to cationic biocides incorporating realism-based and biophysical approaches. *J Ind Microbiol Biotechnol* 49, kuab074. doi: 10.1093/jimb/kuab074

Friedmann, H. C. (2014). Escherich and *Escherichia*. *EcoSal Plus* 6. doi: 10.1128/ecosalplus.ESP-0025-2013

Geurtsen, J., de Been, M., Weerdenburg, E., Zomer, A., McNally, A., and Poolman, J. (2022). Genomics and pathotypes of the many faces of *Escherichia coli*. *FEMS Microbiol Rev* 46, fuac031. doi: 10.1093/femsre/fuac031

Gifford, D. R., Berríos-Caro, E., Joerres, C., Suñé, M., Forsyth, J. H., Bhattacharyya, A., et al. (2023). Mutators can drive the evolution of multi-resistance to antibiotics. *PLoS Genet* 19, e1010791. doi: 10.1371/journal.pgen.1010791

Gilbert, P., and McBain, A. J. (2003). Potential impact of increased use of biocides in consumer products on prevalence of antibiotic resistance. *Clin Microbiol Rev* 16, 189–208. doi: 10.1128/CMR.16.2.189-208.2003

Giraffa, G. (2002). Enterococci from foods. *FEMS Microbiol Rev* 26, 163–171. doi: 10.1111/j.1574-6976.2002.tb00608.x

Goldstein, I. J., Reichert, C. M., and Misaki, A. (1974). Interaction of concanavalin A with model substrates. *Ann N Y Acad Sci* 234, 283–296. doi: 10.1111/j.1749-6632.1974.tb53040.x

Guéneau, V., Charron, R., Costache, V., Bridier, A., and Briandet, R. (2023). "Spatial analysis of multispecies bacterial biofilms," in *Methods in Microbiology*, (Elsevier), 275–307. doi: 10.1016/bs.mim.2023.03.002

Guéneau, V., Rodiles, A., Piard, J.-C., Frayssinet, B., Castex, M., Plateau-Gonthier, J., et al. (2021). Capture and Ex-Situ Analysis of Environmental Biofilms in Livestock Buildings. *Microorganisms* 10, 2. doi: 10.3390/microorganisms10010002

Halder, S., Yadav, K. K., Sarkar, R., Mukherjee, S., Saha, P., Haldar, S., et al. (2015). Alteration of Zeta potential and membrane permeability in bacteria: a study with cationic agents. *Springerplus* 4, 672. doi: 10.1186/s40064-015-1476-7

Han, Y., Zhou, Z.-C., Zhu, L., Wei, Y.-Y., Feng, W.-Q., Xu, L., et al. (2019). The impact and mechanism of quaternary ammonium compounds on the transmission of antibiotic resistance genes. *Environ Sci Pollut Res Int* 26, 28352–28360. doi: 10.1007/s11356-019-05673-2

Heinrichs, D. E., Monteiro, M. A., Perry, M. B., and Whitfield, C. (1998). The assembly system for the lipopolysaccharide R2 core-type of *Escherichia coli* is a hybrid of those found in *Escherichia coli* K-12 and *Salmonella enterica*. Structure and function of the R2 WaaK and WaaL homologs. *J Biol Chem* 273, 8849–8859. doi: 10.1074/jbc.273.15.8849

Høiby, N., Bjarnsholt, T., Givskov, M., Molin, S., and Ciofu, O. (2010). Antibiotic resistance of bacterial biofilms. *Int J Antimicrob Agents* 35, 322–332. doi: 10.1016/j.ijantimicag.2009.12.011

Huang, H.-J., Xiang, D.-R., Sheng, J.-F., Li, J., Pan, X.-P., Yu, H.-Y., et al. (2009). rpoB nested PCR and sequencing for the early diagnosis of tuberculous meningitis and rifampicin resistance. *Int J Tuberc Lung Dis* 13, 749–754.

Hufnagel, D. A., Depas, W. H., and Chapman, M. R. (2015). The Biology of the *Escherichia coli* Extracellular Matrix. *Microbiol Spectr* 3. doi: 10.1128/microbiolspec.MB-0014-2014

Huitric, E., Werngren, J., Juréen, P., and Hoffner, S. (2006). Resistance levels and rpoB gene mutations among in vitro-selected rifampin-resistant *Mycobacterium tuberculosis* mutants. *Antimicrob Agents Chemother* 50, 2860–2862. doi: 10.1128/AAC.00303-06

Ibacache-Quiroga, C., Oliveros, J. C., Couce, A., and Blázquez, J. (2018). Parallel Evolution of High-Level Aminoglycoside Resistance in *Escherichia coli* Under Low and High Mutation Supply Rates. *Front Microbiol* 9, 427. doi: 10.3389/fmicb.2018.00427

Jang, J., Hur, H.-G., Sadowsky, M. J., Byappanahalli, M. N., Yan, T., and Ishii, S. (2017). Environmental *Escherichia coli*: ecology and public health implications-a review. *J Appl Microbiol* 123, 570–581. doi: 10.1111/jam.13468

Jo, J., Price-Whelan, A., and Dietrich, L. E. P. (2022). Gradients and consequences of heterogeneity in biofilms. *Nat Rev Microbiol*. doi: 10.1038/s41579-022-00692-2

Jones, I. A., and Joshi, L. T. (2021). Biocide Use in the Antimicrobial Era: A Review. *Molecules* 26, 2276. doi: 10.3390/molecules26082276

Jutkina, J., Marathe, N. P., Flach, C.-F., and Larsson, D. G. J. (2018). Antibiotics and common antibacterial biocides stimulate horizontal transfer of resistance at low concentrations. *Sci Total Environ* 616–617, 172–178. doi: 10.1016/j.scitotenv.2017.10.312

Kampf, G. (2018). Biocidal Agents Used for Disinfection Can Enhance Antibiotic Resistance in Gram-Negative Species. *Antibiotics (Basel)* 7, 110. doi: 10.3390/antibiotics7040110

Karatzas, K. A. G., Webber, M. A., Jorgensen, F., Woodward, M. J., Piddock, L. J. V., and Humphrey, T. J. (2007). Prolonged treatment of *Salmonella enterica* serovar Typhimurium with commercial disinfectants selects for multiple antibiotic resistance, increased efflux and reduced invasiveness. *Journal of Antimicrobial Chemotherapy* 60, 947–955. doi: 10.1093/jac/dkm314

Koonin, E. V. (1997). Genome sequences: genome sequence of a model prokaryote. *Curr Biol* 7, R656-659. doi: 10.1016/s0960-9822(06)00328-9

Krause, K. M., Serio, A. W., Kane, T. R., and Connolly, L. E. (2016). Aminoglycosides: An Overview. *Cold Spring Harb Perspect Med* 6, a027029. doi: 10.1101/cshperspect.a027029

Lambert, P. A. (2005). Bacterial resistance to antibiotics: modified target sites. *Adv Drug Deliv Rev* 57, 1471–1485. doi: 10.1016/j.addr.2005.04.003

Langsrud, S., Sundheim, G., and Holck, A. L. (2004). Cross-resistance to antibiotics of *Escherichia coli* adapted to benzalkonium chloride or exposed to stress-inducers. *J Appl Microbiol* 96, 201–208. doi: 10.1046/j.1365-2672.2003.02140.x

Laverty, G., Gorman, S. P., and Gilmore, B. F. (2011). The potential of antimicrobial peptides as biocides. *Int J Mol Sci* 12, 6566–6596. doi: 10.3390/ijms12106566

Lee, I. P. A., Eldakar, O. T., Gogarten, J. P., and Andam, C. P. (2022). Bacterial cooperation through horizontal gene transfer. *Trends Ecol Evol* 37, 223–232. doi: 10.1016/j.tree.2021.11.006

Lenski, R. E. (2023). Revisiting the Design of the Long-Term Evolution Experiment with *Escherichia coli*. *J Mol Evol* 91, 241–253. doi: 10.1007/s00239-023-10095-3

Leriche, V., Briandet, R., and Carpentier, B. (2003). Ecology of mixed biofilms subjected daily to a chlorinated alkaline solution: spatial distribution of bacterial species suggests a protective effect of one species to another. *Environ Microbiol* 5, 64–71. doi: 10.1046/j.1462-2920.2003.00394.x

Levin-Reisman, I., Brauner, A., Ronin, I., and Balaban, N. Q. (2019). Epistasis between antibiotic tolerance, persistence, and resistance mutations. *Proc Natl Acad Sci U S A* 116, 14734–14739. doi: 10.1073/pnas.1906169116

Li, M.-C., Lu, J., Lu, Y., Xiao, T.-Y., Liu, H.-C., Lin, S.-Q., et al. (2021). rpoB Mutations and Effects on Rifampin Resistance in *Mycobacterium tuberculosis*. *Infect Drug Resist* 14, 4119–4128. doi: 10.2147/IDR.S333433

Lundborg, C. S., and Tamhankar, A. J. (2017). Antibiotic residues in the environment of South East Asia. *BMJ* 358, j2440. doi: 10.1136/bmj.j2440

Luyckx, K., Millet, S., Van Weyenberg, S., Herman, L., Heyndrickx, M., Dewulf, J., et al. (2016). A 10-day vacancy period after cleaning and disinfection has no effect on the bacterial load in pig nursery units. *BMC Vet Res* 12, 236. doi: 10.1186/s12917-016-0850-1

Maciá, M. D., Blanquer, D., Togores, B., Sauleda, J., Pérez, J. L., and Oliver, A. (2005). Hypermutation is a key factor in development of multiple-antimicrobial resistance in *Pseudomonas aeruginosa* strains causing chronic lung infections. *Antimicrob Agents Chemother* 49, 3382–3386. doi: 10.1128/AAC.49.8.3382-3386.2005

Maifreni, M., Di Bonaventura, G., Marino, M., Guarnieri, S., Frigo, F., and Pompilio, A. (2023). Biofilm formation under food-relevant conditions and sanitizers' tolerance of a *Pseudomonas fluorescens* group strain. *J Appl Microbiol* 134, lxad117. doi: 10.1093/jambio/lxad117

Maillard, J.-Y. (2002). Bacterial target sites for biocide action. *J Appl Microbiol* 92 Suppl, 16S-27S.

Maillard, J.-Y. (2005). Antimicrobial biocides in the healthcare environment: efficacy, usage, policies, and perceived problems. *Ther Clin Risk Manag* 1, 307–320.

Maillard, J.-Y. (2018). Resistance of Bacteria to Biocides. *Microbiol Spectr* 6, 6.2.19. doi: 10.1128/microbiolspec.ARBA-0006-2017

Maillard, J.-Y., and Centeleghe, I. (2023). How biofilm changes our understanding of cleaning and disinfection. *Antimicrob Resist Infect Control* 12, 95. doi: 10.1186/s13756-023-01290-4

Maillard, J.-Y., and Pascoe, M. (2024). Disinfectants and antiseptics: mechanisms of action and resistance. *Nat Rev Microbiol* 22, 4–17. doi: 10.1038/s41579-023-00958-3

Majumdar, C., Nuñez, N. N., Raetz, A. G., Khuu, C., and David, S. S. (2018). Cellular Assays for Studying the Fe-S Cluster Containing Base Excision Repair Glycosylase MUTYH and Homologs. *Methods Enzymol* 599, 69–99. doi: 10.1016/bs.mie.2017.12.006

Mares, J., Kumaran, S., Gobbo, M., and Zerbe, O. (2009). Interactions of lipopolysaccharide and polymyxin studied by NMR spectroscopy. *J Biol Chem* 284, 11498–11506. doi: 10.1074/jbc.M806587200

McDonald, M. J. (2019). Microbial Experimental Evolution - a proving ground for evolutionary theory and a tool for discovery. *EMBO Rep* 20, e46992. doi: 10.15252/embr.201846992

McDonnell, G., and Russell, A. D. (1999). Antiseptics and disinfectants: activity, action, and resistance. *Clin Microbiol Rev* 12, 147–179. doi: 10.1128/CMR.12.1.147

Motiei, M., Pleno de Gouveia, L., Šopík, T., Vícha, R., Škoda, D., Císař, J., et al. (2021). Nanoparticle-Based Rifampicin Delivery System Development. *Molecules* 26, 2067. doi: 10.3390/molecules26072067

Mulcahy, H., Charron-Mazenod, L., and Lewenza, S. (2008). Extracellular DNA chelates cations and induces antibiotic resistance in *Pseudomonas aeruginosa* biofilms. *PLoS Pathog* 4, e1000213. doi: 10.1371/journal.ppat.1000213

Mullis, M. N., Matsui, T., Schell, R., Foree, R., and Ehrenreich, I. M. (2018). The complex underpinnings of genetic background effects. *Nat Commun* 9, 3548. doi: 10.1038/s41467-018-06023-5

Références bibliographiques

Munita, J. M., and Arias, C. A. (2016). Mechanisms of Antibiotic Resistance. *Microbiol Spectr* 4. doi: 10.1128/microbiolspec.VMBF-0016-2015

Murray, C. J. L., Ikuta, K. S., Sharara, F., Swetschinski, L., Robles Aguilar, G., Gray, A., et al. (2022). Global burden of bacterial antimicrobial resistance in 2019: a systematic analysis. *The Lancet* 399, 629–655. doi: 10.1016/S0140-6736(21)02724-0

Nakao, R., Ramstedt, M., Wai, S. N., and Uhlin, B. E. (2012). Enhanced biofilm formation by *Escherichia coli* LPS mutants defective in Hep biosynthesis. *PLoS One* 7, e51241. doi: 10.1371/journal.pone.0051241

Nesse, L. L., Sekse, C., Berg, K., Johannesen, K. C. S., Solheim, H., Vestby, L. K., et al. (2014). Potentially pathogenic *Escherichia coli* can form a biofilm under conditions relevant to the food production chain. *Appl Environ Microbiol* 80, 2042–2049. doi: 10.1128/AEM.03331-13

Nguyen, Y., and Sperandio, V. (2012). Enterohemorrhagic *E. coli* (EHEC) pathogenesis. *Front Cell Infect Microbiol* 2, 90. doi: 10.3389/fcimb.2012.00090

Nikaido, H. (2003). Molecular basis of bacterial outer membrane permeability revisited. *Microbiol Mol Biol Rev* 67, 593–656. doi: 10.1128/MMBR.67.4.593-656.2003

Nordholt, N., Kanaris, O., Schmidt, S. B. I., and Schreiber, F. (2021). Persistence against benzalkonium chloride promotes rapid evolution of tolerance during periodic disinfection. *Nat Commun* 12, 6792. doi: 10.1038/s41467-021-27019-8

Nucci, A., Rocha, E. P. C., and Rendueles, O. (2023). Latent evolution of biofilm formation depends on life-history and genetic background. *npj Biofilms Microbiomes* 9, 53. doi: 10.1038/s41522-023-00422-3

Okshevsky, M., Regina, V. R., and Meyer, R. L. (2015). Extracellular DNA as a target for biofilm control. *Curr Opin Biotechnol* 33, 73–80. doi: 10.1016/j.copbio.2014.12.002

O'Neill, J. (2014). Antimicrobial resistance: Tackling a crisis for the health and wealth of nations. Available at: https://amr-review.org/sites/default/files/AMR%20Review%20Paper%20-%20Tackling%20a%20crisis%20for%20the%20health%20and%20wealth%20of%20nations_1.pdf

Oulahal, N., and Degraeve, P. (2021). Phenolic-Rich Plant Extracts With Antimicrobial Activity: An Alternative to Food Preservatives and Biocides? *Front Microbiol* 12, 753518. doi: 10.3389/fmicb.2021.753518

Pagedar, A., Singh, J., and Batish, V. K. (2011). Efflux mediated adaptive and cross resistance to ciprofloxacin and benzalkonium chloride in *Pseudomonas aeruginosa* of dairy origin. *J Basic Microbiol* 51, 289–295. doi: 10.1002/jobm.201000292

Partridge, S. R., Kwong, S. M., Firth, N., and Jensen, S. O. (2018). Mobile Genetic Elements Associated with Antimicrobial Resistance. *Clin Microbiol Rev* 31, e00088-17. doi: 10.1128/CMR.00088-17

Penesyan, A., Paulsen, I. T., Kjelleberg, S., and Gillings, M. R. (2021). Three faces of biofilms: a microbial lifestyle, a nascent multicellular organism, and an incubator for diversity. *NPJ Biofilms Microbiomes* 7, 80. doi: 10.1038/s41522-021-00251-2

Références bibliographiques

Perry, J., Waglechner, N., and Wright, G. (2016). The Prehistory of Antibiotic Resistance. *Cold Spring Harb Perspect Med* 6, a025197. doi: 10.1101/cshperspect.a025197

Piras, F., Fois, F., Consolati, S. G., Mazza, R., and Mazzette, R. (2015). Influence of Temperature, Source, and Serotype on Biofilm Formation of *Salmonella enterica* Isolates from Pig Slaughterhouses. *J Food Prot* 78, 1875–1878. doi: 10.4315/0362-028X.JFP-15-085

Plesiat, P., Aires, J. R., Godard, C., and Köhler, T. (1997). Use of steroids to monitor alterations in the outer membrane of *Pseudomonas aeruginosa*. *J Bacteriol* 179, 7004–7010. doi: 10.1128/jb.179.22.7004-7010.1997

Poirel, L., Madec, J.-Y., Lupo, A., Schink, A.-K., Kieffer, N., Nordmann, P., et al. (2018). Antimicrobial Resistance in *Escherichia coli*. *Microbiol Spectr* 6, 6.4.14. doi: 10.1128/microbiolspec.ARBA-0026-2017

Poole, K. (2002). Mechanisms of bacterial biocide and antibiotic resistance. *J Appl Microbiol* 92 Suppl, 55S-64S.

Rivera-Betancourt, M., Shackelford, S. D., Arthur, T. M., Westmoreland, K. E., Bellinger, G., Rossman, M., et al. (2004). Prevalence of *Escherichia coli* O157:H7, *Listeria monocytogenes*, and *Salmonella* in two geographically distant commercial beef processing plants in the United States. *J Food Prot* 67, 295–302. doi: 10.4315/0362-028x-67.2.295

Rizvi, S. G., and Ahammad, S. Z. (2022). COVID-19 and antimicrobial resistance: A cross-study. *Sci Total Environ* 807, 150873. doi: 10.1016/j.scitotenv.2021.150873

Roedel, A., Vincze, S., Projahn, M., Roesler, U., Robé, C., Hammerl, J. A., et al. (2021). Genetic but No Phenotypic Associations between Biocide Tolerance and Antibiotic Resistance in *Escherichia coli* from German Broiler Fattening Farms. *Microorganisms* 9, 651. doi: 10.3390/microorganisms9030651

Rosche, W. A., and Foster, P. L. (2000). Determining mutation rates in bacterial populations. *Methods* 20, 4–17. doi: 10.1006/meth.1999.0901

Russell, A. D. (1997). Plasmids and bacterial resistance to biocides. *Journal of Applied Microbiology* 83, 155–165. doi: 10.1046/j.1365-2672.1997.00198.x

Russell, A. D. (2003). Biocide use and antibiotic resistance: the relevance of laboratory findings to clinical and environmental situations. *Lancet Infect Dis* 3, 794–803. doi: 10.1016/s1473-3099(03)00833-8

Ryder, V. J., Chopra, I., and O'Neill, A. J. (2012). Increased mutability of *Staphylococci* in biofilms as a consequence of oxidative stress. *PLoS One* 7, e47695. doi: 10.1371/journal.pone.0047695

Sabnis, A., Hagart, K. L., Klöckner, A., Becce, M., Evans, L. E., Furniss, R. C. D., et al. (2021). Colistin kills bacteria by targeting lipopolysaccharide in the cytoplasmic membrane. *Elife* 10, e65836. doi: 10.7554/eLife.65836

Sadiq, F. A., Flint, S., Li, Y., Liu, T., Lei, Y., Sakandar, H. A., et al. (2017). New mechanistic insights into the motile-to-sessile switch in various bacteria with particular emphasis on *Bacillus subtilis* and *Pseudomonas aeruginosa*: a review. *Biofouling* 33, 306–326. doi: 10.1080/08927014.2017.1304541

Sambaza, S. S., and Naicker, N. (2023). Contribution of wastewater to antimicrobial resistance: A review article. *J Glob Antimicrob Resist* 34, 23–29. doi: 10.1016/j.jgar.2023.05.010

Sanchez-Vizuete, P., Orgaz, B., Aymerich, S., Le Coq, D., and Briandet, R. (2015). Pathogens protection against the action of disinfectants in multispecies biofilms. *Front Microbiol* 6, 705. doi: 10.3389/fmicb.2015.00705

Santé Publique France (2022). Investigation de cas groupés de syndrome hémolytique et urémique (SHU) et d'infections à *E. coli* producteurs de shiga-toxine (STEC) en lien avec la consommation de pizzas Fraîch'Up de marque Buitoni®. Point de situation au 4 mai 2022. Available at: https://www.santepubliquefrance.fr/les-actualites/2022/investigation-de-cas-groupes-de-syndrome-hemolytique-et-uremique-shu-et-d-infections-a-e.-coli-producteurs-de-shiga-toxine-stec-en-lien-avec-la3

Santos-Lopez, A., Marshall, C. W., Scribner, M. R., Snyder, D. J., and Cooper, V. S. (2019). Evolutionary pathways to antibiotic resistance are dependent upon environmental structure and bacterial lifestyle. *Elife* 8, e47612. doi: 10.7554/eLife.47612

Sharma, G., Sharma, S., Sharma, P., Chandola, D., Dang, S., Gupta, S., et al. (2016). *Escherichia coli* biofilm: development and therapeutic strategies. *J Appl Microbiol* 121, 309–319. doi: 10.1111/jam.13078

Shea, J., Halse, T. A., Kohlerschmidt, D., Lapierre, P., Modestil, H. A., Kearns, C. H., et al. (2021). Low-Level Rifampin Resistance and rpoB Mutations in *Mycobacterium tuberculosis*: an Analysis of Whole-Genome Sequencing and Drug Susceptibility Test Data in New York. *J Clin Microbiol* 59, e01885-20. doi: 10.1128/JCM.01885-20

Silhavy, T. J., Kahne, D., and Walker, S. (2010). The bacterial cell envelope. *Cold Spring Harb Perspect Biol* 2, a000414. doi: 10.1101/cshperspect.a000414

Slipski, C. J., Jamieson-Datzkiw, T. R., Zhanel, G. G., and Bay, D. C. (2021). Characterization of Proteobacterial Plasmid Integron-Encoded qac Efflux Pump Sequence Diversity and Quaternary Ammonium Compound Antiseptic Selection in *Escherichia coli* Grown Planktonically and as Biofilms. *Antimicrob Agents Chemother* 65, e0106921. doi: 10.1128/AAC.01069-21

Smith, C. A., and Baker, E. N. (2002). Aminoglycoside antibiotic resistance by enzymatic deactivation. *Curr Drug Targets Infect Disord* 2, 143–160. doi: 10.2174/1568005023342533

Sowlati-Hashjin, S., Carbone, P., and Karttunen, M. (2020). Insights into the Polyhexamethylene Biguanide (PHMB) Mechanism of Action on Bacterial Membrane and DNA: A Molecular Dynamics Study. *J Phys Chem B* 124, 4487–4497. doi: 10.1021/acs.jpcb.0c02609

Steffen, R., Jiang, Z.-D., Gracias Garcia, M. L., Araujo, P., Stiess, M., Nacak, T., et al. (2018). Rifamycin SV-MMX® for treatment of travellers' diarrhea: equally effective as ciprofloxacin and not associated with the acquisition of multi-drug resistant bacteria. *J Travel Med* 25, tay116. doi: 10.1093/jtm/tay116

Tadesse, D. A., Zhao, S., Tong, E., Ayers, S., Singh, A., Bartholomew, M. J., et al. (2012). Antimicrobial drug resistance in *Escherichia coli* from humans and food animals, United States, 1950-2002. *Emerg Infect Dis* 18, 741–749. doi: 10.3201/eid1805.111153

Références bibliographiques

Terlizzi, M. E., Gribaudo, G., and Maffei, M. E. (2017). UroPathogenic *Escherichia coli* (UPEC) Infections: Virulence Factors, Bladder Responses, Antibiotic, and Non-antibiotic Antimicrobial Strategies. *Front Microbiol* 8, 1566. doi: 10.3389/fmicb.2017.01566

Trubenová, B., Roizman, D., Moter, A., Rolff, J., and Regoes, R. R. (2022). Population genetics, biofilm recalcitrance, and antibiotic resistance evolution. *Trends Microbiol* 30, 841–852. doi: 10.1016/j.tim.2022.02.005

Uruén, C., Chopo-Escuin, G., Tommassen, J., Mainar-Jaime, R. C., and Arenas, J. (2020). Biofilms as Promoters of Bacterial Antibiotic Resistance and Tolerance. *Antibiotics (Basel)* 10, 3. doi: 10.3390/antibiotics10010003

Usui, M., Yoshii, Y., Thiriet-Rupert, S., Ghigo, J.-M., and Beloin, C. (2023). Intermittent antibiotic treatment of bacterial biofilms favors the rapid evolution of resistance. *Commun Biol* 6, 275. doi: 10.1038/s42003-023-04601-y

Van Cauteren, D., Le Strat, Y., Sommen, C., Bruyand, M., Tourdjman, M., Jourdan-Da Silva, N., et al. (2018). Estimation de la morbidité et de la mortalité liées aux infections d'origine alimentaire en France métropolitaine, 2008-2013. Available at: http://invs.santepublique france.fr/beh/2018/1/2018_1_1.html

van Hoek, A. H. A. M., Mevius, D., Guerra, B., Mullany, P., Roberts, A. P., and Aarts, H. J. M. (2011). Acquired antibiotic resistance genes: an overview. *Front Microbiol* 2, 203. doi: 10.3389/fmicb.2011.00203

Vanacker, M., Lenuzza, N., and Rasigade, J.-P. (2023). The fitness cost of horizontally transferred and mutational antimicrobial resistance in Escherichia coli. *Front Microbiol* 14, 1186920. doi: 10.3389/fmicb.2023.1186920

Velazquez-Meza, M. E., Galarde-López, M., Carrillo-Quiróz, B., and Alpuche-Aranda, C. M. (2022). Antimicrobial resistance: One Health approach. *Vet World* 15, 743–749. doi: 10.14202/vetworld.2022.743-749

Ventola, C. L. (2015). The antibiotic resistance crisis: part 1: causes and threats. *P T* 40, 277–283.

Vogeleer, P., Tremblay, Y. D. N., Mafu, A. A., Jacques, M., and Harel, J. (2014). Life on the outside: role of biofilms in environmental persistence of Shiga-toxin producing *Escherichia coli*. *Front Microbiol* 5, 317. doi: 10.3389/fmicb.2014.00317

von Wintersdorff, C. J. H., Penders, J., van Niekerk, J. M., Mills, N. D., Majumder, S., van Alphen, L. B., et al. (2016). Dissemination of Antimicrobial Resistance in Microbial Ecosystems through Horizontal Gene Transfer. *Front Microbiol* 7, 173. doi: 10.3389/fmicb.2016.00173

Wang, C., Zhang, H., Wang, J., Chen, S., Wang, Z., Zhao, L., et al. (2021). Corrigendum to "Colanic acid biosynthesis in *Escherichia coli* is dependent on lipopolysaccharide structure and glucose availability" [Microbiol. Res. 239 (October 2020) 126527]. *Microbiol Res* 243, 126656. doi: 10.1016/j.micres.2020.126656

Wesgate, R., Grasha, P., and Maillard, J.-Y. (2016). Use of a predictive protocol to measure the antimicrobial resistance risks associated with biocidal product usage. *Am J Infect Control* 44, 458–464. doi: 10.1016/j.ajic.2015.11.009

Références bibliographiques

Wood, T. K., Knabel, S. J., and Kwan, B. W. (2013). Bacterial persister cell formation and dormancy. *Appl Environ Microbiol* 79, 7116–7121. doi: 10.1128/AEM.02636-13

World Health Organization (2019). *Critically important antimicrobials for human medicine*., 6th rev. Geneva: World Health Organization. Available at: https://iris.who.int/handle/10665/312266 (Accessed November 10, 2023).

World Health Organization (2023). Global research agenda for antimicrobial resistance in human health. Available at: https://cdn.who.int/media/docs/default-source/antimicrobial-resistance/amr-spc-npm/who-global-research-agenda-for-amr-in-human-health---policy-brief.pdf?sfvrsn=f86aa073_4&download=true

World Health Organization (2024). WHO Bacterial Priority Pathogens List 2024. Available at: https://iris.who.int/bitstream/handle/10665/376776/9789240093461-eng.pdf?sequence=1

Yuan, L., Wang, H., Liu, W., Sadiq, F. A., and Zhao, Y. (2022). Editorial: Multi-species biofilms in the food industry. *Front Microbiol* 13, 1023428. doi: 10.3389/fmicb.2022.1023428

Zand, R., Agrawal, B. B., and Goldstein, I. J. (1971). pH-dependent conformational changes of concanavalin A. *Proc Natl Acad Sci U S A* 68, 2173–2176. doi: 10.1073/pnas.68.9.2173

Zhang, G., Meredith, T. C., and Kahne, D. (2013). On the essentiality of lipopolysaccharide to Gram-negative bacteria. *Curr Opin Microbiol* 16, 779–785. doi: 10.1016/j.mib.2013.09.007

Zhang, Y., Gu, A. Z., He, M., Li, D., and Chen, J. (2017). Subinhibitory Concentrations of Disinfectants Promote the Horizontal Transfer of Multidrug Resistance Genes within and across Genera. *Environ Sci Technol* 51, 570–580. doi: 10.1021/acs.est.6b03132

Zhu, S., Yang, B., Jia, Y., Yu, F., Wang, Z., and Liu, Y. (2023). Comprehensive analysis of disinfectants on the horizontal transfer of antibiotic resistance genes. *J Hazard Mater* 453, 131428. doi: 10.1016/j.jhazmat.2023.131428

Zulfiana, R., Suharjono, null, and Kuntaman, null (2021). Genetic profile mutation rpoB in clinical isolate of rifampicin-resistant *Staphylococcus aureus*. *J Basic Clin Physiol Pharmacol* 32, 773–776. doi: 10.1515/jbcpp-2020-0444

Valorisations scientifiques

1. Publications scientifiques

Article 1 (*revue de la littérature*) : Raphaël Charron, Marine Boulanger, Romain Briandet, Arnaud Bridier. Biofilms as protective cocoons against biocides: from bacterial adaptation to One Health issues. *Microbiology*, 2023, 10.1099/mic.0.001340.

Article 2 (*chapitre de méthode*) : Pierre Lemée, **Raphaël Charron**, Arnaud Bridier. Analysis of adaptive mutational events in bacteria undergoing stress exposure. Foodborne Bacterial pathogens-2nd edition, *Methods in Molecular Biology*, Springer, 2024.

Article 3 (*chapitre de méthode*) : Virgile Guéneau*, **Raphaël Charron***, Vlad Costache, Arnaud Bridier, Romain Briandet. Spatial analysis of multispecies bacterial biofilms. MIM 53: Biofilms, Elsevier, 2023, *Methods in Microbiology*, 10.1016/bs.mim.2023.03.002.

Article 4 : Raphaël Charron, Pierre Lemée, Antoine Huguet, Ornella Minlong, Marine Boulanger, Paméla Houée, Christophe Soumet, Romain Briandet, Arnaud Bridier. Impact of biofilm lifestyle on aminoglycoside resistance emergence in *Escherichia coli*.

Article 5 : Raphaël Charron, Pierre Lemée, Antoine Huguet, Ornella Minlong, Marine Boulanger, Pamela Houée, Christophe Soumet, Romain Briandet, Arnaud Bridier. Polyhexamethylene biguanide promotes adaptive cross-resistance to gentamicin in *Escherichia coli* biofilms. *Frontiers in Cellular and Infection Microbiology*, 2023, 10.3389/fcimb.2023.1324991.

Article 6 : Raphaël Charron, Pierre Lemée, Paméla Houée, Patricia Le Grandois, Marine Boulanger, Thibaut Léger, Christophe Soumet, Romain Briandet, Arnaud Bridier. Pivotal role of lipopolysaccharide modulation in biofilm adaptation to triamine biocide and associated antibiotic cross-resistance.

*Ces auteurs ont contribué de manière égale

2. Communications orales

Raphaël Charron, Pierre Lemée, Marine Boulanger, Paméla Houée, Julien Deschamps, Christophe Soumet, Romain Briandet, Arnaud Bridier. Emergence of antibiotic resistant clones in *E. coli* biofilms exposed to biocides. Séminaire Micalis, Jouy-en-Josas, France

Raphaël Charron, Pierre Lemée, Marine Boulanger, Ornella Minlong, Paméla Houée, Julien Deschamps, Antoine Huguet, Christophe Soumet, Romain Briandet, Arnaud Bridier. Adaptation to widely used biocide substances selects for rifampicin resistance in *E. coli* biofilms. Doc'Micalis 2023, Jouy-en-Josas, France

Raphaël Charron, Pierre Lemée, Marine Boulanger, Ornella Minlong, Paméla Houée, Julien Deschamps, Antoine Huguet, Christophe Soumet, Romain Briandet, Arnaud Bridier. Adaptation to widely used biocide active susbtances selects for rifampicin resistance in *E. coli* biofilms. Surf'safe 2023, Porto, Portugal

Raphaël Charron, Marine Boulanger, Pierre Lemée, Ornella Minlong, Paméla Houée, Julien Deschamps, Antoine Huguet, Christophe Soumet, Romain Briandet, Arnaud Bridier.

Adaptation to widely used biocide active susbtances selects for rifampicin resistance in *E. coli* biofilms. Journées scientifiques de l'école doctorale 2024, Saint-Malo, France.

Raphaël Charron, Pierre Lemée, Patricia Le Grandois, Pamela Houée, Thibaut Léger, Marine Boulanger, Ornella Minlong, Antoine Huguet, Christophe Soumet, Romain Briandet, Arnaud Bridier. *E. coli* biofilm adaptation to biocides and impact on antibiotic resistance. Journées Scientifiques et Doctorales de l'ANSES 2024, Maisons-Alfort, France

Raphaël Charron, Pierre Lemée, Paméla Houée, Patricia Le Grandois, Marine Boulanger, Antoine Huguet, Thibaut Léger, Christophe Soumet, Romain Briandet, Arnaud Bridier. L'adaptation de biofilms de Escherichia coli aux biocides sélectionne des résistances à la rifampicine. Réseau National Biofilms 2024, Toulouse, France

3. Posters

Raphaël Charron, Marine Boulanger, Paméla Houée, Christophe Soumet, Romain Briandet, Arnaud Bridier. Biofilm adaptation to biocides and its impact on aminoglycoside resistance. Atlantic Exposome Summer School (ALEXS) 2022, Rennes, France

Raphaël Charron, Pierre Lemée, Marine Boulanger, Ornella Minlong, Paméla Houée, Julien Deschamps, Antoine Huguet, Christophe Soumet, Romain Briandet, Arnaud Bridier. Adaptation to widely used biocide substances selects for rifampicin resistance in *E. coli* biofilms. Fédération Européenne des Sociétés de Microbiologie (FEMS) 2023, Hambourg, Allemagne

Raphaël Charron, Pierre Lemée, Marine Boulanger, Ornella Minlong, Paméla Houée, Julien Deschamps, Antoine Huguet, Christophe Soumet, Romain Briandet, Arnaud Bridier. Adaptation to widely used biocide substances selects for rifampicin resistance in *E. coli* biofilms. Journées Scientifiques et Doctorales de l'ANSES 2023, Maisons-Alfort, France.

Raphaël Charron, Pierre Lemée, Marine Boulanger, Ornella Minlong, Paméla Houée, Julien Deschamps, Antoine Huguet, Christophe Soumet, Romain Briandet, Arnaud Bridier. Adaptation to widely used biocide substances selects for rifampicin resistance in *E. coli* biofilms. Eurobiofilms 2024, Copenhague, Danemark

4. Cours

Raphaël Charron, Arnaud Bridier, Florence Dubois-Brissonnet. Biocides et antibiorésistance de bactéries alimentaires. Master 2 : Analyse des risques alimentaires liés à l'alimentation, AgroParisTech, 2023, Palaiseau, France

5. Encadrements

Raphaël Charron, Arnaud Bridier. Stage de M2 de Marine Boulanger : Impact de l'adaptation des bactéries en biofilm aux biocides sur l'antibiorésistance. Janvier-Juin 2022.

Raphaël Charron, Antoine Huguet, Arnaud Bridier. Stage de M2 de Ornella Minlong : Caractérisation des mécanismes moléculaires impliqués dans l'adaptation aux biocides et la résistance aux antibiotiques chez *E. coli*. Janvier-Juin 2023.

Titre : **Impact de l'adaptation des biofilms bactériens aux biocides désinfectants sur l'antibiorésistance**

Mots clés : Biofilms, Biocides, Antibiotiques, Résistance, Adaptation

Résumé : L'augmentation de la résistance aux antimicrobiens constitue une menace majeure pour la santé publique. L'identification des facteurs contribuant à l'émergence de résistances aux antibiotiques dans les environnements industriels est essentielle pour adapter nos pratiques et limiter leur propagation. Les substances biocides utilisées pour les procédures de désinfection pourraient favoriser la sélection croisée de résistances aux antibiotiques dans les populations bactériennes. Cependant, peu de données existent sur les biofilms, des communautés bactériennes fixées aux surfaces, qui représentent pourtant le mode de vie bactérien principal et qui possèdent des capacités d'adaptation spécifiques. Les objectifs de cette thèse étaient donc de mieux comprendre comment le mode de vie biofilm influence l'adaptation bactérienne face aux stress biocides et la sélection croisée de résistances aux antibiotiques.

Des biofilms de neuf souches d'*Escherichia coli* ont été exposés pendant un mois à quatre substances actives biocides, et la résistance à divers antibiotiques a été quantifiée. Les caractérisations phénotypiques et génomiques des variants résistants ont ensuite permis d'élucider le rôle des biofilms dans la sélection de ces résistances ainsi que les mécanismes sous-jacents.

Des liens entre l'exposition à plusieurs biocides et la sélection croisée de résistances aux antibiotiques ont été identifiés. L'exposition au N-(3-aminopropyl)-N-dodécylpropane-1,3-diamine (Triamine, TMN) et au chlorure de benzalkonium (BAC) a induit la sélection de variants résistants à la rifampicine (RifR) dans les biofilms, par rapport à l'exposition à H_2O. Une récurrence de modifications du LPS a été identifiée dans les variants RifR de la condition TMN. Ils présentaient des avantages compétitifs par rapport aux souches parentales, aussi bien au niveau individuel que collectif dans les biofilms, renforçant ainsi leur risque de dissémination dans la chaîne alimentaire. Une autre association a été trouvée entre l'exposition au polyhexaméthylène biguanide (PHMB) et la sélection de résistances aux aminosides. Les résultats ont montré que le PHMB induisait des modifications structurelles des biofilms, altérant ainsi la réponse physiologique dans diverses souches, ce qui a été associé à l'émergence d'une résistance croisée adaptative à la gentamicine.

Globalement, cette recherche souligne l'importance d'étudier les biofilms, qui façonnent les voies évolutives des bactéries. Les résultats permettront d'évaluer plus précisément le risque lié à l'utilisation des biocides en relation avec la résistance aux antibiotiques, et d'identifier des marqueurs de développement de résistances croisées, utilisables pour développer des outils de surveillance dans la chaîne alimentaire.

Title: **Impact of bacterial biofilm adaptation to biocides on antibiotic resistance**

Keywords: Biofilms, Biocides, Antibiotics, Resistance, Adaptation

Abstract: The increase in antimicrobial resistance increase poses a significant threat to public health. Identifying factors contributing to the emergence of antibiotic resistance in industrial environments is crucial for adapting our practices and limiting the emergence of antimicrobial resistance. Biocidal substances used for disinfection procedures could contribute to the selection of cross-resistance to antibiotics in bacterial populations. However, very few data are available on biofilms, which are surface-associated bacterial communities that represent the primary bacterial lifestyle and exhibit specific adaptation capacities. Therefore, this thesis aimed to better understand how the biofilm lifestyle affects bacterial adaptation to biocidal stresses and the cross-selection of antibiotic resistance.

Biofilms of nine *Escherichia coli* strains were exposed to four biocidal active substances for a month, and resistance to various antibiotics was quantified. Phenotypic and genomic characterizations of resistant variants provided insights into the role of biofilms in the selection of these resistances and the underlying mechanisms.

Links between the exposure to several biocides and antibiotic cross-resistances were identified. Exposure to N-(3-aminopropyl)-N-dodecylpropane-1,3-diamine (Triamine, TMN) and benzalkonium chloride (BAC) led to a significant increase in rifampicin-resistant (RifR) variants in biofilms compared with exposure to H_2O. A recurrence of LPS modifications was identified in the RifR variants from the TMN condition. These variants had competitive advantages over parental strains at both the individual and collective biofilm levels, supporting the likelihood of a higher risk of dissemination throughout the food chain. Another association was found between the exposure to polyhexamethylene biguanide (PHMB) and the selection of resistance to aminoglycosides. Results revealed that PHMB induced structural modulations in biofilms that altered the physiological response in various strains, which was associated with the emergence of an adaptive cross-resistance to gentamicin.

Overall, this research highlights the importance of studying biofilms, which shape the evolutionary pathways of bacteria. Findings will be used to better assess the risks associated with biocide usage in relation to antibiotic resistance, and ultimately identify cross-resistance development markers that can be used to develop surveillance tools in the food chain.